

ADVERTIMENT. La consulta d'aquesta tesi queda condicionada a l'acceptació de les següents condicions d'ús: La difusió d'aquesta tesi per mitjà del servei TDX (www.tesisenxarxa.net) ha estat autoritzada pels titulars dels drets de propietat intel·lectual únicament per a usos privats emmarcats en activitats d'investigació i docència. No s'autoritza la seva reproducció amb finalitats de lucre ni la seva difusió i posada a disposició des d'un lloc aliè al servei TDX. No s'autoritza la presentació del seu contingut en una finestra o marc aliè a TDX (framing). Aquesta reserva de drets afecta tant al resum de presentació de la tesi com als seus continguts. En la utilització o cita de parts de la tesi és obligat indicar el nom de la persona autora.

ADVERTENCIA. La consulta de esta tesis queda condicionada a la aceptación de las siguientes condiciones de uso: La difusión de esta tesis por medio del servicio TDR (www.tesisenred.net) ha sido autorizada por los titulares de los derechos de propiedad intelectual únicamente para usos privados enmarcados en actividades de investigación y docencia. No se autoriza su reproducción con finalidades de lucro ni su difusión y puesta a disposición desde un sitio ajeno al servicio TDR. No se autoriza la presentación de su contenido en una ventana o marco ajeno a TDR (framing). Esta reserva de derechos afecta tanto al resumen de presentación de la tesis como a sus contenidos. En la utilización o cita de partes de la tesis es obligado indicar el nombre de la persona autora.

WARNING. On having consulted this thesis you're accepting the following use conditions: Spreading this thesis by the TDX (www.tesisenxarxa.net) service has been authorized by the titular of the intellectual property rights only for private uses placed in investigation and teaching activities. Reproduction with lucrative aims is not authorized neither its spreading and availability from a site foreign to the TDX service. Introducing its content in a window or frame foreign to the TDX service is not authorized (framing). This rights affect to the presentation summary of the thesis as well as to its contents. In the using or citation of parts of the thesis it's obliged to indicate the name of the author

CONTRIBUTION TO THE ASSESSMENT OF SHELTER-IN-PLACE EFFECTIVENESS AS A COMMUNITY PROTECTION MEASURE IN THE EVENT OF A TOXIC GAS RELEASE

María Isabel Montoya Rodríguez

A dissertation submitted in partial satisfaction of the
requirements for the degree of:

Doctor by the Universitat Politècnica de Catalunya

Supervised by:
Dra. Eulàlia Planas Cuchi

CERTEC – Centre d’Estudis del Risc Tecnològic
Departament d’Enginyeria Química
Escola Tècnica Superior d’ Enginyers Industrials de Barcelona
Universitat Politècnica de Catalunya

Barcelona, September 2010



Chapter 5. Development of an empirical model to estimate single-family dwellings airtightness

Mathematics is the language in which God wrote the universe.
Galileo Galilei

In chapter four, the *ACH* of Catalan dwellings was estimated using the LBNL airtightness model; however, construction techniques, materials and the climatic regions found in the US differ significantly from their equivalents in Catalunya. From available data, air leakage of French dwellings could be the one that better represent Catalan dwellings' situation. Therefore, we used the air leakage database for French single-family dwellings compiled by the Centre d'Études Techniques de L'Équipement (CETE) in Lyon to develop a predictive model for estimating airtightness as a function of dwelling characteristics. Then, the model was used to estimate the airtightness distribution of single-family dwellings in Catalunya using the stochastic simulation, and the results were integrated into the AIM-2 single zone ventilation model (Walker & Wilson, 1998) to predict the *ACH* distribution by season and census tracts for average and extreme meteorological conditions. Figure 5.1 describes the approach followed in this chapter.

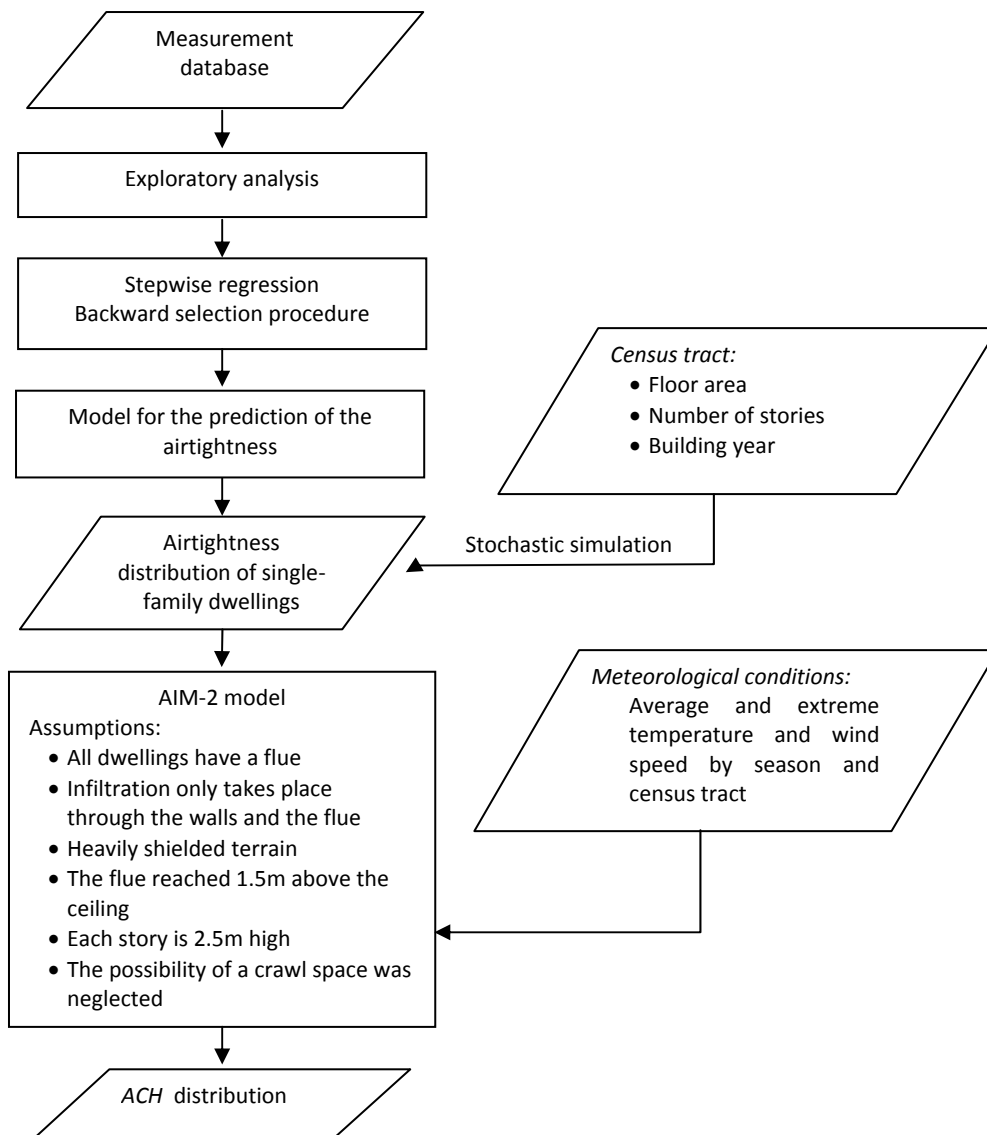
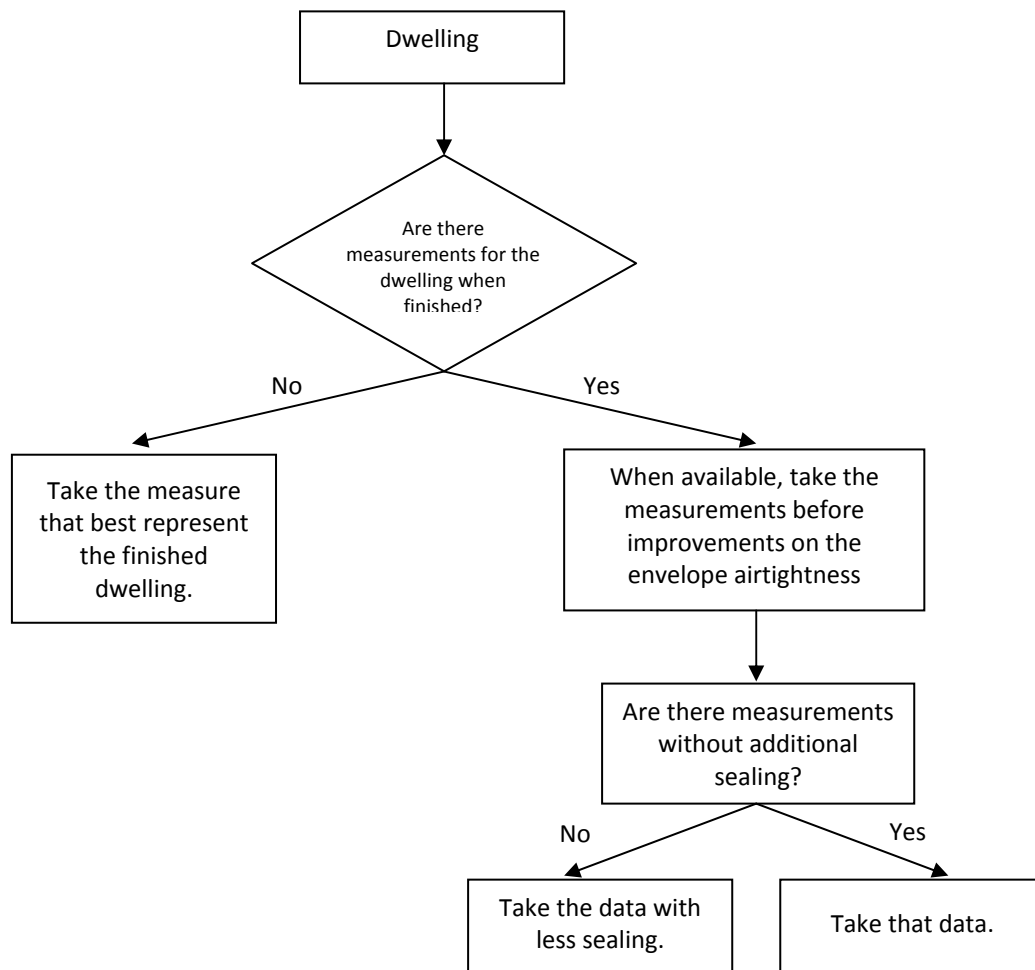


Figure 5.1 Flowchart of the methodology used to estimate the *ACH* distribution in Catalunya

5.1 Database analysis

The CETE de Lyon database contains 483 single-family dwelling pressurization measurements made in a series of studies from 1983 onwards using the pressurization method (see section 2.4.1). The measurements were used to characterize the general envelope airtightness of residential buildings throughout France by identifying the most important leakage paths and possible trends linked to specific structures or materials. Some dwellings were repeated in the

database (i.e. from tests carried out before and after improvements, before and after construction was completed, additional sealing, etc.), so the data was reviewed according to the flow diagram of Figure 5.2 and only the measurement that most accurately reflected the envelope airtightness of each dwelling was used. Two hundred and fifty-one measurements were selected for the analysis after this revision.



In the case of several repetitions under the same conditions, take the mean.

Figure 5.2 Data selection flow diagram

The database contains several fields for each measurement, which describe the characteristics of the dwelling, the exact nature of the test, and the results obtained, as shown in Table 5.1. Concerning the results field, the constants c and N of the power law leakage function are

reported, as well as three airtightness indicators: the air exchange rate at 10 Pa (ACH_{10}), at 50 Pa (ACH_{50}) and the leakage index at 4 Pa (I_4).

Table 5.1 CETE de Lyon database information

Test features	Date of test
	Number of test
	Method used (pressurization, depressurization)
	Specific features of test (state of openings)
Dwelling characteristics	Building material
	Construction type
	Heating system
	Heated volume
	Envelope unheated surface area
	Location
	Insulation type
	Year of construction
Results	Floor area
	c
	N
	ACH at 10 Pa (ACH_{10})
	ACH at 50 Pa (ACH_{50})
	Leakage index at 4 Pa (I_4)

With regards to the dwelling characteristics, some of them refer to the structure and construction of the building while others, like the heating system, refer more to the house adaptation. Among the building materials found in the database there were wood, steel, concrete, mixture steel concrete, mixture wood concrete, fired clay, monomur and cellular concrete. The construction type refers to the structure, which could be structural wall or frame structure. The insulation field covers three types of insulation: exterior insulation, interior insulation and integrated insulation. For the heating system, five types were identified in the database: electric, gas, heating pump, fuel oil and other, predominating the electric heating. Concerning the floor area, recorded values were in the range of 35-255 m², with most of the values (85%) between 70 and 135 m². The number of stories of the dwellings ranged between 1 and 3, but only 2.7% had 3 stories. The year of construction of the dwelling was also recorded in the database, as well as the year in which measurements were taken. However, although there are many fields of information, a lot of data is missed, particularly for older measurements.

The mean, the variance, the standard deviation and the quartiles for I_4 , ACH_{50} , ACH_{10} , c and N are presented in Table 5.2. If we compare these values with the reference value of the CETE to

assess the permeability from a point of view of energy efficiency ($I_4 < 0.8$) (see Table 2.13), it can be said that around 50% of the dwellings have a good airtightness.

Since N had a small range of variability and more than 90% of the values lied in the range 0.58 - 0.7 (see Figure 5.3), the value of N was fixed at $2/3$, which is the typical value for a residential building, as mentioned in Chapter 2. However, to reduce the implicit error done when assuming a constant N , a new parameter called c' was defined. This parameter captures the effect of c and N on the calculation of the airflow for a given pressure difference. As expressed in Eq. 5.1, the value of c' is the value of c that, when applied with an N of $2/3$ and at a given pressure difference, would produce the same airflow as the real c and N values. The reference pressure difference (ΔP_r) under typical meteorological conditions in the US and southern Europe is 4 Pa (ASHRAE, 2005; Carrié *et al.*, 2006). Thus, c' was defined at a reference pressure difference of 4 Pa (Eq. 5.2).

$$Q = c \cdot (\Delta P_r)^N = c' (\Delta P_r)^{2/3} \quad \text{Eq. 5.1}$$

$$c' = c \cdot (4)^{N-2/3} \quad \text{Eq. 5.2}$$

Table 5.2 Quartiles and descriptive statistics for the database airtightness indicators

	I_4	ACH_{10}	ACH_{50}	c	N	c'
Mean	0.813	1.082	3.035	0.0173	0.648	0.0165
GM	0.686	0.952	2.700	0.0140	0.645	0.0136
Q₂₅	0.475	0.668	1.942	0.0092	0.610	0.0091
Q₅₀	0.669	0.980	2.702	0.0133	0.650	0.0130
Q₇₅	1.015	1.349	3.729	0.0224	0.690	0.0211
Q₉₀	1.386	1.883	5.108	0.0344	0.790	0.0321
Data used	221	251	251	251	251	251

As shown in Figure 5.4, values of c and c' fit a log-normal distribution and show similar behaviours, which was expected because most values of N lay around the fixed value of $2/3$.

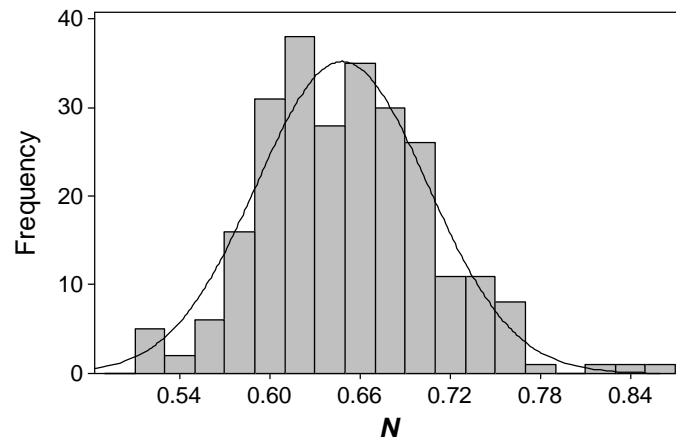


Figure 5.3 Frequency histogram and normal distribution of N

The adjustment to a log-normal distribution was confirmed through the Anderson-Darling test (0.383 and 0.361 respectively), for which P-values above 0.05 were obtained. Therefore, in the subsequent analysis the natural logarithm of c' ($\ln(c')$) is used, instead of c' itself, since the analysis of variance and the regression analysis assumed that the data is normally distributed.

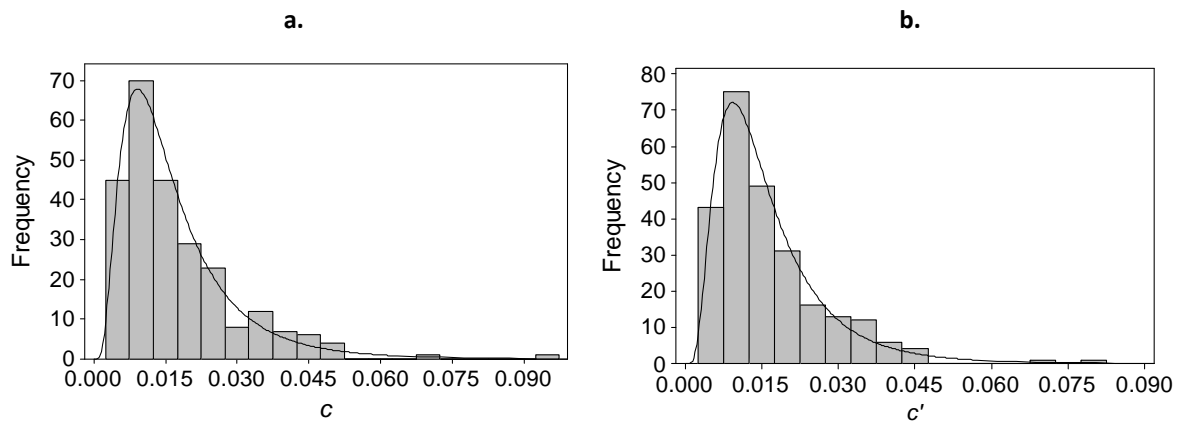


Figure 5.4 Histograms and Log-normal distributions. a) c values, b) c' values.

5.1.1 Exploratory analysis

In order to identify any significant relation between building characteristics and $\ln(c')$, an exploratory analysis was conducted. For categorical variables a boxplot diagram and an analysis of variance (ANOVA) were made, while for quantitative variables, a scatter plot and a regression were accomplished. The significance of each variable was assessed according to the

P -value of the F -test, applying a significance level of 5%. P -values higher than 0.05 denote no significant difference between the means of the variable analyzed, while lower P -values denotes higher significant difference and therefore, a possible relation between the $\ln(c')$ and the variable. Variables analyzed comprise dwelling's characteristics available in the dataset (see Table 5.1), described as follows.

Structure type (ST)

In the database there are information available concerning the building material (wood, steel, concrete, mixture steel concrete, mixture wood concrete, fired clay, monomur and cellular concrete), and the construction type (structural wall or frame structure). An initial analysis of this two variables show that dwellings built with wood and steel were the leakiest, which in addition always have a frame structure. This type of construction in wood or steel is considered a light construction; which is generally accepted to be leakier than those with a heavy structure (Litvak *et al.*, 2000a). Heavy-structured dwellings are those built with other materials such as concrete, cellular concrete, fired clay, masonry and/or within a structural wall. Therefore, a classification was made grouping both, the construction material and the construction type in light or heavy-structures. A light structure was assigned when the construction material was wood or steel, and the construction type was a frame structure, in the others cases a heavy structure was assigned. For this variable, 72.1% of the data presented a heavy structure, 21.5% a light structure and 6.4% lacked of information. The prevalence of a heavy structure in this case, also reflects a general trend in single-family dwelling construction stock in France.

Figure 5.5 shows the box plot for this variable, where an important difference between the means for light and heavy structures can be observed. Values for dwellings with a light structure are higher, confirming the fact that light structures are leakier than heavy structures. Also, from the width of the boxes the proportion of the sample size that belongs to each structure can be seen, being the heavy structure the one with the largest representation (72.1%), as mentioned above. From the ANOVA test (Annex D), a statistical difference between the means was also found (Table 5.3).

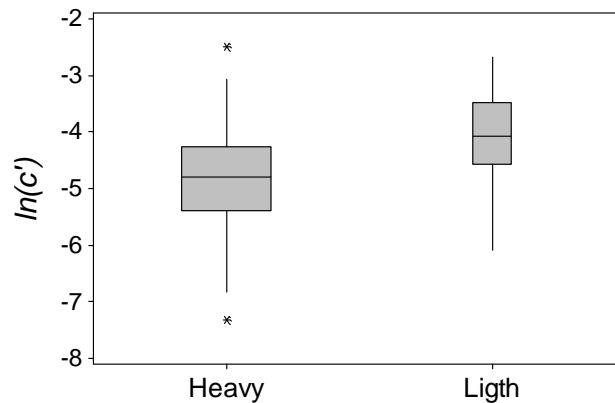


Figure 5.5 Box plot for the structure type (width of the box proportional to the sample size)

Insulation (IT)

In the database three types of insulation can be identified: exterior insulation (4.4%), interior insulation (34.3%) and integrated insulation (17.6%). No data were available for 43.7% of the dwellings. The mean for interior insulation was the smallest, which shows that dwellings with this type of insulation are more airtight (Figure 5.6). The highest mean was recorded for exterior insulation, which supports the fact that dwellings with this type of insulation tend to be leakier than others. However, it should be noted that only 4.4% of the dwellings had exterior insulation, and in addition they are all more than one story dwellings, therefore the lack of representation of the exterior insulation could have influenced this result.

Statistically, the hypothesis of different means should not be rejected outright, but the statistical significance of this variable in the ANOVA test was lower than that of the other variables (Table 5.3).

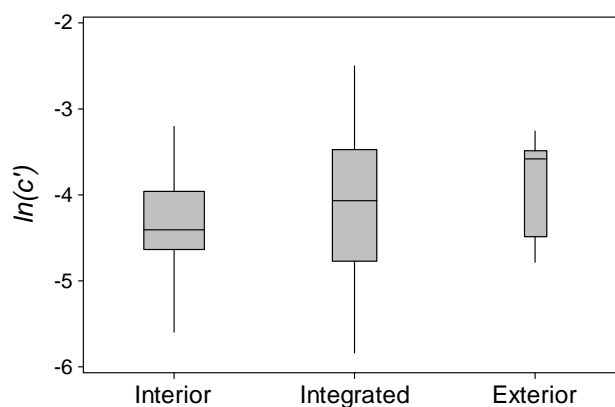


Figure 5.6 Box plot for the insulation type (width of the box proportional to the sample size)

Heating system (HS)

The heating system variable refers to the nature of the heating source. Five types of heating systems were identified in the database: electric (25.5%), gas (18%), heating pump (0.4%), fuel oil (2.4%) and other (5.1%). No data were available for 48.6% of the cases. Since few dwellings had heating pump, fuel oil, gas and other heating systems, we considered only two options for this variable: electric heating, or non-electric heating. This selection was also made taking into account that French dwellings with electric heating are under a more exigent regulation, then, they were expected to be more airtight. From Figure 5.7, a difference between the means can be seen, being the dwellings with non-electric heating systems less airtight than electric ones. However, this difference is not confirmed by the results of the ANOVA test, where a P -value higher than 0.05 was obtained (Table 5.3).

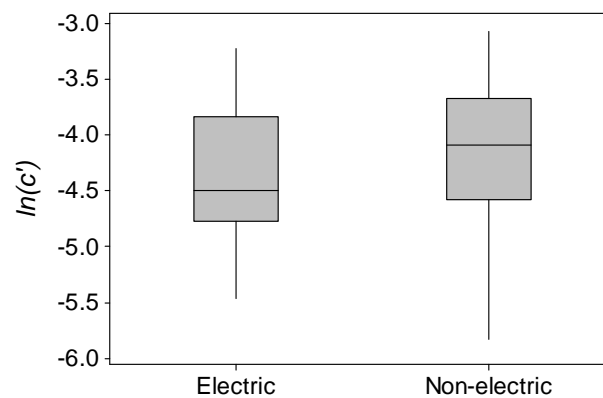


Figure 5.7 Box plot for the heating system (width of the box proportional to the sample size)

Age

The age variable is the age of the dwelling at the time of testing. The year in which measurements were taken is recorded in the database for all the dwellings, while the year of construction is only available for 88.4% of the cases. Consequently, the building age at testing could not be obtained for 11.6% of the dwellings. In addition, the oldest measurement in the database is from 1983, and the oldest year of construction is also 1983. This is due to the fact that most of the measurements made belong to projects concerning the study of energy efficiency of residences, and therefore they were interested on the performance of the new constructions. From Figure 5.8, a trend for the means can be seen in which the airtightness decreases with the age of the dwellings, with an exception for age 3. This difference was also confirmed to be statistically significant from the results of the ANOVA test (Table 5.3). The

oldest building age is 9 years, so this value constitutes the limiting age for the model development.

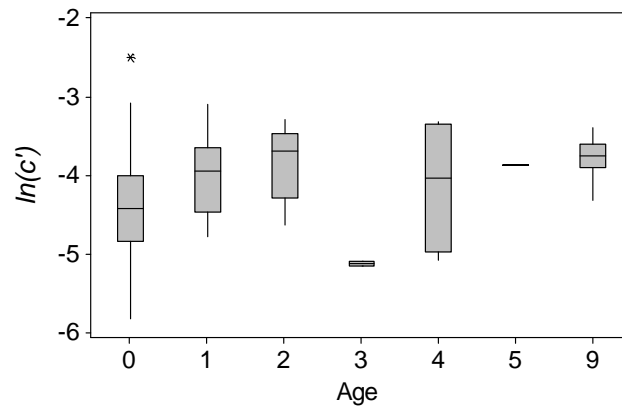


Figure 5.8 Box plot for the Age variable

Floor area (Area)

Initially there were very few entrances for the floor area in the database, thereby, the available reports at the CETE de Lyon were reviewed and the floor area was taken from them when reported, if not (22.3% of the data), it was estimated as the quotient between the heated volume and the standard height of one story 2.5 m. The value of $\ln(c')$ followed a clear trend and increased in direct proportion to the floor area of the dwelling, as presented in Figure 5.9. This trend was expected, since larger floor areas increase the surface area through which infiltration takes place. The floor area data range from 35.2 to 255 m², with most of the data (85%) located between 70 and 135 m², and a mean of 96 m².

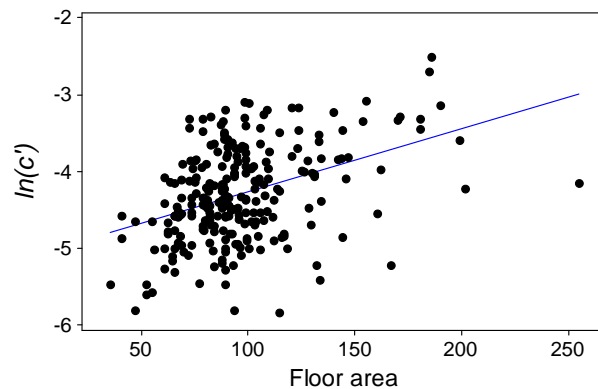


Figure 5.9 Scatter plot for the floor area

Number of stories (NS)

In the database, neither the number of stories nor the height was reported. Nevertheless, as it could be an important variable influencing the airtightness, especially the fact that the dwelling have one or more stories, due to the probable leakage path in the junction of the ceiling/floor and the external wall that increase the leakage as mentioned by Kalamees (2007), the reports available were reviewed and the number of stories was extracted from them. In total, 92.4% of the entrances were filled with this variable. As there were very few measures with three stories (2.7%), and no significant difference was found between the means of these dwellings and those with two stories, only the fact of having one or more than one stories was analyzed.

From Figure 5.10, a big difference can be seen between the means of the two groups, being leakier the dwellings with more than one story. From the ANOVA test (Table 5.3), the statistical significance of this variable was born out, showing the existence of a strong relation between these variables.

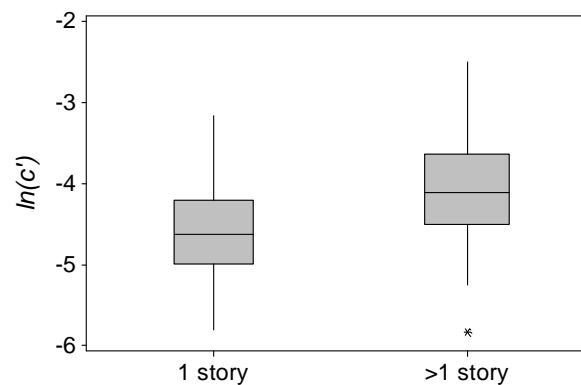


Figure 5.10 Box plot for the number of stories (width of the box proportional to the sample size)

Climate zone (CZ)

The climate zone where the measurements came from might have some influence on the airtightness of the dwellings, as in the case of the LBNL airtightness model. One may expect that tighter dwellings are located in regions with more severe climatic conditions, while more leaky dwellings would be found in moderate climatic conditions. However, this statement is also subjected to the fact that airtightness should be more influenced by constructions techniques prevailing in the zone, than by the climatic conditions themselves. Nevertheless, it

could be an interesting variable to analyze, since it can also capture other features of construction practices that are not included within the construction variables.

The climatic zones were assigned according to those defined in the French Thermal Regulation (RT, 2000), with reference to the sun exposure conditions: H1, H2 and H3, as shown in Figure 5.11. To assign the climatic zone to each measurement the post code reported in the address was used. Final distribution by climatic zone shows that 50% of the data came from zone H1, 45% from zone H2 and 5% from zone H3, this proportion is represented by the width of the boxes of Figure 5.12. It should be noted that this distribution fairly correspond to the distribution of the territory.

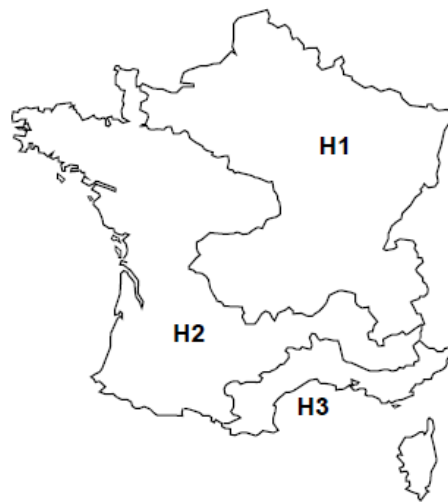


Figure 5.11 Climatic zones in France according to the RT2000

For this classification of climatic zones, a difference between the means of the airtightness for each zone is observed (Figure 5.12). This difference was confirmed through the ANOVA test, where a statistical significance was attributed to this variable (Table 5.3). More airtight constructions are located in the H2 zone, while dwellings in the H1 and H3 zones are leakier.

Concerning the relation between the structure type and the climatic zone, Figure 5.13 shows the box-plot for the structure type by climatic zone, where the width of the boxes represent the proportion to the sample size.

From this figure we can see that zones H1 and H2 have dwellings with the two structures types, being more uniform the distribution in zone H1, while zone H3 only presents heavy structures. Looking at the difference between heavy and light structures in zones H1 and H2,

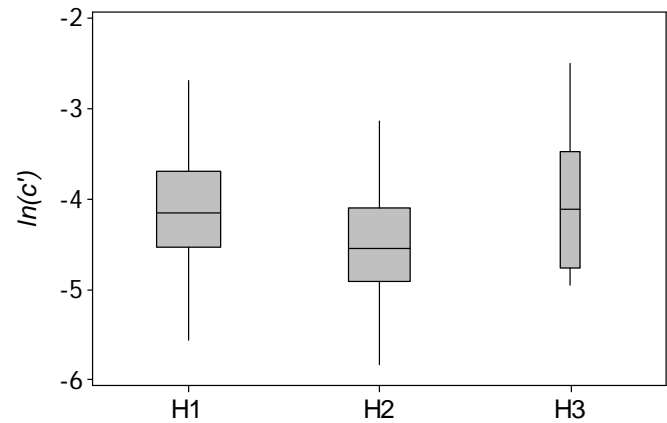


Figure 5.12 Box plot for the climatic zone (width of the box proportional to the sample size)

we can see a clear difference between the means as in the case of the structure type variable (Figure 5.5). Comparing heavy structures among zones, those of zone H2 are tighter than those of zone H1, while those of zone H3 are the leakiest. According to this, we can say that the tightest of zone H2 (Figure 5.12) may be influenced by the larger proportion of heavy structures in this zone. However, an ANOVA (see Annex D) conducted only over heavy structures shows that there is a significant difference between the means for the three climatic zones.

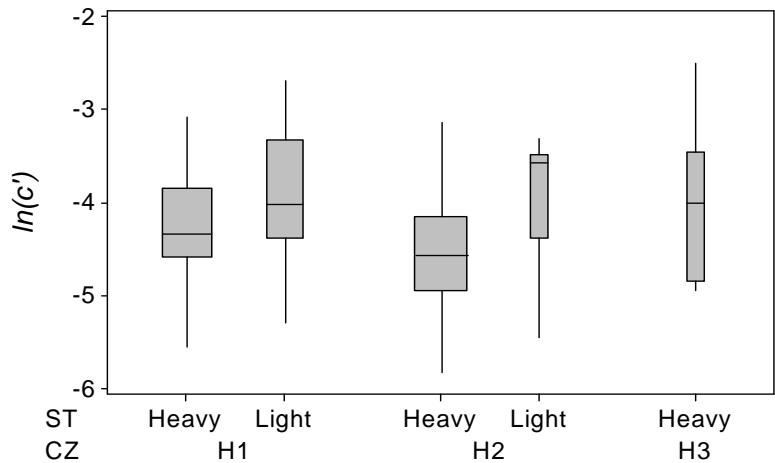


Figure 5.13 Box plot for the structure type by climatic zone (width of the box proportional to the sample size)

Table 5.3 summarizes the main results of the ANOVA test conducted to identify significant relations between building characteristics and $\ln(c')$. Complete results of ANOVA test for each variable can be found in Annex D. The significance of each variable was assessed according to

the P -value of the F -test, as described before. From these results, most significant variables ($P < 0.05$) are, in order of significance, the NS , the ST , the CZ , the $Area$, the Age and the IT , while no statistical significance was observed for HS . Regarding the proportion of data used most of the variables account with almost 90% of the data, while the heating system and the insulation variables lack more than 40% of the data. A prevalence of a heavy structure and an interior insulation was also observed.

Table 5.3 Main results of the ANOVA test

Building feature	Variable	% data used	Mean $\ln(C')$	F	P-value
<i>NS</i>	1 story	43.4	-4.588	46.63	0.000
	>1 story	49.0	-4.070		
	Missed	7.60			
<i>ST</i>	Heavy	72.1	-4.401	27.45	0.000
	Light	21.5	-3.926		
	Missed	6.40			
<i>IT</i>	Exterior	4.40	-3.903	3.470	0.034
	Interior	34.3	-4.364		
	Integrated	17.5	-4.159		
	Missed	43.8			
<i>HS</i>	Electric	25.5	-4.368	3.670	0.058
	Non electric	25.9	-4.162		
	Missed	48.6			
<i>CZ</i>	H1	50.0	-4.141	11.60	0.000
	H2	45.0	-4.491		
	H3	5.00	-4.045		
	Missed	0.00			
<i>Area</i>	36 – 255 m	100		4.860	0.000
	Missed	0.00			
<i>Age</i>	0 – 9 years	88.5		3.650	0.002
	Missed	11.5			

5.2 Model development

To develop a predictive model (multiple linear model), we applied the stepwise regression technique using the backward selection procedure (Draper & Smith, 1998) with the building variables. This procedure consists of carrying out an initial regression with all the variables, and then, starts to eliminate from the model the variables with coefficients of low significance one

by one. Each time a variable was taken out; the resulting adjusted R-square and the significance of the variables regression coefficient (P -value) were observed. According to the results, we decided whether the variable should be kept. If the adjusted R-square increased or remained at approximately the same value, the variable was discarded, but if it decreased significantly, the variable was kept. We also have into account the percentage of data used for the regression, with the aim of obtaining the best correlation coefficient with the highest proportion of data.

The initial model proposed (Eq. 5.3) includes all the building characteristics defined in last section. In the model, the parameters β_{H1} , β_{H2} , β_{area} , β_{ST} , β_{Age} , β_{NS} , β_{IT} and β_{HS} represent the coefficients for climatic zone H1, climatic zone H2, floor area, structure type, building age, number of stories, insulation type and heating system, respectively. Climatic zone $H3$ is not explicitly expressed in the model, since it is linearly correlated with climatic zones H1 and H2, therefore, its effect is included within the independent term α . H1, H2, ST, IT and HS are the indicators that we considered for categorical variables, they take values of 0 or 1 depending on the condition of the variable. For climatic zones indicators H1 and H2, a value of 1 is assigned to the zone where the dwellings is located and a value of 0 for the other zone, if the dwelling is located in zone H3, a 0 is assigned to indicators H1 and H2. The ST indicator takes a value of 0 for heavy structures and 1 for light structures. In the case of the IT indicator, it takes a value of 0 for interior or integrated insulation and 1 for exterior insulation. Possible values for the HS indicator represent electric heating, $HS = 0$, and non-electric heating, $HS = 1$. The heating system was also analyzed because, although its P -value was not significant from the ANOVA test, it was very close to the significance threshold level (0.05). Concerning the number of stories, NS, we must remember that in the exploratory analysis only two possibilities were considered: dwellings with one or more than one story, since there was no significant difference between dwellings with 2 or 3 stories and also, due to the lack of representation of 3 storied houses. Thereby, the NS variable takes a value of 1 for single-story dwellings and 2 for those with more than one story.

$$\begin{aligned} \ln(c') = & \alpha + \beta_{H1} \cdot H1 + \beta_{H2} \cdot H2 + \beta_{area} \cdot Area + \beta_{ST} \cdot ST + \beta_{Age} \cdot Age + \\ & \beta_{NS} \cdot NS + \beta_{IT} \cdot IT + \beta_{HS} \cdot HS \end{aligned} \quad \text{Eq. 5.3}$$

Results of this first regression (see Table 5.4) show an adjusted R^2 of 34.9%; this means that the model can explain the 34.9% of the variability of the data. With regards to the statistical

significance of the coefficients, we found no significance for the climatic zones and the *NS* variables, which do not agree with the results of the exploratory analysis. This may be due to the fact that only 33.5% of the data was used in this regression, since the other entries of the database lack of information concerning one or more variables. Therefore a second regression (Eq. 5.4) was proposed eliminating the *HS* variable, which is one with a low representation in the database (51.4%), and for which no significance was found from the exploratory analysis.

$$Ln(c') = \alpha + \beta_{H1} \cdot H1 + \beta_{H2} \cdot H2 + \beta_{area} \cdot Area + \beta_{ST} \cdot ST + \beta_{Age} \cdot Age + \beta_{NS} \cdot NS + \beta_{IT} \cdot IT \quad \text{Eq. 5.4}$$

In this second regression (see Table 5.4) the adjusted R^2 increased to 40%, but the percentage of data used only increase to 46.6% which is still a low proportion of the data available, and might cause a bias in the data analyzed. This situation can also lead to the low significance of the coefficients for the climatic zones and the *NS* variables. Thereby a third regression was proposed (Eq. 5.5) where the *IT* variable was eliminated.

$$Ln(c') = \alpha + \beta_{H1} \cdot H1 + \beta_{H2} \cdot H2 + \beta_{area} \cdot Area + \beta_{ST} \cdot ST + \beta_{Age} \cdot Age + \beta_{NS} \cdot NS \quad \text{Eq. 5.5}$$

With the elimination of the *IT* variable, the proportion of data used in regression 3 greatly increases (80.1%), as well as the significance of the *NS* and *ST* coefficients (Table 5.4), as was expected since from the exploratory analysis these variables were found to have a strong influence on the $Ln(c')$. By contrast, although the P-value of the climatic zones coefficients improve, they are still larger than 0.05 to consider these variables significant. With regards to the correlation coefficient, we can say that even if the data increased by almost the double, the adjusted R^2 stayed around the same value (38.4%). For the next regression (Eq. 5.6), the climatic zones variables were eliminated since they were the ones that lack of significance in regression 3.

$$Ln(c') = \alpha + \beta_{area} \cdot Area + \beta_{ST} \cdot ST + \beta_{Age} \cdot Age + \beta_{NS} \cdot NS \quad \text{Eq. 5.6}$$

The proportion of data used in regression 4 was the same of regression 3 (80.1%), since climatic zone was a variable available for all the entries. In relation to the variables' coefficients, all were found to have a statistical significance (P-value<0.05) while the adjusted R^2 remains almost the same (37.5%). Looking at the coefficients' standard errors for all the

Table 5.4 Coefficients and adjusted R-squares for each regression (see Annex D)

Coefficients	Regression 1		Regression 2		Regression 3		Regression 4	
	Eq. 5.3	P-value	Eq. 5.4	P-value	Eq. 5.5	P-value	Eq. 5.6	P-value
α	- 5.5438 ± 0.4060	0.000	- 5.5078 ± 0.3118	0.000	- 5.4049 ± 0.2304	0.000	- 5.6815 ± 0.1463	0.000
H1	0.1076 ± 0.3220	0.739	- 0.1411 ± 0.2073	0.497	- 0.1388 ± 0.1725	0.422		
H2	0.0488 ± 0.3293	0.883	- 0.2538 ± 0.2133	0.237	- 0.2861 ± 0.1698	0.094		
β_{area}	0.00641 ± 0.0020	0.002	0.01020 ± 0.0017	0.000	0.00709 ± 0.0012	0.000	0.00698 ± 0.0012	0.000
β_{ST}	0.3107 ± 0.1359	0.025	0.3239 ± 0.1231	0.010	0.4798 ± 0.0893	0.000	0.5075 ± 0.0858	0.000
β_{NS}	0.1240 ± 0.1305	0.345	0.1764 ± 0.1107	0.114	0.2931 ± 0.0777	0.000	0.34504 ± 0.0737	0.000
β_{Age}	0.08807 ± 0.0238	0.000	0.07039 ± 0.0221	0.002	0.06987 ± 0.0200	0.001	0.0784 ± 0.0192	0.000
β_{T}	0.5832 ± 0.2174	0.009	0.4288 ± 0.2115	0.045				
β_{HS}	0.4105 ± 0.1279	0.002						
Adj- R ² (%)	34.9%		40.0%		38.4%		37.5%	
Data used	33.5%		46.6%		80.1%		80.1%	

regressions, we can see that they decreased from regression 1 to regression 4, being the last the one with the lowest standard errors. This might be due to the proportion of data used, being regression 3 and 4 the ones with more data, which generate a more accurate illustration of the influence of the variables. Therefore, of the models proposed, the linear combination of Eq. 5.6 appeared to be the best statistical approximation for estimating the $\text{Ln}(c')$.

Figure 5.14.a shows the dispersion plot of predicted and observed values for the $\text{Ln}(c')$. The range of the predicted values varied between -5 and -3, while the range of the observed values lied between -6 and -3.5; it is, a narrower range for the predicted values was obtained. From the residuals plot (Figure 5.14.b), an homogeneous distribution could be seen, with a mean of 0 and a standard deviation of 0.49, it could also be seen that most of the residuals lied between -1 and 1.

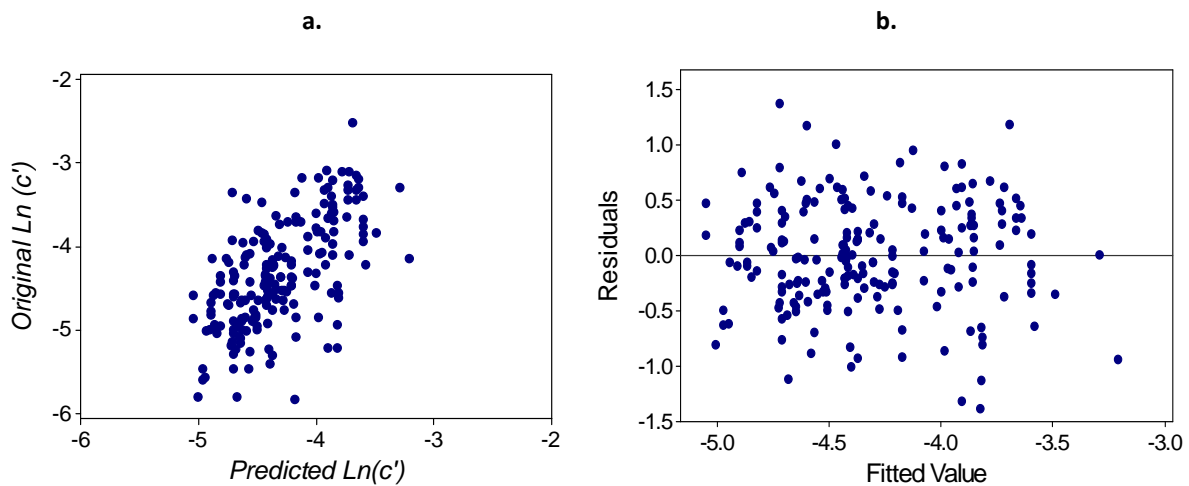


Figure 5.14 a) Predicted vs observed values of $\text{Ln}(c')$, b) Model residuals

Original and predicted distributions of c' are shown in Figure 5.15. Predicted values vary in the range of 0.006 to 0.043, with most of the data staying between 0.005 and 0.015 as in the original data, however the data does not fit a log-normal distribution. Figure 5.16 presents the observed and predicted cumulative distributions, which are very similar. Since there is no experimental data available to assess the accuracy of the model prediction, we decided to evaluate if there was any statistical difference between the distribution of predicted c' and original data distribution. To accomplish this, the Kruskal-Wallis test was used, which is a non parametric method for the analysis of variance (Montgomery & Runger, 2007). Result of this test with a P -value of 0.68 (see Annex D), higher than 0.05, reject the hypothesis of any significant difference between the medians of the distributions with a 95% confidence. The

geometric mean, the arithmetic mean and the median of the predicted values of c' are 0.0133, 0.0144, 0.0122; these values are very similar to those of the original data (Table 5.2), showing errors of 2.3%, 12.7% and 3.6% respectively; which are lower than those obtained for individual predictions, and therefore the model should be better used for the estimation of airtightness population distributions.

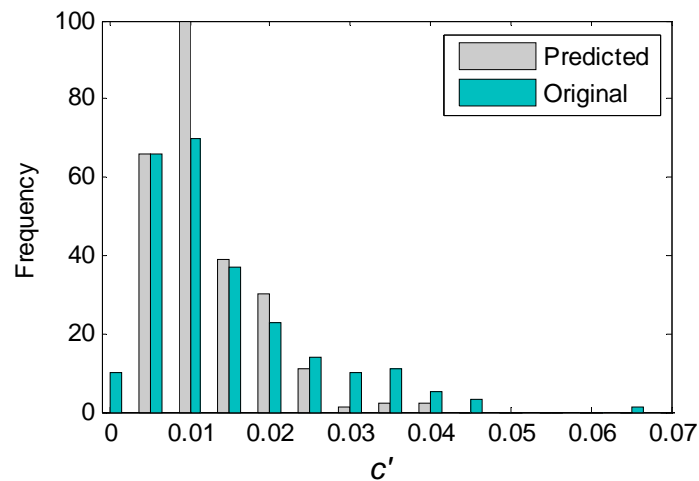


Figure 5.15 Distribution of the original and predicted values of c'

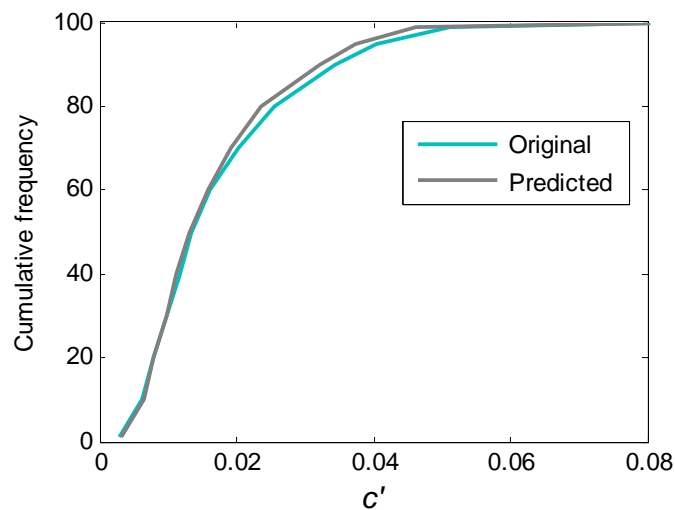


Figure 5.16 Cumulative frequency of the original and predicted values of c'

5.2.1 Adjustment of the Age coefficient

As mentioned before, maximum building age to which the model can be applied is 9 years. However, most of the current building stock of single-family dwellings in Catalunya is older

than 9 years (Figure 4.1). Therefore, we adapted the model (Eq. 5.6) for houses older than 9 years by incorporating a new term. The European Standard EN-13465 2004 gives ACH_{50} values for single-family dwellings as a function of a range of construction years (< 1940, 1941 - 1960, 1961 - 1975, 1976 - 1988, > 1989) and construction types (airtight, average and leaky), so, with this information we can capture the effect of age on ACH_{50} . The underlying assumption behind this statement is that the difference in airtightness depending on construction year, is more due to the aging process than to the construction techniques used in that period. Although the change in the ACH_{50} is also known to be affected by more factors than the aging process only, as it is assumed here, this is the best approximation that could be made with available data. This clearly points out the work needed in this field. The behaviour of ACH_{50} with age was determined by performing a linear regression between the ACH_{50} , the construction type (CT) and the building age, as shown in Eq. 5.7. The age was estimated as the period from the year in which the standard was introduced (taken to be the tested year, 2004) and the year of construction (taken as the mean of the range of years for which ACH_{50} was reported). β'_{age} and β'_{CT} , are the coefficients for the age and construction technique variables respectively, and α' is the independent term. The CT parameter represents the construction technique variable, which is defined as airtight ($CT = 1$), average ($CT = 2$) or leaky ($CT = 3$).

$$ACH_{50} = \alpha' + \beta'_{age} \cdot Age + \beta'_{CT} \cdot CT \quad \text{Eq. 5.7}$$

Table 5.5 shows the regression results of Eq. 5.7, which exhibits a high correlation. The model explained 94% of the data variability, and all coefficients were found to have a high level of significance. The value for the age coefficient means that the change in ACH_{50} , due to the aging process, per year is $6.33 \cdot 10^{-5} \text{ s}^{-1}$ (0.228 h^{-1}).

Table 5.5 Coefficients and adjusted R-squared for regression of Eq. 5.7.

Coefficients	Eq. 5.7	P-value
α'	$-0.00239 \pm 3.59 \cdot 10^{-4}$	0.000
β'_{Age}	$6.33 \cdot 10^{-5} \pm 5.76 \cdot 10^{-6}$	0.000
β'_{CT}	$0.00131 \pm 1.31 \cdot 10^{-4}$	0.000
Adj- R^2	94%	
Data used	15	

In addition, the earliest year reported in the EN-13465 is 1940, thus we assumed that the aging process had no further effect on airtightness for buildings more than 64 years old. Therefore, the variation of ACH_{50} between specific ages can be expressed as follows:

$$\Delta ACH_{50} = \beta'_{age} \cdot (Age_1 - Age_2), \quad Age_2 < Age_1 \leq 64 \quad \text{Eq. 5.8}$$

From Eq. 2.40 and Eq. 2.41, the change in $ACH_{\Delta P}$ can be expressed in terms of Δc , as shown in the following expression:

$$\Delta ACH_{\Delta P} = \frac{\Delta c \cdot \Delta P^N}{V} \quad \text{Eq. 5.9}$$

If we combine Eq. 5.8 and Eq. 5.9, and assume that the volume can be estimated as the product of the floor area (Area) and the standard height of one story (2.5 m), the change in c' (which implies $N = 2/3$) due to the aging process can be determined through the following expression.

$$\Delta c' = \beta'_{age} \cdot (Age_1 - Age_2) \cdot Area \cdot 2.5 / 50^{2/3}, \quad Age_2 < Age_1 \leq 64 \quad \text{Eq. 5.10}$$

To extend the application of the model developed to dwellings more than 9 years old, Eq. 5.10 was combined with the expression for predicting c' (Eq. 5.6), fixing a value of 9 for the variable Age_2 . In this way, we obtained an improved model for estimating the airtightness of dwellings with different ages (hereafter called the UPC-CETE model), as shown in Eq. 5.11 to Eq. 5.13.

For dwellings with $Age \leq 9$:

$$c' = \exp(-5.6815 + 0.00698 \cdot Area + 0.5075 \cdot ST + 0.0784 \cdot Age + 0.345 \cdot NS) \quad \text{Eq. 5.11}$$

For dwellings with $9 < Age \leq 64$:

$$c' = \exp(-5.6815 + 0.00698 \cdot Area + 0.5075 \cdot ST + 0.0784 \cdot 9 + 0.345 \cdot NS) + \left(Area \cdot \frac{2.5}{50^{2/3}} \cdot 6.33 \cdot 10^{-5} \cdot (Age - 9) \right) \quad \text{Eq. 5.12}$$

For dwellings with Age > 64:

$$c' = \exp(-5.6815 + 0.00698 \cdot Area + 0.5075 \cdot ST + 0.0784 \cdot 9 + 0.345 \cdot NS) + \left(Area \cdot \frac{2.5}{50^{2/3}} \cdot 6.33 \cdot 10^{-5} \cdot (64 - 9) \right) \quad \text{Eq. 5.13}$$

5.3 Application of the UPC-CETE model to Catalan dwellings

After the development of the model, this was used to estimate the airtightness of Catalan dwellings, c' , by census tract as done in Chapter 4 for the LBNL airtightness model. Several stochastic simulations were performed for a sample of census tracts with different numbers of dwellings, in order to determine whether the predicted distribution of c' varied within simulations. This was accomplished using the same methodology and criterion explained in section 4.3.2. First, we determined the number of simulations required to obtain a constant cumulative average (Eq. 4.3) for a sample of census tracts with different number of dwellings. The criterion used was that the difference between actual (r) and previous ($r-1$) cumulative average were lower than 1%. Second, we performed an analysis of variance of the predicted distributions for each census tract of the sample.

$$C = \frac{\sum_{r=1}^{N \text{ simulations}} \sum_{i=1}^{N \text{ dwellings}} c_{r,i}}{r \cdot i} \quad \text{Eq. 4.3}$$

Table 5.6 shows the results for the first test, where we observe no relation between the required number of simulations and the number of dwellings of the census tract. We also see that 2 to 14 simulations were needed to fulfill the criterion. In relation to the standard deviation and the 10th, 50th and 90th percentiles determined for each simulation by census tract, little variation was observed for these indicators within simulations (results of these simulations are shown in Annex C).

Table 5.6 Required simulations to obtain a constant cumulative average

Number of dwellings	Section	Number of simulations	Number of dwellings	Section	Number of simulations
10	801509044	7	180	807601002	6
20	801503002	14	200	818707001	5
30	801507015	4	250	812601001	7
40	801507005	6	300	813601005	6
50	801507010	11	400	820002013	3
60	800801001	7	499	4313701001	10
70	801907188	2	599	804201001	7
80	801907067	6	699	4302801001	5
90	810201001	5	792	820505001	4
100	810201001	4	902	823401001	2
120	801502001	14	967	829101001	4
140	800902002	2	1648	802301001	3
160	256101001	3			

Since not all the predicted distributions of c' followed a log-normal distribution, we evaluated the variability between groups by applying the Kruskal-Wallis test, which is a non-parametric method for the analysis of variance in data that do not follow a given probability distribution (Montgomery and Runger, 2007). The results showed P -values higher than 0.05, which reject the hypothesis of any significant difference between the medians of c' distributions with 95% confidence for each of the census tracts analyzed (see Annex C).

To apply the UPC-CETE model, we used the buildings characteristics (area, number of stories and year of construction) obtained from the stochastic simulation develop in section 4.3.2, where data was only simulated for census tracts with more than 10 dwellings, and the number of data simulated was equal to the number of single-family dwellings in the census tract, so we use the same data for the application of the two models. The predicted distribution of c' obtained with the UPC-CETE model for Catalunya is shown in Figure 5.17. Although this distribution looks like a log-normal distribution, the hypothesis of fitting a log-normal behavior was rejected through the Lilliefors' test. If we compare these values with empirical data on the distribution for French houses (Figure 5.4b), we can see that predicted values of c' are higher for Catalan dwellings. This result was expected, since more than 90% of Catalan single-family dwellings are more than 9 years old and therefore leakier.

From c' we can also estimate ELA for each dwelling through Eq. 4.2 assuming a C_D of 1 and $\rho = 1.2 \text{ m}^3/\text{kg}$ (air density at 1 atm and 293.15 K). The ELA distribution obtained is shown in Figure 5.18. $ELAs$ predicted with this model are slightly smaller than those estimated with the LBNL

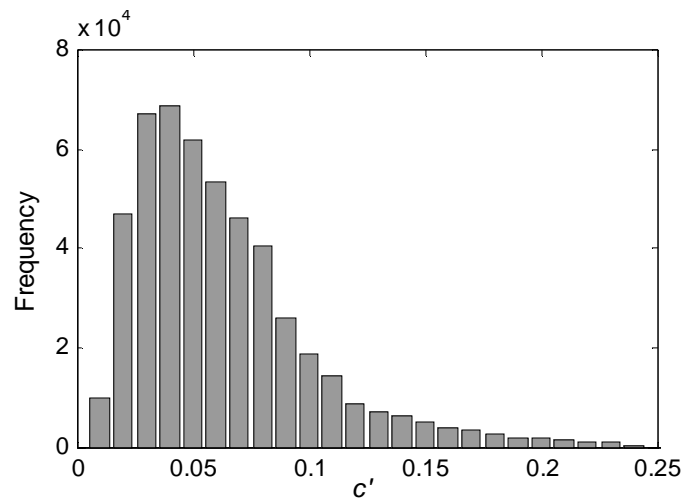


Figure 5.17 Histogram of c' distribution of Catalan dwellings

airtightness model (Figure 4.19), as we expected, since lower ACH had been reported for French dwellings than for US dwellings (Orme *et al.*, 1998), from which the LBNL airtightness model came. Even though, there are no data available for making a direct comparison with dwellings in Catalunya. As mentioned in section 4.3.2, $ELAs$ reported by Chan *et al.* (2005) for US dwellings range from 0.04 m^2 to 0.3 m^2 , therefore as in the case of the LBNL airtightness model, predicted $ELAs$ are closer to the lower value. Under French regulations the value used as reference for energy performance calculations in terms of ELA , is 0.0153 m^2 (as described in section 4.3.1), which is much lower than predicted $ELAs$ with both models, the LBNL airtightness model and the UPC-CETE model.

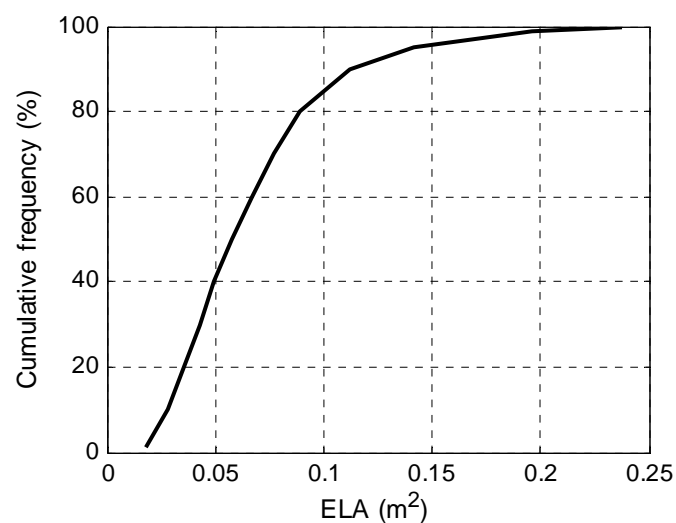


Figure 5.18 ELA cumulative distribution of Catalan single-family dwellings obtained with the UPC-CETE model

To estimate average and extreme *ACH* distribution by seasons, with predicted c' , we used the AIM-2 air infiltration model (see section 2.4.2) as in Chapter 4, where airtightness was estimated through the LBNL airtightness model. We also made the same assumptions as in section 4.3.1 (also shown in Figure 5.1), and used an indoor temperature of 20 °C for winter, spring and autumn, and 25 °C for summer. Figure 5.19 and Figure 5.20 show the geometric mean for each census tract across Catalunya for average and extreme meteorological

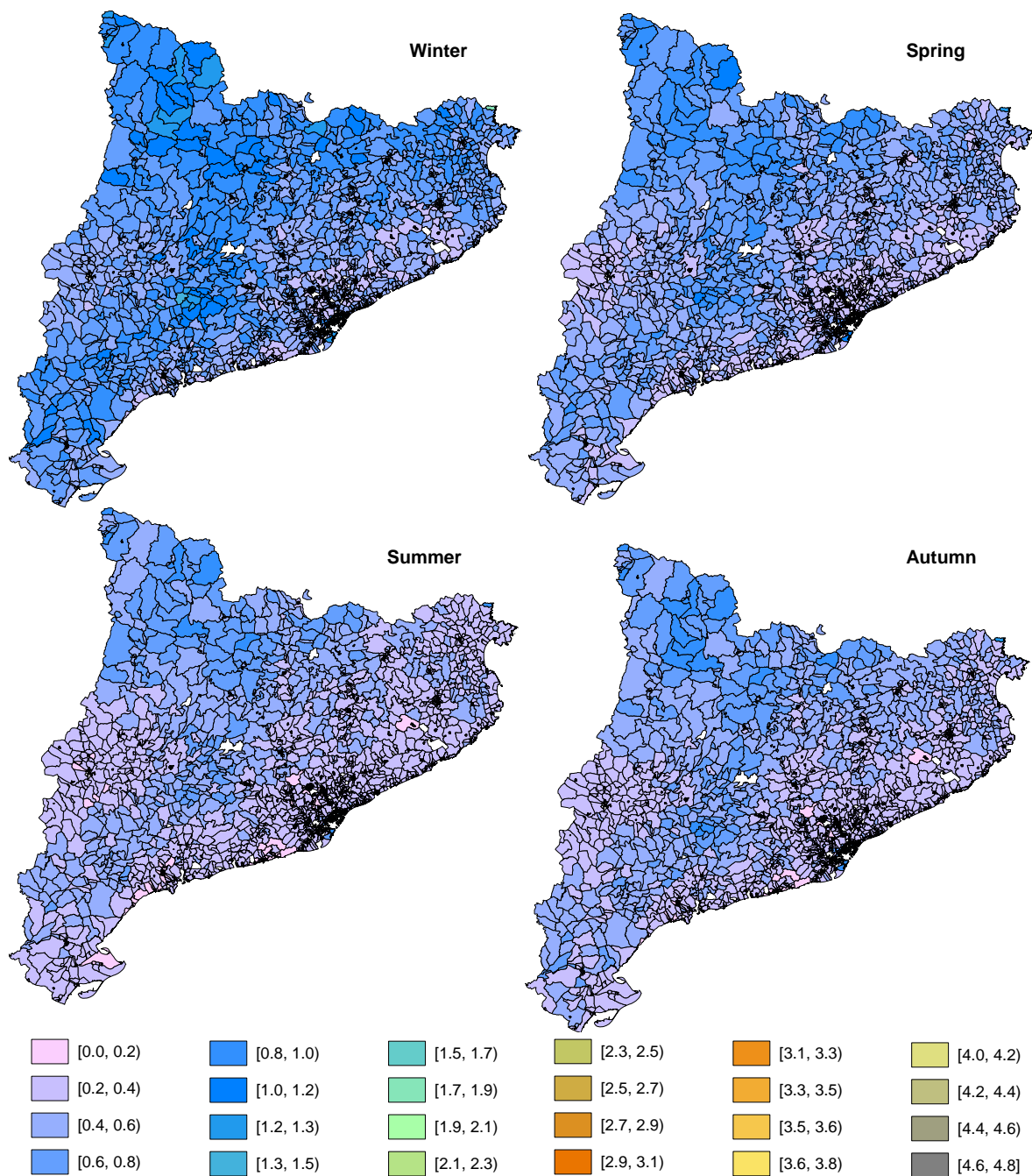


Figure 5.19 Geometric means of the *ACH* for average meteorological conditions by census tract obtained using the stochastic simulation and the UPC-CETE model

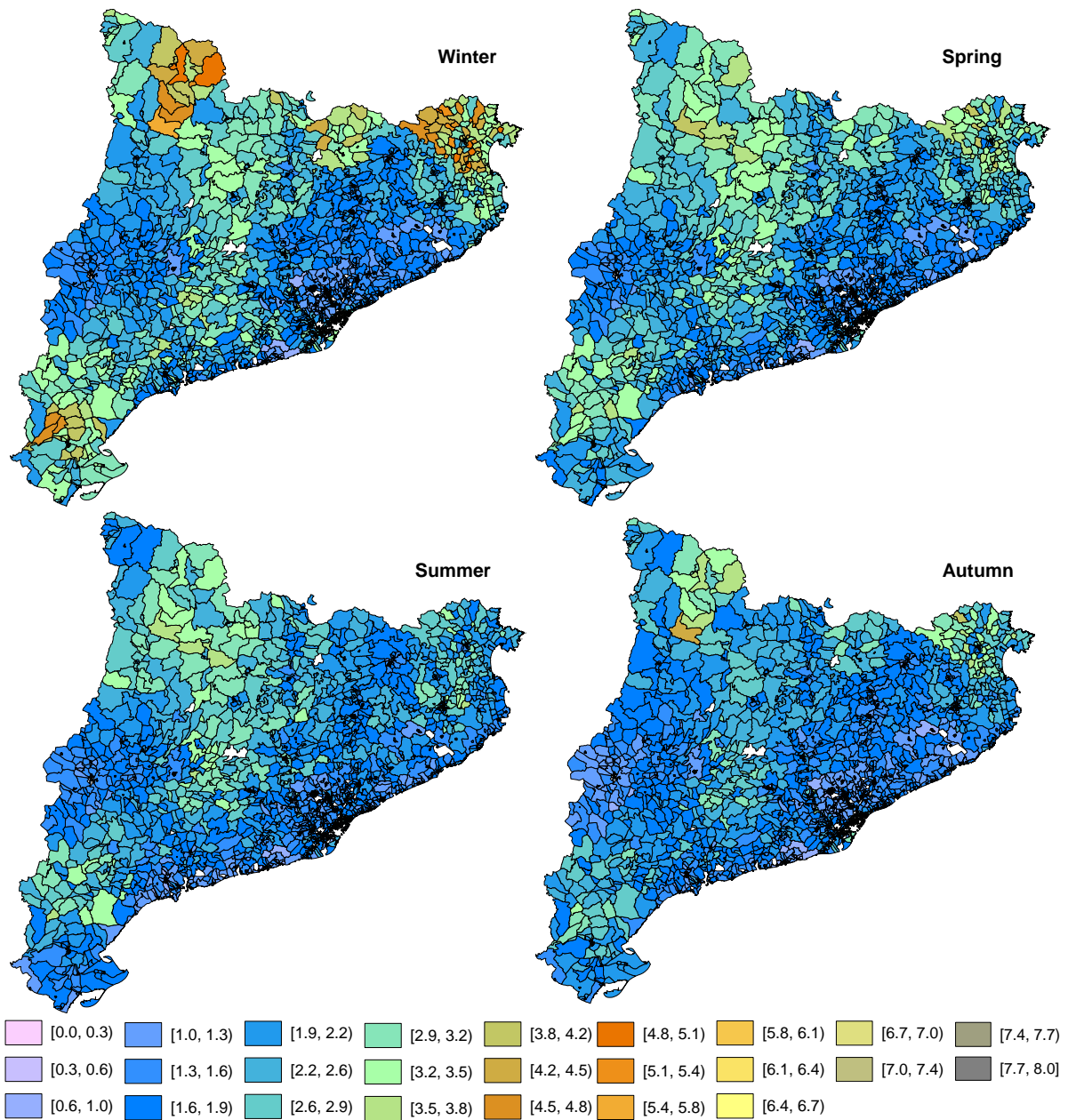


Figure 5.20 Geometric means of the *ACH* for extreme meteorological conditions by census tract obtained using the stochastic simulation and the UPC-CETE model

conditions, respectively. From these figures we can see that mean *ACHs* are lower than 1.5 h^{-1} for average conditions while they are between 0.6 and 4.2 h^{-1} in the case of extreme conditions. In comparison with geometric means obtained with the LBNL airtightness model (Figure 4.20 and Figure 4.21), predicted *ACHs* are lower, increasing the difference in those census tracts located in the dry climatic zone (Figure 4.11), as is logical since the NL_{cz} coefficient for this zone in the LBNL airtightness model is larger than that for the humid zone, leading to higher values of *ACH*.

The results for average and extreme ACH cumulative distributions within seasons are shown in Figure 5.21 and Figure 5.22, respectively. Highest ACH s belong to winter due to severe meteorological conditions during this season, while lowest values were recorded in summer for average meteorological conditions, and in autumn for extreme average meteorological conditions.

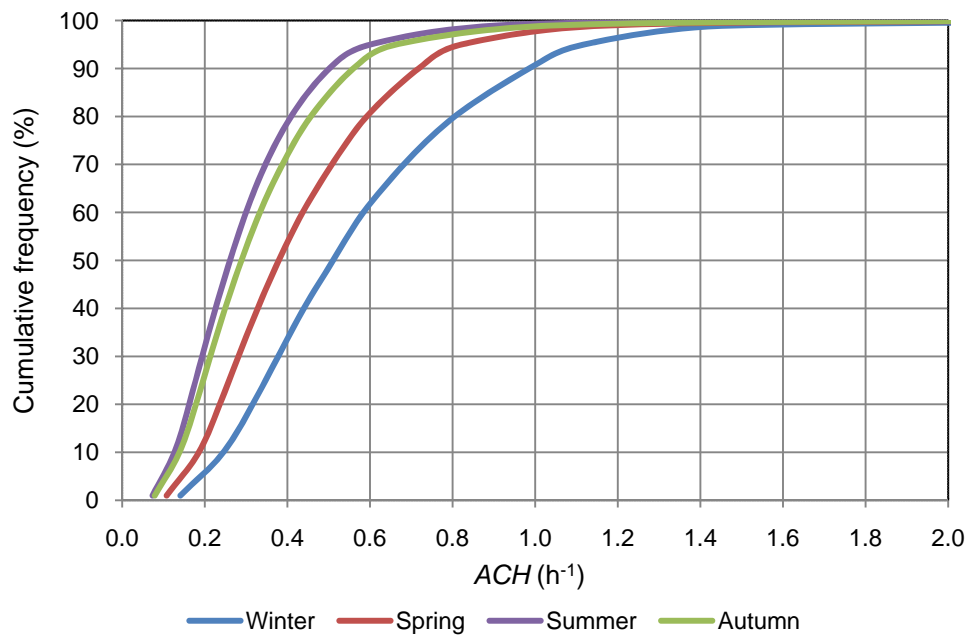


Figure 5.21 Cumulative distribution of the ACH for average meteorological conditions obtained with the UPC-CETE model and the stochastic simulation by census tract

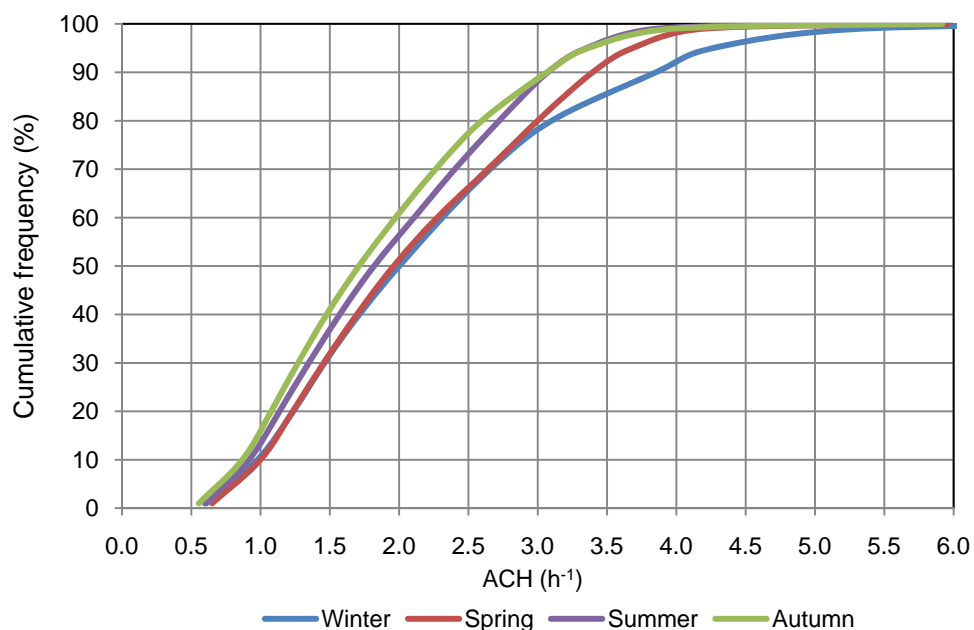


Figure 5.22 Cumulative distribution of the ACH for extreme meteorological conditions obtained with the UPC-CETE model and the stochastic simulation by census tract

Since we used the same infiltration model to estimate the *ACH* for the *c* predicted with the UPC-CETE and LBNL airtightness models, the difference between *ACH* distributions given by the two models followed the same pattern as the difference between predicted *ELAs* (Figure 5.18 and Figure 4.19 respectively). Largest differences were found in cumulative frequencies lower than 20% and higher than 80%, whereas those between the 20th and 80th percentiles were very close and showed differences of less than 10%.

In summer and autumn 80% of dwellings showed *ACHs* lower than 0.5 h⁻¹ for both the UPC-CETE and the LBNL airtightness models (Figure 4.22), whereas in spring and winter 70% and 50% of dwellings showed *ACHs* lower than 0.5 h⁻¹, respectively. If we compare these results with residential *ACH* distribution by season in the US (Table 2.17), where *ACHs* lower than 0.5 h⁻¹ were reported for 60% of dwellings in winter, 50% in spring, 80% in autumn and only 25% in summer, we can see that similar values were obtained in autumn while the largest difference was recorded in summer. However, as mentioned in section 2.4.4 *ACH* distribution of US dwellings in summer, presented in Table 2.17, was not expected and might be a consequence of open doors or windows during tracer gas tests. Under extreme conditions, only 10% of dwellings showed *ACHs* lower than 1 h⁻¹ in all seasons, whereas 90% of dwellings in summer and autumn and 80% of dwellings in winter and spring showed *ACHs* below 3 h⁻¹.

Chapter 6. Air exchange rates of Catalan single-family dwellings: Experimental measurements

*"A pessimist sees the difficulty in
every opportunity; an optimist sees
the opportunity in every difficulty"*
Winston Churchill

In this chapter we describe the experimental campaign carried out in order to determine the *ACH* of some Catalan dwellings, as well as the air exchange of an interior room where expedient measures were applied. The aim of using expedient measures was to assess the reduction of air infiltration, and the increase in the protection offered by sheltering. To accomplish this, we tested 16 dwellings across Catalunya using the concentration decay technique and CO₂ as tracer gas. Experimental measurements were performed during two different seasons to contrast the effect of meteorological conditions. The first part of this chapter deals with the description of the concentration decay technique, the use of CO₂ as tracer gas and the use of expedient measures, while the second part presents the experimental design, the methodology followed and the results obtained.

6.1 Concentration decay technique

The concentration decay technique is one of the procedures available to determine the *ACH* of a single-zone volume using a tracer gas and is probably the most used due to its simplicity and advantages over other procedures, like the constant injection or constant concentration, mentioned in section 2.4.4. A single-zone volume is defined by the ASTM E-471 (2001) standard as a space or set of spaces wherein the concentration of the tracer gas is maintained uniformly throughout and that only exchanges air with the outside. This type of spaces, where concentrations could remain uniform or where perfect mixing can be assumed, are mostly places with low internal resistance to airflow (i.e. few internal partitions), uniform temperature, and low or null momentum effects (i.e. infiltration through small openings, no mechanical ventilation systems). The results of this test are also subjected to the meteorological conditions prevailing during the test.

This technique comprised the injection of a quantity of tracer gas uniformly into the zone to reach a fixed concentration and then measure tracer gas concentration at known times. To ensure uniformity, ventilation fans could be used to aid the mixing process, however, uniformity implies that gas concentrations measured at representatives locations throughout the zone shall differ by less than 10% of the average concentration for the zone (ASTM E741-00, 2001). Finally, the average air exchange rate for the testing period can be calculated from Eq. 2.54 Taking logarithms at both sides, the difference between the logarithms of the initial ($C_{t=t_1=0} = C_1$) and final ($C_{t=t_2} = C_2$) tracer gas concentrations divided by the time period ($t = t_2 - t_1$) gives the average air exchange rate (see Eq. 6.1).

$$ACH = \frac{\ln(C_1 - C_o) - \ln(C_2 - C_o)}{(t_2 - t_1)} \quad \text{Eq. 6.1}$$

One can also monitor any fluctuation of the air exchange during the test taking additional measurements throughout the test. In this case we can use Eq. 6.2, the linear presentation of Eq. 2.54 Therefore, performing a regression analysis of the logarithms or a plot of the logarithms versus time, we can estimate the slope which represents the air exchange rate. This procedure assumes a steady-state through the measuring period, and is more accurate than just using a pair of measurements as in Eq. 6.1.

$$\ln(C_i(t) - C_o) = \ln(C_{i(t=0)} - C_o) - ACH \cdot t \quad \text{Eq. 6.2}$$

One of the advantages of the concentration decay over the constant injection or constant concentration techniques is that because logarithms of concentrations are used, only relative concentrations are needed, which can simplify the calibration of the measuring equipment and minimize the error associated to equipment calibration (ASHRAE, 2005). Another advantage is that the gas injection rate is not needed, although it must be controlled to assure that gas concentrations are within the limits of the concentration measuring device. By contrast, constant concentration and constant injection techniques require the measurement of absolute concentrations and injection rates, and requires longer measurement periods, more control and automatization. Nevertheless, they are more suitable to measure airflow into each zone, and air exchanges rates that vary with time. Among the disadvantages of the concentration decay, the most important is the imperfect mixing of the tracer gas with indoor air, at the initial injection and during the decay period; however this is a problem also in the other techniques (ASHRAE, 2005).

The entire procedure for this test is completely described in the standard ASTM E-471 (2001), and resumed in Figure 6.1.

6.1.1 Use of CO₂ as tracer gas

Gases used as tracers should have some especial characteristics like detectability, nonreactivity, nontoxicity, neutral buoyancy, relatively low concentration in ambient air and low cost (ASHRAE, 2005). Common gases used as tracers comprise sulphur hexafluoride (SF₆), carbon dioxide (CO₂), and perfluorocarbon compounds (PFTs). The SF₆ is perhaps the most used in the estimation of the *ACH* in residential buildings; however, the SF₆ and PFTs decay techniques are more complex and expensive than CO₂ techniques, since experienced operators and special equipment (i.e. gas chromatograph) are needed to perform the measurements and the analysis. Another advantage of using CO₂ is that it has a lower molecular weight than SF₆ or PFT, facilitating the mixing process and the homogenization. The use of CO₂ as a tracer gas has usually been addressed in two ways: using injected CO₂, like with other gases, or using metabolic CO₂ generated by people. The use of metabolic CO₂, also linked to the assessment of indoor air quality (Persily, 1996) and long-term studies in occupied buildings, has been widely

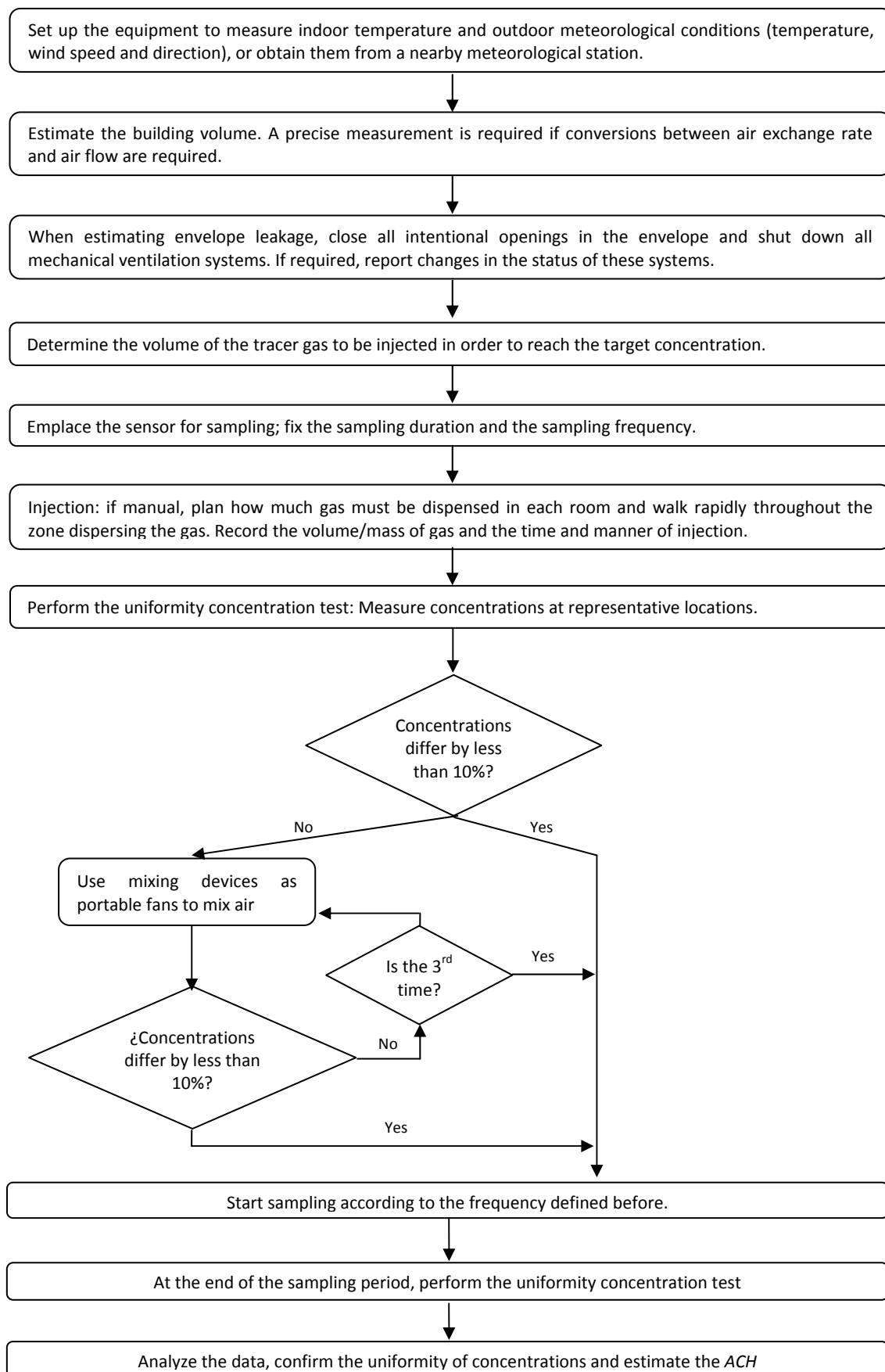


Figure 6.1 Flowchart of the concentration decay procedure

used in the *ACH* estimation of residential rooms, schools classrooms, office rooms and commercial buildings departments (Guo & Lewis, 2007; Penman, 1980; Morse *et al.*, 2009; Lawrence & Braun, 2006; You *et al.* 2007), while injected CO_2 has usually been applied in the *ACH* estimation of greenhouses, animal transport cabins, test rooms and for the assessment of mechanical ventilation systems' effectiveness (You *et al.*, 2007; Purswell, 2006; Borhan & Hao, 2007). One reason for using metabolic CO_2 instead of a tracer gas is the risk of objections being raised by or on behalf of the occupants to breathing a tracer for a long period of time.

The use of metabolic CO_2 for the estimation of *ACH* in dwellings, however, has some drawbacks in relation to injected gases: test times are longer (several days or even weeks), the state of the openings and occupants' behavior is more difficult to control, as well as, assuring an uniform concentration since CO_2 is generally emitted in a specific location (i.e. rooms at night). Also, depending on the procedure considered, constant injection or concentration decay, the rate at which CO_2 is generated has to be taken into account. For the constant injection technique the CO_2 generated by the people inside must be determined. Usually this generation rate is approximated assuming an average CO_2 emission for a single person multiplied by the number of people (Penman 1980). Moreover, for the concentration decay technique the dwelling must be empty and the data used should exhibit an exponential decay behavior. Therefore, data commonly used in this case correspond to that recorded after people left dwellings in the morning, when CO_2 concentration might be the highest under normal usage of the dwelling. Guo and Lewis (2007) developed an interesting work that consists of determining the *ACH* of six Irish single-family dwellings. To accomplish this, they used the pressurization technique to determine the airtightness (ACH_{50}), the tracer gas concentration decay technique with SF_6 to estimate the *ACH* of the whole house and the metabolic CO_2 concentration measured in an occupied room. They monitored the CO_2 concentration continuously for 2 to 7 days in order to calculate the *ACH* based on the constant injection technique. These authors support the selection of a bedroom to represent the whole house *ACH* (using the metabolic CO_2), on the assumption that a small-scale enclosure inside the house can represent the infiltration and ventilation performance of the whole structure. To analyze the *ACH* with the CO_2 measurements, the authors took the average of the *ACH*s found every night during the steadily increasing concentration periods. From their results, the highest correlation (87%) was found between ACH_{CO_2} and the ACH_{50} , while for ACH_{CO_2} and ACH_{SF_6} it was 68%, and for ACH_{SF_6} and ACH_{50} 63%. Concerning the results with CO_2 and SF_6 ,

similar values were obtained for half of the dwellings studied, with differences lower than 12% (based on the SF₆ results), while the others exhibit differences of around 25%.

In the case of non residential rooms, one of the earlier studies was that of Penman (1980), who determined experimental *ACH* of two large rooms at Exeter University Library, mechanically ventilated, measuring the amount by which occupants raises CO₂ concentration. He argued that the rooms were kept at positive pressure with respect to the rest of the building and therefore, infiltration of internal air should be little, and all incoming air was assumed as fresh. From his work, he concluded that this procedure is applicable when the incoming air is known to be fresh, or if the concentration of the other internal source is provided. The problem then is the difficulty on determining the relative importance of each source. In a subsequent study, Penman and Rashid (1982) investigated a natural ventilated office room that had connections with other internal spaces (corridor and ceiling), as well as with the outside. In this case, the authors monitored the CO₂ concentration in the adjacent spaces too (outside, corridor and ceiling), and determine the airflow pertaining to each connection solving the set of differential equations resulting from the mass balance. This type of procedure is generally used to test the *ACH* of non residential rooms, as also described by Smith (1988), who measured the ventilation rates at Tidcombe Lane School using the CO₂ produced by students. He monitored CO₂ concentrations in every room and their occupancy, and then solved the set of differential ventilation equations finding the flow rates among rooms and within the outside. He also measured the *ACH* of each room with SF₆, using solely the data from the measurements of its decay in that room, since no information about SF₆ concentration in the others rooms was available. He mentioned that this procedure was only adequate after the release of the gas, when concentrations in the other rooms were small, because if a significant built-up of the gas occurs in one or more of the other rooms, then the result would underestimate the real value, as he reported for room 2 (the most interconnected), while estimations for rooms 1 and 3, agreed with those obtained with the CO₂.

Regarding the use of injected CO₂, it has been mostly used to assess the *ACH* of non occupied rooms, as mentioned before. You *et al.* (2007), analyzed the performance of the decay method using injected CO₂ in a test chamber where the airflow was controlled, with the aim of validate the usage of this procedure in the determination of the *ACH* in apartments, offices, classrooms, dormitories and meeting rooms involving metabolic CO₂ measurements during

several days (3 - 5 days). These authors reported that, for the chamber test, duplicate precision was within 10% and measured *ACH* were among 90% to 120% of the real *ACH*. By the other hand, Borhan and Hao (2009) used the continuous injection method with CO₂ to investigate the *ACH* of a greenhouse at various levels of roof vent openings and weather conditions. The objective of these authors was to develop a ventilation model that lead to the optimization of CO₂ enrichment under several ventilated and meteorological conditions. For the experiments, they used a target concentration of 1000 ppm, and registered CO₂ concentrations each minute, during 15 min.

6.2 Expedient measures

Expedient sheltering, as mentioned in chapter 2, consists of taking simple measures to reduce the *ACH*. A common strategy in the case of a toxic release, consist of advising people to close all windows, doors, any other openings, and go into an interior room, seal with tape the joints of doors and windows, and stay there until emergency managers announce that it is safe to exit. These measures offer additional protection to people beyond the protection provided by the house, since indoor air of the rest of the dwelling will act as a mattress that slow down the toxic gas concentration while it travels and infiltrates to the shelter. Nevertheless outdoor air would also infiltrate to the interior room if it has any connection with the outside. Therefore two different situations can take place. The first, if the room is completely interior and has no vents or connections with the outside, in this case all the air infiltrated would be from the rest of the dwelling (Figure 6.2.a). The other situation, when the room is connected with the outside (i.e. windows, doors, vents), comprise the air exchange with both indoors and outdoors, as shown in Figure 6.2.b. In this last case a limiting situation where all the air infiltrates from outdoors can also take place, which corresponds to the worst scenario in the event of a toxic gas release (Figure 6.2.c).

Experimental *ACH* studies concerning the use of expedient measures in dwellings for a shelter-in-place situation, comprises those developed by Jetter and Whitfield (2005), Blewett and Arca (1999) and Rogers *et al.* (1990). Blewett and Arca (1999) analyzed the effect that sorption and expedient measures have on shelter-in-place protection. To accomplish this, they exposed a two-room cottage of wooden construction to a series of transient vapor challenges with sarin,

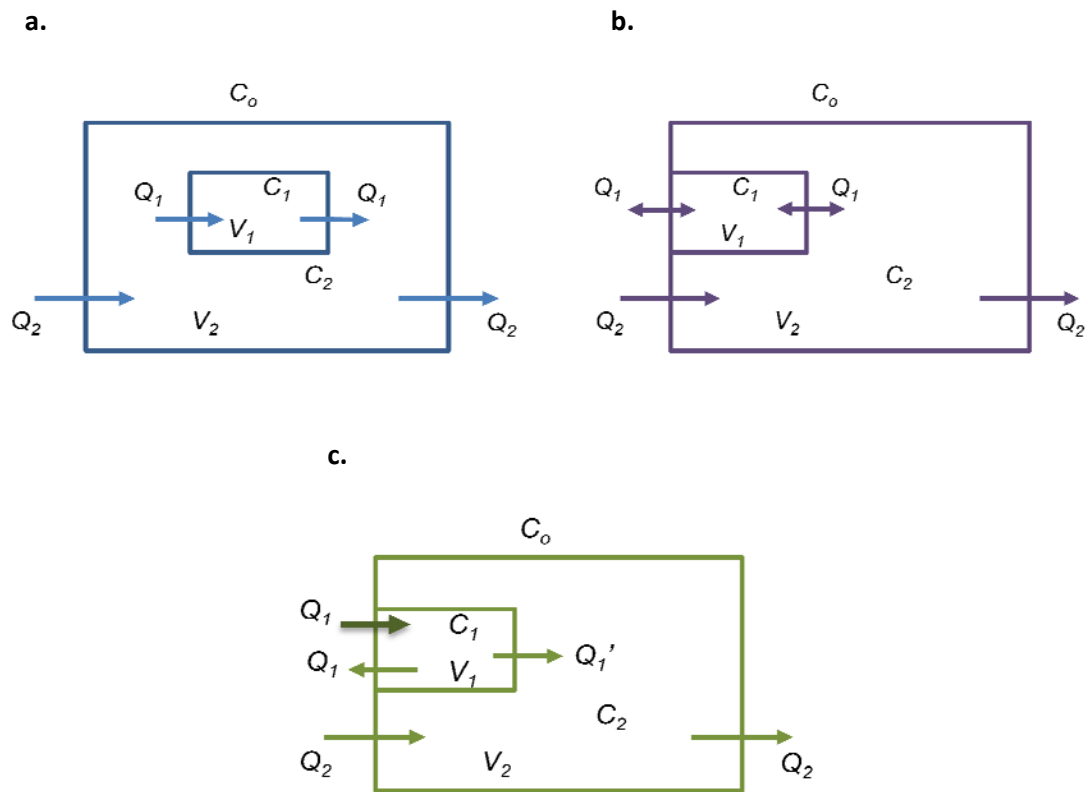


Figure 6.2 Possible situations of air exchange of a room: a) Only with indoors, b) With indoors and outdoors, c) Air infiltrate only from outdoors

mustard gas and methyl salicylate (a surrogate for mustard gas), and measured the *ACH* and the airtightness of the two rooms by means of the tracer gas method using SF_6 and the pressurization test, respectively. Each room had an exhaust, a door to the outside and an electrical connection to the outside. The wall separating the two rooms did not have any penetration. They performed *ACH* tests with different configurations: with the exhaust fan tapped, with no sealing or fully sealed, and found reductions in the *ACH* of around 65% in the case of fully sealed and 40% for the exhaust fan tapped in relation to the *ACH* without sealing. From their results, we can also see a reduction of around 50% in the dosage measured inside the test rooms (5 h dosage) and a double in the protection factor when they are fully sealed in comparison with no sealing, for the methyl salicylate trial. Also, experimental protection factors reported were higher than those calculated using the *ACH* measured due to the effect of sorption, which was stronger in the case of mustard gas, the less volatile of the three substances. The protection factor calculated by these authors, presented in Eq. 6.3, is defined as the ratio between the cumulative exposure outdoors over the cumulative exposure indoors;

where the cumulative exposure is given by the integration of the concentration over time, it is, as the TL for and n of 1.

$$PF = \frac{\int C_o dt}{\int C_i dt} \quad \text{Eq. 6.3}$$

Moreover, Rogers *et al.* (1990) investigated features like the amount of time it takes to complete expedient measures and the degree of reduced infiltration associated with each in-place shelter option. To accomplish this they performed *ACH* measurements of the whole house and an interior room used as shelter in 12 single-family dwellings using Freon as tracer gas. Shelters were mainly bathrooms, and the *ACH* was first measured with a towel under the door and then using expedient measures, which were applied by household members using written instructions. From their results, a 55% average reduction was achieved in the *ACH* of the sealed room in comparison to the *ACH* of the room without sealing. Concerning the *ACH* of the whole house, 58% of the dwellings presented lower *ACH* than the sealed rooms. This situation can take place because interior structure tends to be leakier than exterior structure (Voisin, 2007). Commonly, joints of indoor windows and door frames are not as tight as exterior, since more attention is paid to the shell due to insulation and thermal efficiency; therefore most of the air exchange of the room is within indoor air rather than outdoor air. Nevertheless, these authors did not make any description of the dwellings tested.

Another interesting work developed to determine the effectiveness of expedient sealing measures in reducing the air infiltration rate of a room selected as shelter is that of Blewett *et al.* (1996), carried out between July and October of 1995. They tested bathrooms, windowless bathrooms and walk-in closets, using the decay technique and SF_6 as tracer, in 8 single-family dwellings, 2 mobile homes and 2 apartments. Expedient measures applied by these authors comprised placing a wet rolled towel at the base of the door, put duct tape over the vent or exhaust and tape electrical outlets (Method 1), or placing, in addition, duct tape around the perimeter of the door and plastic sheet over the window (Method 2). The approach used by them consisted of releasing the SF_6 through the whole dwelling; close the shelter or shelters when the uniformity of concentration was reached (if there was more than one room to be tested in the dwelling), and measure concurrently the *ACH* of the shelter and the dwelling, monitoring concentrations in different locations of the dwelling. With this type of preparation, and measuring the SF_6 concentration decay in the dwelling simultaneously; these authors

assumed that the air exchange of the sealed room was with the outdoors. Even though, this assumption is not very accurate, since air exchange within indoor air comprise an important fraction of the air exchange of a room as mentioned before. From the results reported for bathrooms with windows, most of the trials without sealing presented higher or equal *ACH* than the houses. In the case of method 1 only two measurements were found to be higher than the *ACH* of the dwellings, and an average reduction of 16.5% was reported in the *ACH* of the shelter with respect to that of the dwelling. For method 2, only tested in 5 bathrooms (belonging to 2 dwellings and a mobile home), all the *ACH* measured were lower than those of the houses, showing an average reduction of 34% with respect to the *ACH* of the whole dwelling. For the other type of shelters tested by these authors, windowless bathrooms, an average reduction of 22% with respect to the house, was reported for no expedient measures, and 30% when sealing measures of method 1 were applied. For walk-in closets, the reduction in the *ACH* was almost the same (around 30%), with and without expedient measures. Another interesting feature about this work was that the variability in the *ACH* was greater among shelters than among the dwellings, as expressed by the standard deviation reported for each set of trials (according to the type of shelter and expedient method applied). The authors conclude that this may be due to inconsistent or inadequate sealing methods and or leakage paths not addressed by the expedient measures such as the sole plate.

Jetter and Whitfield (2005) also performed a recent study to determine the effectiveness of expedient measures in an interior room. They performed 18 experiments in a single-story, wood frame dwelling during two periods of the year, using SF_6 as tracer gas. Experiments consisted of monitoring the time needed by the participants (men and women of various ages and occupations) to implement expedient measures in an interior bathroom with a vent and no exterior walls, and record SF_6 concentration in the house and shelter simultaneously. As Blewett *et al.* (1996), they released the SF_6 in the whole dwelling and after a uniform concentration was reached, the shelter was closed. However, their approach was different and consisted of assuming a two-zone ventilation model, where the shelter only exchanges air with the house. Therefore, to analyze the data, they solved simultaneously the set of differential equations resulting from the two-zone model and estimated the airflow rate to the house and to the shelter. These airflows divided by the volume of the house and the shelter, respectively, gave the *ACH*, being those of the shelter higher than those of the house. These authors reported protection factors for the shelter 1.3 to 10 times greater than those for the house, being the difference between protection factors larger for short exposures (outdoor exposures

times tested: 0.25, 1, 2 h) and small temperature differences between the dwelling and the exterior, than for long exposures and large temperature differences. From other trials made by these authors with the bathroom door closed but with no sealing, they said that the concentration of the tracer remained the same as the concentration in the rest of the dwelling, while if only the door was sealed, the concentration in the shelter decrease faster than that of the rest of the dwelling. They concluded that these results were probably a consequence of the stack effect of the unsealed bathroom vent.

6.3 Experimental design

The objective of this chapter is to determine the distribution of single-family dwellings' *ACH* across Catalunya, during two periods of the year: summer and winter, using the tracer gas decay technique, and to assess the performance of the UPC-CETE model, developed in chapter 5. To accomplish this, we employed injected CO₂ as tracer gas, and therefore, the CO₂ concentration was the response variable. Generally, experimental data of air exchange rates follow a log-normal distribution, thereby; we focused our efforts on the inference of the parameters that describe this distribution: the geometric mean (GM) and the geometric standard deviation (GSD).

6.3.1 Estimation of sample size

To determine the size of the sample, we must take into account the desired confidence level (α), usually taken as 95%, the error of the mean estimation to be considered in the calculation (f_{GM}), which is generally between 1 and 5%, and the standard deviation of the population (σ). Generally, the standard deviation of the population is unknown, so, this is commonly taken from previous studies either on the same population, or on the same variable but in other populations (i.e. other regions or countries) (Azorin & Sánchez, 1986). The estimation of sample size also depends on the distribution that the variable has (e.g. a normal distribution, log-normal, etc), so the expressions to calculate the sample size depend on both the distribution exhibited by the variable and the parameter you want to infer (Castañeda *et al.*, 2002).

In our case, we planned to infer the GM, therefore we used the expression proposed by Hewett (1995) to estimate the sample size (n_{GM}) for a variable that follows a log-normal distribution (Eq. 6.4). Since we needed an estimation of the standard deviation to perform the calculation, we used different GSD reported in experimental studies developed in the US (Murray & Burmaster, 1995). In addition, we also used the GSD obtained from the French air leakage database, when the power law equation (Eq. 2.40) was applied with a pressure difference of 4 Pa (see Table 6.1). Afterwards, assuming a calculation error of 10% (f_{GM}) and a confidence level of 95%, we obtained the sample sizes shown in Table 6.1.

$$n_{GM} \cong \frac{t_{(\alpha/2, n-1)}^2 (\ln(GSD))^2}{\left[\frac{1}{2} \cdot \ln \left(\frac{1+f_{GM}}{1-f_{GM}} \right) \right]^2} \quad \text{Eq. 6.4}$$

Table 6.1 Sample sizes estimated to infer the GM and the GSD of Catalan dwellings

	GSD source			
	France (4Pa) ¹	US summer, HDDS <2500 ²	US summer, 2500<HDDS<5500 ²	US, summer ²
GM (h⁻¹)	0.5360	0.4552	0.5549	0.4391
GSD (h⁻¹)	1.745	1.573	1.844	1.996
n³	250	37	34	332
f_{GM}	0.1	0.1	0.1	0.1
t-student (95%)	2.255	2.339	2.348	2.252
n_{GM}	157	112	205	240

¹Data obtained from the power law coefficients reported in the CETE Air leakage database with a ΔP of 4 Pa

²Data taken from Murray and Burmaster (1995)

³Size of the study from which the GSD was taken

Calculated sample sizes are very large and depend specially on the GSD used. Larger GSD lead to larger sample sizes. In this case we considered that the better estimate was the one obtained with the French data (157), since it probably resemble more to Catalunya, and also came from a reasonable number of data. However, due mainly to restrictions concerning dwellings availability, time and cost as described below, we could only measure 16 dwellings.

- Dwellings availability: it is difficult to get the houses since not everyone would leave you his dwelling to make an experiment where a gas would be injected. Therefore, possible dwellings may come from friends. Also, since the owners must remain outside during the

trial period (at least 6 h), it is sometimes an obstacle because they should eat outside, or stay outside when it is cold, etc.

- Time: the time is also a limiting factor since you need a day for each trial; therefore, measuring 157 dwellings (or even 112) equal a long term, which would exceed the period of meteorological conditions of interest.
- Economy: the cost of the trials is another feature to look at, since beyond the gas and equipment, one should also consider the displacement and transport of the equipment, which is not possible through economic public transport (bus or train).

Apart from the sample size, another important feature that has been taken into account when selecting sampling units is the stratification. Stratification refers to the division of the population into more homogeneous subgroups, i.e. groups having a common feature. Since the distribution of units within the population is heterogeneous, we decided to stratify the population according to the characteristics that we believe influence the airtightness, and therefore the degree of infiltration, such as: floor area, year of construction and number of stories. To accomplish this, we selected the ranges used by the IDESCAT to tabulate the buildings' census data (see Figure 4.1). Then, the sampling units that should be included in each range could be estimated proportionally to the real distribution of the population. Nevertheless, although the stratification is a very good technique that leads to a better selection of the sampling units, we could not apply it because dwellings availability took priority over this criterion. Table 6.2 shows the hypothetic distribution of the sampling units taking the stratification into account, and the real distribution of the dwellings tested.

6.3.2 Experimental planning

Since the *ACH* vary with meteorological conditions, we decided to carry out two experimental campaigns in order to analyze the effect of outdoor conditions. To accomplish this we carried out the first set of measurements through summer (2009), where outdoor temperature is high and wind speeds are small, while the second experimental set was performed in winter (2010) where outdoor temperature is low and wind speeds were supposed to be higher. A total of 27 trials were done, 14 in the first campaign and 13 in the second campaign. In the first campaign we tested 14 dwellings and not 16, because we only account with 14 dwellings at that time.

Table 6.2 Distribution of the 16 sampling units according to the stratification

Number of stories		Distribution		Floor area m ²		Distribution	
		Hypothetic	Real			Hypothetic	Real
1	40%	6	0	<30	0.2%	0	0
2	45%	7	12	30-39	0.4%	0	0
≥3	15%	3	4	40-49	1.3%	0	0
				50-59	2.3%	0	0
				60-69	5.4%	1	0
				70-79	7.8%	1	2
Year of construction							
<1900	12.1%	2	0	80-89	9.8%	2	3
1900-1920	4.1%	1	0	90-99	17.6%	3	0
1921-1940	4.8%	1	0	100-109	12.3%	2	0
1941-1950	4.4%	1	2	110-119	5.9%	1	2
1951-1960	8.4%	1	1	120-129	9.2%	1	1
1961-1970	11.1%	2	1	130-139	3.3%	1	1
1971-1980	15.5%	2	1	140-149	3.4%	1	2
1981-1990	18%	3	2	150-179	8.8%	1	4
1991-2001	21%	3	4	180-209	6.7%	1	1
> 2001	0.5%	0	5	>209	5.5%	1	0

For the second campaign, although we got 2 more dwellings, only 11 dwellings of the 14 tested in the first campaign could be repeated. Table 6.3 shows the schedule of the trials, which was subjected to owners' availability. That was why some trials were performed at the end or out of the summer and winter period. However, since meteorological conditions for those dates are not so severe, we could also assess the *ACH* during those conditions.

Table 6.3 Chronogram of the trials

Dwelling	First campaign: summer 2009	Second campaign: winter 2010
1	05/07/2009	
2	04/07/2009	12/03/2010
3	04/07/2009	
4	11/07/2009	05/02/2010
5	13/07/2009	20/02/2010
6	09/07/2009	06/02/2010
7	10/07/2009	04/02/2010
8	07/07/2009	
9	06/08/2009	13/02/2010
10	26/08/2009	27/03/2010
11	27/08/2009	10/04/2010
12	25/09/2009	15/02/2010
13	29/09/2009	17/02/2010
14	13/10/2009	16/02/2010
15		27-28/01/2010
16		13/03/2010

Also, in order to inform people about the objective of trials, what they were and how they developed, we designed an informative brochure, where we explained in a clear and simple way who we were, which was the aim of the trials and which was the procedure of the trials. We also remarked the profit of these trials from the energetic and the risk assessment views, and clarify that the trials were safe and CO₂ concentrations to be studied did not pose any danger, and could even be reached in a closed room during night due to breathing. This brochure is shown in Annex E, in Spanish and Catalan presentations, respectively.

To design the trials and the experimental protocol, we took into account the following considerations:

- In order to optimize the use of CO₂, the test was performed first in the shelter and then in the house. Thus, the CO₂ remaining in the shelter and that infiltrated into the house could be used in the second test.
- Trials in dwellings located nearby were programmed together; it is, on the same dates, so we went to that location only once.
- For the sealing, we used masking tape in order to avoid any damage to the wall paint or surface.
- Concentrations were measured at mid-height of each story.
- Temperatures were monitored inside and outside, as well as wind speed, since the *ACH* measured is specific to those conditions. If wind speed could not be measured onsite, we took it from the nearest meteorological station.
- Any event during the testing time that could affect concentrations was recorded, like changes in fans, doors or windows operation, and the presence of people or animals.
- Fans could be used to aid the good mixing of the gas.
- We took photos of the dwelling and the surroundings.
- Dwellings characteristics involved in the shell leakage sites, like number and size of exterior doors and windows, vents, etc, were recorded.
- Notes on dwellings construction features, like floor area, number of stories, and those than could be related with the airtightness were taken.
- The status of all mechanical ventilation and heating systems was annotated.
- We made draws or obtained the plans of the dwellings with dimensions, so that all the spaces could be identified, as well as outdoor openings, and the volume could be determined.

- Outdoor gas concentration and in the zone was measured prior to injecting the tracer gas.
- The proper function of the measuring devices was verified prior to each trial.
- To assure a uniformity of concentrations, spatial samplings through the whole tested space are necessary. We separately sampled each individual room of zones that had interconnecting rooms.

6.3.3 Target or reference concentration

The reference concentration refers to the desired initial concentration of CO₂ that should be reached after injection and from which the trial would start. The standard (ASTM E-471, 2001) advises to use the highest detection limit of the gas analyzer as the target concentration. Nevertheless it also mentions that the maximum safe/allowable concentration for tracer gases is the PEL (permissible exposure limit 8 h), 5000 ppm for CO₂, and thus concentrations to be used might be around one tenth of that concentration. In our case, the maximum measuring limit of the sensor was 10000 ppm (see Table 6.5), which is the double of the PEL and might not be used. In addition, one tenth of the PEL (500 ppm) is a very low concentration, very close to normal levels of CO₂ in the ambient (~300 ppm). Therefore, to establish the reference concentration we revised the maximums concentrations of CO₂ used in other studies (Smith, 1988; Guo & Lewis, 2007; You *et al.*, 2007) and found that initial CO₂ concentrations varied between 1200 and 2000 ppm, which comprised CO₂ concentration reached in rooms during nights. Then, assuming an initial concentration of 1500 ppm we plot the evolution of the concentration for two common ACH: 1 and 0.5 h⁻¹ through Eq. 2.54 (Figure 6.3), in order to analyze the usefulness of this concentration.

From the figure it can be seen that 1500 ppm is a good target concentration since it leads to good concentration decay in two hours, the trials time, and outdoor concentration had not been reached for that period of time.

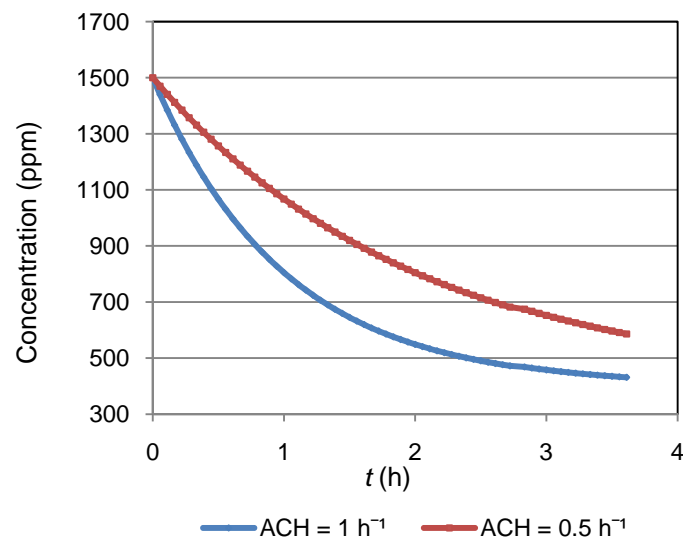


Figure 6.3 Theoretical evolution of the CO₂ concentration in a dwelling with different ACH

6.4 Materials and methods

6.4.1 Equipment and measuring devices

Table 6.4 lists the equipment and measuring devices used during the trials. Measuring devices are described in more detail in the following paragraphs.

Table 6.4 Equipment and measuring devices used for the trials

Equipment		Measuring devices
Extensions cords	Cutter	CO ₂ sensor
Batteries (3A and 9V)	Meter	Thermometers
Bottle of CO ₂	Bungee cords	Balance
Compass	Scissors	
Camera	Data loggers	
Laptop	Plastic box	
Folding wheelbarrow	Masking tape	

CO₂ sensor

The CO₂ concentrations were monitored with the Testo IAQ probe (Indoor air quality) and were recorded by the Testo 435-2 instrument. This probe is a portable, real-time sensor that also measures temperature, relative humidity and absolute pressure. It uses the Nondispersive Infrared (NDIR) technique to detect CO₂ in a gaseous environment through its characteristic absorption. The key components of this type of sensors (NDIR sensors) are an infrared source, a light tube, an interference (wavelength) filter, and an infrared detector. The gas is pumped or diffuses into the light tube, and the electronics measure the absorption of the characteristic wavelength of light. Table 6.5 shows the specifications of the sensor.

All the readings recorded were downloaded to a laptop using the USB connection and the Testo Comfort Software X-435 v 3.4, included with the instrument. Each recorded measurement contains a number (assigned chronologically), the date, the hour, the CO₂ concentration, the absolute pressure, the temperature and the relative humidity.

Table 6.5 Specifications of the CO₂ sensor

CO₂	
Measuring range	0 to 10000 ppm
Accuracy	±(50 ppm CO ₂ ±2% of mv) (0 to +5000 ppm CO ₂) ±(100 ppm CO ₂ ±3% of mv) (5001 to +10000 ppm CO ₂)
Resolution	1 ppm
Temperature	
Measuring range	0 to +50 °C
Accuracy	±0.3 °C
Resolution	0.1 °C
Relative humidity	
Measuring range	0 to +100% HR
Accuracy	±2% HR (+2 to. +98% HR)
Resolution	0.1%
Absolute pressure	
Measuring range	+600 to +1150 hPa
Accuracy	±5 hPa
Resolution	0.1 hPa
Recording frequency	from 1s
Storage capacity	10000 readings
Usage conditions	-20 to +50 °C
Feeding	Batteries (3A) or AC adapter
Dimensions	225 x 74 x 46 mm
PC connection	PC software and USB data transmission



Thermometer

Indoor and outdoor temperatures were recorded using contact thermometers, and the CO₂ sensor. Since the CO₂ sensor also measure temperature, it was recorded together with the CO₂ concentration. Concerning the thermometers, we used three contact thermometers PCE-T395, and three thermocouples (TP-K01). These thermometers are four channel digital thermometers for use with any K-type thermocouple as temperature sensor. Their internal memory can keep up to 6000 records per channel. They use a RS232 interface to perform bi-directional communication with PC. Their specifications are given in Table 6.6.

All the readings recorded were downloaded to a laptop using a RS-232 connector and the software TestLink PCE-T395 SE-309, included with the instrument. Each recorded measurement contained the date, the hour and the temperature.

Table 6.6 Specifications of the PCE-T395 Thermometers

Measuring range	-200 to +1370 °C
Accuracy	±0.2% of reading up to 200 °C ±0.5% of reading from 200 °C to 400 °C 0.2 °C from 400 °C
Resolution	°C from -200 to +200 °C 1 °C from +200 to +1370
Recording frequency	4 readings in 3 seconds
Storage capacity	10000 readings
Usage conditions	-20 to +50 °C
Feeding	Batteries (9V)
Dimensions	184 x 64 x 30 mm
PC connection	PC software and RS-232 connector
TP-K01 probe	
Range	-50 to 200 °C
Accuracy	±2.2 or ±0.75% of reading



CO₂ Bottle

We used liquefied CO₂ for the trials in small bottles of 7 kg of CO₂. We used this type of bottles since they were easy to transport in a standard car and contained enough quantity of CO₂ to test around 5 to 7 dwellings. Table 6.7 presents the specifications of the bottles. The safety data sheet of the CO₂ is shown in Annex E.

Table 6.7 Specifications of the liquefied CO₂ bottles

Bottle type	B10
Diameter	~150 mm
Height	~900 mm
Pressure	39.5 bar
Mass of CO ₂	7kg
Bottle weight	~20 kg
Purity	>99.99%



Balance

To control the CO₂ injection, we used a balance to monitor the CO₂ bottle weight and consequently the amount of CO₂ released. The balance used was a high capacity precision balance Mettler Toledo SB32000, which has a very good readability (1 g) and a high capacity at the same time. We took the readings manually before and after each injection. The following table presents the specifications of the balance.

Table 6.8 Specifications of the Mettler Toledo SB32000 balance

Measuring range	0 to 32100.0 g
Accuracy	± 0.5 g
Resolution	1 g
Stabilization time	2.5 s
Feeding	AC adapter
Dimensions	381 x 321 x 92 mm
Interface	RS-232C, Sub-D 9 pin



6.4.2 Dwellings characteristics

We tested a total of 16 single-family dwellings from different locations throughout Catalunya, the dwellings show different years of construction, typology, floor areas and number of stories, representing the range of actual dwellings found in Catalunya. All of them consist of heavy structures, as is typical in Catalunya, and were built with materials such as concrete, masonry and bricks. Also, they were dominated by natural ventilation provided by windows, doors and grille vents in kitchens and storage rooms with non electric boilers. Electrical

exhaust fans were only present in kitchens, as is mandatory in Spain, and windowless bathrooms, commonly, interior bathrooms with no exterior walls. Around half of the dwellings had a fire place and therefore a flue, so we closed the damper during the trials, to mimic shelter-in-place conditions. The main features of the dwellings analyzed are shown in Table 6.9, where the year of construction parameter refers to the actual year of construction if no substantial improvements had taken place or the year of improvements. The dwelling type refers to the type of construction concerning the surroundings of the dwelling; a detached house is completely separated from the other houses, a semi-detached correspond to a pair of dwellings connected by one side, a terraced middle correspond to a dwelling located in the middle of a line of houses connected by the left and right sides, while a terraced-end refers to the first and last dwelling of a line of houses. With regards to the number of stories, we reported the actual number of stories of the dwelling and the stories tested. This number differ for dwellings 5, 7, 14 and 16, since they all have the garage and storage rooms on the ground floor, which are commonly very leaky, unconditioned and are only connected with the rest of the house by a door (which implied a restriction to airflow and mixing), thus we did not consider them and the connecting door was kept closed during the trials. In the case of dwelling 3, the last 2 stories were unfinished and consequently leakier than the others; therefore, the door that connected these stories with the rest of the dwelling was closed and those stories were not taken into account. In relation to dwelling 5, it consists of 2 stories plus a terrace, connected by a staircase located at one side of the main structure, but only the first floor comprises the inhabited space, since the ground floor comprises an unfinished garage and the last floor is an open terrace. In addition, dwellings 3 and 12, also had the garage on the ground floor, from which a lot of air infiltrates, thereby, the door that connected it with the rest of the floor was closed for the trials and the garage was not taken into account. Concerning the floor area reported in the table, it corresponds only to the tested area. Finally, the shelter type parameter refers to whether the shelter was windowless or not. Windowless shelters were all interior bathrooms containing an exhaust fan connected with the outside. The other shelters were exterior, with one wall and a window facing the outside. Also, shelters 6, 9, 15 and 16 had a false ceiling.

Table 6.9 Main features of dwellings analyzed

Dwelling	Year of construction ¹	Type	Actual Number of stories	Tested Number of stories	Floor area (m ²)	Shelter volume m ³	Shelter type	Chimney	Location
1	1994	Terraced middle	2	2	72	9	Exterior	Yes	Cambrils (Tarragona)
2	2009	Terraced middle	4	4	87	10.7	Exterior	No	Vandellòs (Tarragona)
3	1945	Terraced middle	4	2	86.1	7.8	Exterior	Yes	Vandellòs (Tarragona)
4	2003	Detached	2	2	112.6	8	Exterior	Yes	Campelles (Girona)
5	1958	Terraced-end	2	1 ²	82 ²	8.9	Exterior	No	Lleida (Lleida)
6	1977	Detached	2	2	147.7	9	Exterior	Yes	Centelles (Barcelona)
7	2003	Terraced-end	4	3	141.3	9.6	Windowless	Yes	Centelles (Barcelona)
8	1950	Detached	2	2	172	12.8	Exterior	No	Barcelona (Barcelona)
9	2004	Terraced middle	4	4	172.3	4.7	Windowless	No	San Adreu (Barcelona)
10	1989	Detached	3	3	176	5.8	Exterior	Yes	Abrera (Barcelona)
11	1995	Semi-detached	2	2	84.5	12.3	Exterior	No	Creixell (Tarragona)
12	1989	Terraced middle	2	2	137	10.6	Windowless	No	San Adreu (Barcelona)
13	1965	Terraced middle	2	2	74	18.8	Exterior	No	San Adreu (Barcelona)
14	1990	Terraced middle	4	3	142.3	7.9	Windowless	Yes	San Adreu (Barcelona)
15	1997	Detached	2	2	127.3	29	Exterior	No	Barcelona (Barcelona)
16	2004	Detached	3	2	182	7.5	Exterior	Yes	Hospitalet de L'Infant (Tarragona)

¹ Year of construction or year of substantial improvements

² This area differs from summer (96 m²) to winter (86 m²), since during summer we consider the staircase that connect the dwelling with the outside. Which actually was an unheated space did not taken into account in winter. Consequently, the number of stories also changed from 2 in summer to 1 in winter

6.4.3 Methodology

For each house or trial, we conducted two measurements following the tracer gas decay technique described in the standard ASTM E741-00, first in the shelter and then in the whole dwelling. During the measurements the instrument was placed at a height of around 1 to 1.2 m. The following paragraphs describe the steps for the preparation of the dwelling, the shelter test and the dwelling test. The detailed protocol is included in Annex E.

Dwelling preparation

First, we measured the outside concentration of CO₂ in the area surrounding the dwelling, and determined the orientation of the dwelling. Then, if the plans of the dwellings were not available, we draw a plan for the house with its distribution and measured its dimensions for the subsequent preparation of the test. We also measured all external doors and windows and locate them in plans. Afterwards, we placed the thermometers, one outside and the others inside (one per floor), and started recording temperatures. Concerning the dwelling, the preparation consisted of closing all intentional openings, lowering the blinds, numbering all the rooms of the house in the plan, selecting the room that would serve as the shelter, estimating the volume of the shelter and the dwelling, entering the shelter and sealing the joint between the window and window-frame or the exhaust fan with masking tape, depending on whether the room is windowless or not. The sealing was intended to reduce or avoid the infiltration airflow through these paths. People in the dwelling had to leave, excluding the two researchers performing the test. Finally we measured the CO₂ concentration and the temperature in each room.

Shelter test

Using the temperature and the initial CO₂ concentration in the shelter, we estimated the amount of CO₂ to be injected in order to reach the target concentration established as 1500 ppm. To compute the amount of CO₂, we implemented Eq. 6.5 and Eq. 6.6 in an excel spreadsheet. Therefore, with the volume of the shelter (V_s), the initial concentration of CO₂ (C_s), the absolute pressure (Pa) and the temperature (T_s), the mass of CO₂ was estimated.

$$V_{CO_2} = (C_{ref} - C_s) \cdot 10^{-6} \cdot V_s \quad \text{Eq. 6.5}$$

$$m_{CO_2} = \frac{P_a \cdot V_{CO_2} \cdot 44}{T_s \cdot 8.314} \quad \text{Eq. 6.6}$$

After the calculations, one of the researchers entered the shelter, closed the door, injected the computed amount of CO₂ and started a fan to mix the air and the CO₂ released until the uniformity condition was achieved (difference between measured concentrations and the average concentration are less than 10%), approximately 5 to 10 min. At this point, the sensor was programmed to record the CO₂ concentration every 5 seconds, then the researcher left the shelter and immediately sealed the door and door-frame joint with masking tape on the out side. Afterwards, we left the house and waited one hour and a half or two hours depending on the dwelling availability (owner's disposition). After this time, we entered the house, took off the masking tape from the door and one researcher entered the shelter, stopped the recording procedure and measured the concentration at three different locations in the shelter to perform the uniformity test. Next, he took the masking tape from the window frame or exhaust fan, left the shelter, measured the CO₂ concentration and temperature in each one of the numbered rooms and started the protocol for the dwelling test.

Dwelling test

Using the concentrations throughout the dwelling, the amount of CO₂ to reach the target concentration was estimated and the discharging process started. Since the discharge was manual, we injected the gas in every room as quick as possible, and controlled the amount of CO₂ discharged through the weight of the bottle. To assure a good mixing, we started the fans and walked throughout the dwelling with a small one, until the uniformity condition was achieved (it took around 40 – 80 minutes). After this, we programmed the sensor to record the CO₂ concentration every 5 seconds, turned off the fans and left the house immediately. After two hours, we entered, stopped the recording process and measured the CO₂ concentration in each room to perform the uniformity test.

The outside temperature was recorded during the whole trial, as well as the indoor temperature in each story, while wind speeds were taken from the nearest meteorological station. Because we used CO₂ as tracer gas, we can see that the experiments were designed in such a way that metabolic CO₂ could only influence the values of the uniformity tests. Since

the amount of CO₂ emitted by a human being is low, 0.005 l/s (Guo & Lewis, 2007), the shelter environment would be the most affected (as it has a small volume), however, assuming a volume of 10 m³ the increase in the concentration by the presence of a person would be of 20 ppm/min, that is, around 40 ppm in the 2 minutes that the uniformity test lasts, which represents an error of 2% in the reading, the same percentage as the sensor uncertainty. In the case of the whole dwelling, where the volume is larger, the influence would be smaller for this period of time. Therefore the effect of metabolic CO₂ can be ignored. We may also remark that although the reference concentration was 1500 ppm, the initial concentration achieved after injection was generally higher since dwelling furniture diminishes the empty volume available in the house.

Data processing

The data recorded during each trial correspond to the CO₂ concentration decay within time, as represented in Figure 6.4 for dwelling 11.

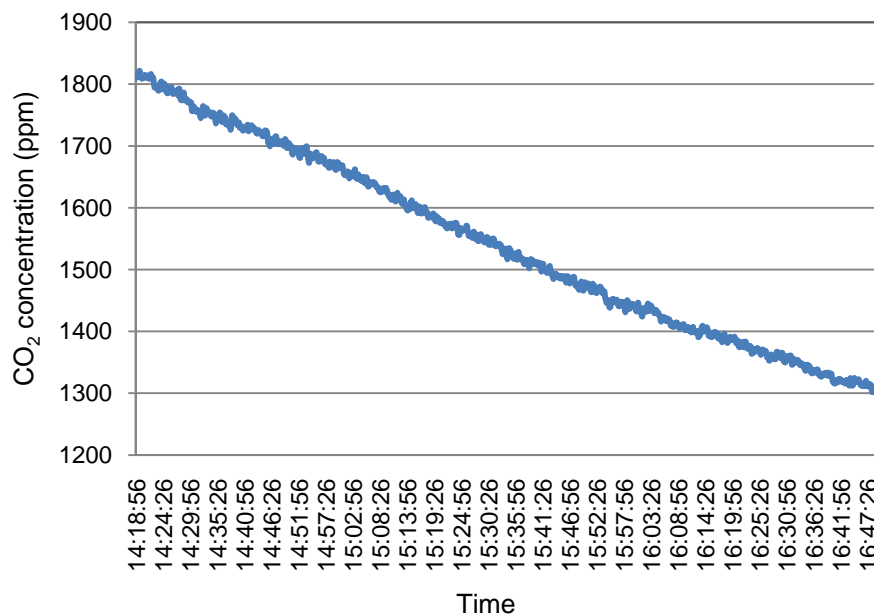


Figure 6.4 Concentration decay obtained for dwelling 11 during the second campaign of the trials

Then, to analyze the data according to Eq. 6.2, we obtained the natural logarithm of the difference between the measured concentration and the outdoor concentration for each time recorded. With these data, we made a plot of the natural logarithm versus time (see Figure 6.5) and performed a linear regression, as shown in Table 6.10. Therefore, the slope obtained

represents the *ACH* of the dwelling, $4.68 \cdot 10^{-5} \pm 4.93 \cdot 10^{-8} \text{ s}^{-1}$ ($0.168 \pm 1.7 \cdot 10^{-4} \text{ h}^{-1}$) in this case. Outdoor concentration used for the calculation was taken as the average of outdoor concentration registered, and was considered constant through the whole trial.

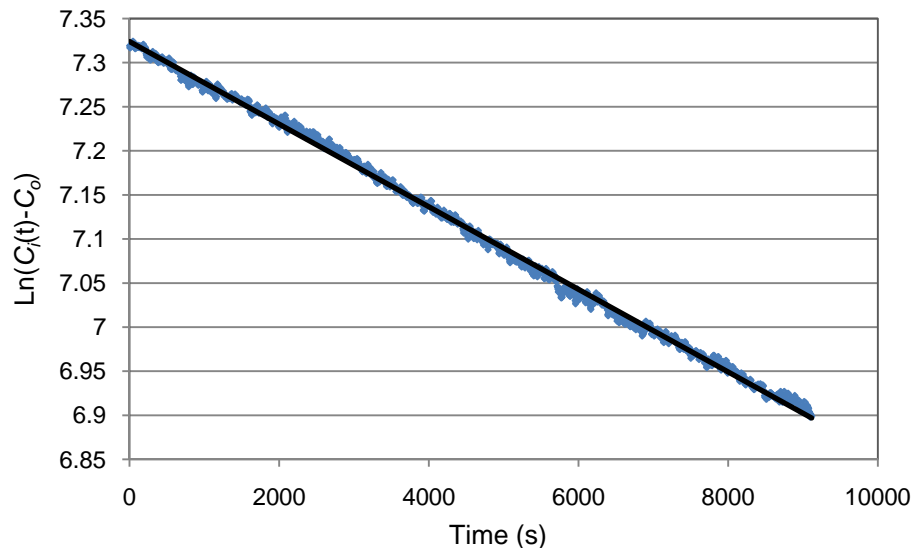


Figure 6.5 Plot of the natural logarithms of concentrations difference versus time for dwelling 11 during the second campaign

Table 6.10 Linear regression results

Regression statistics	
R^2	0.9979
Adjusted R^2	0.9979
Standard error	0.00554
Observations	1824

	Coefficients	Error	t- statistic	P-value	Lower confidence limit 95%	Upper confidence limit 95%
Intercept	7.3238	0.00025	28225.85	0	7.32333	7.32435
Slope	-4.683E-05	4.929E-08	-949.95	0	-4.693E-05	-4.673E-05

In the case of the shelters, the behavior of the concentration decay at the beginning was different to that of dwellings as shown in Figure 6.6. This happened since fresh air enters the shelter when the person inside opens the door in order to exit, thus an initial decrease is recorded, but then, the concentration increased reaching a maximum (at this moment we can say that homogeneity within the shelter was reached) and started the decay. Consequently, we only analyze the data that follow the maximum concentration, and neglect the previous

one. From the different shelters we could see that it took around 10 to 20 minutes to reach the maximum concentration. We also observed that this time was related to the volume of the shelter, higher volumes lasting longer.

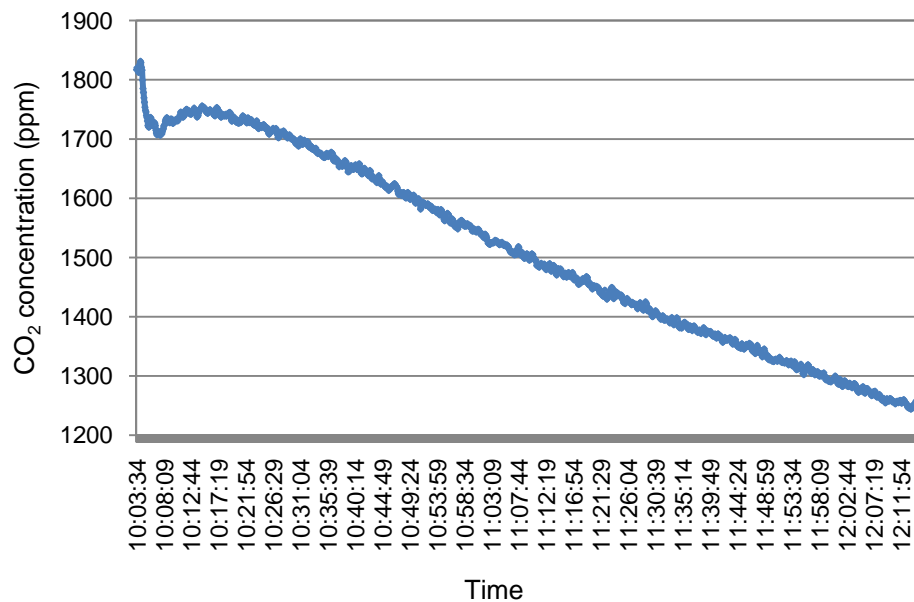


Figure 6.6 CO₂ concentration decay with time for the shelter of dwelling 12 in winter

To account for the concentration of the infiltrated air, we might consider the possible situations that can take place, as mentioned in section 6.2. According to this and looking at Table 6.9, all shelters exhibit some connection with the outside, which mean that air could infiltrate from both indoors and outdoors. Therefore, as it was not possible to monitor both the shelter's and the dwelling's concentration simultaneously, we evaluate two cases for the concentration of the air infiltrated to the shelter: in the first we assumed this concentration as outdoor concentration; while for the second we used initial indoor average concentration. Actually the air infiltrated should come from both sources; therefore the *ACH* obtained with these assumptions would give an approximation of the real value. Since we also measured concentrations in each room before and after the shelter trial, these values could serve to estimate the fraction of CO₂ infiltrated to the dwelling.

6.5 Results and analysis

6.5.1 ACH Results

Table 6.11 shows the experimental results obtained during the trials for the shelters and dwellings. In the case of the shelters, two values were reported concerning the *ACH* estimated assuming the concentration of the air infiltrated as the outdoor concentration (C_o) or as the initial average indoor concentration (C_o'). With regards to the latter consideration, it was not possible to calculate the *ACH* in four cases (dwellings 3, 7 and 8 in summer and dwelling 9 in winter) since we did not have initial concentrations before the test. Concerning the magnitudes of the *ACH* for the shelters, those estimated with the initial average indoor concentration were higher than the ones obtained with the outdoor concentration, as was expected since at a higher incoming concentration more fresh air would be needed to lower the concentration, than if the fresh air exhibits a lower concentration. Also, we can see that the difference in the *ACHs* for each shelter is proportional to the concentrations' difference.

In relation to the magnitude of the *ACH* measured, it varied between 0.056 and 0.579 h⁻¹ for shelters, with a geometric mean of 0.158 h⁻¹, while it ranged between 0.074 and 0.541 h⁻¹ for dwellings, with a geometric mean of 0.226 h⁻¹. In general, *ACH* for shelters were lower than *ACH* for dwellings. Only in 5 cases (18.5%) the *ACH* of the shelter, obtained with both concentrations, was larger (see Figure 6.7, dwellings: 2, 9 and Figure 6.8, dwellings: 10, 12, 16); while in 2 cases one was above (the one obtained with the initial average indoor concentration) and the other below (the one estimated with outdoor concentration) the *ACH* of the dwelling (see Figure 6.7 dwelling 13 and Figure 6.8 dwelling 6). Nevertheless, in this last situation the *ACH* of the shelters that were above only exceeded those of the dwellings by less than 1%. Analyzing the fact that the *ACH* of the shelter is larger than that of the dwelling, we observe that this is not repetitive, and only happened in one of the trials (campaign) performed in the dwelling. For example, for dwelling 2 and 9 the *ACH* of the shelter was higher in the first campaign (summer) while it was lower for the second (winter). Therefore, this situation might be mainly influenced by the combination of the tightness of indoor structure and the meteorological conditions; however the quality of the sealing during the first and the second campaign may have also influenced this result, although we tried to do it on the same way. This behavior, as mentioned in section 6.2, has also been reported by Rogers *et al.* (1990)

Table 6.11 Experimental air exchange rates obtained

Dwelling	Campaign	Shelter					Dwelling				
		C_o^1	ACH (h^{-1})	Ti ($^{\circ}C$)	To ($^{\circ}C$)	v^2 ($m \cdot s^{-1}$)	ACH (h^{-1})	Ti ($^{\circ}C$)	To ($^{\circ}C$)	v^2 ($m \cdot s^{-1}$)	Uniformity ³ (%)
1	Summer	$C_o=300$	0.289±0.0007	27.9	28.4	2	0.331±0.0008	28.6	30.6	1.8	3.2
		$C_o'=403$	0.314±0.0007								
2	Summer	$C_o=303$	0.310±0.0010	28.4	28.6	1	0.281±0.0080	26.4	28.7	0.4	22.4
		$C_o'=390$	0.330±0.0005								
	Winter	$C_o=306$	0.146±0.0002	14.7	10.6	1.1	0.223±0.0005	14.1	8.6	3	28
		$C_o'=522$	0.168±0.0003								
3	Summer	$C_o=302$	0.057±0.0003	26.3	28	2.5	0.417±0.0028	27	30	2.1	5.2
4	Summer	$C_o=299$	0.077±0.0006	19.3	17.3	3.7	0.122±0.0007	19.4	20.3	2.2	3.5
		$C_o'=358$	0.079±0.0003								
	Winter	$C_o=267$	0.111±0.0003	14.7	5.6	1.6	0.155±0.0003	16.1	8	1.5	7
		$C_o'=327$	0.115±0.0004								
5	Summer	$C_o=290$	0.143±0.0005	30.6	33.6	2.8	0.316±0.0009	31.3	33.4	2.5	7.7
		$C_o'=342$	0.148±0.0005								
	Winter	$C_o=316$	0.241±0.0007	17.8	12.3	4	0.359±0.0009	16	14.8	3.1	6
		$C_o'=714$	0.286±0.0008								
6	Summer	$C_o=352$	0.113±0.0011	22.4	19.8	1.5	0.366±0.0014	22	19.6	1.7	13.6
		$C_o'=429$	0.119±0.0005								
	Winter	$C_o=329$	0.151±0.0005	22.8	9.5	0.6	0.206±0.0007	19.2	11.2	0.5	10.7
		$C_o'=829$	0.207±0.0006								
7	Summer	$C_o=320$	0.401±0.0011	23.4	21.1	1.1	0.541±0.0030	23.2	23	1.9	32.4
	Winter	$C_o=374$	0.307±0.0004	19.1	3.4	1.4	0.479±0.0005	16.6	5.6	1.4	23
		$C_o'=548$	0.339±0.0004								
8	Summer	$C_o=300$	0.178±0.0021	27.1	23.3	2	0.201±0.0007	25.6	23	2.6	4.4
9	Summer	$C_o=308$	0.322±0.0016	28.2	30.5	3.3	0.178±0.0007	29.8	30.4	3.1	21.9
		$C_o'=370$	0.334±0.0016								
	Winter	$C_o=340$	0.309±0.0002	21.1	5.6	1.7	0.314±0.0004	19.3	6.6	1.8	15
		$C_o'=760$	0.129±0.0005								
10	Summer	$C_o=310$	0.106±0.0012	28.5	32.6	2.2	0.152±0.0005	28.1	31.3	4.7	13
		$C_o'=444$	0.110±0.0007								
	Winter	$C_o=312$	0.103±0.0004	21.2	14.5	2.1	0.093±0.0002	22.2	20.6	3.6	25.6
		$C_o'=760$	0.129±0.0005								
11	Summer	$C_o=300$	0.077±0.0005	26.8	32	3.6	0.154±0.0004	27.4	32	2.6	3
		$C_o'=411$	0.081±0.0003								
	Winter	$C_o=305$	0.064±0.0002	16.7	16	4.2	0.168±0.0002	18	19.4	3.7	6.6
		$C_o'=443$	0.068±0.0003								

Table 6.11 Experimental air exchange rates obtained (continuation)

Dwelling	Campaign	Shelter					Dwelling				
		C_o^1	ACH (h^{-1})	Ti ($^{\circ}C$)	To ($^{\circ}C$)	v^2 ($m \cdot s^{-1}$)	ACH (h^{-1})	Ti ($^{\circ}C$)	To ($^{\circ}C$)	v^2 ($m \cdot s^{-1}$)	Uniformity ³ (%)
12	Summer	$C_o=321$	0.117 ± 0.0009	24.7	26.5	2.6	0.159 ± 0.0009	25	26	3.3	18.8
		$C_o'=403$	0.123 ± 0.0005								
	Winter	$C_o=389$	0.243 ± 0.0003	13.3	6.1	2.4	0.176 ± 0.0002	16.5	12.4	2.9	6.7
		$C_o'=535$	0.281 ± 0.0003								
13	Summer	$C_o=300$	0.201 ± 0.0012	24.2	25.8	3.9	0.205 ± 0.0007	25	27	3.3	5.3
		$C_o'=423$	0.207 ± 0.0004								
	Winter	$C_o=351$	0.163 ± 0.0007	14.2	12.4	2.4	0.309 ± 0.0003	15.8	14.1	3.5	9.5
		$C_o'=436$	0.175 ± 0.0008								
14	Summer	$C_o=265$	0.081 ± 0.0003	25.5	21.7	2	0.210 ± 0.0015	25.5	22.5	2	35
		$C_o'=344$	0.085 ± 0.0002								
	Winter	$C_o=331$	0.121 ± 0.0002	13.6	8.6	1.9	0.223 ± 0.0009	13.5	8.9	2	5.2
		$C_o'=728$	0.147 ± 0.0003								
15	Winter	$C_o=319$	0.056 ± 0.0002	9.5	5.6	11	0.074 ± 0.0002	10.1	4.2	9.1	4.5
		$C_o'=541$	0.062 ± 0.0002								
16	Winter	$C_o=303$	0.521 ± 0.0007	18.7	6.1	5	0.386 ± 0.0008	18.6	11.3	4	10.3
		$C_o'=411$	0.579 ± 0.0008								
	Geometric mean		0.158				0.226				
	Maximun		0.579				0.541				
	Minimun		0.056				0.074				

¹ This parameter refers to the concentration of the air infiltrating to the shelter used to estimate the ACH. Therefore the first concentration reported for each trial was outdoor concentration (C_o), while the second was the initial average indoor concentration (C_o') as explained in section 0.

² Wind speeds taken from the nearest meteorological station (Servei Meteorologic de Catalunya) and corrected to a height of 10m with the LBL model, assuming a flat terrain with some isolated obstacles (see Table 2.11). Meteorological stations used for each dwelling are listed in Annex F.

³ This parameter shows the largest difference between measured concentrations and the average concentration obtained at the end of the dwelling trial. As described in section 0 the uniformity was achieved if the difference is less than 10%.

and Blewett *et al.* (1996). For further analysis concerning the ACH of the shelter, we decided to use those obtained employing outdoor concentration, since it better represents the worst scenario in the event of a toxic gas release, which assumes that all the air infiltrates from outdoors.

With respect to the uniformity criterion we observed that it was not achieved in around half of the trials, which represent dwellings with three or four stories (2, 7, 9, 10, 14, 16), and dwellings with 2 stories but with a floor area larger than 140 m² (6, 12). However, in the case

of dwelling 10 if we do not consider the ground floor, that contains the garage through which a higher infiltration took place, the uniformity criterion would be met in the other stories, 8.8% and 4% for summer and winter respectively. In this dwelling, the ground floor is connected to the other stories through a door that is usually closed. Therefore, from the point of view of a shelter-in-place situation we could only consider the first and second story. From Figure 6.7 and Figure 6.8 we can also see that larger differences between the two ACH calculated for shelters took place during winter, up to 40% with regards to the ACH calculated with outdoor concentration, while for summer differences remained below 10%. This may happen because initial indoor concentrations during winter were larger than those during summer, because in winter windows and doors remained closed before the test, as is typical in winter to avoid heat losses; while this is not the case for summer during which windows tend to be open and then metabolic CO_2 produced by the inhabitants is easily removed.

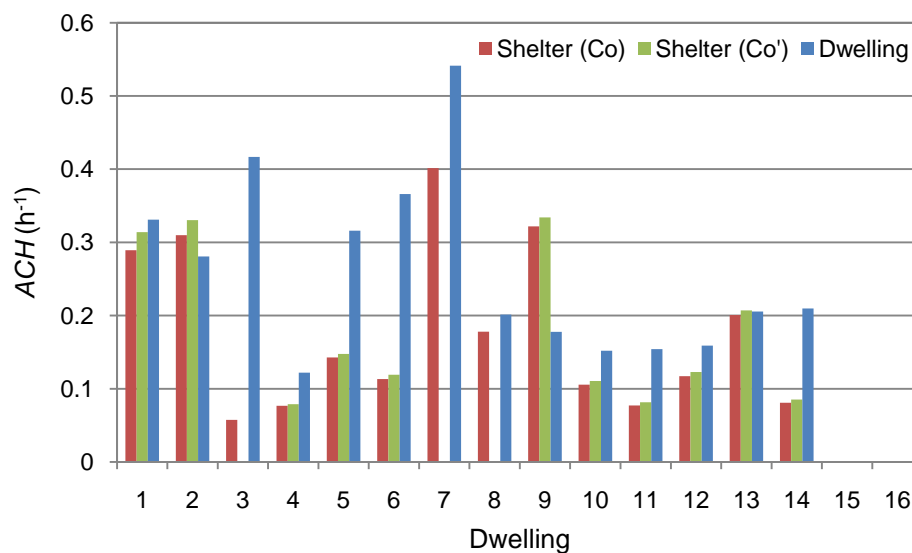


Figure 6.7 ACH obtained during the summer campaign

In general, comparing the ACH during summer and winter, similar values were obtained and no significant difference is observed. With regards to meteorological conditions, we see from Figure 6.9 that wind speeds were similar during the two periods and most of them were equal to or less than $4 \text{ m}\cdot\text{s}^{-1}$, only in the case of dwelling 15 wind speeds reported reached more than $9 \text{ m}\cdot\text{s}^{-1}$. Concerning temperatures differences, the summer period was characterized by values between 0.5 and $4.5 \text{ }^{\circ}\text{C}$, while during the winter larger values were recorded due to the use of heating, which ranged between 1.5 and $12 \text{ }^{\circ}\text{C}$ (Figure 6.10). However, for dwellings 10,

11 and 13, the temperature difference in winter was lower than that of summer as a consequence of the delay on the date of the trials.

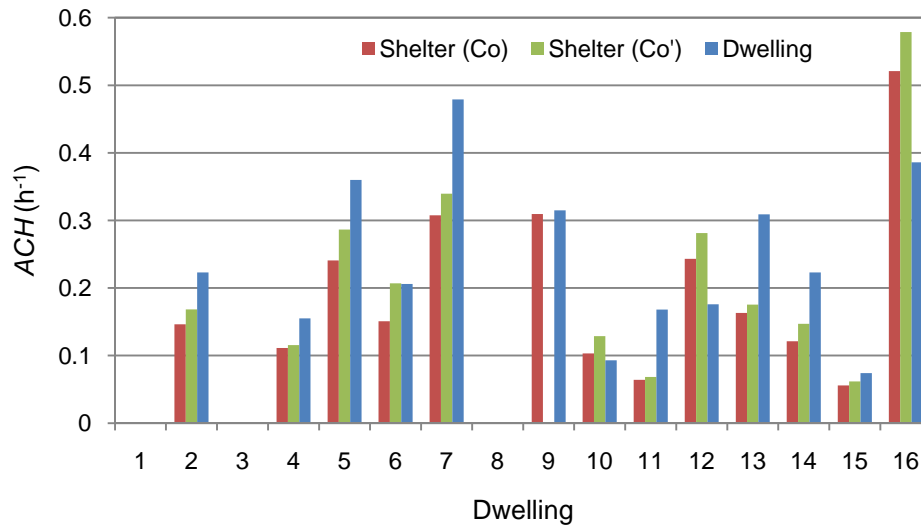


Figure 6.8 ACH obtained during the winter campaign

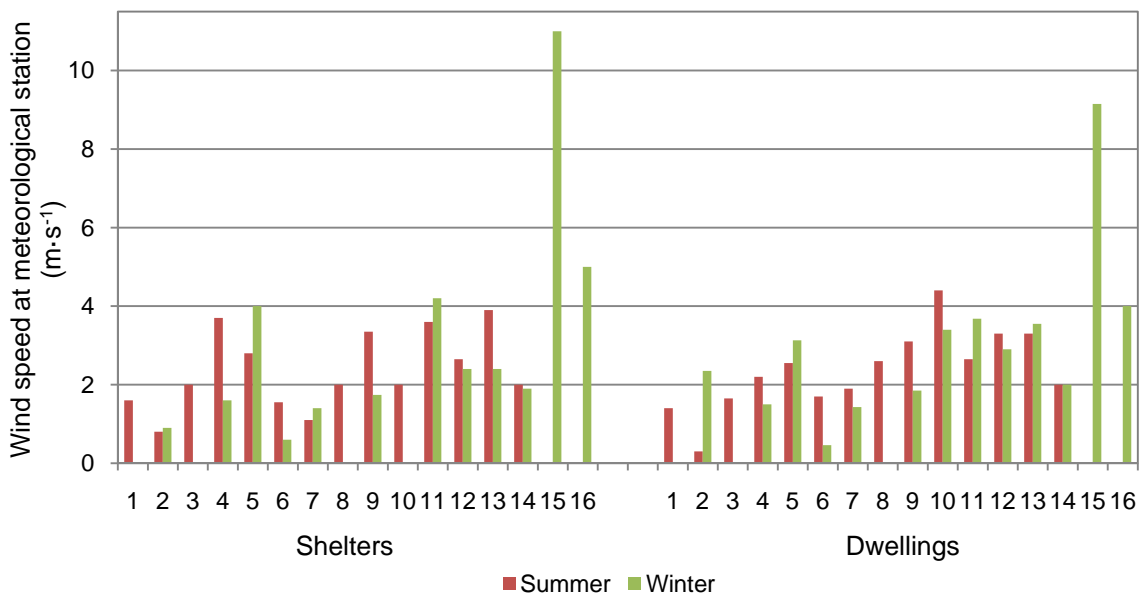


Figure 6.9 Wind speed for shelters and dwellings during summer and winter

During the trials some incidents took place, such as the incomplete sealing of the shelter door, which would probably affect the ACH obtained. From Table 6.12, which sums up those incidents, we can see that for dwelling 12 the exhaust fan of the shelter was not sealed, therefore in winter due to a larger temperature difference (7.2 °C) the stack effect should have increased, generating a higher airflow through the shelter. Also, the sealing of the kitchen

vents in dwelling 6 during winter lowered the leakage sites of the dwelling reducing the infiltration flow, which is reflected on the *ACH* obtained.

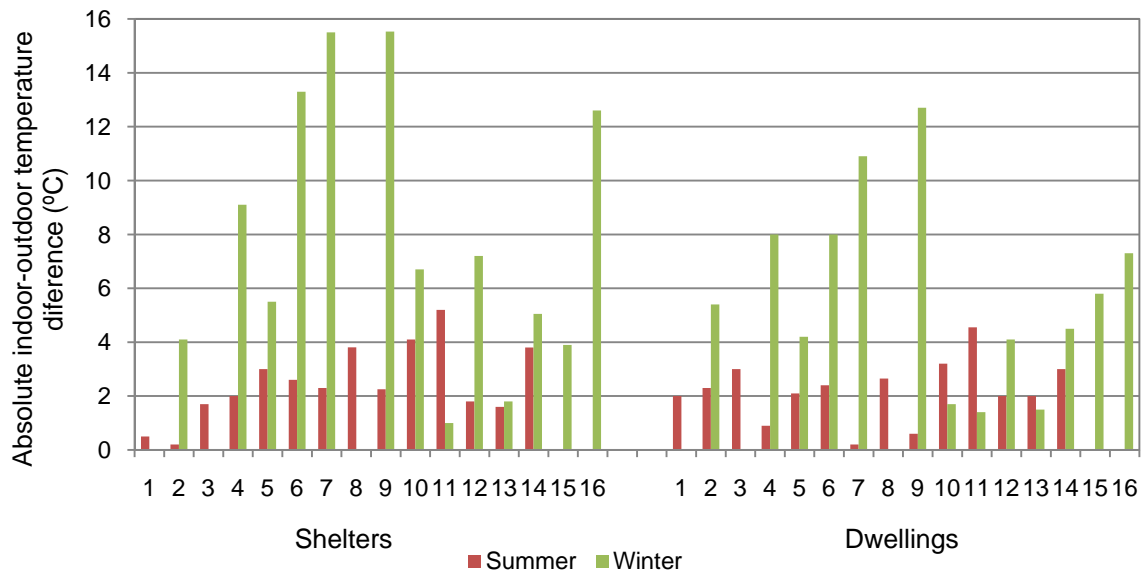


Figure 6.10 Absolute indoor-outdoor temperature difference for shelters and dwellings

Table 6.12 Main incidents taking place during the trials

Dwelling	Campaign	Notes
1	Summer	<ul style="list-style-type: none"> Only half of the door and door frame joint was sealed.
2	Summer	<ul style="list-style-type: none"> One person remained inside the dwelling during the shelter trial in a different story.
3	Summer	<ul style="list-style-type: none"> Two people remained inside the dwelling during the shelter trial in the same story of the shelter.
6	Winter	<ul style="list-style-type: none"> The vents of the kitchen had been sealed with plastic tape by the owner. The window of the shelter remained sealed during the dwelling test.
5	Winter	<ul style="list-style-type: none"> The stairs that connect the dwelling with the outdoor were not taken into account since there was a large temperature difference between the heated space of the dwelling and the stairs.
11	Summer	<ul style="list-style-type: none"> Only the upper and lower parts of the shelters' door were sealed
12	Summer and winter	<ul style="list-style-type: none"> The exhaust fan was not sealed We did not take the garage into account, which was located on the ground floor and was connected to the rest of the dwelling through a door, since air infiltration in it was really high due to several grids on the door that face the outside. Therefore, we kept the door closed during the trials, as it is normally kept by the owner.
15	Winter	<ul style="list-style-type: none"> Two people remained inside the dwelling during the shelter trial in a different story. The blinds were not lowered.
16	Winter	<ul style="list-style-type: none"> Two blinds were not lowered for the shelter test.

6.5.2 ACH distribution

Measured *ACH* for shelters and dwellings also fit a log-normal distribution (see Figure 6.11 and Figure 6.12, respectively), as experimental *ACH* reported by other authors (Murray & Burmaster, 1995). In the case of shelters, the *P*-value for the Anderson Darling statistic was 0.389 at the 95% confidence level, while it was 0.586 for dwellings. Both values were above the significance level (0.05), which borne out the log-normal behavior of the data. The mean and the standard deviation for the natural logarithm of the *ACH* for shelters' and dwellings' distributions were -1.871 ± 0.623 and -1.488 ± 0.487 , respectively. From these results, we can see that the shelters show lower *ACH* than the dwellings but exhibit a larger standard deviation, which represents more dispersion among the *ACH* of shelters.

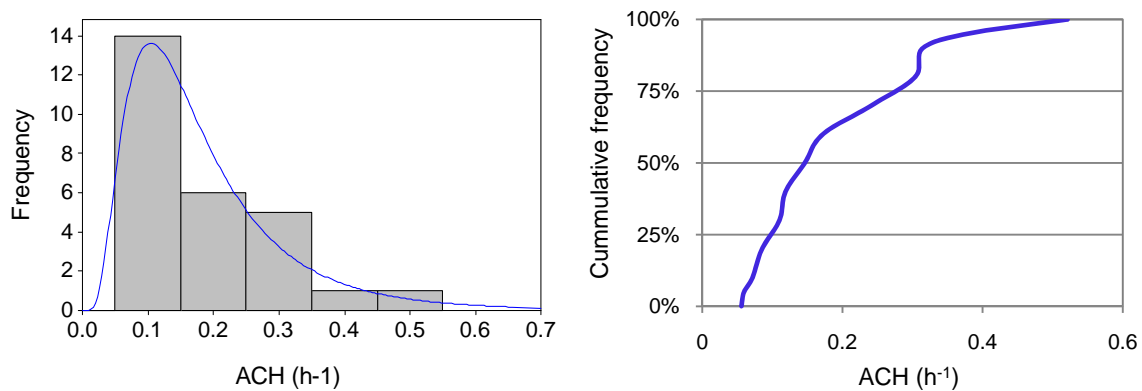


Figure 6.11 Log-normal distribution and cumulative frequency for the *ACH* of the shelters

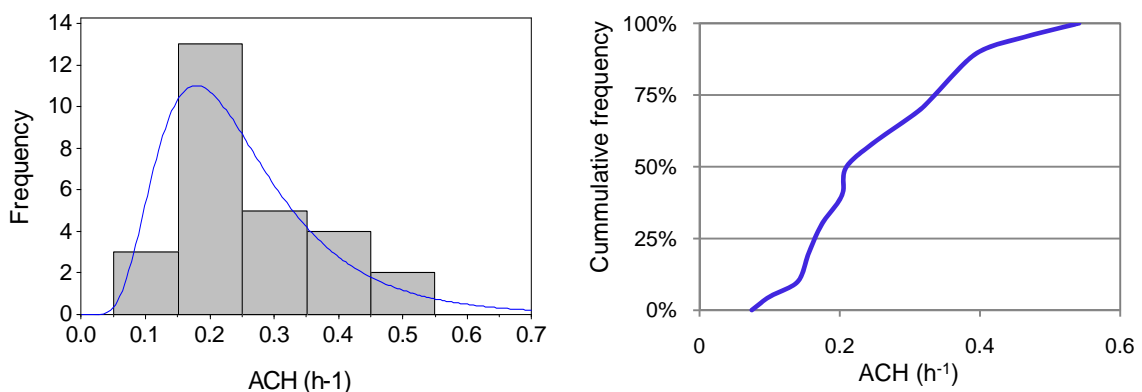


Figure 6.12 Log-normal distribution and cumulative frequency for the *ACH* of the dwellings

In relation to other experimental data reported by Blewett *et al.* (1996) and Rogers *et al.* (1990), concerning the *ACH* of sealed shelters (see Figure 6.13), we can say that our data range

was on the same interval as their data, between 0.1 and 0.5 h^{-1} , with most of the data located close to the lower limit. With regards to the dwellings the behavior is similar to that of shelters, they range on the same intervals although data reported by Rogers *et al.* (1990) cover a wider range and is more disperse, probably due to the low number of measurements.

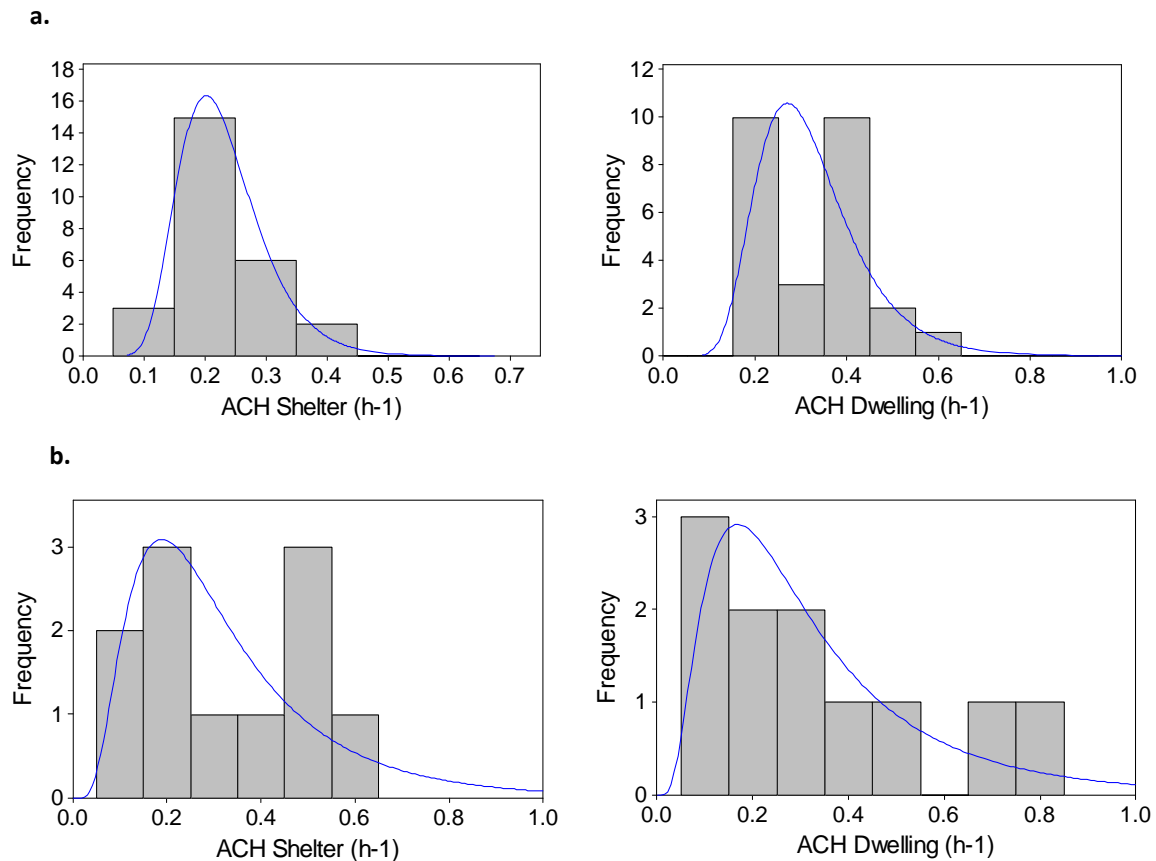


Figure 6.13 Experimental data on the *ACH* of sealed shelters and dwellings from other authors:
a) Blewett *et al.*, 1996, b) Rogers *et al.*, 1990

In general, concerning the *ACH* distribution obtained for Catalan dwellings with those reported for North American dwellings (see section 2.4.4), we observe that Catalan dwellings tend to be more airtight with a geometric mean of 0.226 h^{-1} while for the US it is 0.56 h^{-1} (see Table 2.17), around double. This tendency, as also mentioned in chapters 4 and 5 is logical since most constructions techniques in Catalunya are based on heavy materials like concrete or bricks, while in the US light materials such as wood and wood frame structure dwellings are common, which are leakier. Nevertheless we should remember that the size of the sample concerning US dwellings is much larger than the one used in this work for Catalunya. Regarding the data reported by Sfakianaki *et al.* (2008) concerning the *ACH* of 20 single-family dwellings in Greece

during the summer, they found a geometric mean of 0.76 h^{-1} , which in relation to our data is a high value, showing that Catalan dwellings tend to be more airtight than Greek dwellings.

ACH reduction

With the results obtained we can also estimate the reduction on the *ACH* gained by sheltering in a sealed room with regards to the *ACH* of the dwelling without expedient measures. Therefore, excluding the trials where the shelters' *ACH* were higher than those of the dwellings' and considering the worst scenario in the event of a toxic gas release, that is, all the air infiltrates to the shelter from outdoors; reductions from 1.5% to 84% were achieved (Figure 6.14), with an average of 35%. Blewett *et al.* (1996) obtained a similar reduction percentage when applying Method 2 in bathrooms, as mentioned in section 6.2. This reduction represents an increase in the protection offered by expedient sheltering, which in fact should be higher since part of the infiltration would come from indoor air and not directly from outdoors, where toxic gas concentration is higher.

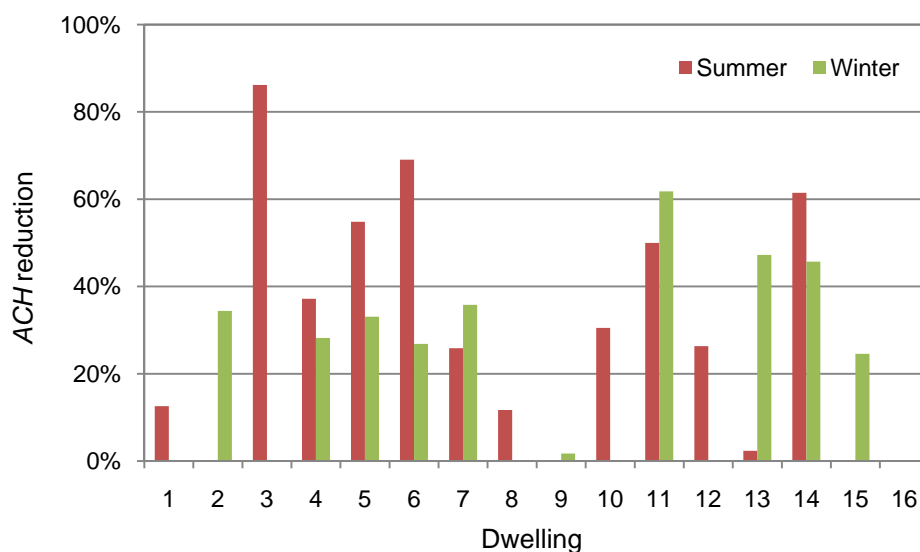


Figure 6.14 *ACH* reduction achieved in sealed shelters with regards to dwellings *ACH*

6.5.3 Possible relations of the *ACH* with different parameters

In order to explore any relationship between the *ACH* of the shelters, the *ACH* of the dwellings and the *ACH* reduction achieved in the sealed shelters with meteorological conditions and dwelling features, we obtained the correlation matrix for these variables in Minitab 2007 16.1

(see Table 6.13) in order to assess the linear relationship between them. For the analysis, we used the natural logarithms of the ACH instead of the original values since they exhibit a log-normal distribution; we analyzed the whole data, and the data classified according to the campaign and the shelter type. Among the variables studied we have the shelter area, the floor area, the number of stories, the number of stories used for the trial, the year of construction, the absolute temperature difference between the shelter and the outside ($\Delta T_{\text{shelter}}$), the wind speed during the shelter trial (v_{shelter}), the maximum temperature difference between floors inside the dwelling (Max ΔT dwelling), the absolute temperature difference between the dwelling and the outside ($\Delta T_{\text{dwelling}}$) and the wind speed during the dwelling trial (v_{dwelling}). From these results we can observe that the ACH of the shelter and the dwelling exhibit a high correlation in all situations analyzed, being slightly larger in the case of winter and windowless shelters.

Table 6.13 Correlation matrix for the ACH of shelters and dwellings

	$\ln(ACH_{\text{shelter}})$					$\ln(ACH_{\text{dwelling}})$			ACH reduction
	All data	Summer	Winter	Windowless	Exterior	All data	Summer	Winter	All data
$\ln(ACH_{\text{shelter}})$	1.00	1.00	1.00	1.00	1.00	0.59	0.44	0.76	-0.64
$\ln(ACH_{\text{dwelling}})$	0.59	0.44	0.76	0.68	0.52	1.00	1.00	1.00	0.17
Shelter area	-0.16	0.06	-0.19	-0.06	0.02	-	-	-	0.07
Floor area	0.23	0.03	0.49	0.41	0.15	-0.12	-0.18	0.07	-0.43
Number of stories	0.13	0.20	0.11	0.30	-0.11	0.31	0.26	0.37	0.05
Number of stories used for the trial	0.28	0.53	0.02	0.44	0.05	0.00	-0.04	0.04	-0.37
Year of construction	0.18	0.37	0.12	0.27	0.16	-0.19	-0.18	-0.08	-0.32
$\Delta T_{\text{shelter}}$	0.33	-0.49	0.64	0.30	0.29	-	-	-	-
v_{shelter}	-0.31	-0.39	-0.10	-0.27	-0.07	-	-	-	-
Max ΔT dwelling	0.21	0.61	-0.10	0.56	0.04	-0.13	0.14	-0.29	-0.41
$\Delta T_{\text{dwelling}}$	-	-	-	-	-	0.17	-0.16	0.45	-0.06
v_{dwelling}	-	-	-	-	-	-0.54	-0.53	-0.40	-0.11
ACH Reduction	-0.64	-0.67	-0.59	-0.47	-0.71	0.17	0.29	0.01	1.00

With regards to the dwelling features, the *ACH* of the dwelling just show some correlation with the number of stories, while the correlation with the other variables is negligible. The *ACH* of the shelter presents larger correlations with dwelling features than the *ACH* of the dwelling; nevertheless they are small and negligible, with the exception of the correlation for the number of stories used for the trial, in which higher correlations were obtained for the summer campaign and windowless shelters. This trend concerning the *ACH* of the shelters and the number of stories used in the trial might be linked with the maximum ΔT inside the dwelling, which also presents a large correlation with the *ACH* of the shelters. In the case of windowless shelters 3 of the 4 dwellings with this type of shelter were 3 and 4 storey dwellings, that is, dwellings where higher temperature differences inside took place generating a stronger stack effect. Moreover, this behavior is also in agreement with the fact that most of the air infiltrated to the shelter in the case of windowless shelters comes from the rest of the dwelling rather than the outdoor. In relation to meteorological conditions, shelters show higher correlations with indoor-outdoor temperature difference than with wind speeds; by contrast, dwellings present larger correlations with wind speeds. This makes sense since the indoor-outdoor temperature difference generates an indoor vertical air movement (the stack effect) producing more infiltration to the shelter from indoor air, also, if the shelter is windowless or the external walls of the shelter do not face the wind directly it would not create a significant pressure difference within the shelter. In relation to the *ACH* of the dwelling they are generally more affected by the wind speed than by the temperature difference, except during winter, in which the correlation with the temperature difference is higher, as is logical since wind speeds were not high and temperature differences increased, enlarging the stack effect.

Concerning the sign of the correlation coefficients for the temperature difference and the wind speed, we should expect them to be positive as the *ACH* increase with the increase of those parameters, however that statement is true for constant shell airtightness, which is not the case analyzed here, since the airtightness of the dwellings may differ from one another. On the other hand, this comparison is valid for each one of the 11 dwellings tested during the two campaigns, for which we can observe (see Figure 6.7 to Figure 6.10) that higher *ACH* were obtained for the campaign where both parameters were larger (dwellings 5, 6, 7, 10, 14) except for dwelling 2. With regards to the dwellings where one parameter was higher in one campaign but the other was lower (dwellings 4, 9, 11, 12, 13), the *ACH* varied according to the strength of each effect.

In relation to temperature differences inside the dwelling (see Figure 6.15) and the dwellings' features, larger differences between the ground and the top floor took place in 3 or more than 3 storey dwellings, as well as in dwellings with larger areas. Also, larger temperature differences were most frequent during winter due to the use of heating in some stories, and are also associated with the dwellings where the concentrations' difference for the uniformity criterion was larger (see Table 6.11), that is, mostly dwellings with 3 or more stories.

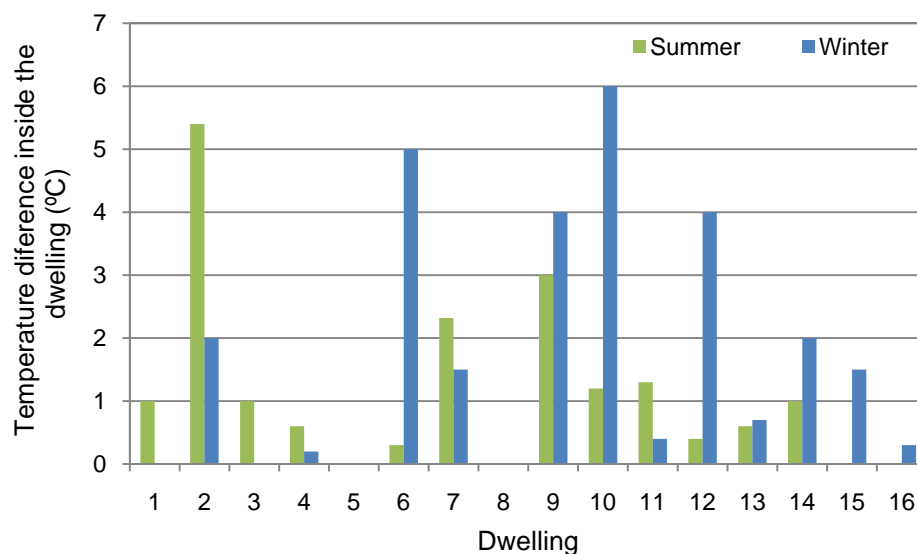


Figure 6.15 Temperature difference inside the dwellings

With regards to the relationship between the dwelling type (see Table 6.9) and the ACH of the dwellings, we found a significant difference between the means of the $\ln(ACH)$ for the different dwellings types, as presented on Figure 6.16, with a P -value of 0.009 for the ANOVA test. The largest differences belong to the terraced-end dwellings, which show the highest ACH , and the detached and semi-detached dwellings, which present the lowest ACH . The terraced middle dwellings are located on the middle. This trend is somewhat consistent with the fact that detached dwellings tend to be more airtight since they have a larger outdoor surface through which energy (heating) is lost, and therefore more attention is paid to the shell. For the $\ln(ACH)$ of the shelter, they follow the same trend as that of the dwellings but do not present a significant difference (P -value of 0.072).

Concerning the reduction gained on the ACH , we observe a high correlation with the ACH of the shelter, as is logical, and with the floor area, the number of stories tested, the year of construction and the maximum temperature difference inside the dwelling. With all these

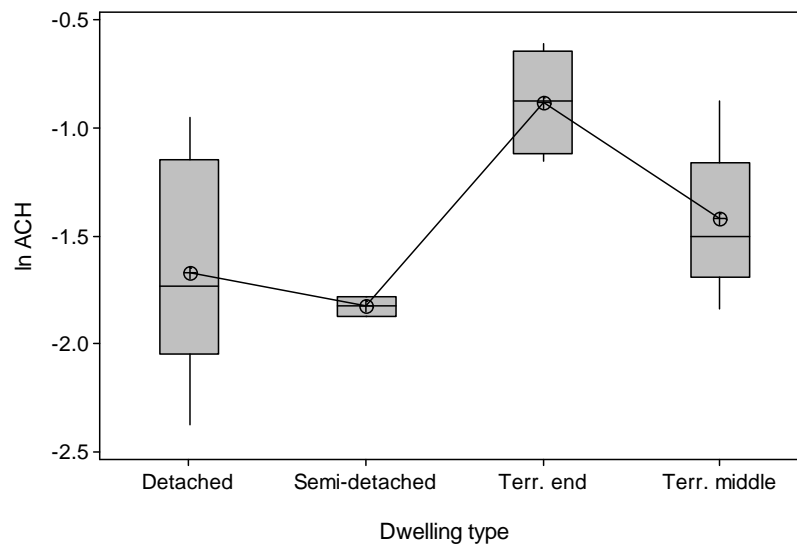


Figure 6.16 Boxplot for the $\text{Ln}(ACH)$ and the dwelling type

variables the ACH reduction presents and inverse behavior where it decreases as they increases. As the maximum temperature difference inside the dwelling is directly related to the number of stories tested, we expect the ACH reduction to decrease as they increase since the stack effect would be stronger, as mentioned before. This situation is probably related to the floor area too; by one side, larger floor areas tend to be associated with several numbers of stories while by the other, larger floor areas are also linked to larger spaces where uniform temperature conditions are less probable, generating internal airflows. Concerning the year of construction, this trend must be related to the fact that newer dwellings present a more airtight structure, as is consistent with increasing regulations mainly in the field of energy efficiency in buildings. Therefore, according to these results we can say that higher ACH reductions could be achieved in old dwellings, with small floor areas and few stories.

6.5.4 CO_2 fraction infiltrated to indoors

As we also measured indoor concentrations before and after the shelter test, we can make an estimate of the fraction of air infiltrated to the dwelling from the shelter, taking into account the concentration decay in the shelter and the initial and final indoor concentrations of the dwelling. To accomplish this, we performed a mass balance around the dwelling considering the shelter as an internal source with a constant emission (S), as shown in Eq. 6.7. Therefore,

knowing the volume of the dwelling, the ACH , the CO_2 outdoor concentration, the initial and final CO_2 indoor concentration and the elapsed time, we can estimate the source strength. For this calculation we took the time (t) as the period elapsed between the start of the shelter measures and the indoor concentration measures after the shelter finished; the ACH as that measured in the dwelling; the volume as the volume tested minus the volume of the shelter, and indoor concentrations as the average of the initial and final concentrations. In the case of dwellings where 3 or 4 stories were used for the trial, indoor concentrations were taken as the average concentrations of the story where the shelter was located, since for these dwellings, concentrations significantly differ from the ground story to the last. Following this procedure, we estimated the source strength in cm^3 of CO_2 per second, thus we divided it by the dwelling volume in order to obtain this rate in $ppm \cdot s^{-1}$.

$$C_i(t) = C_o + \frac{S}{V \cdot ACH} + \left(C_{i(t=0)} - C_o - \frac{S}{V \cdot ACH} \right) \exp(-ACH \cdot t) \quad \text{Eq. 6.7}$$

We could also calculate from the plot of CO_2 concentration versus time, the rate at which CO_2 decays in the shelter, it is, the rate at which CO_2 leaves. Assuming a constant decay rate, the slope of the decay line would give the decay concentration rate ($ppm \cdot s^{-1}$), as presented in Figure 6.17.

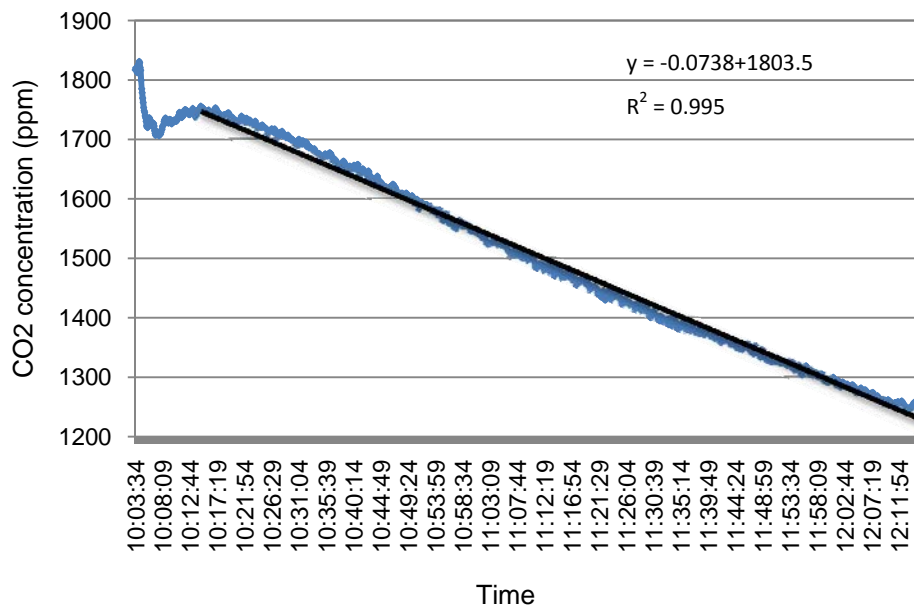


Figure 6.17 Estimation of the CO_2 concentration decay rate for the shelter of dwelling 12 in winter

Finally, with the source rate and the decay rate we calculated the fraction of CO₂ infiltrated to the dwelling, as shown in Table 6.14. For dwellings 3, 8 and 9 (winter) we did not have concentrations after the shelter test, so it was not possible to estimate the infiltrated fraction. In relation to the values obtained, we can see that most of them are between 0.15 and 0.80 with a geometric mean of 0.38, therefore the tendency observed is that more air exfiltrate to the outdoors rather than to the indoors. In relation to the trends of the infiltration fraction, we observe that it decreases as the floor area and the number of stories increase. From the table we also see that in 3 cases, fractions estimated were higher than one and the source rates were larger than the shelter's decay rates. Although in section 6.4.3 we mentioned that the effect of metabolic CO₂ could be negligible for short times (i.e. 2 minutes); probably in these cases, people stayed for a longer time before leaving the dwelling at the beginning of the shelter trial or while measuring indoor concentration at the end of the trial, causing a significant increase on the indoor concentration.

Table 6.14 Fraction of CO₂ infiltrated to the dwelling

Dwelling	Campaign	Source rate (ppm·s ⁻¹)	Shelter decay rate (ppm·s ⁻¹)	Infiltrated fraction to the dwelling
1	Summer	0.051	0.107	0.471
2	Summer	0.034	0.123	0.280
	Winter	0.047	0.068	0.700
4	Summer	0.022	0.042	0.536
	Winter	0.011	0.051	0.220
5	Summer	0.033	0.064	0.518
	Winter	0.048	0.168	0.284
6	Summer	0.017	0.049	0.347
	Winter	0.026	0.077	0.339
7	Winter	0.038	0.160	0.240
9	Summer	0.044	0.151	0.288
10	Summer	0.038	0.089	0.432
	Winter	0.036	0.064	0.563
11	Summer	0.038	0.044	0.866
	Winter	0.058	0.042	1.381
12	Summer	0.027	0.057	0.472
	Winter	0.017	0.074	0.229
13	Summer	0.051	0.083	0.617
	Winter	0.069	0.058	1.207
14	Summer	0.057	0.034	1.650
	Winter	0.023	0.076	0.302
15	Winter	0.024	0.036	0.679
16	Winter	0.022	0.161	0.135

Anyway, we must take into account that this is just an approximation made in order to have a rough idea of the fraction of CO₂ infiltrated to the dwelling and therefore an approximation of the fraction of air exchanged with indoor air; in which several assumptions were made and also several sources of errors exist. Possible sources of errors are:

- The opening of the shelter door after starting the recording process, and open it again after the trial time to extract the sensor. This allows some air exchange directly with the dwelling.
- The presence of people (maximum 2) at the beginning and end of the shelter trial for around 4 minutes; which corresponds to the time while the shelter door was sealed (2 minutes) and during concentrations measurement after the trial (2 minutes). Since the average CO₂ emission rate of a person is 0.005 l/s (ASHRAE, 2005), 2 people would discharge around 2.4 l of CO₂ during 4 minutes. Therefore, this situation could have increased indoor concentration from 5 to 15 ppm, in bigger and smaller dwellings respectively; generating an overestimation in the source rate up to 3%, mainly in smaller dwellings.
- In dwellings 2 and 15, presence of one person inside the dwelling during the trial.

Despite these possible sources of errors, we have borne out that effectively there is a fraction of air exchanged with indoor air.

6.6 UPC-CETE model accuracy

In order to assess the applicability of the model developed in the previous chapter (Eq. 5.11 to Eq. 5.13), we applied it to the dwellings studied in this chapter with the aim of estimating the airtightness (c'), and then the ACH using the AIM-2 ventilation model. To accomplish this we assumed a heavy structure type for all dwellings ($ST = 0$) and used the dwellings parameters reported in Table 6.9. The age was estimated as the difference between 2009 and the year of construction or substantial improvements. The NS parameter was assigned according to the tested number of stories shown in Table 6.9, it took a value of 1 for one-storey dwellings and 2 for dwellings with two or more stories. Finally, the area parameter corresponds to the floor area presented in Table 6.9. Concerning the terrain class, we assigned it according to the surroundings of the dwellings and the estimates of shelter coefficients reported in Table 2.10,

as shown in Table 6.15. Meteorological conditions used correspond to those presented in Table 6.11, but in relation to wind speeds, they were now corrected at the height of the dwelling using the *LBL* model (Eq. 2.53). The absolute pressure and the relative humidity also needed for density calculations were taken as the average of the values registered by the CO₂ sensor.

Table 6.15 Terrain classes assigned to tested dwellings in order to apply the AIM-2 ventilation model

Dwelling	Terrain class	Dwelling	Terrain class
1	1	9	4
2	2	10	2
3	2	11	2
4	1	12	4
5	3	13	4
6	2	14	4
7	2	15	3
8	3	16	1

Figure 6.18 shows the results of the airtightness, expressed as the power law flow coefficient c' for each dwelling, and Figure 6.19 presents the results for predicted and experimental *ACH*. From these results we can see that the predicted *ACH* greatly differs with the real values in some cases, while good predictions were obtained in others. Also, we can see that for almost half of the dwellings (44%) experimental values were underestimated, while the other half were overestimated (56%). Looking at the values, we observe that the dwellings where the *ACH* was highly underestimated (underestimations larger than 30%), correspond to dwellings of 4 stories (dwellings: 2, 7, 9). Then this behavior must be directly related to this situation, as is consistent with the fact that for the development of the airtightness model we did not account with data from 4 storey dwellings and only have three measurements from 3 storey dwellings. Therefore, although we did not find any significant difference between the means of the $\ln(c')$ for 2 and 3 storey dwellings in section 5.1.1, probably due to the lack of representation for 3 storey dwellings; we effectively have borne out from these experimental results, that there is a significant difference that must be taken into account in the prediction model. Nevertheless, in the case of dwelling 10, a 3 storey dwelling, the trend is contrary and the experimental values are highly overestimated by the predicted ones, which make us consider *ACH* for this dwelling as outliers. Reviewing specific characteristics of dwelling 10, we found that this is the unique dwelling from those tested that has a radiant-floor heating

system, so we thought this could directly affect the airtightness of the dwelling since less holes though the walls are needed than in dwellings with a radiator heating system. Moreover, apart from these situations, we should mention that the AIM-2 ventilation model also tends to underestimate the airflow by about 10% (Wang *et al.*, 2009) which is probably the case of dwellings: 1, 4, 12, 13 and 16.

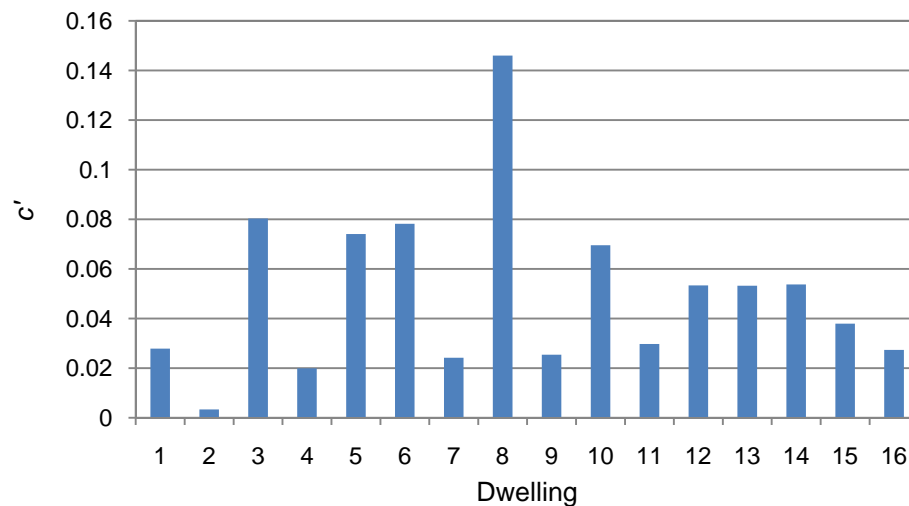


Figure 6.18 Airtightness estimated with the UPC-CETE model for each dwelling

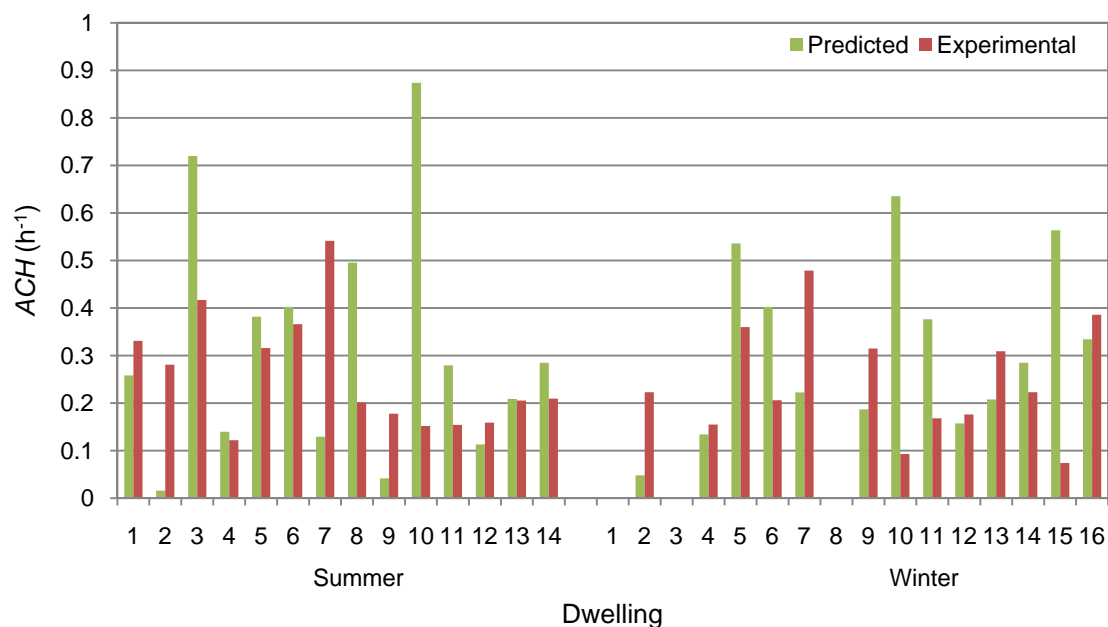


Figure 6.19 Experimental and predicted ACH

Figure 6.20 shows the dot plot for experimental versus predicted values of the ACH, from this plot we can see that some points are very dispersed and far from the diagonal line, while

others lied very close to it. The mean absolute deviation of the data is 0.18 h^{-1} and the squared correlation coefficient between predicted and experimental values obtained is 0.006, a very low value, which gives the sense that the model could not explain any variance of the experimental data. As shown in the plot, *ACH* corresponding to 3 or more than 3 storey dwellings (red dots) comprise the outer values, which is logical since for the model development we only considered data from dwellings with one or two stories, as mentioned in the previous paragraph. Therefore if we did not consider the data from dwellings with 3 or more stories, and the *ACH* for dwelling 15, which also seems to be an outlier; the squared correlation increases to 0.4. This squared correlation is better and is also similar to that obtained in the development of the airtightness model (see regression 4 in Table 5.4), which bears out that the model could explain around 40% of the *ACH* variance. The mean absolute deviation in this case is 0.11 h^{-1} , which means that the predicted values present an average deviation of 0.11 h^{-1} with respect to the observed value.

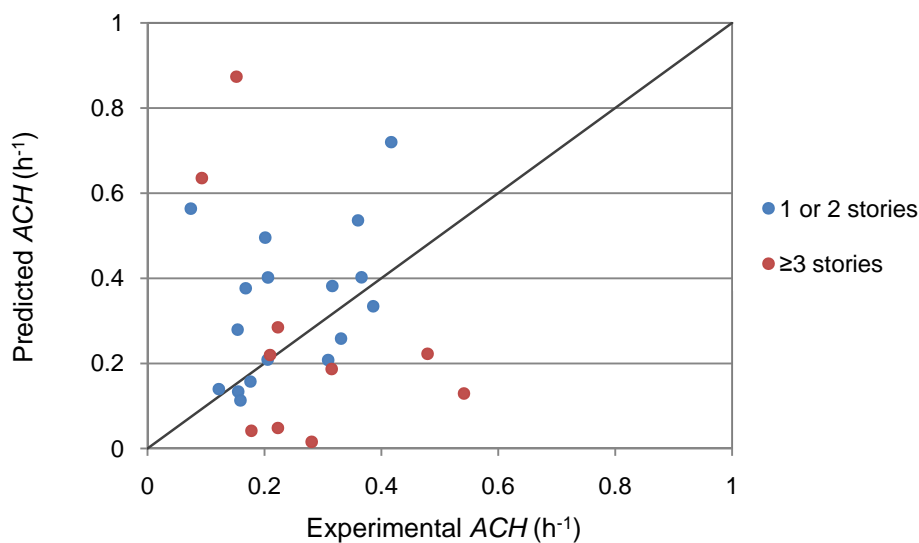


Figure 6.20 Experimental versus predicted *ACH* dot plot

6.7 Adjustment of the airtightness model

From the point of view of a shelter-in-place event, emergency managers should work taking into account a conservative situation. Therefore, the usefulness of any model, as in this case the model to estimate the *ACH*, should be restricted by its predicted accuracy in the sense that predictions might overestimate real values rather than underestimate them. Therefore, in

order to adapt the airtightness model to dwellings with more than 2 stories, which we thought are the principal source of underestimation, we redefined the NS parameter of the airtightness model (Eq. 5.11 to Eq. 5.13). In this case we considered that the NS parameter takes the value concerning the number of stories of the dwelling, for example, the NS take a value of 3 for a 3-storey dwelling. Thereby, for the application of the model to the tested dwellings applying this modification to the NS parameter, we consider the NS as the tested number of stories reported in Table 6.9. With this modification, predictions for dwellings 2, 7, 9 and 16 improved (see Figure 6.21), obtaining overestimations for the winter campaign. However, the underestimation continued for the summer campaign, although it decreased. This situation, in which predictions improve only for one season (winter) let us think that the problem is probably with the ventilation model, which performs better at high indoor-outdoor temperatures differences. In the case of dwelling 10, the overestimation increases as the NS parameter increases from 2 to 3.

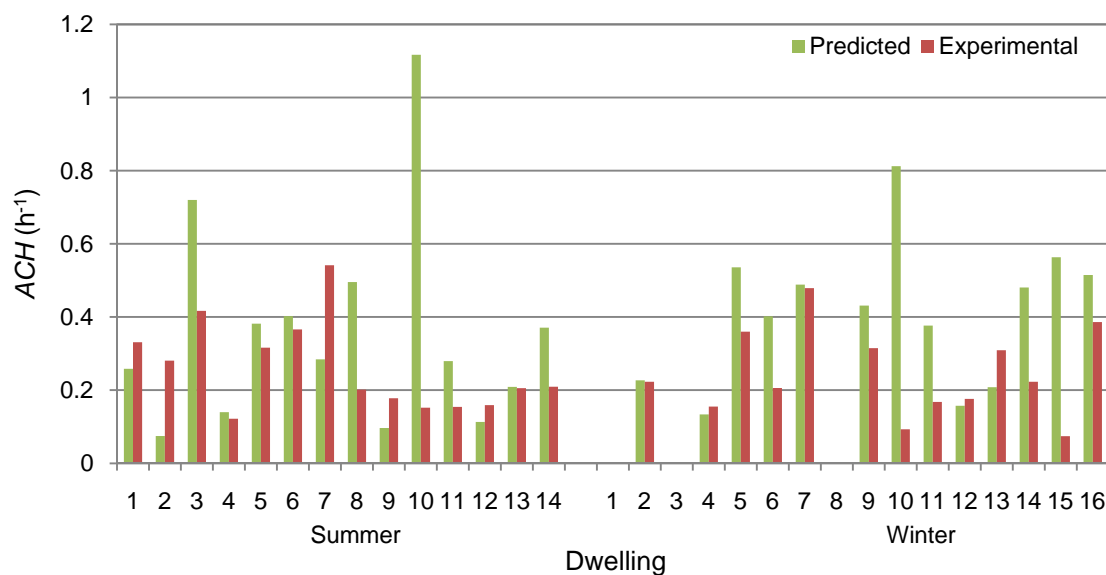


Figure 6.21 Experimental and predicted ACH modifying the NS parameter of the UPC-CETE model

From these results, we see that the application of the UPC-CETE model modifying the NS parameter gave better results from the point of view of the risk assessment, since it overestimate rather than underestimate actual ACH in most cases (70%). In addition, if we assume that terrain class for all the dwellings consist of class 1, no obstructions or local shielding, we obtained the values shown in Figure 6.22. In this situation, underestimation reduced to 15%. Concerning the magnitude of the ACH , the highest prediction reached is 1.2

h^{-1} while all the experimental values and most of the predicted ones (80%) stayed below 0.8 h^{-1} . That is, *ACH* were much lower than the common value generally used in delimiting actuation zones in the case of a toxic gas release (2 h^{-1}), considered as a conservative value. Therefore, under these conditions (assuming a terrain class with no obstructions or local shielding and modifying the *NS* parameter to be the actual number of stories), we can state that the usage of this model in the estimation of the *ACH* of Catalan dwellings, with the purpose of delimiting actuation zones in the event of a shelter-in-place situation, is a good tool that improves actual determination of the *ACH* assuming it as a fix value, and thus gives better and more accurate estimations of the *ACH*.

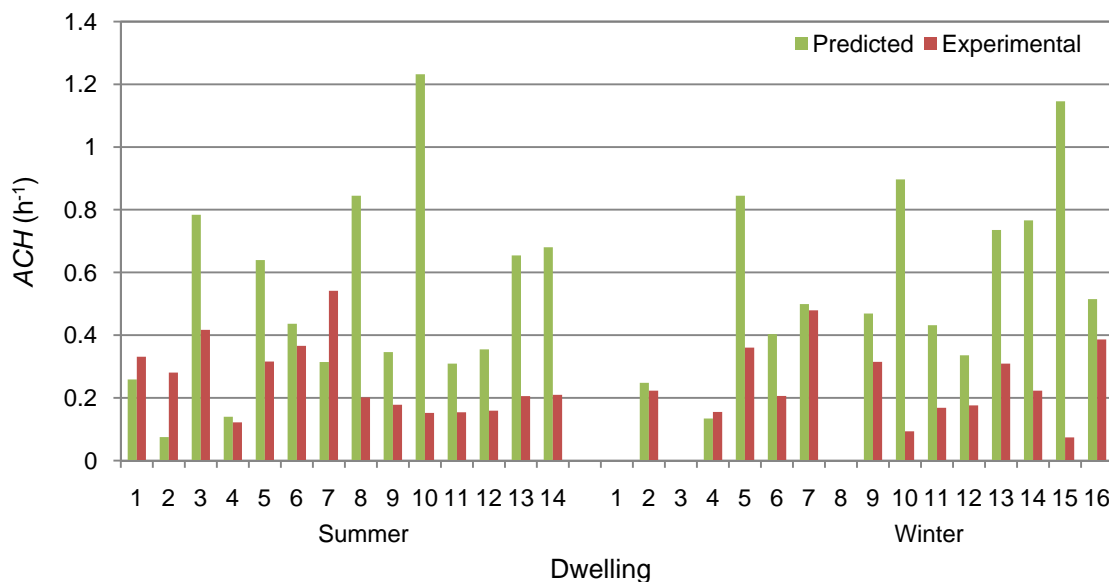


Figure 6.22 Experimental and predicted *ACH* modifying the *NS* parameter of the UPC-CETE model and assuming a terrain class of no obstruction or local shielding to apply the AIM-2 model

Chapter 7. Assessment of shelter-in-place effectiveness and estimation of the evacuation radius in Catalunya.

A case study

"For believers, God is in the beginning, and for me He is at the end of all considerations..."
Max-Planck

This chapter presents how to incorporate the estimation of the airtightness distribution obtained with the UPC-CETE model, in the assessment of shelter-in-place effectiveness in Catalunya using a geographic information system. As described in Chapter 2 the assessment of shelter-in-place effectiveness is subjected to three main stages: the calculation of the outdoor gas dispersion after the release, the estimation of indoor concentration from outdoor concentration and the evaluation of human vulnerability. We specially focus this chapter on the step concerning the determination of indoor concentration at a community scale, for which we employ a methodology similar to that used in Chapter 4 and Chapter 5 in the estimation of the *ACH* distribution in Catalunya. Therefore we assessed a hypothetical case study taking place in an industrialized area of Catalunya. In this example we considered the urbanized area, the census tracts and the real number and characteristics of single-family

dwellings present in the affected zone, in order to account for air leakage variability among dwellings which lead to a more accurate description of shelter-in-place effectiveness in a residential community (Chan *et al.*, 2007b). Apart from considering the air-leakage variability or not (assuming a constant airtightness value), we also analyzed the situation where constant adsorption takes place and expedient measures are implemented.

7.1 Scenarios analyzed

In order to assess the effect that constant leakage, air leakage variability, possible adsorption over indoor surfaces and implementation of expedient measures, have on the estimation of the evacuation radius, we defined 4 possible scenarios that consider these situations in the estimation of indoor concentration, named: the base case, constant adsorption, expedient sheltering, and constant airtightness. The base case considers the implementation of normal sheltering (closing all external openings and shut down mechanical ventilation systems) and the use of the airtightness distribution by census tract to account for air leakage variability. This scenario represents the most general shelter-in-place situation in a community. The constant adsorption scenario includes the same considerations of the base case but in addition, contemplates the case of constant adsorption over indoor surfaces; therefore this scenario would only represent the case when substances adsorb over indoor surfaces (see section 2.2). The third scenario, expedient sheltering, only differs with the base case in that it considers sheltering in a room with expedient measures, besides closing external openings and shutting down ventilation systems. Finally, the constant airtightness scenario does not take into account building's air leakage variability and assumes a fixed value equal to the 90th percentile of the airtightness distribution in Catalunya. Commonly, emergency managers used a fixed value of the *ACH* to perform calculations; however, the *ACH* of a building is a changing value that depends on meteorological conditions and the airtightness, therefore it is more accurate to use a fixed airtightness. In this case, we used the 90th percentile of the airtightness (c') distribution in Catalunya obtained with the UPC-CETE model.

Other considerations made to perform calculations were:

- People initiate shelter from the beginning of the release.

- Shelter-in-place should terminate as soon as outdoor concentration falls below indoor concentration, but since termination time in a community would be different for each building depending on the downwind distance from the source, besides taking into account that the advice to exit shelters should be given to the whole community; a unique termination time must be established. Therefore, we considered that shelter-in-place finished when the cloud had completely passed over the affected area and there was not residual outdoor concentration. At this time we assumed people ventilate dwellings quickly or went outside, thus, no further exposure was considered.
- Concerning the mechanism that lower indoor concentration, as chemical reactions, sorption over indoor surfaces or filtering by building envelope, we only considered the possibility of sorption over indoor surfaces.
- Criteria to establish an evacuation area or define a zone where shelter-in-place could be implemented are subjected to local authorities and emergency managers. They commonly involve the assessment of human vulnerability through a threshold value or toxic load limit computed from a LOC (AEGL, ERPG, TEEL, IDHL) or a casualty' probability. For the scenarios studied here, we established two different criteria, in order to define the evacuation radius:
Criterion 1: The largest distance within which casualties inside dwellings exceed 0.1%.
Criterion 2: The largest distance where the indoor toxic load (TL_i) exceeds the toxic load limit (TLL) based on the AEGL-3 threshold concentration.

7.2 Case study definition

Our hypothetical case consists of a chlorine facility near the city of Terrassa, with the center of the plant located at the following coordinates: 415863, 4601800 (UTM31). The largest quantity of chlorine corresponds to the one storage in a pressurized vessel situated in the middle of the installation. The storage vessel is a horizontal cylinder, 10 m long and 2.6 m in diameter, with a maximum capacity of 80000 kg of chlorine, and an average amount of 60000 kg. The temperature in the vessel is 15 °C, and since the product is 2-phase the pressure in the tank is 5.87 bar. Therefore we analyze the event of the entire content release (60000 kg) in 10 min, which implies a release rate of 100 kg/s. For the calculations we considered the terrain as an industrial area with a ground roughness (z_0) of 0.3 m. For meteorology we made the analysis using a wind speed of 4 m/s and neutral stability (4D), since this is a frequent meteorological

situation, for which outdoor heavy gas dispersion models like ALOHA or SLAB, gave similar results and have been more studied. Average temperature and humidity are 15 °C and 66%, respectively. Acute exposure guideline levels (AEGL) for chlorine defined at different times by the EPA, are shown in Table 7.1.

Table 7.1 AEGL values for Chlorine ppm ($\text{mg}\cdot\text{m}^{-3}$)

	10 min	30 min	60 min	4 h	8 h
AEGL 1	0.50 (1.41)	0.50 (1.41)	0.50 (1.41)	0.50 (1.41)	0.50 (1.41)
AEGL 2	2.8 (8.29)	2.8 (8.29)	2.0 (5.92)	1.0 (2.96)	0.71 (2.10)
AEGL 3	50 (148.18)	28 (81.19)	20 (59.27)	10 (29.63)	7.1 (21.04)

Source term

Chlorine is stored at 15 °C as a saturated liquid in a pressurized vessel; consequently, due to the depressurization it is released to the atmosphere in a two phase flow for which the flash plus aerosol fraction is 37%. This fraction means that 37 kg/s will instantaneously evaporate when coming out, while the other 63% would fall to the ground from which it will evaporate. However, under these conditions the evaporation rate of chlorine is equivalent to the rate of liquid chlorine falling to the ground (63 kg/s), therefore, it immediately incorporates to the gas cloud. Consequently, we assumed the entire release flow (100kg/s) as a direct gas flow from the ground.

7.3 Methodology

As mentioned above and discussed in Chapter 2, the assessment of shelter-in-place effectiveness consists on the evaluation of three main stages: outdoor gas dispersion, indoor concentration and human vulnerability. With the aim of incorporating the air leakage variability in the calculations and perform the assessment in a geo-referenced way, the steps shown in Figure 7.1 were proposed. Detailed explanation of each step is given in the following paragraphs.

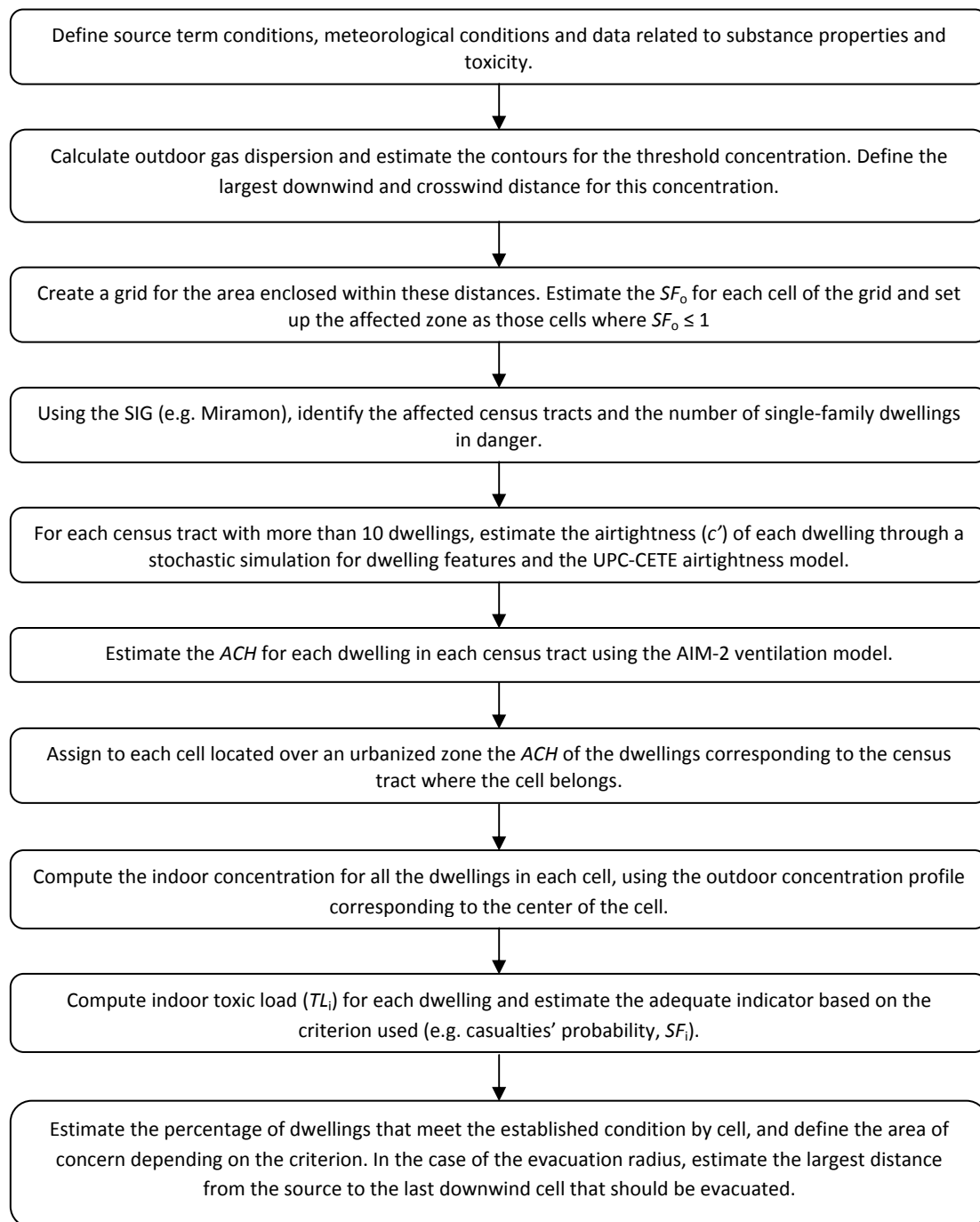


Figure 7.1 Flow diagram to estimate an area of concern (evacuation, shelter-in-place) given a toxic gas release

7.3.1 Outdoor dispersion

To compute outdoor dispersion of heavy gases, like chlorine, we should use heavy gas dispersion models. Among widely-used dense gas models we found ALOHA, HGSYSTEM, SLAB,

SCIPUFF, PHAST and TRACE. A recent study performed by Hanna *et al.* (2008), focused on the comparison of these dispersion models when modeling three chlorine accidents. They concluded that given the same source emissions rates, for a 10-min average concentration, centerline concentrations at downwind distances ranging from 0.1 to 10 km, agree with each other within plus and minus a factor of two most of the time. They also stressed that real concentrations were expected to be lower than those calculated with the dispersion models, since they do not take into account outdoor removal processes like dry deposition at the surface or chemical reactions (e.g. photolysis). One major observation made by these authors is that the estimation of the source or release term is very important to obtain reliable results.

For our study case we calculate outdoor dispersion using the SLAB, which is a dispersion model developed in the 1980s by the Lawrence Livermore National Laboratory of the US department of energy. This code had been incorporated into different commercial risk assessment packages like BREEZE HAZ software or EFFECTS. One advantage of using this model is that it generates a result sheet that contains several calculations parameters at different times and distances from which the user could estimate outdoor concentrations at different times and locations applying the equation of the transient puff mode of the model (Ermak, 1990), without having to read concentration from a graphic or running the program several times. Consequently, as in this study case we need to know the concentration profile over time at many locations, we took advantage of the result sheet generated by SLAB, and developed a Matlab code to calculate the concentration profile over time at different locations using the transient puff mode equation and the calculation parameters of the result sheet. Figure 7.2 shows a copy of the result sheet generated by SLAB, which contains the transient puff mode equation and the parameters needed to solve the equation.

Therefore, in order to set the limits of the zone where the concentration is greater than the threshold concentration, the AEGL-3 at 10 min in this case (see Table 7.1), we first run our study case in BREEZE HAZ version 4 using the SLAB model and obtained the maximum width and downwind distance of the plume for the threshold concentration, and the result sheet. With the maximum width and downwind distance we created a grid using cells of 50 x 50 m length in Matlab and estimated outdoor concentrations profiles for the center of each cell (all the calculations involving the cells correspond to the center of the cells). Afterwards, outdoor plume contours for the threshold were generated in Matlab and written in topographic files so that they could be opened with the GIS (Miramon). Afterwards, for each cell of the grid we


```

time averaged (tav = 600. s) volume concentration: concentration contour parameters
c(x,y,z,t) = cc(x) * (erf(xa)-erf(xb)) * (erf(ya)-erf(yb)) * (exp(-za*za)+exp(-zb*zb))

c(x,y,z,t) = concentration (volume fraction) at (x,y,z,t)
x = downwind distance (m)
y = crosswind horizontal distance (m)
z = height (m)
t = time (s)

erf = error function
xa = (x-xc+bx)/(sr2*betax)
xb = (x-xc-bx)/(sr2*betax)
ya = (y+b)/(sr2*betac)
yb = (y-b)/(sr2*betac)
exp = exponential function
za = (z-zc)/(sr2*sig)
zb = (z+zc)/(sr2*sig)
sr2 = sqrt(2.0)

x      cc(x)    b(x)    betac(x)    zc(x)    sig(x)    t      xc(t)    bx(t)    betax(t)
-1.86E+01  0.00E+00  1.67E+01  4.68E+00  0.00E+00  0.00E+00  5.96E+00  0.00E+00  1.86E+01  1.52E-01
-1.49E+01  6.94E-03  1.70E+01  5.29E+00  0.00E+00  1.27E+00  7.06E+00  1.86E+00  2.06E+01  1.68E-01
-7.43E+00  7.87E-03  1.78E+01  6.13E+00  0.00E+00  2.20E+00  9.43E+00  5.57E+00  2.46E+01  2.01E-01
-3.72E+00  8.22E-03  1.84E+01  6.63E+00  0.00E+00  2.53E+00  1.07E+01  7.43E+00  2.66E+01  2.17E-01
2.86E-06  8.49E-03  1.92E+01  7.19E+00  0.00E+00  2.81E+00  1.21E+01  9.29E+00  2.86E+01  2.34E-01
3.72E+00  8.68E-03  2.01E+01  7.81E+00  0.00E+00  3.03E+00  1.35E+01  1.11E+01  3.06E+01  2.50E-01
7.43E+00  8.82E-03  2.11E+01  8.49E+00  0.00E+00  3.22E+00  1.51E+01  1.30E+01  3.26E+01  2.66E-01
1.11E+01  8.89E-03  2.23E+01  9.21E+00  0.00E+00  3.38E+00  1.67E+01  1.49E+01  3.46E+01  2.83E-01
1.86E+01  8.90E-03  2.48E+01  1.08E+01  0.00E+00  3.65E+00  2.01E+01  1.86E+01  3.86E+01  3.15E-01
:      :      :      :      :      :      :      :      :      :

```

Figure 7.2 Result sheet generated by SLAB

estimated the outdoor toxic load and the outdoor safety factor (Eq. 2.8) in order to establish the affected zone, the area in which people standing outside can experience severe health affections or even death. We defined this zone as the area where the TL_o exceeded the TLL (Eq. 7.2), it is, those cells that exhibited a $SF_o \leq 1$. Later, we identified the affected census tracts and the number of single-family dwellings involved, using the grid and the SIG (Miramon) information concerning the census tract, the urbanized area and the census information.

$$SF_o = \left[\frac{TLL}{TL_o(t)} \right]^{\frac{1}{n}} \quad \text{Eq. 7.1}$$

$$TLL = (AEGL - 3_{at10min})^n \cdot 10min \quad \text{Eq. 7.2}$$

7.3.2 Indoor concentration

Air exchange rate

To estimate indoor concentration we first performed a stochastic simulation for dwellings characteristics (as in section 4.3.2) in each census tract with more than 10 dwellings in order to estimate the airtightness of each dwelling by applying the UPC-CETE airtightness model. In this case we used the UPC-CETE airtightness model with the number of stories parameter modified NS' (Eq. 5.11 to Eq. 5.13), it is, using the real number of stories instead of the NS indicator, which only took a value of 1 or 2. This modification of the airtightness model made in section 6.7 allows us to make more conservative predictions, since the model tends to overestimate rather than underestimate the airtightness.

For dwellings with Age ≤ 9 :

$$c' = \exp(-5.6815 + 0.00698 \cdot Area + 0.5075 \cdot ST + 0.0784 \cdot Age + 0.345 \cdot NS') \quad \text{Eq. 7.3}$$

For dwellings with $9 < Age \leq 64$:

$$c' = \exp(-5.6815 + 0.00698 \cdot Area + 0.5075 \cdot ST + 0.0784 \cdot 9 + 0.345 \cdot NS') + \left(Area \cdot \frac{2.5}{50^{2/3}} \cdot 6.33 \cdot 10^{-5} \cdot (Age - 9) \right) \quad \text{Eq. 7.4}$$

For dwellings with Age > 64 :

$$c' = \exp(-5.6815 + 0.00698 \cdot Area + 0.5075 \cdot ST + 0.0784 \cdot 9 + 0.345 \cdot NS') + \left(Area \cdot \frac{2.5}{50^{2/3}} \cdot 6.33 \cdot 10^{-5} \cdot (64 - 9) \right) \quad \text{Eq. 7.5}$$

In addition to calculate the airtightness distribution for the affected census tracts, we also estimated the airtightness distribution for the whole Catalunya using the UPC-CETE model with the number of stories parameter modified NS' , in order to obtain the 90th percentile of the airtightness distribution to assess the constant airtightness scenario.

After calculating the airtightness, the ACH was estimated for each dwelling through the AIM-2 ventilation model, assuming an indoor temperature of 25 °C. In the case of the constant airtightness scenario, we also computed the ACH for each dwelling since we needed the height

(a function of the number of stories) to compute the infiltration flow through the AIM-2 model, and the volume to estimate the *ACH*. Therefore, unless we considered a constant airtightness, the *ACH* of the dwellings was not constant since it depends on dwellings characteristics. With the purpose of applying the AIM-2 model, the following assumptions were made:

- The presence of a flue was considered for all dwellings, as this is a typical construction feature in single-family dwellings in Catalunya.
- Each story was 2.5 m high.
- The flue outlet was 1.5 m above the upper ceiling.
- Crawl space foundations were not considered. Single-family dwellings in Catalunya are typically constructed using heavy materials, and crawl spaces in this type of construction are very well insulated, so the potential air infiltration through this space is considered negligible.
- All infiltration was assumed to take place through the walls and the flue. Infiltration through floor and ceiling was not considered, since the techniques and materials used in residential constructions in Catalunya ensure that these components are very airtight.
- The relation between the flue flow coefficient (c_{flue}) and the total flow coefficient (c_1), Y (Eq. 2.52) was assumed to be 0.2, which is a typical value reported by Walker and Wilson (1998).
- A terrain with no obstructions or local shielding (Table 2.10) was assumed as the shelter situation for the buildings. More conservative *ACH* from the point of view of a shelter-in-place situation were obtained for this terrain class in the previous chapter (see section 6.7) with regards to other terrain classes.
- The flue was considered unsheltered.

Indoor concentration

After calculating the *ACH* for each dwelling, we assigned to each cell located over an urbanized zone the dwellings corresponding to the census tract where the cell belongs. Then, for the base case, the constant airtightness and the expedient sheltering scenario, we computed indoor concentration through Eq. 2.22 for every dwelling, using the outdoor concentration profile corresponding to the center of the cell. Nevertheless, in the case of the expedient sheltering scenario, we assessed the protection gained by sheltering in a room with expedient

measures, assuming that the *ACH* of the shelter consisted of a 65% of the dwelling *ACH*. This reduction (35%) corresponded to the average reduction obtained from the experimental trials described in Chapter 6.

In relation to the constant adsorption scenario, we considered the case where sorption over indoor surfaces occurs, considering an adsorption velocity (v_d) of $1.4 \cdot 10^{-4} \text{ m} \cdot \text{s}^{-1}$, which is the highest value for chlorine (see Table 2.2) and an indoor surface to volume ratio (A/V) of 3.5 m^{-1} . Indoor concentration in this scenario was calculated through Eq. 2.23 for every dwelling in each cell, using the outdoor concentration profile corresponding to the center of the cell. Thereby, with indoor concentrations profiles by dwelling, we could estimate indoor concentration distribution for each cell at different times. Besides, since we considered all the dwellings of the census tract by cell, we included all the possible *ACH* that could take place at that location, not just some, which reduces any underestimation.

7.3.3 Indicators of shelter-in-place effectiveness

The purpose of shelter-in-place is to provide a protected space where people could remain safe while the toxic cloud passes. Therefore, in the case of a community where buildings are different we should evaluate shelter-in-place effectiveness in every building, depending on its airtightness and location, in order to define the area where shelter-in-place could be implemented and the area where this measure does not provide enough protection and has to be evacuated. To accomplish this, we assessed individual and collective indicators of shelter-in-place effectiveness at different times. First we calculated the indoor toxic load (Eq. 2.1) received inside the dwellings at different times after the beginning of the release. Then, with the TL_i and the probit equations (Eq. 2.2 and Eq. 2.3) we computed the casualty probability inside each dwelling, using the constants of Table 3.10 for chlorine, and we estimated the percentage of dwellings that exhibited a casualty probability greater than 0.1%. Cells that contained any dwelling with a casualty probability equal or higher than 0.1% comprised the evacuation zone according to criterion 1. In relation to criterion 2, we estimated the indoor safety factor through Eq. 7.9, based on the AEGL-3 threshold, and computed the percentage of dwellings with a SF_i lower than 1 by cell. Therefore, those cells with a percentage of dwellings higher than 0, defined the area to be evacuated.

$$TL_i = \int_0^t C_i^n dt \quad \text{Eq. 7.6}$$

$$P_r = a + b \cdot \ln(TL) \quad \text{Eq. 7.7}$$

$$P = \frac{1}{2} \left[1 + \operatorname{erf} \left(\frac{P_r - 5}{\sqrt{2}} \right) \right] \quad \text{Eq. 7.8}$$

$$SF_i = \left[\frac{TLL}{TL_i(t)} \right]^{\frac{1}{n}} \quad \text{Eq. 7.9}$$

Since the toxic load is a cumulative variable, the areas defined based on this parameter increased with time. After the toxic cloud passed through a specific location, indoor concentration starts to decrease but the TL_i continue increasing due to the residual indoor concentration. Therefore, the time at which indoor concentration began to decrease, it is, when outdoor concentration becomes lower than indoors, should be the time to finish sheltering. However, at a community scale we must assure a safe outdoor concentration in the whole area that does not represent any risk from that time on. The most conservative case therefore, is to consider the sheltering termination time as the time needed by the cloud to completely pass over the maximum downwind distance where the $SF_o \leq 1$, as already mentioned in section 7.1.

7.3.4 Possible simplifications

In order to simplify and speed up the calculations concerning indoor concentration, shelter-in-place effectiveness indicators and the definition of the zones of concern (i.e. evacuation, shelter-in-place), we can take advantage of the airtightness (c') distribution by census tract instead of performing all the calculations for each dwelling. In this sense, we must look first at the criterion established to define the zones of interest (criterion 1 or 2 for example) and the shelter-in-place indicator that could be used to define them (e.g. percentage of casualties, SF_i). Then, knowing the shelter-in-place indicator wanted and the percentage of dwellings associated to the indicator, we can select the appropriate c' percentile to develop the calculations. For example, if we want to determine the area (cells) in which all the dwellings

(100%) provide a secure shelter based on the SF_i criterion ($SF_i > 1$), we should use the maximum value of the c' distribution (100th percentile), to assure that all the dwellings met the fixed condition. By the other hand, if we want to define the area in which at least a given percentage of dwellings show a $SF_i \leq 1$ (i.e. 20%), we should use 100 minus the given percentile (100th – 20th = 80th) of the c' distribution to define that zone. Therefore, the c' to be used is directly related to the percentage of dwellings that would at least meet the given criterion: the same percentage if the area to be defined is above the criterion or 100 minus the given percentage if the area is below the criterion. This simplified methodology, based on the airtightness distribution leads to a quick identification of the area of concern, and the rapid estimation of a certain indicator for a percentage of dwellings. For example, emergency managers could assess the casualty probability for the 50% or 90% of the dwellings by cell, or calculate the SF_i for the 95th percentile of c' and identify the cells with $1 < SF_i < 2$ in order to plan the emergency response in a toxic release event. The chart of Figure 7.3 sums up the steps followed to identify the zone of concern using this simplified methodology.

In order to apply this simplified methodology to our study case, for which we defined evacuation zones using criteria 1 and 2; we used the c' corresponding to the 100th percentile of the distribution since the area to implement shelter-in-place involves the area (cells) with a casualty probability lower than 0.1% and the area where 100% of the dwellings present a $SF_i > 1$, according to the evacuation zone condition of criteria 1 and 2, respectively.

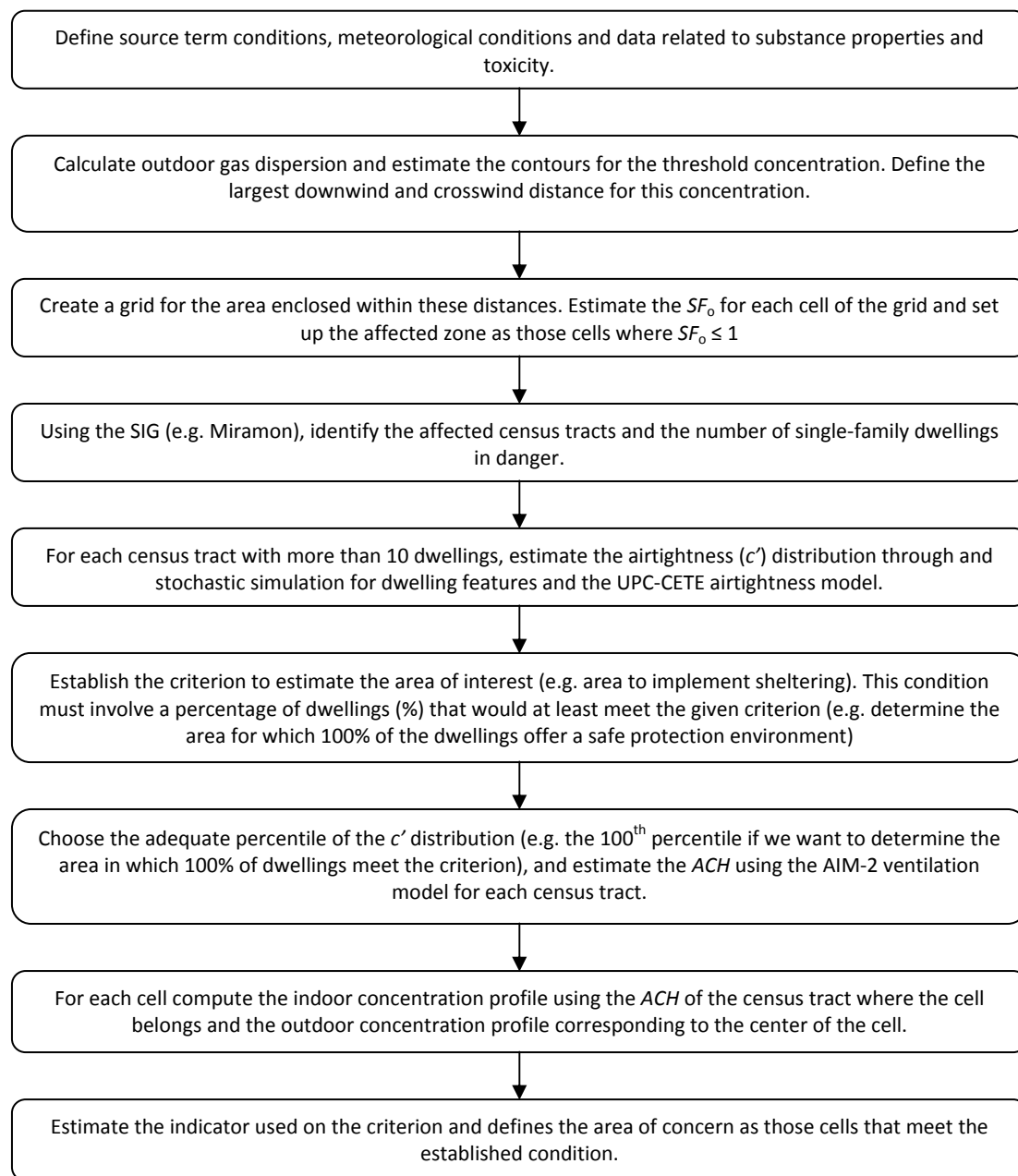


Figure 7.3 Steps used to estimate an area of concern for a given criterion when using shelter-in-place as a protection measure in the case of a toxic gas release in a geo-reference way

7.4 Results

7.4.1 Outdoor dispersion

Figure 7.4 shows the plume contour for the threshold concentration (148 mg/m^3) at 10, 15, 20 and 25 minutes from the beginning of the release. It took around 27 min for the toxic cloud to attain concentrations below the threshold concentration in the downwind direction. The largest distance reached by the cloud for the threshold concentration in the downwind direction was 7100 m, and 450 m in the crosswind direction.

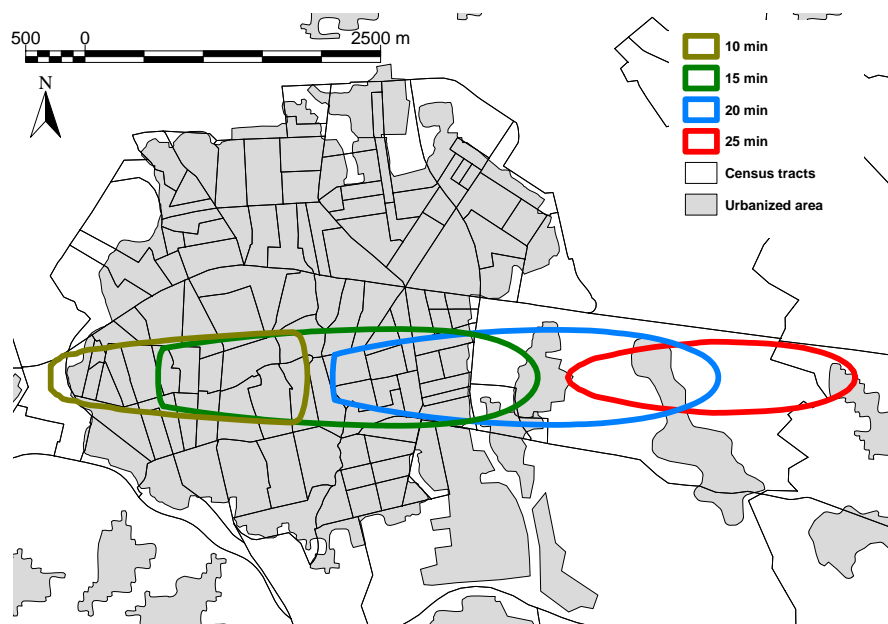


Figure 7.4 Plume contour for the threshold value at different times

The affected area, as defined by the cells where the $SF_o \leq 1$ (see Figure 7.5), comprised 3912500 m^2 being the maximum distance from the source 6500 m. From this area 68.4% belong to an urbanized zone, represented as the gray surface on the figure. In total, the number of affected census tracts summed up 61 and the number of single-family dwellings within these census tracts was 6231. It took around 45 minutes to the toxic cloud to completely pass over this area.



Figure 7.5 Area where the outdoor safety factor remains equal or below 1 ($SF_o \leq 1$)

7.4.2 Airtightness and air exchange rate

Airtightness distribution in Catalunya, estimated with the UPC-CETE model modifying the NS parameter (Eq. 5.11 to Eq. 5.13), is shown in Figure 7.6. As we can see from the figure, more than 80% of the dwellings show a c' below $0.1 \text{ m}^3 \cdot \text{s}^{-1} \cdot \text{Pa}^{-0.67}$, which is very similar to the trend found without modifying the model (see Figure 5.17). The difference of considering the real number of stories is mostly reflected on the higher percentiles, which is logical since the percentage of dwellings with more than 2 stories is around 20% (see Figure 4.1). Nevertheless, since most of the dwellings are three stories the difference is small and only for the highest percentiles ($>99^{\text{th}}$) the difference is significant (from 0.25 to 0.65). To develop the scenario of the constant airtightness we employed the value corresponding to the 90^{th} percentile, $0.1198 \text{ (m}^3 \cdot \text{s}^{-1} \cdot \text{Pa}^{-0.67})$.

The 50^{th} and 90^{th} percentiles of the ACH distribution estimated for each census tract, as a result of applying the UPC-CETE airtightness model and the AIM-2 ventilation model to each dwelling in the different census tracts, are shown in Figure 7.7 and Figure 7.8. As we can see in Figure 7.7, the ACH_{p50} ranged among 0.73 and 1.97 h^{-1} while the ACH_{p90} are between 1.27 and

2.44 h^{-1} (Figure 7.8). In total 12 census tracts have an ACH_{p90} greater than 2 h^{-1} , which is one value commonly used when the ACH is unknown. Therefore, we have a variety of ACH by census tract that ranged from the tightest to the leakiest. In the figures there are also some census tracts (6) without a value, this is because they have less than 10 dwellings or do not have single-family dwellings.

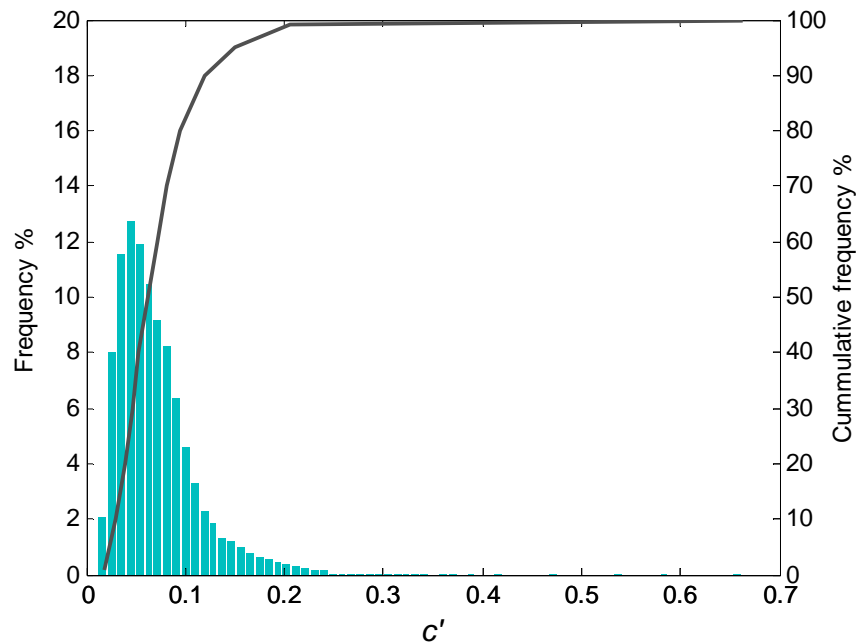


Figure 7.6 Airtightness distribution in Catalunya estimated with the modified UPC-CETE model

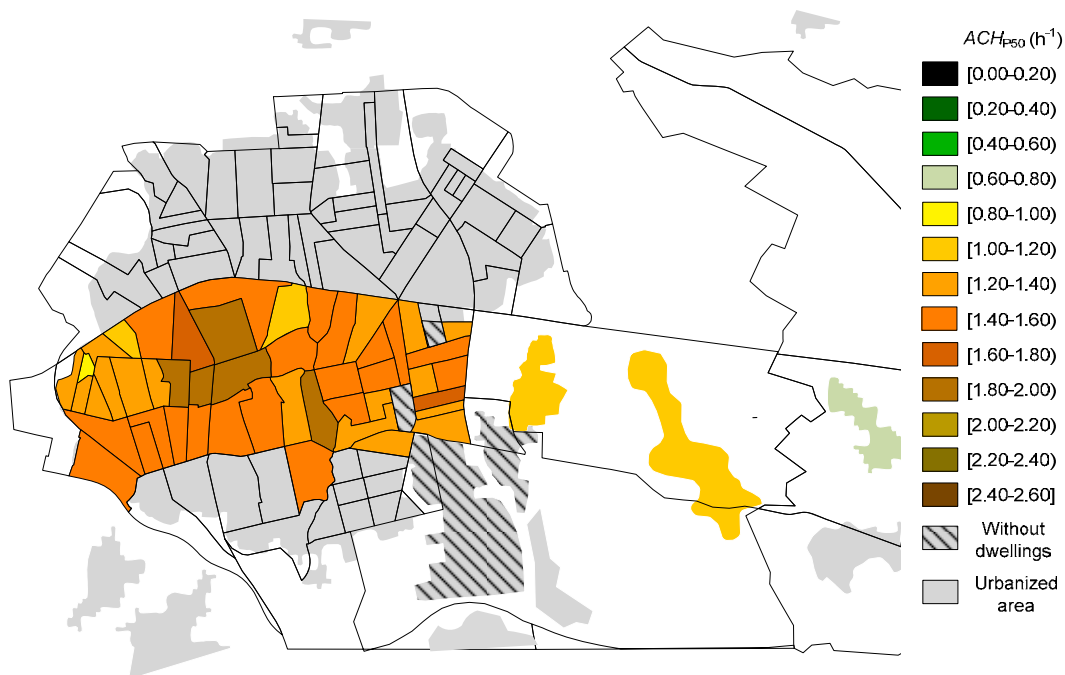


Figure 7.7 50th percentile of the ACH distribution by census tract

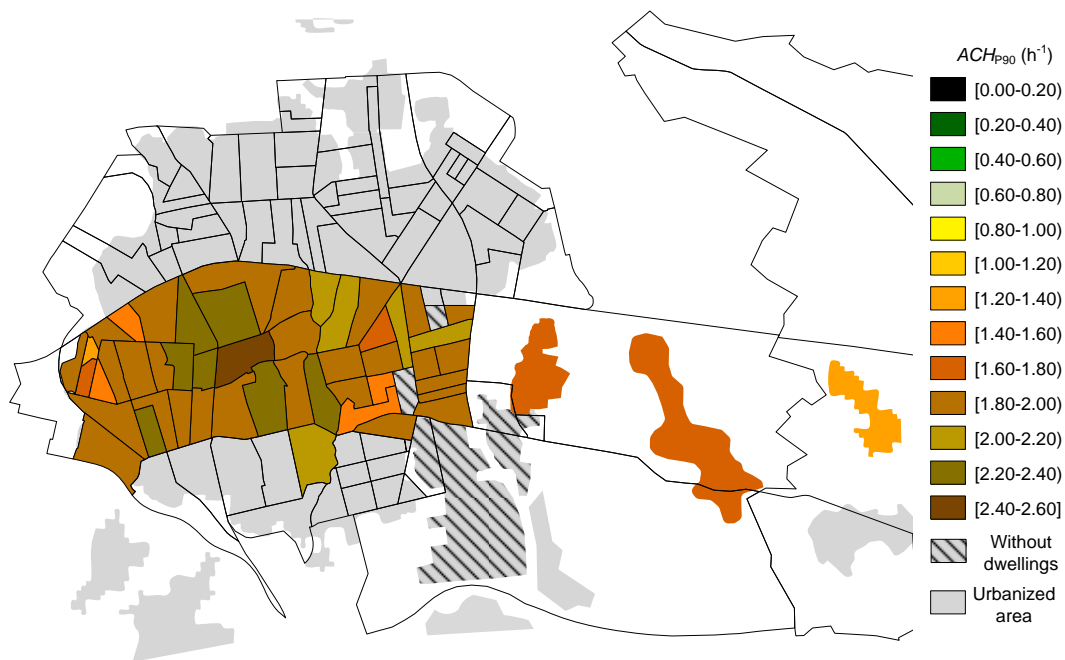


Figure 7.8 90th percentile of the ACH distribution by census tract

7.4.3 Indoor concentration

Figure 7.9 and Figure 7.10 presented the 50th and the 90th percentiles of the indoor concentration distribution by cell, in a geo-referenced way, at 5, 10, 15, 20, 25, 30 and 35 minutes after the release started. Since the behavior of indoor concentration followed the same pattern, first increase and then decrease after outdoor concentration decrease, we only showed the geo-referenced distribution for the base case scenario. These percentiles represent the concentrations below which 50% and 90% of the single-family dwellings stayed. They allowed us to see the progress of indoor concentration with time, if it is increasing or decreasing. Largest values for the 50th and 90th percentiles were 4471 and 5719 mg/m³ respectively, and took place at minute 15. From the figures we can also see that largest distances for indoor concentrations greater than the threshold value (148.18 mg/m³) were achieved at minute 20, 2200 m and 2500 m for the 50th and the 90th percentiles, respectively. After that time the area with an indoor concentration higher than 148.18 mg/m³ started to decrease. Also, looking at the values for indoor concentration we could see the effect of having different ACH between cells located on different census tracts, for example, there is one census tract at minute 20 in Figure 7.9 that only has some cells with concentrations greater than 148.18 mg/m³ while the adjacent census tract, which is located further concerning the downwind distance, presented more cells with concentrations greater than 148.18 mg/m³.

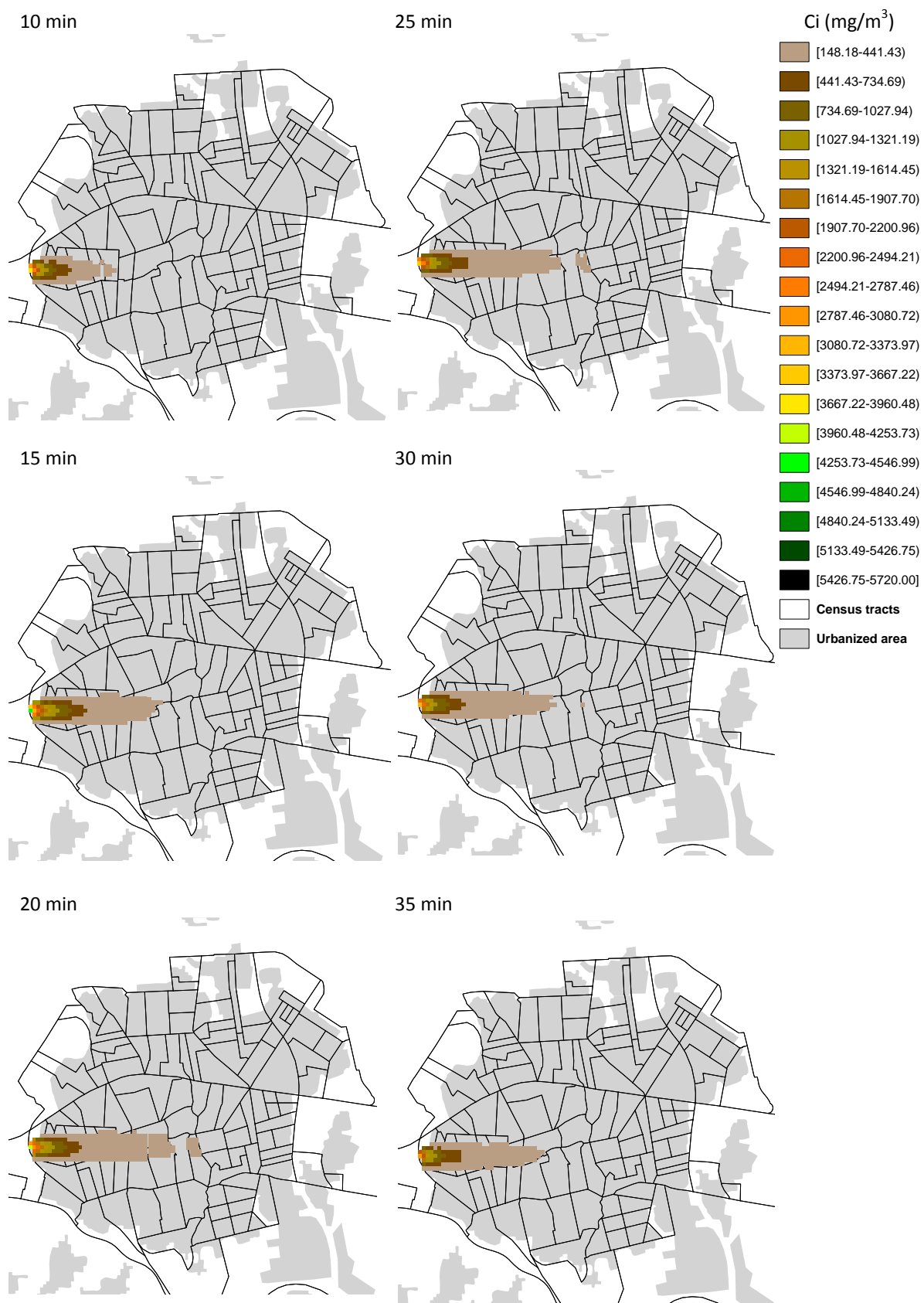


Figure 7.9 50th percentile of the indoor concentration distribution inside each cell at different times

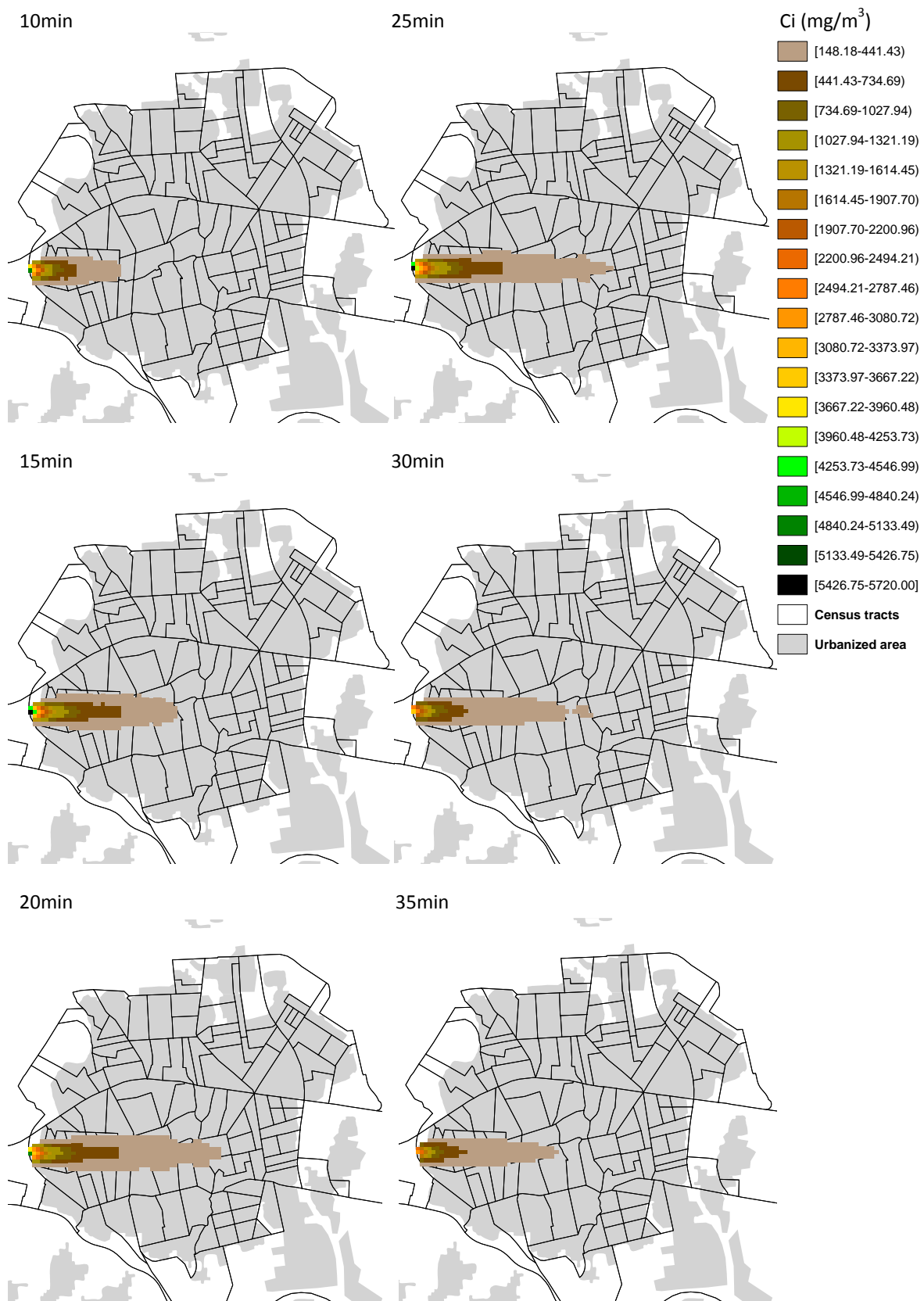


Figure 7.10 90th percentile of the indoor concentration distribution inside each cell at different times

7.4.4 Evacuation area

For our case study, the cloud needed 45 min to completely pass at a downwind distance of 6500 m therefore we considered 45 min as the shelter termination time. Consequently, we computed the TL_i and assessed the SF_i and the casualty' probability at 15, 25, 35 and 45 min. Figure 7.11 to Figure 7.26 present shelter-in-place indicators estimated at these times, for the base case scenario using the complete and the simplified methodology. Figure 7.15 to Figure 7.18 present the indicators for the expedient sheltering scenario, Figure 7.19 to Figure 7.22 for the constant adsorption scenario and Figure 7.23 to Figure 7.26 for the constant airtightness scenario. Figure 7.11, Figure 7.15, Figure 7.19 and Figure 7.23 show the percentage of dwellings by cell that exhibit a casualty' probability greater than 0.1% (complete methodology) for each scenario; therefore, considering criterion 1 all the area delimited by cells with percentages higher than zero should be evacuated while the remaining area where the percentage is zero, because casualty' probability inside dwellings is lower than 0.1%, illustrates the zone where shelter-in-place represents a good protection measure to the population (area with blue diagonal patterns in the figures). Figure 7.12, Figure 7.16, Figure 7.20, Figure 7.24 present the percentage of dwellings by cell that show a $SF_i \leq 1$ for each scenario. Therefore, with regards to the second criterion, the evacuation area comprised the cells with percentages greater than zero while shelter-in-place zone is defined by cells with percentages of zero (area with blue diagonal patterns in the figures). Looking at the figures, we also see that the area where dwellings present an indoor casualty' probability greater than 0.1% is smaller than the one defined by dwellings with a $SF_i \leq 1$, as is logical. This happened because the toxic load limit is different; for criterion 1 we used the Probit analysis which involved a percentage of casualties while in the second the TLL was estimated from the AEGL-3, which is a threshold value that does not involve any casualty.

In relation to the use of the simplified methodology, Figure 7.13, Figure 7.17, Figure 7.21 and Figure 7.25 show the casualty probability for each cell obtained using the maximum value (100th percentile) of the airtightness distribution of its census tract, while Figure 7.14, Figure 7.18, Figure 7.22 and Figure 7.26 show the SF_i for each cell using also the maximum value of the airtightness distribution. In these cases, we represented on the maps the casualty probability and the SF_i by cell, therefore, the evacuation area could be established directly from the two criteria. From the figures, we can see the variability in the percentage of

dwelling by cell that met the given criteria or on the indicators, which reflects both the effect of location and air exchange rate variability.

Table 7.2 presents the results for the evacuation area, the area where shelter-in-place could be implemented and the evacuation radius, obtained for each scenario and criterion. The evacuation radius corresponds to the distance from the source to the furthest cell that met the given criterion. Looking at the table we see that the use of the complete and the simplified methodology lead to the same results, which born out the good performance of the simplified methodology. There was only one difference concerning the area and the radius estimated with criterion 1 for the base case scenario, in which the area and the radius computed using the complete calculations included one more cell.

Concerning the area to be evacuated, smallest areas were obtained for the expedient sheltering scenario, followed by the case where adsorption was considered, the basic case and the constant airtightness. Therefore we can say that more protection is gained by sheltering in a room with expedient measures than by assuming that the substance adsorbs over indoor surfaces. Nevertheless evacuation radiuses for these scenarios were the same for criterion 1 and only differ by one cell (50 m) for criterion 2, which show that evacuation areas were wider in the case of constant adsorption, and the furthest distances to the cell that met the given criteria in the cross-wind direction, were larger. With regards to the constant adsorption scenario, larger evacuation areas and evacuation radiuses were obtained, areas increased by 29% and radiuses between 16 and 19% in relation to the base case scenario. Therefore, to consider a constant airtightness equal to the 90th percentile of the c' distribution in Catalunya, avoid the real distribution in the affected area and lead to higher overestimations, while advising people to take shelter in a room and implement expedient measures could decrease the evacuation radius by 19% in relation to no expedient sheltering, a reduction of the same order of considering a substance that adsorbs over indoor surfaces. Therefore, with concern to calculations efforts, the application of the simplified methodology really simplifies and speeds up calculations without losing accuracy.

Table 7.2 Evacuation and shelter-in-place areas estimated for the different cases

Scenario	Criterion*	Zone of concern	Complete calculations		Simplified methodology	
			Area (m ²)	Evacuation radius (m)	Area (m ²)	Evacuation radius
Base case	1	Evacuate	1037500	2900	1035000	2850
		Shelter-in-place	1520000		1522500	
	2	Evacuate	1240000	3400	1240000	3400
		Shelter-in-place	1317500		1317500	
Expedient sheltering	1	Evacuate	787500	2350	787500	2350
		Shelter-in-place	1770000		1770000	
	2	Evacuate	945000	2700	945000	2700
		Shelter-in-place	1612500		1612500	
Constant adsorption	1	Evacuate	822500	2350	822500	2350
		Shelter-in-place	1735000		1735000	
	2	Evacuate	967500	2750	967500	2750
		Shelter-in-place	1590000		1590000	
Constant airtightness	1	Evacuate	1337500	3450	1337500	3450
		Shelter-in-place	1220000		1220000	
	2	Evacuate	1597500	3950	1597500	3950
		Shelter-in-place	960000		960000	

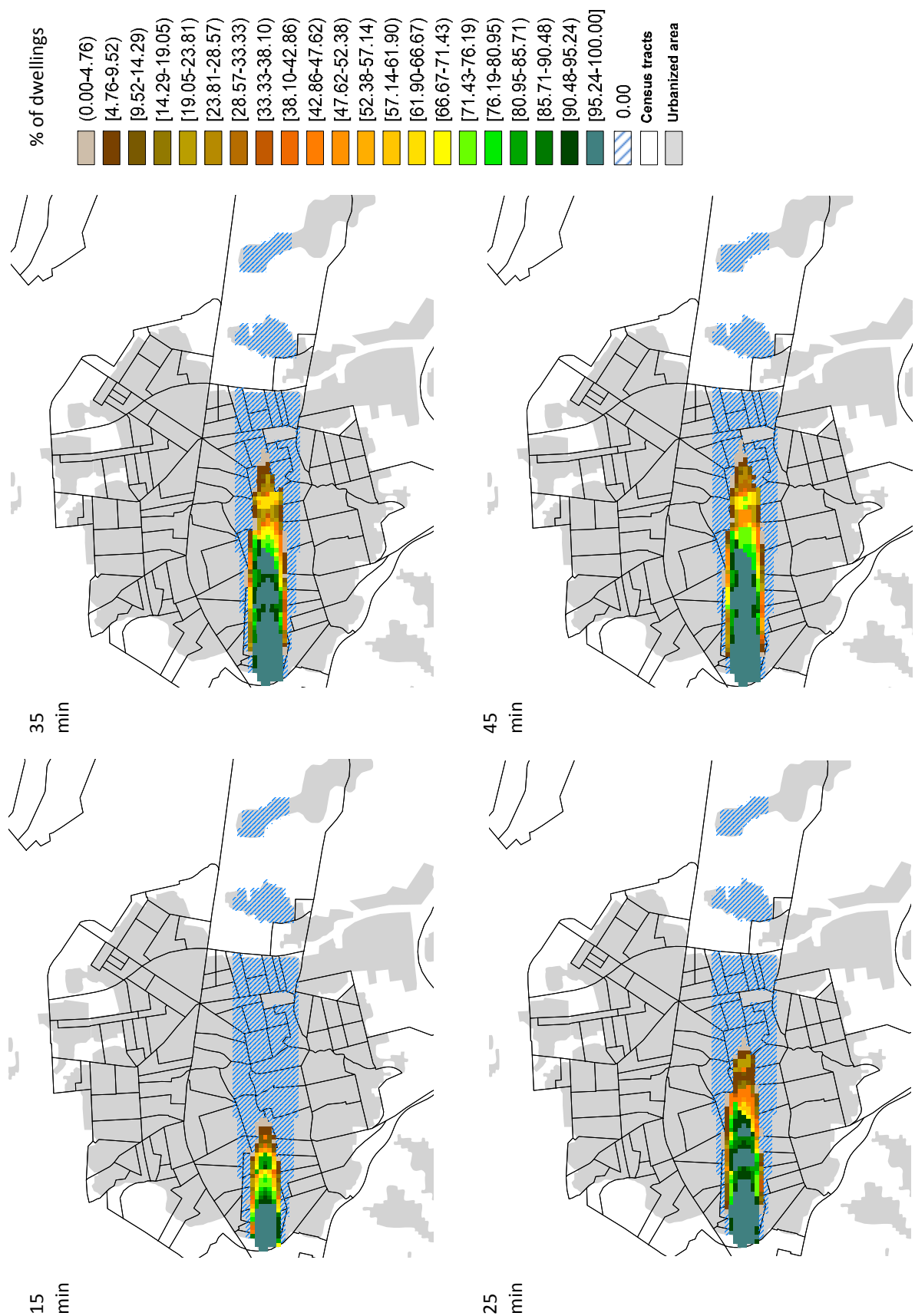


Figure 7.11 Percentage of dwellings with a casualties' probability equal or greater than 0.1%. Base case scenario

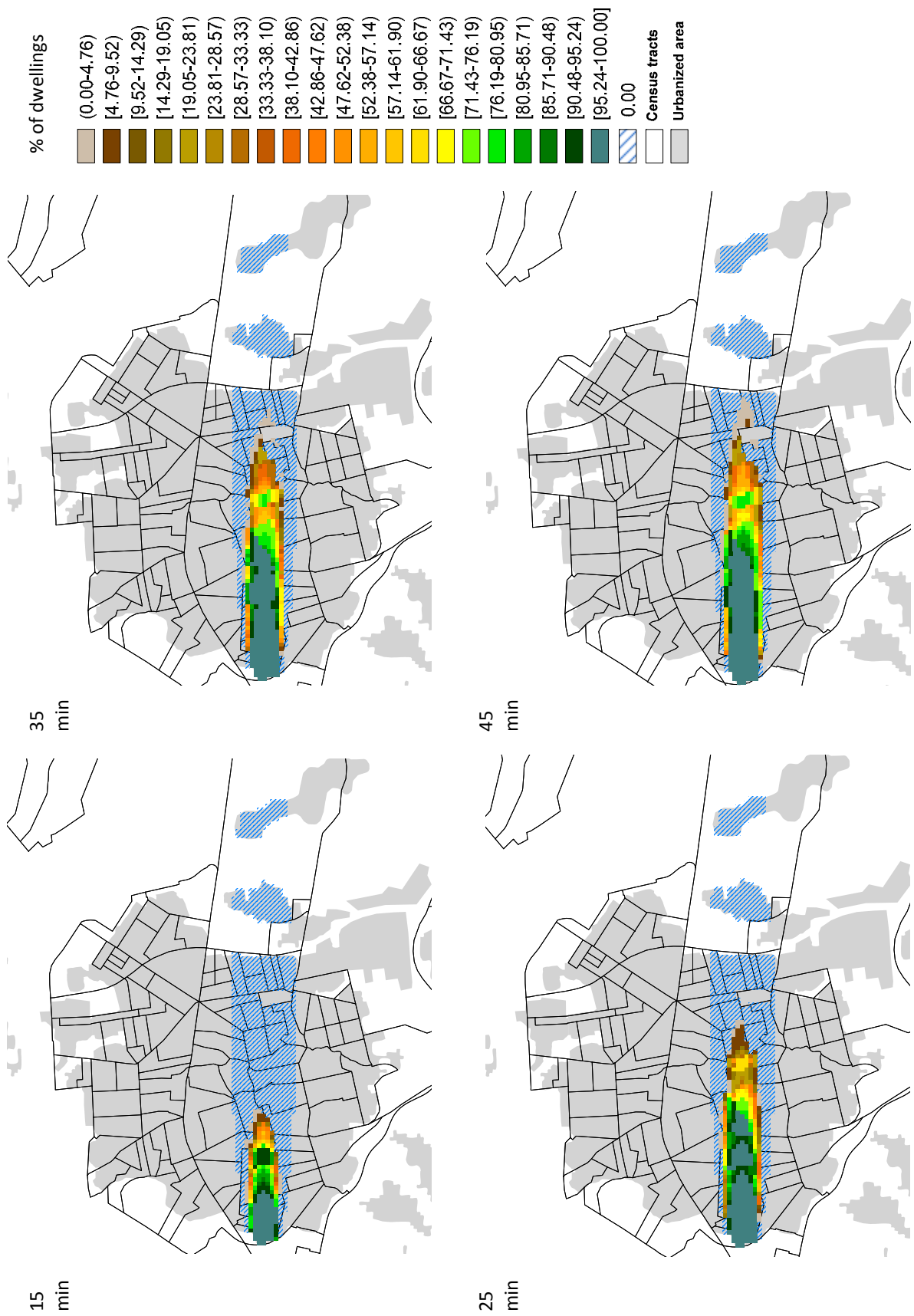


Figure 7.12 Percentage of dwellings where the $SF_1 \leq 1$. Base case scenario

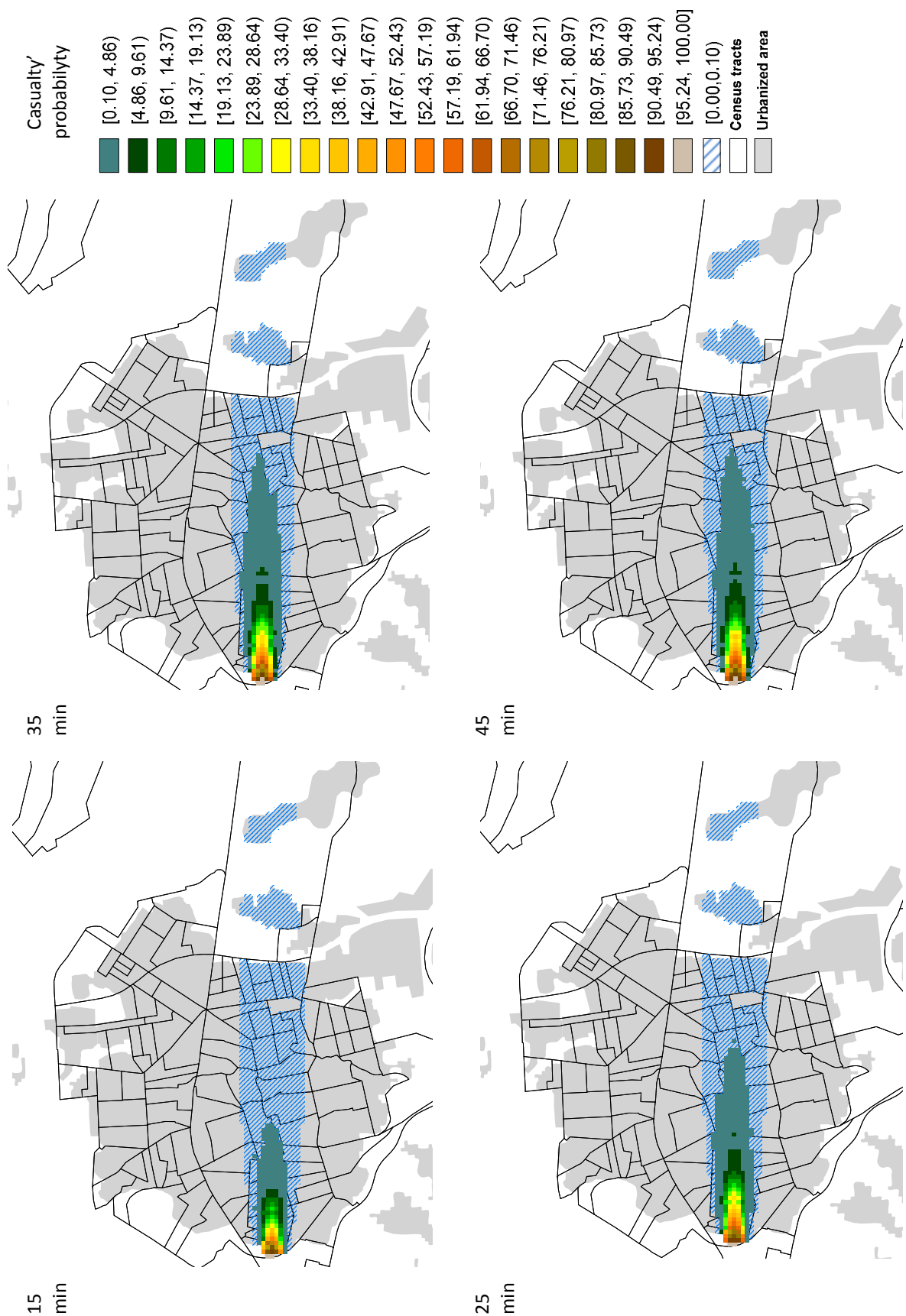


Figure 7.13 Casualty' probability for the 100th percentile of the airtightness (c') distribution. Base case scenario (simplified methodology).

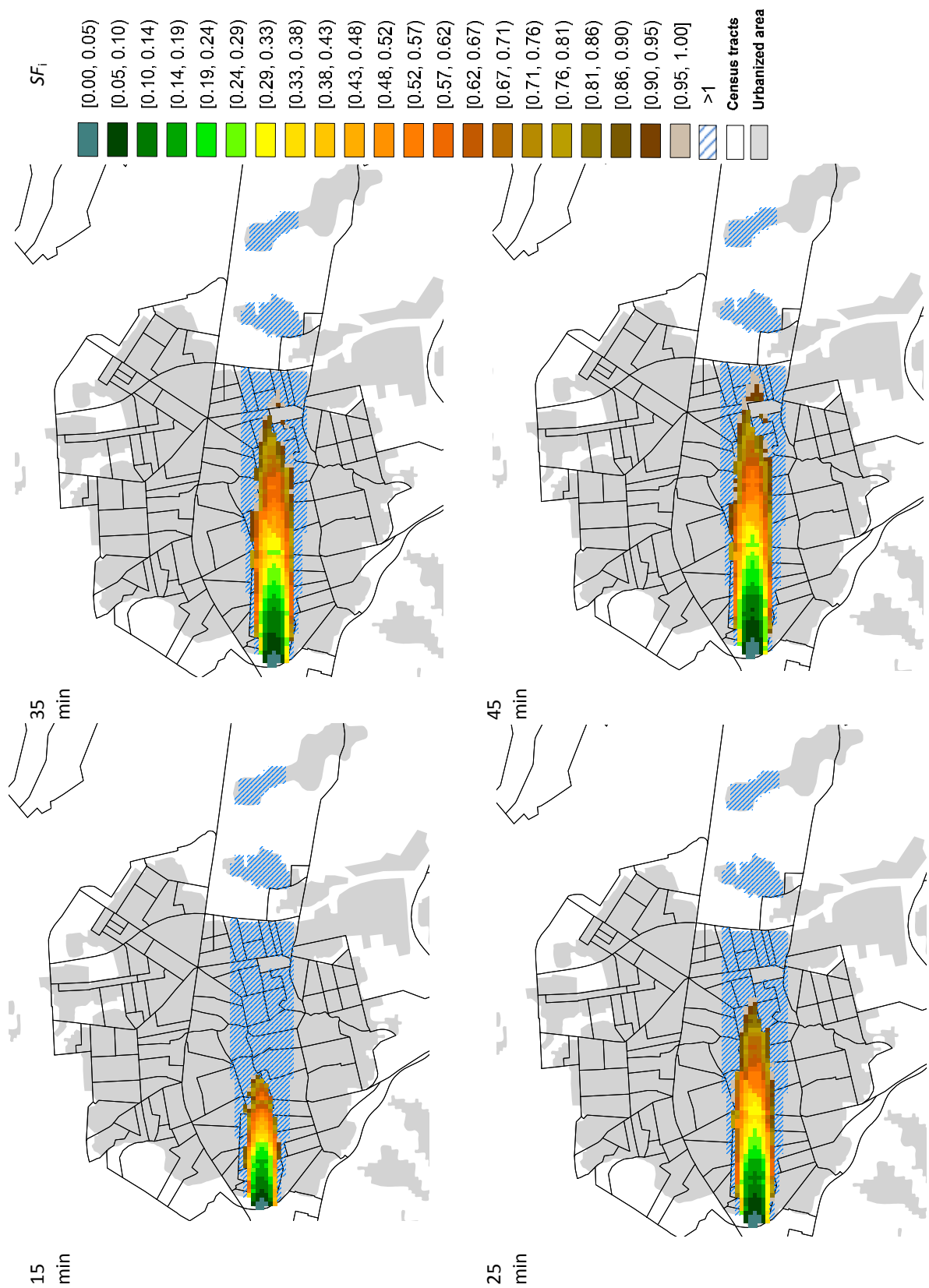


Figure 7.14 SF_i for the 100th percentile of the airtightness (c') distribution. Base case scenario (simplified methodology).

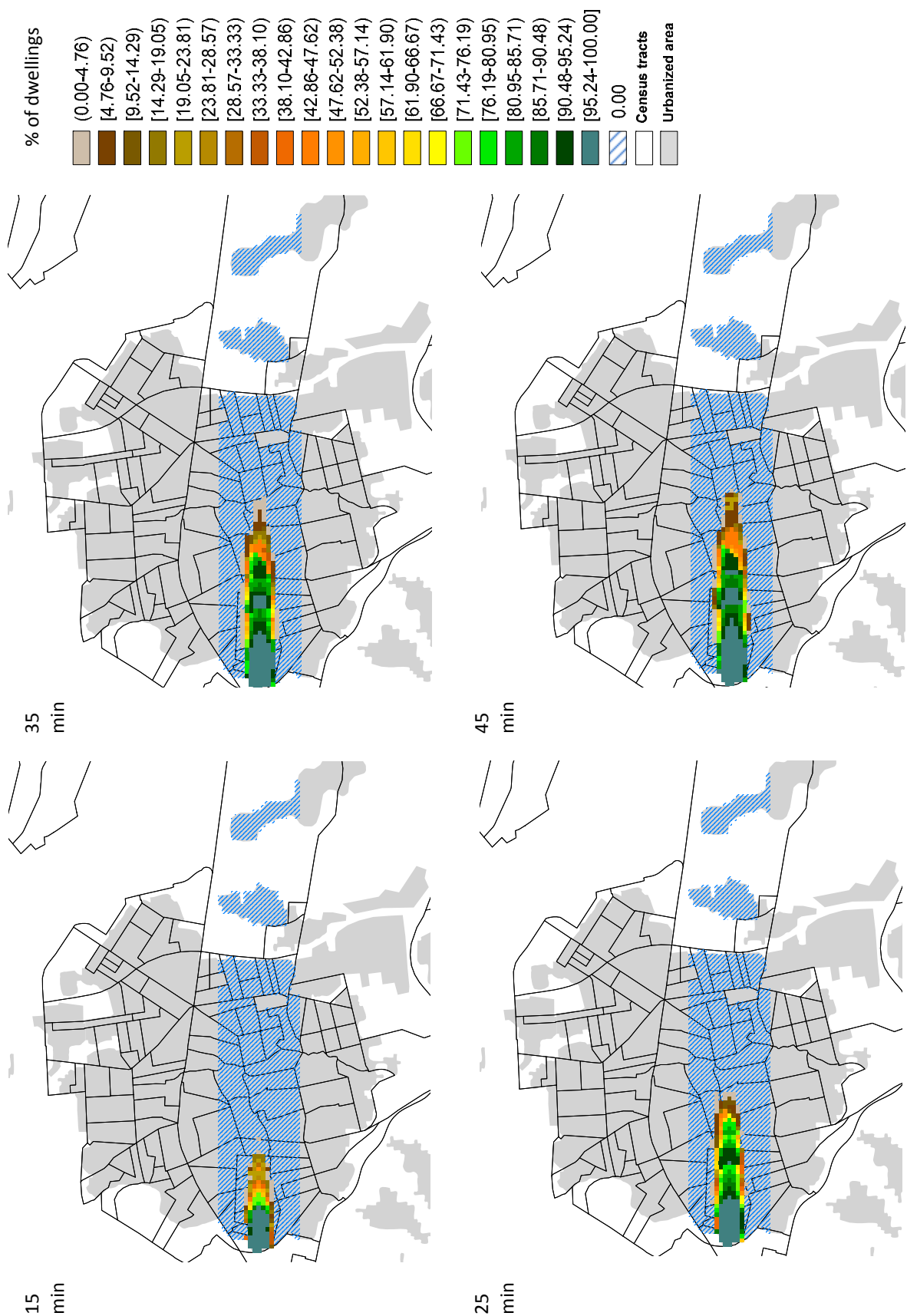


Figure 7.15 Percentage of dwellings with a casualties' probability equal or greater than 0.1%. Expedient sheltering scenario.

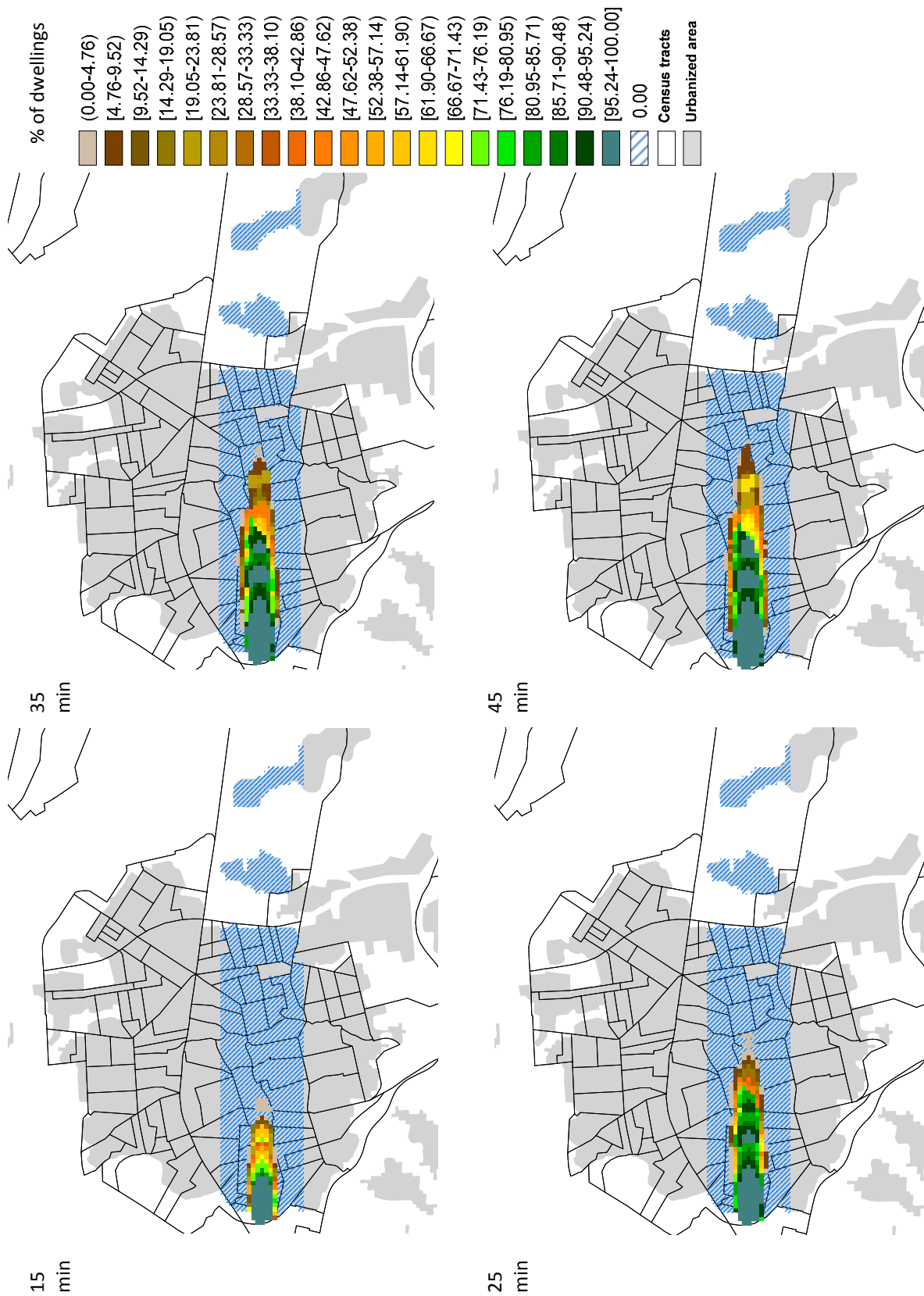


Figure 7.16 Percentage of dwellings where the $SF_i \leq 1$. Expedient sheltering scenario.

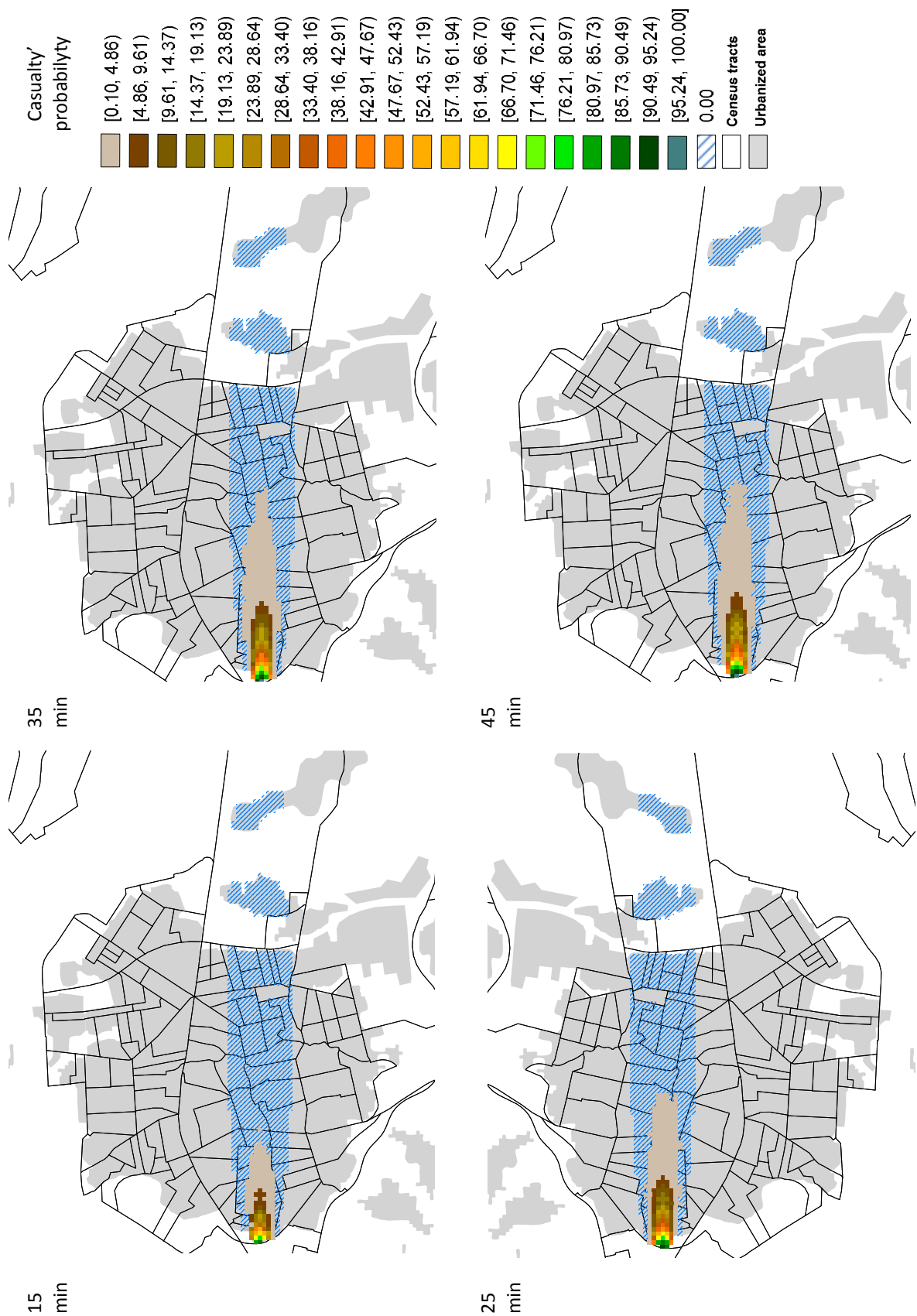


Figure 7.17 Casualty' probability for the 100th percentile of the airtightness (c') distribution. Expedient sheltering scenario (simplified methodology).

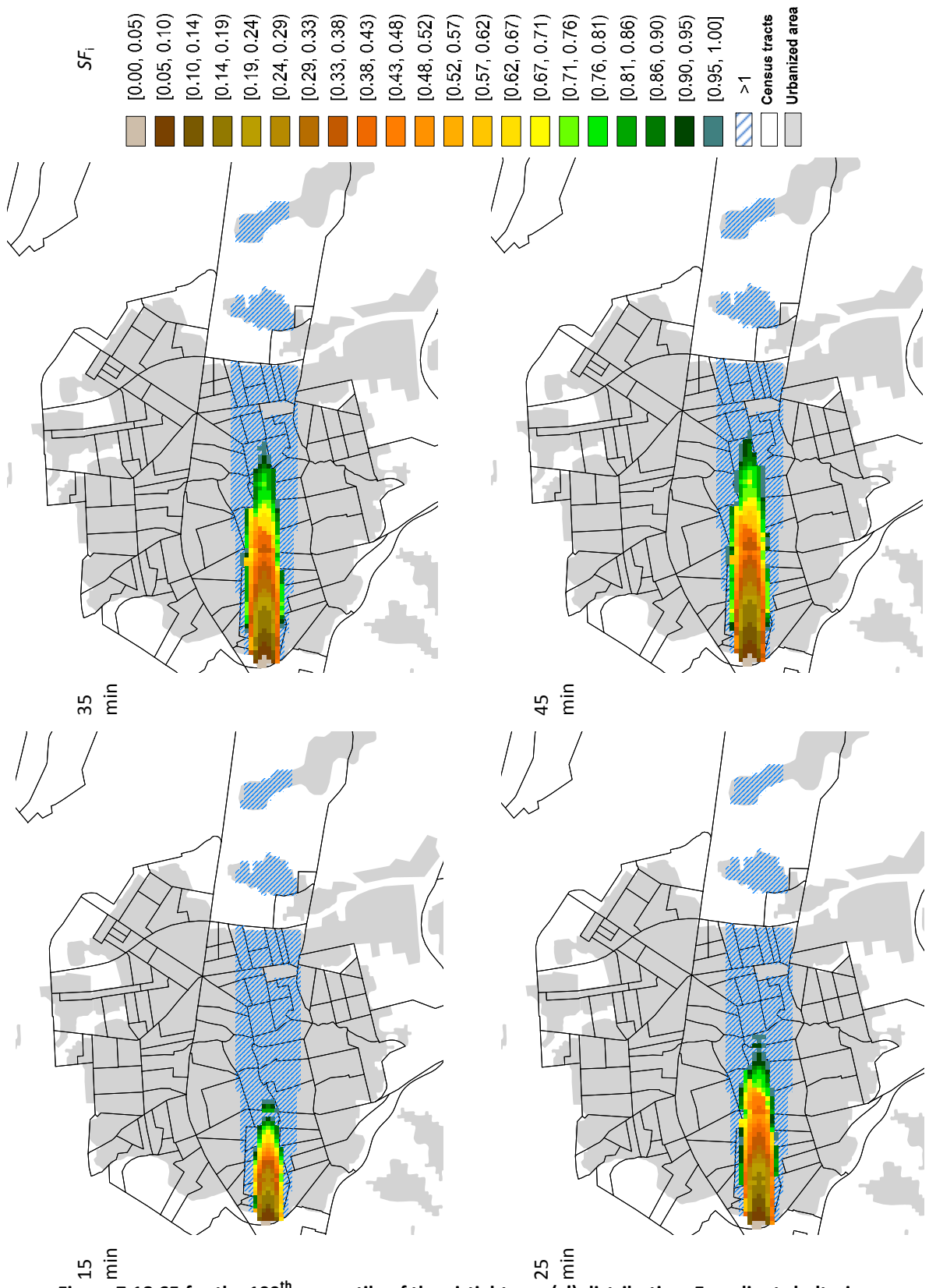


Figure 7.18 SF_i for the 100th percentile of the airtightness (c') distribution. Expedient sheltering scenario (Simplified methodology).

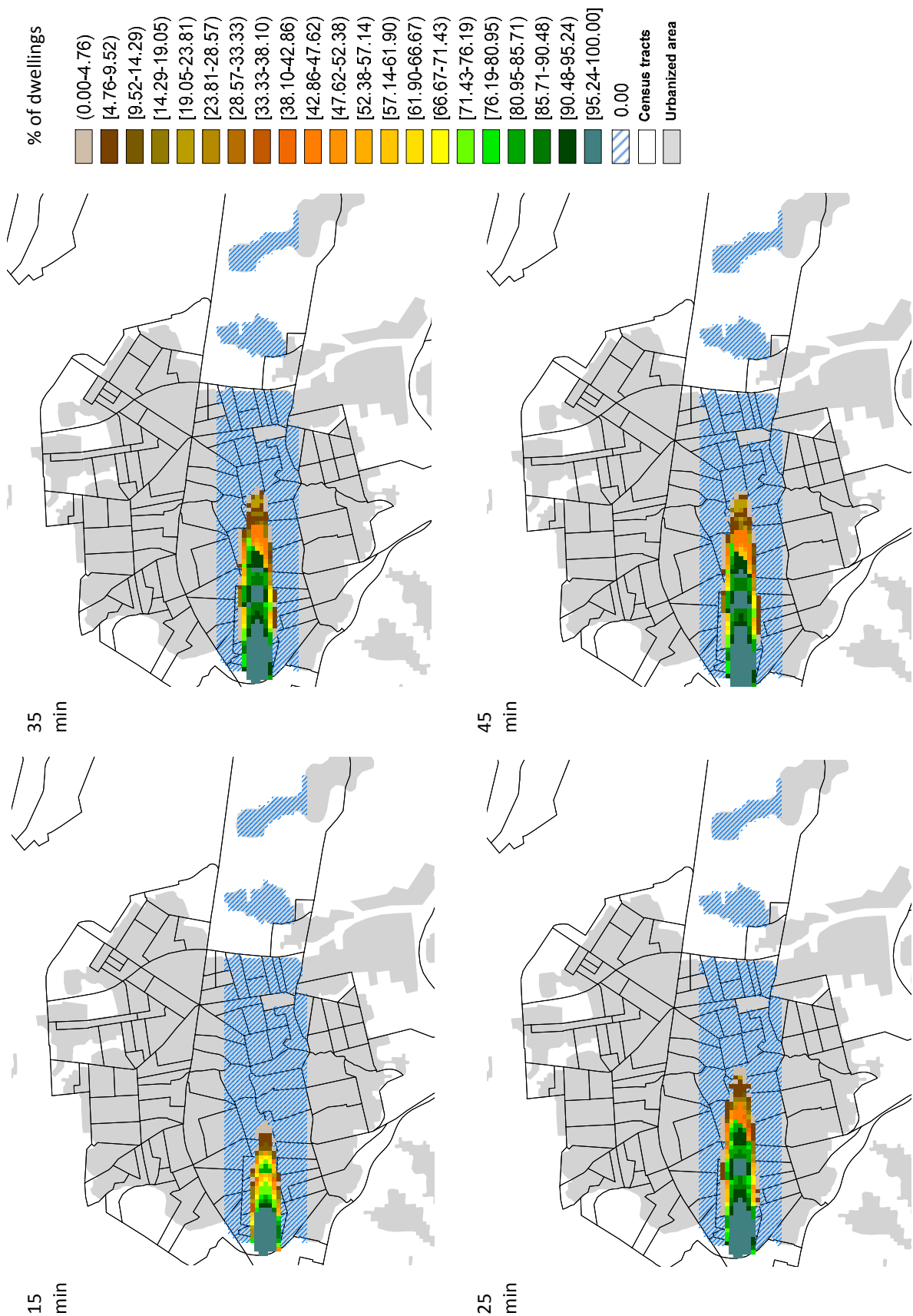


Figure 7.19 Percentage of dwellings with a casualties' probability equal or greater than 0.1%. Constant adsorption scenario.

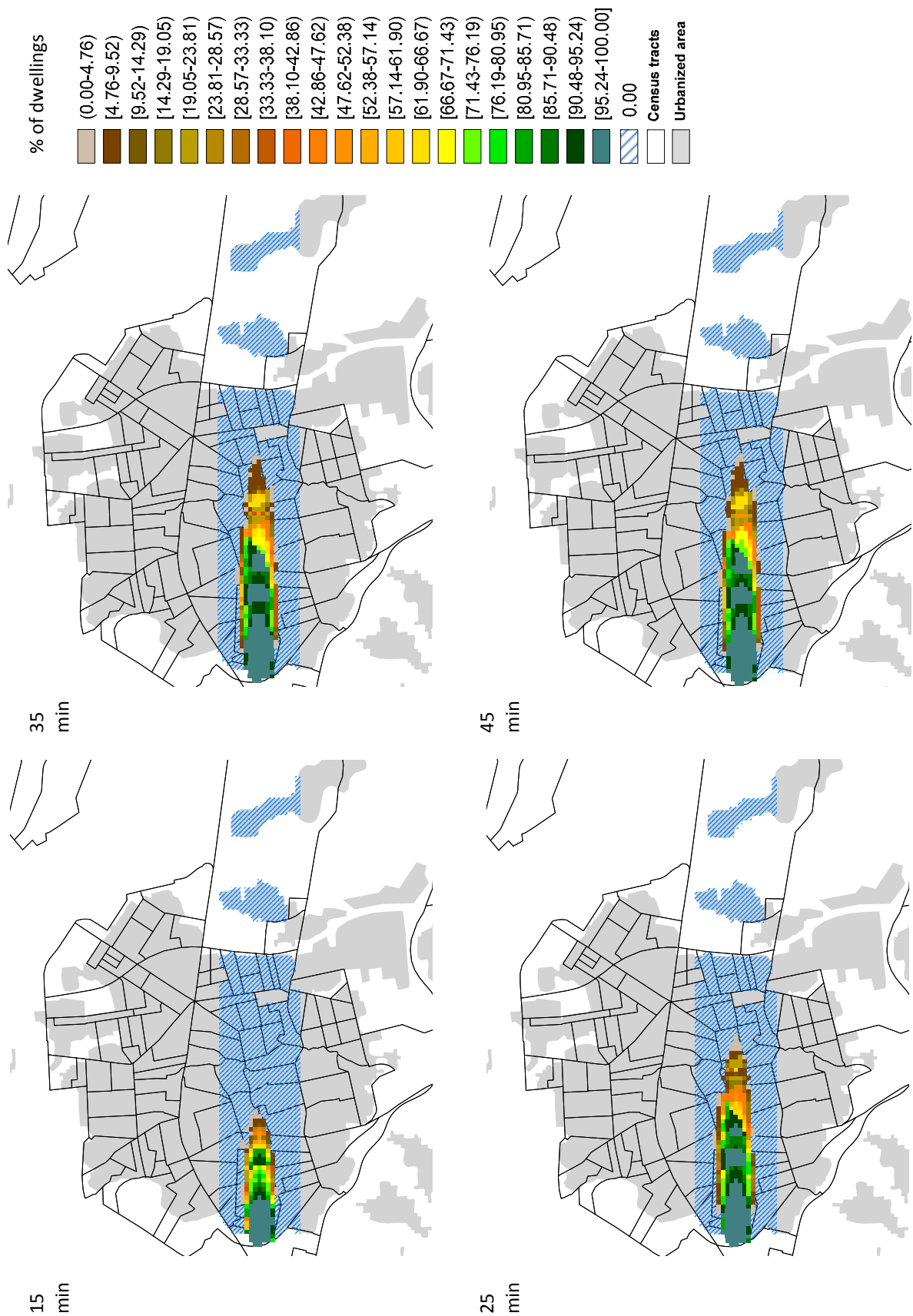


Figure 7.20 Percentage of dwellings where the $SF_1 \leq 1$. Constant adsorption scenario.

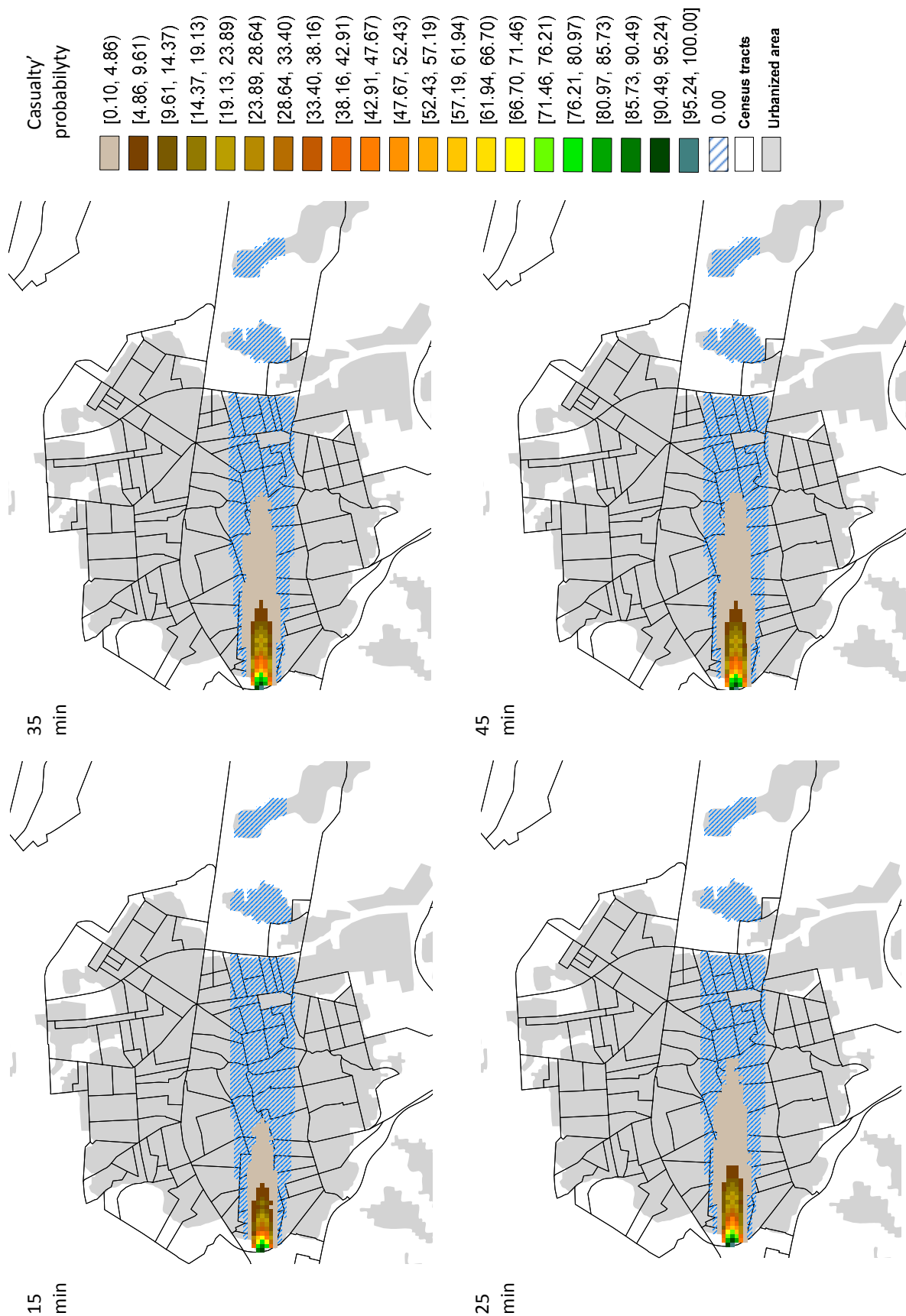


Figure 7.21 Casualty' probability for the 100th percentile of the airtightness (c') distribution. Constant adsorption scenario (simplified methodology).

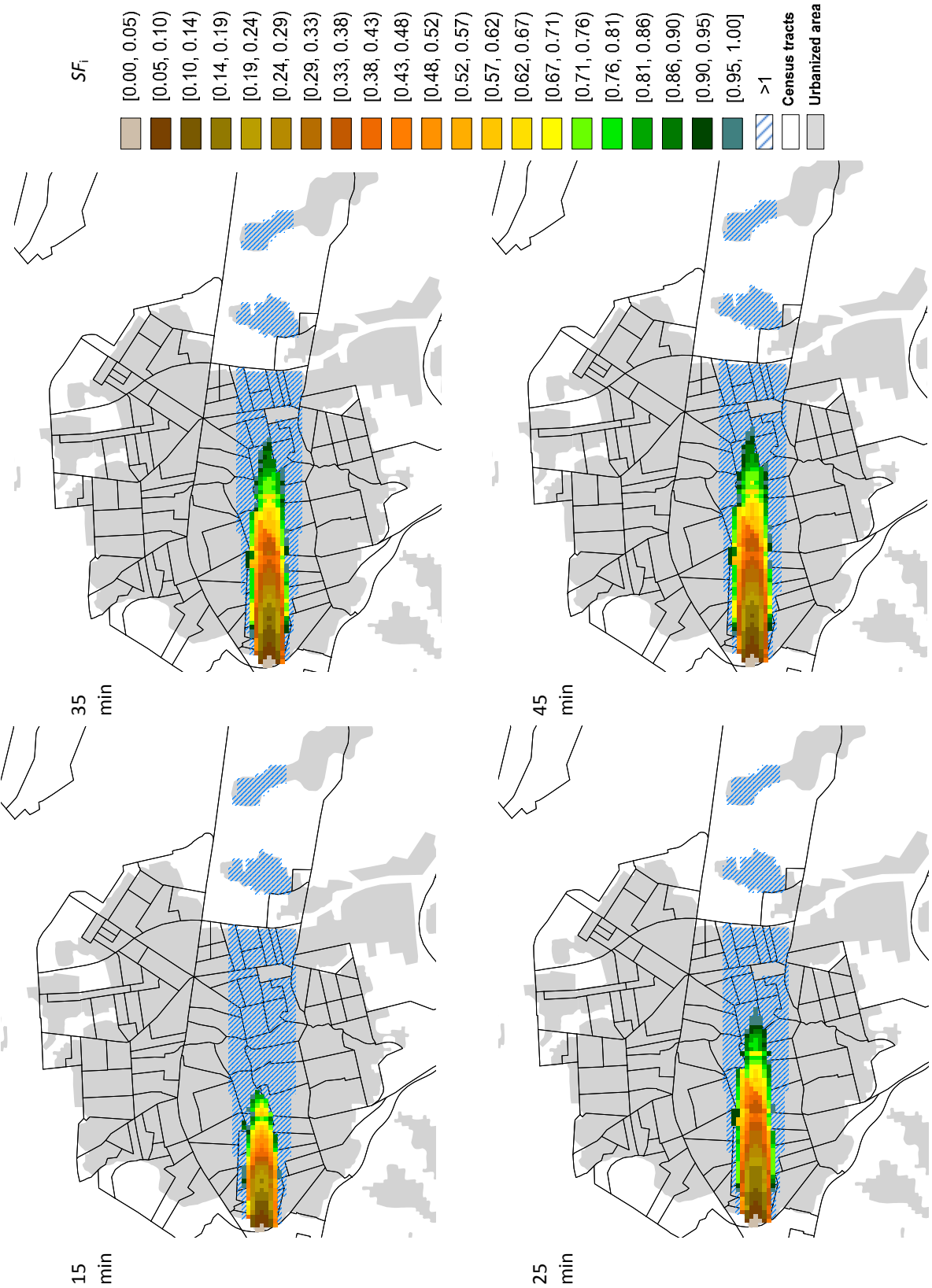


Figure 7.22 SF_1 for the 100th percentile of the airtightness (c') distribution. Constant adsorption scenario (Simplified methodology).

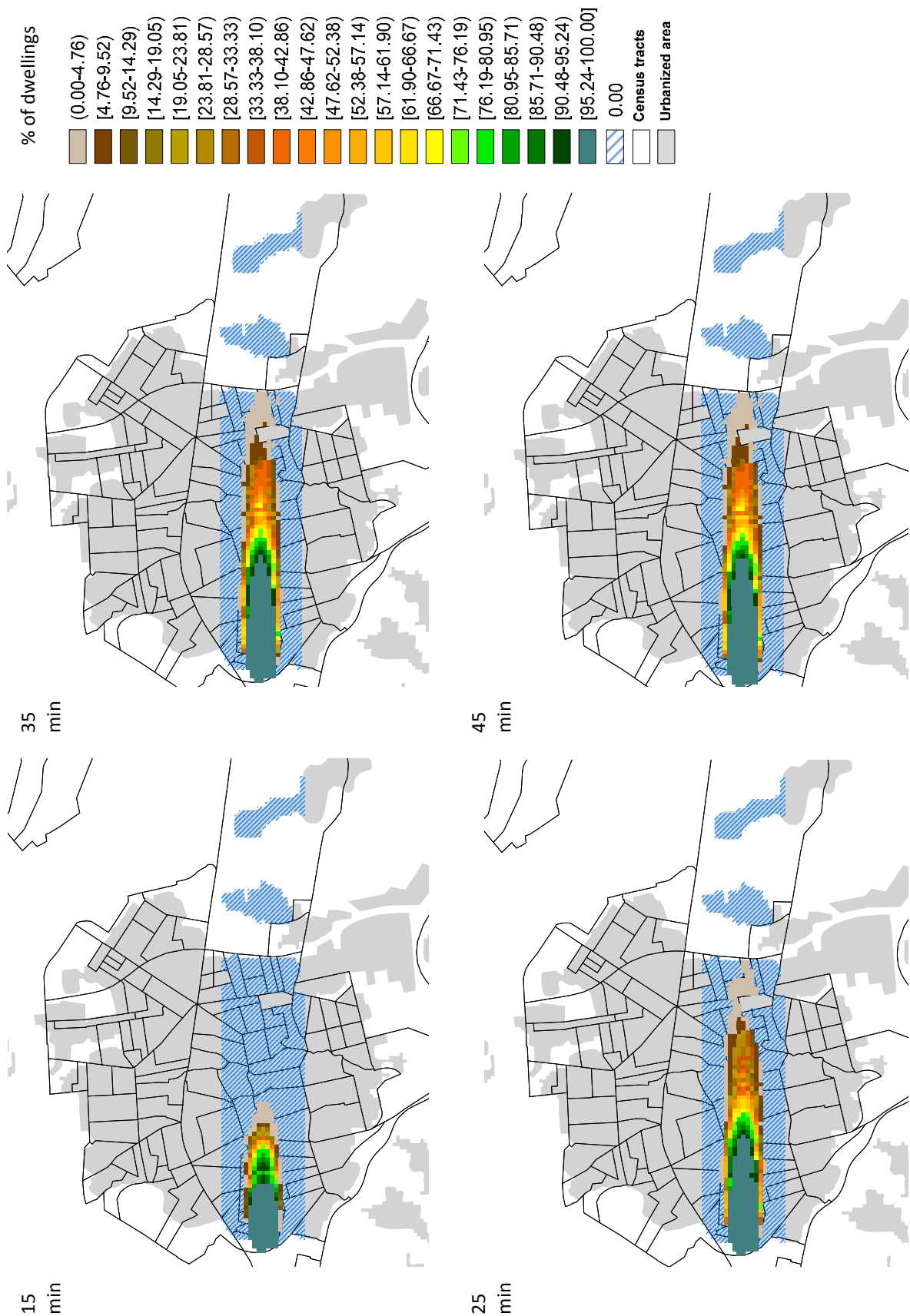


Figure 7.23 Percentage of dwellings with a casualties' probability equal or greater than 0.1%. Constant airtightness scenario.

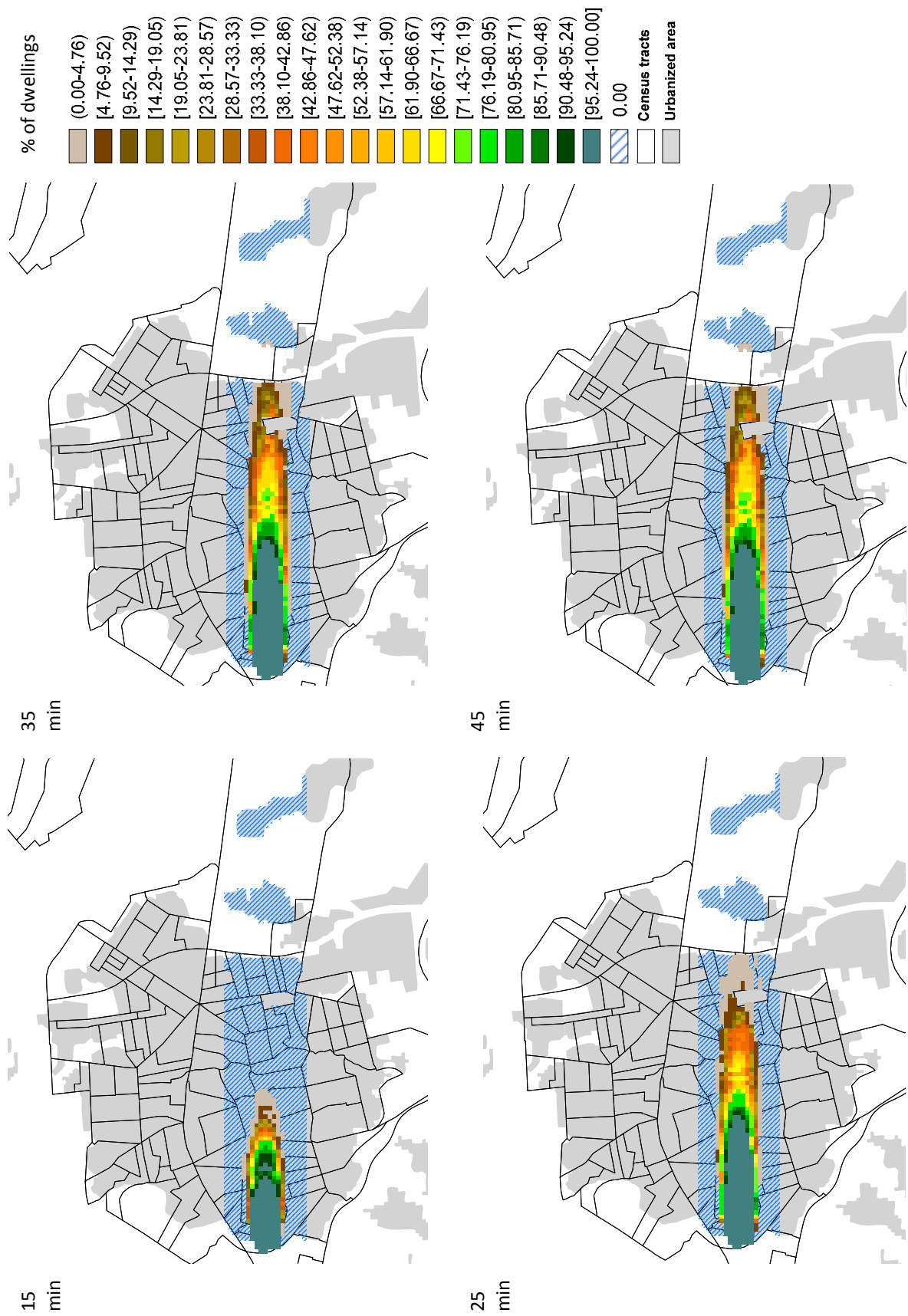


Figure 7.24 Percentage of dwellings where the $SF_1 \leq 1$. Constant airtightness scenario.

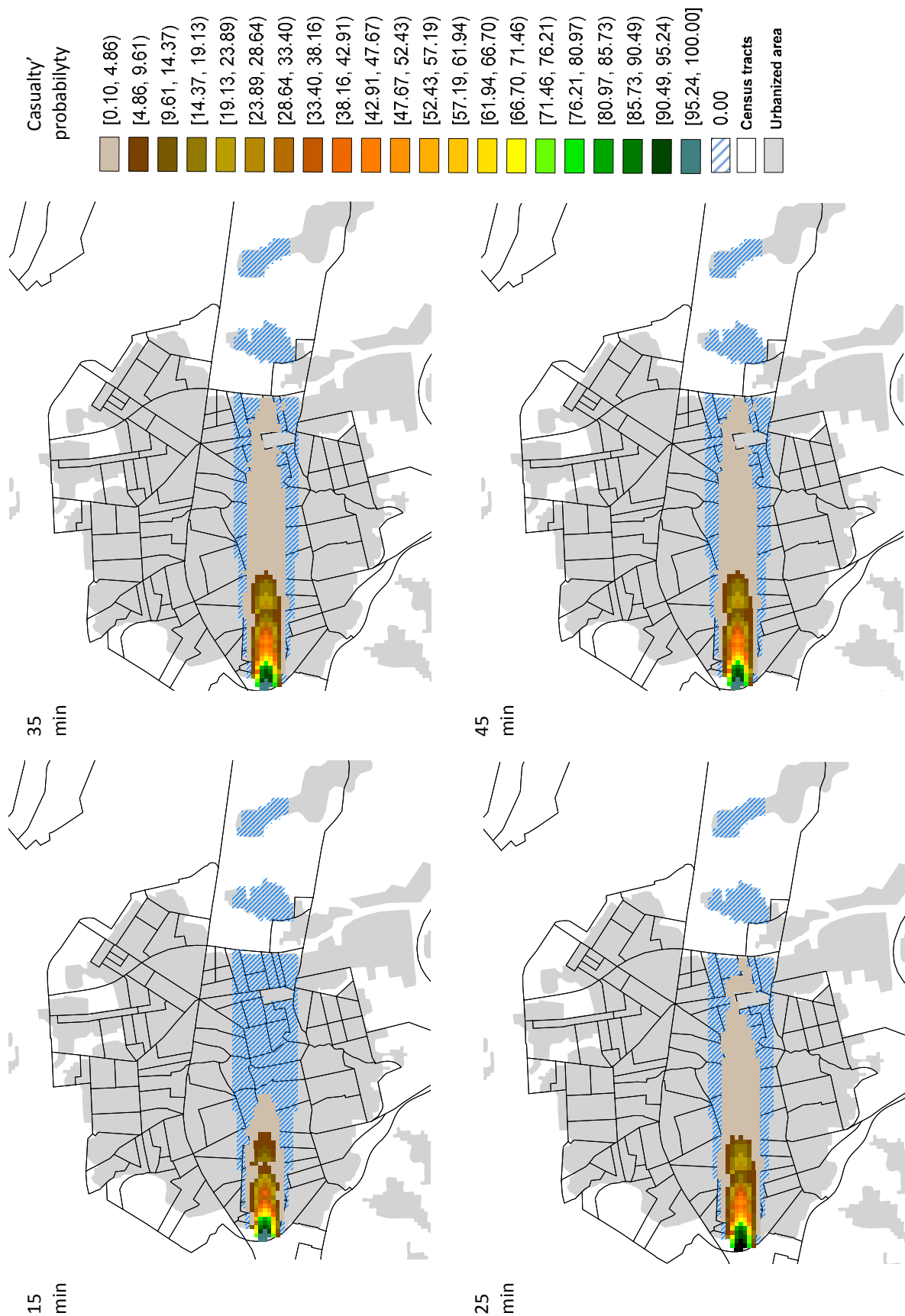


Figure 7.25 Casualty' probability for the 100th percentile of the airtightness (c') distribution. Constant airtightness scenario (simplified methodology).

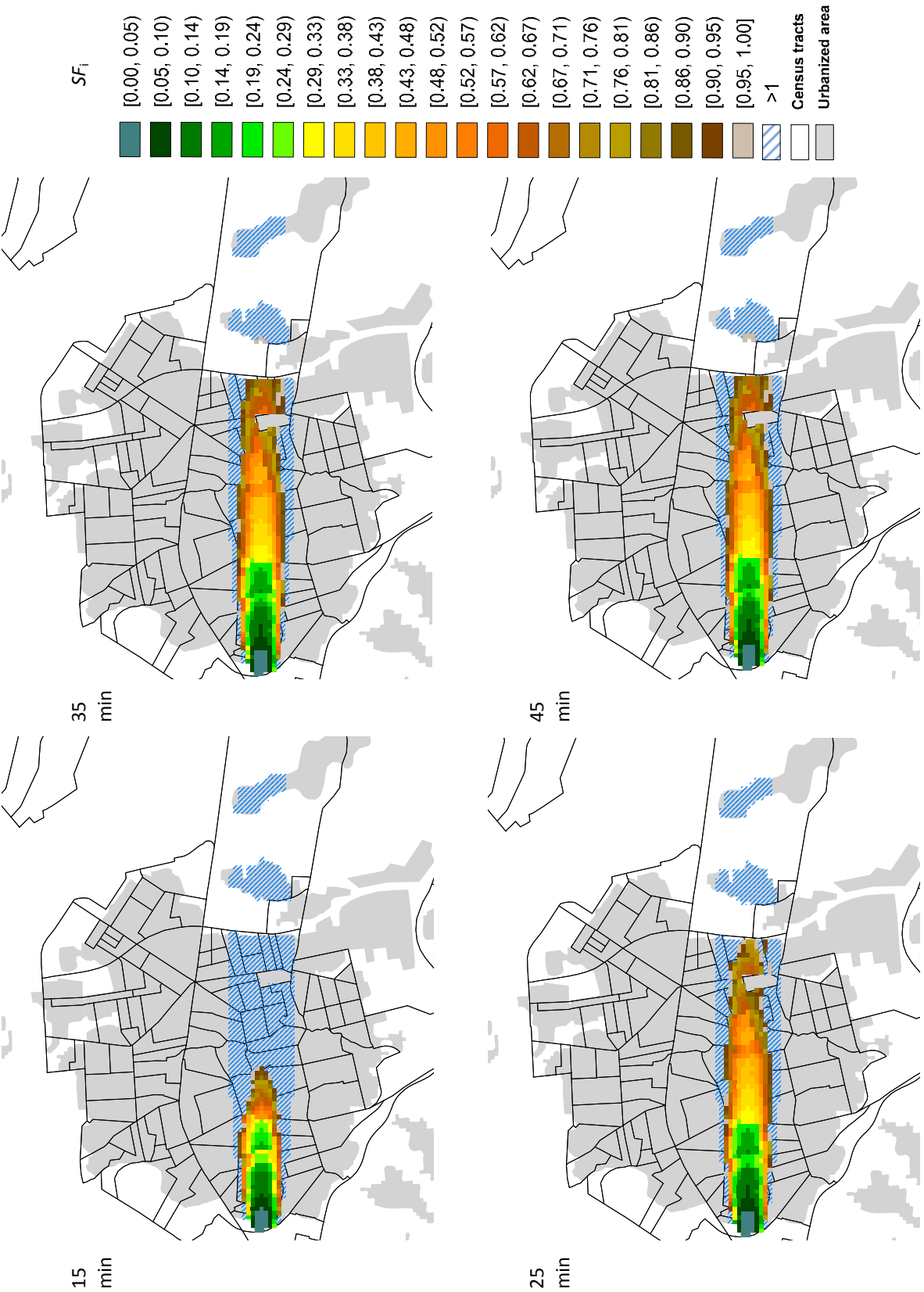


Figure 7.26 SF_i for the 100th percentile of the airtightness (c') distribution. Constant airtightness scenario (Simplified methodology).

Conclusions

The work done and the results obtained through the development of this thesis have led to the following conclusions.

1. Toxic gas clouds, although less common than other major hazards like fires, can affect larger areas. Besides, depending on the toxicity of the substance, they could have a great potential to kill, harm and pollute zones for weeks or even months. Therefore, in the event of an outdoor toxic gas release, the assessment of indoor concentration is essential to predict the efficiency of sheltering as an emergency protective measure. In this thesis, we have reviewed several models to estimate indoor concentration on the basis of the outdoor situation. These models vary in complexity, and the decision of which one to use depends on the desired accuracy and the availability of the parameters required by each model. The simplest models do not take into account the adsorption of toxic gases over indoor material surfaces. More complex models consider the effects of filtration in narrow air entrances, constant or variable adsorption, and desorption of the gas in the final stages of the event. Analytical solutions of these models for continuous and temporary sources, modeled with a Gaussian dispersion model, were obtained.
2. The survey of indoor concentration models also indicates that the main difficulty in estimating indoor concentration as a function of outdoor concentration lies not in the mathematical model to be applied, but in the lack of data on adsorption and desorption

properties of many substances. This kind of information has recently been published for VOCs, but for toxic substances it remains scarce. Further research should be done in this area.

3. A sensitivity analysis has been performed to assess the effect of diverse parameters on the effectiveness of shelter-in-place. From this analysis we found that adsorption processes significantly reduce maximum indoor concentration in relation to the situation of no adsorption. The presence of adsorption really improves shelter-in-place effectiveness, being its effect stronger in the case of cumulative substances ($n = 1$) than in peak substances ($n > 1$). Also, the presence of adsorption led to a quick stabilization of the indoor toxic load after the passage of the plume especially in peak substances, in a way that shelter-in-place effectiveness becomes independent of shelter duration. By contrast, in the case of non adsorption, the indoor toxic load increased with time (particularly for cumulative substances) and the shelter duration becomes an important parameter for shelter success.

In relation to the different adsorption models, we did not observe a significant difference among them, especially the one-sink and the sink-diffusion models performed almost equally, therefore an accurate estimation of shelter-in-place effectiveness can be obtained using the less complex model for which adsorption parameters are available, especially in the case of peak chemicals.

4. The air exchange rate comprises the unique parameter that people can manipulate in the case of a shelter-in-place situation, and its variation has a great effect on the effectiveness of shelter-in-place. From the sensitivity analysis, we saw that shelter-in-place effectiveness is favored at low air exchange rates, it specially affected the indoor safety factor and its effect was larger in the case of peak substances that adsorb over indoor surfaces, because the peak concentration reduction decrease as the air exchange rate increases, and the speed of gas entrance increases while adsorption velocity remains constant. Therefore, the knowledge of the distribution of this parameter among buildings becomes one of the most important things when assessing shelter-in-place effectiveness in a community, as well as the magnitude of reduction on the air exchange rate that could be achieved if expedient measures are implemented.

5. A review of available methods to estimate the air exchange rate, which comprised semi-empirical approaches and empirical measurements of different buildings in North America and Europe, has been done. The semi-empirical approach consists of determining the building airtightness, empirically or through airtightness models, and then applies a ventilation model that takes into account meteorological conditions, while the empirical approach consists of the direct measurement of the air exchange rate. Unfortunately we found nothing concerning Spanish buildings.
6. The LBNL airtightness model has been applied to Catalan single-family dwellings. It has been observed that it can give an approach of the airtightness distribution. However, the airtightness obtained is highly affected by the climatic zone distribution, pointing out that census tracts located in the dry climatic zone are less airtight, which is not the case for Catalunya, since differences in construction quality or materials among the different regions are negligible.
7. Since French dwellings and French climate are more likely to the Catalan situation, we prepared and performed a statistical analysis of the air leakage database of French single-family dwellings available at the Centre d'Études Techniques de L'Équipement (CETE) in Lyon. From this analysis we found that buildings characteristics that mainly affect single-family dwellings airtightness were the structure type, the number of stories, the floor area and the building age. From this database, we have also developed a statistical model, the UPC-CETE model, for predicting the airtightness of single-family dwellings in France and Spain. In addition, due to the similarities of dwellings' features across the south of Europe (Portugal, Italy, Greece), the model developed will probably give good estimations of the airtightness of dwellings in these areas too.

In the case of Catalunya, for which no experimental data regarding airtightness or air exchange rates were available, this model constitutes the first proposal for estimating the airtightness distribution of single-family dwellings. Airtightness distribution predicted with this model give smaller values than those obtained with the LBNL airtightness model.

8. A total of 27 trials to measure the air exchange rate, using the tracer gas technique, have been carried out in 16 single-family dwellings across Catalunya. These trials comprised the measurement of the whole dwelling air exchange rate, and the measurement of the air exchange rate of a room with expedient measures that could be used as an indoor shelter.

The reductions on the air exchange rates gained by sheltering in the sealed room with regards to the air exchange rate of the dwelling ranged from 1.5% to 84% with an average of 35%. Higher reductions were achieved in old dwellings, with small floor areas and few stories. Therefore, sheltering in an interior room with expedient measures in these types of dwellings, would really improve the effectiveness of shelter-in-place.

9. The approach used in this thesis is based on the assumption that indoor concentration is distributed homogeneously over indoor space. Considering the experimental trials, we found that homogeneity (in terms of the uniformity criterion) was achieved in dwellings with one or two stories, and with floor areas smaller than 140 m^2 (a volume of approximately 350 m^3), which represent 76% of Catalan single-family dwellings stock. Nevertheless, in the case of two and three story dwellings where the garage and the ground floor could be isolated from the rest of the dwelling closing a door, respectively, this criterion could also be met.

However, although homogeneity is harder to happen in dwellings with four or more stories (0.4% of Catalan single-family dwellings stock), and care should be taken when using models that assume perfect mixing to assess shelter-in-place effectiveness in a community with a high representation of these dwellings, the modification performed on the UPC-CETE airtightness model lead us to expect overestimations rather than underestimations of the airtightness and consequently the *ACH*, which is more conservative from the point of view of a shelter-in-place situation. Nevertheless, the model performs better in dwellings with one or two stories and small floor areas.

10. A simplified approach to estimate the fraction of air exchanged with outdoor and within indoor air, in the case of the room with expedient measures, has been used. Despite of the possible sources of errors, we borne out that effectively there is a fraction of air exchanged with indoor air. In general the tendency found was that more air exfiltrate to outdoor rather than to indoor and an average of 38% of the air exfiltrates to the indoor environment.
11. The usage of the UPC-CETE model in the estimation of the air exchange rate of Catalan dwellings, with the purpose of delimiting actuation zones in the event of a shelter-in-place situation, is a good tool that improves actual determination of the air exchange rate

(assuming it as a fix value), and thus gives better and more accurate estimations of this parameter.

From the case study developed in chapter 7, the scenario that considers a constant airtightness equal to the 90th percentile of the c' distribution in Catalunya, which avoided the real distribution of the air exchange rate in the affected area, leaded to a higher overestimation of the evacuation radius, while for the scenario that considers taking shelter in a room with expedient measures, the evacuation radius decreased by 19% in relation to no expedient sheltering scenario. In this case study, the usage of expedient measures also entailed a reduction on the evacuation radius of the same order of that obtained when the substance adsorbs over indoor surfaces.

With regards to calculations efforts, the application of the simplified methodology really makes easier and speeds up calculations without losing accuracy.

12. This thesis is only focused on the assessment of shelter in place effectiveness in single-family dwellings; which are the simplest residential units that could be considered as single zone volumes. However, more complex buildings, such as multifamily-dwellings and non-residential buildings (i.e. offices, educational buildings) also comprise a large proportion of buildings stock where people are usually found. Therefore further research concerning the assessment of shelter-in-place effectiveness in these types of buildings, including the calculation of air leakage and indoor concentration distribution across indoor space, should continue.

Nomenclature

Acronyms and Abbreviations

AEGL	Acute Exposure Guideline Levels
AIM-2	Alberta air infiltration model
AIVC	Air Infiltration and Ventilation Centre
ANOVA	Analysis of variance
ASHRAE	American Society of Heating, Refrigerating and Air-Conditioning Engineers
CFD	Computational fluid dynamics
CETE	Centre d'Études Techniques de L'Équipement in Lyon
DMMP	Dimethyl methylphosphonate, surrogate for sarin (GB)
DEEP	Diethyl ethylphosphonate, surrogate for soman (GD)
det	Determinat
EPA	U.S Environmental Protection Agency
erf	Error function

ERPG	Emergency Response Planning Guidelines
GIS	Geographical Information System
GM	Geometric mean
GSD	Geometric standard deviation
HDD	Heating degree day
IDESCAT	Statistical Institute of Catalunya
IDHL	Immediately Dangerous to Life or Health
LBNL	Lawrence Berkeley National Laboratory
LOC	Toxic level of concern
MS	Methyl salicylate, surrogate of mustard gas.
PEL	Permissible exposure limit at 8h
TEEL	Temporary Emergency Exposure Limits
TNO	The Netherland Organization for Applied Scientific Research
TEP	Triethyl phosphate, surrogate for tabun (GA)
US	United States of America
VX	Nerve agent VX, a extremely toxic substance

Symbols

a	Probit constant (-)
a_1, a_2, a_3	Solutions to the homogeneous system for indoor concentration. Eq. 3.1 - Eq. 3.3
A	Indoor surface area (m ²)
ACH	Air infiltration exchange rate or ventilation frequency, (s ⁻¹ , h ⁻¹)
$Area$	Floor area (m ²)
Age	Actual age of the dwelling (year)

B_1	Wind and stack effect pressure interaction coefficient in the AIM-2 ventilation model ($B_1 = -0.33$)
b	Probit constant (-)
c	Power law flow coefficient ($\text{m}^3 \cdot \text{s}^{-1} \cdot \text{Pa}^{-n}$)
c'	Adjusted power law flow coefficient for a pressure difference of 4 Pa, as defined in Eq. 5.2 ($\text{m}^3 \cdot \text{s}^{-1} \cdot \text{Pa}^{-n}$)
c_1	Power law flow coefficient including the flue in the AIM-2 ventilation model ($\text{m}^3 \cdot \text{s}^{-1} \cdot \text{Pa}^{-n}$)
c_{flue}	Power law flow coefficient of the flue in the AIM-2 ventilation model ($\text{m}^3 \cdot \text{s}^{-1} \cdot \text{Pa}^{-n}$)
C_D	Discharge coefficient for openings. Assumed as 1 (-)
C_i, C_o	Indoor and outdoor concentration ($\text{kg} \cdot \text{m}^{-3}$; ppm in Chapter 6)
C_o'	Initial indoor concentration in the dwelling during the trials (ppm)
C_{ref}	Reference concentration of CO_2 used for the trials (1500 ppm)
C_s	Concentration of CO_2 in the shelter (ppm)
C_1, C_2	Initial and final tracer gas concentrations during the experimental trials (ppm)
CRF	Casualty reduction factor (-)
CT	Construction type indicator in Eq. 5.7 (-)
CZ	Climate zone parameter (-)
d_1, d_2, d_3	Constants defined by initial conditions in Eq. 3.1 - Eq. 3.3
D	Number of different sorptive materials
dm_j/dt	Gas flux to or from surface of material j ($\text{kg} \cdot \text{m}^{-2} \cdot \text{s}^{-1}$)
ELA	Effective air leakage area (m^2)
f_i, f_o	Internal and external filtration factor, respectively ($\text{kg} \cdot \text{m}^{-3}$)
f_{GM}	Error of the mean estimation in Eq. 6.4

f_w, f_s	Wind and stack factors in the AIM-2 ventilation model, respectively (-)
g	Gravity acceleration ($9.8 \text{ m}\cdot\text{s}^{-2}$)
h	Source height of the release above ground (m)
H, H_o	Height of the building and height of one story, respectively (m)
H_1, H_2	French climate zone indicators. A value of 1 is assigned to the zone where the dwelling is located and 0 for the other zone
HS	Heating system indicator for the UPC-CETE model. Takes a value of 0 for electric heating systems and 1 for dwellings with non-electric heating systems
$I_{\Delta P}$	Leakage index ($\text{m}^3\cdot\text{s}^{-1}\cdot\text{m}^2$)
I_y, I_z	Parameters for the calculations of dispersion coefficients in the Gaussian dispersion model (see Table 2.6)
IT	Insulation type indicator for the UPC-CETE model. Takes a value of 0 for interior or integrated insulation, and 1 for exterior insulation (-)
J_y, J_z	Parameters for the calculations of dispersion coefficients in the Gaussian dispersion model (see Table 2.6)
k_1, k_2	Mass transfer coefficients in the two sink model (s^{-1})
k_a	Adsorption constant ($\text{m}\cdot\text{s}^{-1}$)
k_d	Desorption constant (s^{-1})
k_{dif}	Effective mass transfer coefficient (s^{-1})
K_y, K_z	Parameters for the calculations of dispersion coefficients in the Gaussian dispersion model (see Table 2.6)
m_{CO_2}	Mass of CO_2 to be injected during the experimental trials (g)
m_j	Amount of gas deposited on the surface of material j per unit of area, in the one-sink model ($\text{kg}\cdot\text{m}^{-2}$)
$m_{1,j}, m_{2,j}$	Amount of gas in the surface and inside of material j per unit of area in the diffusion and two sink model, respectively ($\text{kg}\cdot\text{m}^{-2}$)

n	Toxic load exponent (-)
N	Power law exponent (-)
NL	Normalized leakage (-)
NL_{CZ}	Normalized leakage coefficient for each climatic zone in the LBNL airtightness model, Eq. 2.45 (-)
N_{story}	Number of stories in the LBNL airtightness model, Eq. 2.45. Height of the building divided by the height of a single story, 2.5 m, (-)
NS	Number of stories parameter for the UPC-CETE model (Eq. 5.11 - Eq. 5.13). Takes a value of 1 for one-storey dwellings and 2 for more than one-storey (-)
NS'	Adjusted number of stories parameter for the UPC-CETE model (Eq. 7.3 - Eq. 7.5). Represent the real number of stories (-)
p	Parameter for the calculation of dispersion coefficients in the Gaussian dispersion model (see Table 2.6)
p_1, p_2, p_3	Constants defined by initial conditions in Eq. 3.4 - Eq. 3.6
P	Casualties' probability
P_a	Absolute pressure (Pa)
P_{eff}	Probability of an energy-efficient house in the LBNL airtightness model, Eq. 2.45 (-)
P_{floor}	Probability of floor leakage in the LBNL airtightness model, Eq. 2.45 (-)
P_i	Indoor casualties' probability (-)
P_{Li}	Probability of a low income house in the LBNL airtightness model, Eq. 2.45 (-)
P_o	Outdoor casualties' probability (-)
PF	Protection factor (-)
Pr	Probit function (-)
q	Amount of material instantaneously released (kg)
\dot{q}	Release source strength (kg·s ⁻¹)

Q	Air infiltration flow ($\text{m}^3 \cdot \text{s}^{-1}$)
Q_1	Air exfiltration flow ($\text{m}^3 \cdot \text{s}^{-1}$)
Q_2	Air recirculation flow due to mechanical ventilation systems ($\text{m}^3 \cdot \text{s}^{-1}$)
Q_3	Flow of make-up air of the mechanical ventilation system ($\text{m}^3 \cdot \text{s}^{-1}$)
Q_w, Q_s	Air infiltration flow due to the wind and the stack effect, respectively ($\text{m}^3 \cdot \text{s}^{-1}$)
R	Toxic substance removal rate ($\text{kg} \cdot \text{s}^{-1}$)
R^2	Squared correlation coefficient (-)
S	Toxic substance gain rate ($\text{kg} \cdot \text{s}^{-1}$)
S_f	Envelope unheated surface area (m^2)
S_w	Shelter coefficient in the AIM-2 ventilation model (see Table 2.10)
SF_i, SF_o	Indoor and outdoor safety factor, respectively (-)
SFM	Safety factor multiplier (-)
ST	Structure type indicator for the UPC-CETE model. Takes a value of 0 for a heavy structure and 1 for a light structure (-)
size	Area parameter in the LBNL airtightness model, Eq. 2.45. Floor area divided by 100 m^2 (-)
t	Time (s) Time elapsed from the plume's arrival at the house in Eq. 2.30, Eq. 2.36 - Eq. 2.38 (s) t -student statistic in Eq. 6.4
t_1	Duration of the release (s). In Eq. 6.1 denotes the time at which initial tracer gas concentration was measured
t_2	Time at which final tracer gas concentration was measured
t'	Time elapsed from the beginning of the release (s)
T_i, T_o	Indoor and outdoor temperature, respectively ($^{\circ}\text{C}$)
T_s	Shelter temperature ($^{\circ}\text{C}$)

TL	Toxic load $((\text{kg}\cdot\text{m}^{-3})^n \cdot \text{s})$
TL_i, TL_o	Indoor and outdoor toxic load $((\text{kg}\cdot\text{m}^{-3})^n \cdot \text{s})$
TLL	Toxic load limit $((\text{kg}\cdot\text{m}^{-3})^n \cdot \text{s})$
$TLRF$	Toxic load reduction factor (-)
v	Average wind velocity $(\text{m}\cdot\text{s}^{-1})$
v_d	Constant adsorption velocity $(\text{m}\cdot\text{s}^{-1})$
$v_z, v_{z'}$	Required and measured wind speed at level z and z' above ground, respectively $(\text{m}\cdot\text{s}^{-1})$
V	Building volume (m^3)
V_s	Shelter volume (m^3)
V_{CO_2}	Volume of CO_2 to be injected in the experimental trials (m^3)
x	Downwind distance from the release source (m)
x_{ij}	Coefficients of the eigenvector matrix X , Eq. 3.1 - Eq. 3.6 (-)
y	Cross-distance to the downwind direction (m)
Y	Flue leakage fraction, (-)
z	Height at which the concentration is estimated (m)
z_o	Terrain surface roughness (m)
ΔP	Pressure difference (Pa)
ΔP_r	Reference pressure difference (4 Pa)
ΔT	Absolute indoor-outdoor temperature difference ($^{\circ}\text{C}$)

Greek symbols

α	Independent coefficients for regressions of Eq. 5.3 - Eq. 5.6 (-)
	Confidence level in Eq. 6.1 (-)
α'	Independent coefficients for regressions of Eq. 5.7 (s^{-1})

δ, δ'	Constants dependent on onsite and offsite terrain conditions to convert wind speed in Eq. 2.53, respectively (-)
β_{Age}	UPC-CETE model coefficient for the age (year^{-1})
β'_{Age}	UPC-CETE model coefficient for the age when dwellings are older than 9 years ($\text{year}^{-1} \cdot \text{s}^{-1}$)
β_{area}	UPC-CETE model coefficient for the floor area (m^{-2})
β'_{CT}	Construction technique coefficient for regression of Eq. 5.7 (s^{-1})
β_{IT}	UPC-CETE model coefficient for the insulation type (-)
β_{H1}, β_{H2}	Coefficients for climate zones H1 and H2 in Eq. 5.3 - Eq. 5.5 (-)
β_{HS}	UPC-CETE model coefficient for the heating system (-)
β_{NS}	UPC-CETE model coefficient for the number of stories (-)
ϕ_{area}	LBNL airtightness model coefficient for the area (-)
ϕ_{height}	LBNL airtightness model coefficient for the height of the dwelling (-)
ϕ_e	LBNL airtightness model coefficient for energy-efficient dwellings (-)
ϕ_{age}	LBNL airtightness model coefficient for the age (-)
ϕ_{floor}	LBNL airtightness model coefficient for the floor leakage probability (-)
$\phi_{LI,age}$	LBNL airtightness model coefficient for the age of a low income dwelling (-)
$\phi_{LI,area}$	LBNL airtightness model coefficient for the area of a low income dwelling (-)
ϕ_{LI}	LBNL airtightness model coefficient for a low income dwelling (-)
γ, γ'	Constants dependent on onsite and offsite terrain conditions to convert wind speed in Eq. 2.53, respectively (-)
η_{GM}	Sample size in Eq. 6.4
$\lambda_1, \lambda_2, \lambda_3$	Eigenvalues of the coefficient matrix in Eq. 3.2 - Eq. 3.6 (-)
ρ	Air density ($\text{kg} \cdot \text{m}^{-3}$)
$\sigma_x, \sigma_y, \sigma_z$	Dispersion coefficients of the Gaussian model for a continuous source (m)

$\sigma_{x,i}$, $\sigma_{y,i}$, $\sigma_{z,i}$ Dispersion coefficients of the Gaussian model for an instantaneous source (m)

References

Angell W., Grimsrud D.T., Lee H. (2004). Survey and Critical Review of Scientific Literature on Indoor Air Quality, Ventilation, and Building-Related Health Effects in Residences. Chap. 6: Residential ventilation. US EPA 2004. Available at: <<http://mniaa.org/iaqresidential.html>>

Anuari de dades meteorològiques 2003. Servei Meteorològic de Catalunya (Meteorological Service of Catalunya). Available at: <http://www.meteocat.com/marcs/marc_clima.html>

Arroyo L.F., Pérez J.I. (2008). Construcción de edificios 2003 – 2007, licencias municipales de obra. Series estadísticas. Ministerio de Fomento. Available at: <<http://www.fomento.es/NR/rdonlyres/1A1EC825-4EA6-4A84-8282-4C0879E5C0F5/36397/CONSTRUCCIONDEEDIFICIOS2007.pdf>>

ASHRAE. (2005). ASHRAE handbook fundamentals. Chap. 27: Ventilation and Infiltration. SI Edition.

ASTM. Standard E741-00. Test Method for Determining Air Change in a Single Zone by Means of a Tracer Gas Dilution. American Society for Testing and Materials, 2000. Philadelphia, PA.

Azorin F., Sánchez-Crespo J.L. Métodos y aplicaciones del muestreo. Alianza Editorial, Madrid 1986.

Blewett W.K., Reeves D.W., Arca V.J., Fatkin D.P., Cannon B.D. (1996). Expedient sheltering in place: An evaluation for the chemical stockpile emergency preparedness program. Edgewood, Research Development and Engineering Center . U.S. Army Chemical and Biological Defense Command, Edgewood, Maryland.

Blewett W.K., Arca V.J. (1999). Experiments in sheltering in place: How filtering affects protection against sarin and mustard vapour. Edgewood Chemical Center, U.S. Army, Edgewood, Maryland.

Borhan M.S., Hao X. (2007). Development of a natural ventilated model for a tall, gutter-vented, multi-span double-layer Polyethylene greenhouse. Proceedings IS on Greensys 2007, 481-486.

Bouhamra W., Elkilani A. (1999). Development of a model for the estimation of indoor volatile organic compounds concentration based on experimental sorption parameters. Environmental Science and Technology, 33, 2100–2105.

Building Science Consulting. Consulted in April 18th of 2007. Available at: <<http://www.buildingscienceconsulting.com/designsthatwork/hygro-thermal.htm>>

Carrari C.L., Aparicio L.V., Bandoni J.S., Tonelli S.M. (2004). Utilización de Modelos de Dispersión Atmosférica para la estimación de Dosis de Exposición. Mecánica Computacional vol. XXIII (1-17). G.Buscaglia, E.Dari, O.Zamonsky (Eds.). Available at: <<http://www.cab.cnea.gov.ar/enief/dirjobs/CCarrari.resumen.pdf>>

Carrié R., Jobert R., Fournier M., Berthault S. 2006. Perméabilité à l'air de l'enveloppe des bâtiments. Généralités et sensibilisation. CETE de Lyon. Available at: <http://www.cete-lyon.equipement.gouv.fr/home_fichiers/domainesactivite/auhc/generalites_et_sensibilisation_v2.32-600dpi.pdf>

Casal J. (2008). Evaluation of the effects and consequences of major accidents in industrial plants (1st ed.). In: Industrial safety series, Vol. 8. Elsevier.

Casal J., Montiel H., Planas E., Vílchez, J.A. (1999a). Análisis del riesgo en instalaciones industriales. Barcelona, Spain: Ediciones UPC.

- Casal J., Planas E., Casal J. (1999b). Sheltering as a protective measure against airborne virus spread. *Journal of Hazardous Materials*, A68, 179–189.
- Castañeda A., Pérez A., Gil J. (2002). Tamaño de muestra requerido para estimar la media aritmética de una distribución lognormal. *Revista Colombiana de Estadística*, 25, 31-41.
- Chan, W. R., Price, P. N., Gadgil, A. J., & Nazaroff, W. W. (2004). Modeling shelter-in place including sorption on indoor surfaces. *Proceedings of the 84th American Meteorological Society Annual Meeting*, Seattle, WA.
- Chan W.R., Nazaroff W.W., Price P.N., Sohn M.D., Gadgil A.J. (2005) Analyzing a database of residential air leakage in the United States. *Atmospheric Environment*, 39, 3445-3455.
- Chan W.R., Nazaroff W.W., Price P.N., Gadgil A.J. (2007a). Effectiveness of urban shelter-in-place—I: Idealized conditions. *Atmospheric Environment*. 41, 4962–4976
- Chan W.R., Nazaroff W.W., Price P.N., Gadgil A.J. (2007b). Effectiveness of urban shelter-in-place—II: Residential districts. *Atmospheric Environment*. 41, 7082–7095.
- Chávez J., Goula X., Roca A., Mañá F., Presmanes J.A., López-Arroyo A. Escenarios de daños sísmicos en Cataluña (Seismic damage scenarios in Catalunya). 1er Congreso Nacional de Ingeniería Sísmica, Murcia 1999.
- Chen Q. (2009). Ventilation performance prediction for buildings: a method overview and recent applications. *Building and Environment*, 44, 848–858.
- Cozzani V., Smeder M., Zanelli S. (1998). Formation of hazardous compounds by unwanted reactions in industrial accidents. *Journal of Hazardous Materials* A63, 131–142.
- CPR 16E (Green Book). 1989. *Methods for the determination of possible damage*. Chap. 6: Protection against toxic substances by remaining indoors. TNO, Voorburg, The Netherlands, 1989.
- CPR 18E (Purple Book). 2005. *Guidelines for Quantitative Risk Assessment*. Directorate General for Social Affairs and Employment, TNO, The Hague, The Netherlands, 2005.

Dandrieux, A., Dimbour, J.P., Dusserre, G. (2006). Are dispersion models suitable for simulating small gaseous chlorine release?. *Journal of Loss Prevention in the Process Industries* 19, 683-689.

Digital Climatic Atlas of Catalunya (Atlas Climático Digital de Catalunya), 2001. Meteorological Service of Catalunya. Available at: <<http://magno.uab.es/atles-climatic/catala/minimes.htm>>

Draper NR, Smith H. Applied regression analysis. Wiley Series in Probability and Statistics. 3rd ed. John Wiley & Sons; 1998.

EN 13829:2001, European standard. Thermal performance of buildings. Determination of air permeability of buildings. Fan pressurization method. January 2001.

EN 13465:2004. European standard. Ventilation for buildings: calculation methods for the determination of air flow rates in dwellings. 2004.

Emmerich S.J. (2001). Validation of IAQ modeling of residential scale buildings: a review. *ASHRAE Transactions*, 107(2), 619–628.

Engelmann R.J. (1992). Sheltering effectiveness against plutonium provided by buildings. *Atmospheric Environment* 26A, 11, 2037-2044.

EPA. 2009. U.S Environmental Protection Agency. Website available at: <<http://www.epa.gov/oppt/aegl/>>

Ermak D.L. (1990). User's manual for SLAB: An atmospheric dispersion model for denser-than-air releases. University of California, Lawrence Livermore National Laboratory. UCRL-MA-105607.

Espinar J. 2005. Estudi comparatiu dels paràmetres de toxicitat i vulnerabilitat de substàncies perilloses. Undergraduate final work. Universitat Politècnica de Catalunya. Escola Tècnica Superior d'Enginyeria Industrial de Barcelona, Departament d'Enginyeria Química.

Glickman T.S., Ujihara A.M. (1990). Deciding between in-place protection and evacuation in toxic vapor cloud emergencies. *Journal of Hazardous Materials*, 23, 57–72.

Guo L., Lewis O. (2007). Carbon dioxide concentration and its application on estimating the air change rate in typical Irish houses. *International Journal of Ventilation*, 6(3), 235-345.

- Hanna S., Dharmavaram S., Zhang J., Sykes I., Witlox H., Khajehnajafi S., Koslan K. (2008). Comparison of six widely-used dense gas dispersion model for three recent chlorine railcar accidents. *Process Safety Progress*, 27 (3), 248-259.
- Hartman H.M. (2002). Evaluation of risk assessment guideline levels for the chemical warfare agents mustard, GB, and VX. *Regulatory Toxicology and Pharmacology* 35, 347–356.
- Heath MT. Scientific computing: an introductory survey. Chapter 13 – random numbers and stochastic simulation. 2002. Available at: <http://www.cse.uiuc.edu/heath/scicomp/notes/chap13_8up.pdf>
- Hewett P. (1995). Sample size formulae for estimating the true arithmetic or geometric mean of lognormal exposure distributions. *American Industrial Hygienist Association Journal*, 56, 219-225.
- Irwin J.S. (1979). A theoretical variation of the wind profile power-law exponent as a function of surface roughness and stability. *Atmospheric Environment* 13, 191-194.
- Jetter J.J., Whitfield, C. (2005). Effectiveness of expedient sheltering in place in a residence. *Journal of Hazardous Materials*, A119, 31–40.
- Jetter J., Proffitt D. (2006). Effectiveness of Expedient Sheltering in Place in Commercial Buildings. *Journal of Homeland Security and Emergency Management*, 3(2), article 4. Available at: <<http://www.bepress.com/jhsem/vol3/iss2/4>>
- Jørgensen R.B., Bjørseth O. (1999). Sorption behavior of volatile organic compounds on material surfaces: the influence of combinations of compounds and materials compared to sorption of single compounds on single materials. *Environment International*, 25, 17–27.
- Jørgensen R.B., Bjørseth O., Malvik B. (1999). Chamber testing of adsorption of volatile organic compounds (VOCs) on material surfaces. *Indoor Air*, 9, 2–9.
- Jørgensen R.B., Dokka T.H., Bjørseth O. (2000). Introduction of a sink-diffusion model to describe the interaction between volatile organic compounds (VOCs) and material surfaces. *Indoor Air*, 10, 27–38.
- Jonsson L., Karlsson E., Thaning L. (2005). Toxic gas clouds: effects and implications of dry deposition on concentration. *Journal of Hazardous Materials*, A124, 1–18.

- Kalamees T. (2007). Air tightness and air leakages of new lightweight single-family detached houses in Estonia. *Building and Environment* 42, 2369–2377.
- Karlsson E. (1994). Indoor deposition reducing the effect of toxic gas clouds in ordinary buildings. *Journal of Hazardous Materials*, 38, 313–327.
- Karlsson E., Huber U. (1996). Influence of desorption on the indoor concentration of toxic gases. *Journal of Hazardous Materials*, 49, 15–27.
- Khan F.I., Abbasi S.A. (1999). Major accidents in process industries and an analysis of causes and consequences. *Journal of Loss Prevention in the Process Industries*, 12, 361–378.
- Lawrence T.M., Braun J.E. (2006). Evaluation of simplified models for predicting CO₂ concentrations in small commercial buildings. *Building and Environment* 41, 184–194.
- Litvak A., Guillot K., Kilberger M., Boze D. (2000a). Airtightness of French dwellings: Results from field measurement studies. *Proceedings 21st AIVC Annual Conference, "Innovations in Ventilation Technology"*, 26-29 September 2000, paper 60.
- Litvak A., Kilberger M., Guillot K. (2000b). Field measurement results of the airtightness of 64 French dwellings. Submitted to ROOMVENT 2000 (9-12 July 2000)
- Litvak A., Boze D., Kilberger M. (2001). Airtightness of 12 non residential large buildings results from field measurement studies, *22nd AIVC Conference*, Bath, UK, September 2001.
- Mannan M.S., Kilpatrick D.L. (2000). The pros and cons of shelter-in-place. *Process Safety Progress* 19 (4), 210–218.
- Matlab. The Language of Technical Computing. Version 7.8.0.347 (R2009a). License number: 107001.
- McWilliams J., Jung M. (2006). Development of a mathematical air-leakage model from measured data. Lawrence Berkeley Laboratory Report: No. 59041.
- Meininghaus R., Uhde E. (2002). Diffusion studies of VOC mixtures in a building material. *Indoor Air*, 12, 215–222.

Montgomery DC, Runger GC. Applied statistics and probability for engineers. John Wiley & Sons, Inc. Fourth edition. 2007.

Morse R.G., Haas P., Lattanzio S.M, Zehnte D., Divine M. (2009). A cross-sectional study of schools for compliance to ventilation rate requirements, *J. Chem. Health Safety*, 16 (6), 4-10.

Murray D.M., Burmaster D.E. (1995). Residential air exchange rates in the United States: empirical and estimated parametric distribution by season and climatic region. *Risk Analysis*, 15, 459–465.

NICS. National Institute for Chemical Studies. (2001). Sheltering in place as a public protection action. Available at: <<http://www.nicsinfo.org/shelter%20in%20place.pdf>>

Oggero A., Darbra R.M., Muñoz M., Planas E., Casal J. (2006). A survey of accidents occurring during the transport of hazardous substances by road and rail. *Journal of Hazardous Materials A133*, 1–7.

Orme M., Liddament M.W., Wilson A. (1998). An analysis and data summary of the AIVC numerical database. AIVC Technical Note, 44. International Energy Agency.

Orme M., Leksmono N. (2002). Ventilation modeling data guide. In: AIVC guide, Vol. 5. International Energy Agency.

Pandian, M.D., Behar, J.V., et al. (1998). Correcting errors in the nationwide data base of residential air exchange rates. *Journal of Exposure Analysis and Environmental Epidemiology* 8(4): 577-86.

Penman J. M. (1980). An Experimental Determination of Ventilation Rate in Occupied Rooms Using Atmospheric Carbon Dioxide Concentration. *Building and Environment*, Vol. 15, pp. 45-17.

Penman J.M., Rashid A.A.M. (1982). Experimental determination of air-flow in a naturally ventilated room using metabolic carbon dioxide. *Building and Environment*, Vol. 17, pp. 253-256.

Perfil Ambiental de España 2005. Informe basado en indicadores. Apartado 2.14: Riesgos naturales y tecnológicos (269-285). Ministerio de Medio Ambiente. Available at:

<http://www.mma.es/secciones/calidad_contaminacion/indicadores_ambientales/perfil_ambiental_2005/>

Perfil Ambiental de España 2008. Informe basado en indicadores. Apartado 2.14: Desastres naturales y tecnológicos (304-323). Ministerio de Medio Ambiente. Available at: <http://www.mma.es/portal/secciones/calidad_contaminacion/indicadores_ambientales/perfil_ambiental_2008/pdf/2_14Desastres.pdf>

Persily A.K. (1996). The relationship between indoor air quality and carbon dioxide. In: 7th Indoor Air Quality and Climate, 2: 961-966. July 1996, Nagoya, Japan.

Persily A.K. (1999). Myths about buildings envelopes. ASHRAE Journal, March, 39-47.

Piadé J., D'Andrés S.D., Sanders E.B. (1999). Sorption phenomena of nicotine and ethenylpyridine vapors on different materials in a test chamber. Environmental Science and Technology, 33, 2046–2052.

PLASEQCAT 2005. Pla d'Emergència Exterior del Sector Químic de Catalunya (Emergency Plan for the Chemical Sector at Catalunya). Generalitat de Catalunya, Direcció General de Protecció Civil. Available at: <<http://www.gencat.cat/interior/emergencies/plans/quimic/emergencia/index.htm>>

PLASEQCAT 2007. Pla d'Emergència Exterior del Sector Químic de Catalunya (Emergency Plan for the Chemical Sector at Catalunya). Generalitat de Catalunya, Direcció General de Protecció Civil. Available at: <<http://www.gencat.cat/interior/emergencies/plans/quimic/emergencia/index.htm>>

Price P.N., Shehabi A., Chan R. (2006). *Indoor-Outdoor Air Leakage of Apartments and Commercial Buildings*. California Energy Commission, PIER Energy-Related Environmental Research Program. CEC-500-2006-111.

Purswell J.L., Gates R.S., Lawrence L.M., Jacob J.D., Stombaugh T.S., Coleman R.J. (2006). Review of "Air exchange rate in a horse trailer during road transport". Transactions of the American Society of Agricultural and Biological Engineers, Vol. 49 (1): 193-201.

Renau J.M. (2008). Part III Senyals del Risc. Risc Industrial. Informe 2008: Aigua font de vida, font de risc. Observatori del Risc. Available at: <<http://www.seguretat.org/ides/ca/observatori-del-risc/informe-2008/sumari.html?pag=2>>

Renau J.M. (2009). Indicadors del Risc. Risc Industrial. Informe 2009 de l'Observatori del Risc. Available at: <<http://www.seguretat.org/docroot/ides/includes/senyals/fitxers/entrada9661/complet743/RISC-INDUSTRIAL.pdf>>

Rogers G.O., Watson A.P., Sorensen J.H., Sharp R.D., Carnes S.A. (1990). Evaluating protective actions for chemical agent emergencies. U.S. Department of the Army. Prepared by the Oak Ridge National Laboratory. ORNL-6615.

RT 2000. Arrêté du 29 novembre 2000 relatif aux caractéristiques thermiques des bâtiments nouveaux et des parties nouvelles de bâtiments, Ministère de l'Équipement, des Transports et du Logement, DGUHC.

Seinfeld J.H., Pandis S.N. Atmospheric Chemistry and Physics: From Air Pollution to Climate Change. Wiley Interscience Publication, New York 1998, 926-950.

Serida. Safety environmental Risk Database. Version 1.30, 1999.

Sfakianaki A., Pavlou K., Santamouris M., Livada I., Assimakopoulos M.-N., Mantas P., Christakopoulos A. Air tightness measurements of residential houses in Athens, Greece. Building and Environment 43 (2008) 398–405.

Shair F.H., Heitner K.L. (1974). Theoretical model for relating indoor pollutant concentrations to those outside. Environmental Science and Technology, 8, 444–451.

Sherman M., Grimsrud D. (1980). Infiltration–pressurization correlation: simplified physical modeling. ASHRAE Transactions, 86, 778.

Sherman M.H. (1992). Superposition in Infiltration Modeling. Indoor Air, 2, 101-114.

Sherman M. H., Dickerhoff D. (1998). Air-Tightness of U.S. Dwellings. ASHRAE Transactions, 104 (2), 1359-1367.

Sherman M. (2008). Air leakage of US homes. Proceedings of the 29th AIVC Conference. Vol. 3, 333-340. Kyoto, JP.

- Singer B.C., Revzan K.L., Hotchi T., Hodgson A.T., Brown N. (2004). Sorption of organic gases in a furnished room. *Atmospheric Environment*, 38, 2483–2494.
- Singer B.C., Hodgson A.T., Destailats H., Hotchi T., Revzan K.L., Sextro R.G. (2005a). Indoor sorption of surrogates for sarin and related nerve agents. *Environmental Science and Technology*, 39, 3203–3214.
- Singer B.C., Hodgson A.T., Hotchi T., Ming K.Y., Sextro R.G., Wood E.E. (2005b). Sorption of organic gases in residential bedrooms and bathrooms. *Proceedings, Indoor Air: 10th International Conference on Indoor Air Quality and Climate*, Beijing, China.
- Smith P.N. (1988). Determination of ventilation rates in occupied buildings from metabolic CO₂ concentrations and production rates. *Building and environment*, 23 (2), 95-102.
- Sorensen J.H., Vogt B.M. (2001). Will duct tape and plastic really work? Issues related to expedient shelter-in-place. Federal Emergency Management Agency. Prepared by OAK Ridge National Laboratory. ORNL/TM-2001/154.
- Ten Berge W. F. (1986). Concentration time mortality response relationship of irritant and systematically acting vapors and gases. *Journal of Hazardous Materials*, 13, 301-309.
- Van Der Wal J.F., Hoogeveen A.W., Van Leeuwen L. (1998). A quick screening method for sorption effects of volatile organic compounds on indoor materials. *Indoor Air*, 8, 103–112.
- Van Loy M.D., Lee V., Gundel L.A., Daisey J.M., Sextro R.G., Nazaroff W.W. (1997). Dynamic behavior of semivolatile organic compounds in indoor air.1. Nicotine in a stainless steel chamber. *Environmental Science and Technology*, 31, 2554–2561.
- Van Loy M.D., Riley W.J., Daisey J.M., Nazaroff W.W. (2001). Dynamic behavior of semivolatile organic compounds in indoor air. 2. Nicotine and phenanthrene with carpet and wallboard. *Environmental Science and Technology*, 35, 560–567.
- Vílchez J.A., Sevilla S., Montiel H., Casal J. (1995). Historical analysis of accidents in chemical plants and in the transportation of hazardous materials. *Journal of Loss Prevention in the Process Industries*, 8 (2), 87-96.

- Voisin G. (2007). Influence de la perméabilité à l'air des bâtiments sur la pénétration de polluants extérieurs toxiques dans un local de confinement. Étude numérique et expérimentale pour le développement d'un outil opérationnel de prévention du risque toxique. Master Recherché MEGA, Génie Civil, Insa Lyon.
- Walker I.S., Wilson D.J. (1998). Field Validation of Algebraic Equations for Stack and Wind Driven Air Infiltration Calculations. ASHRAE HVAC&R Research Journal, Vol. 4(2), 119-139.
- Wang L., Chen Q. (2008). Evaluation of some assumptions used in multizone airflow network models. Building and Environment, 43, 1671–1677.
- Wang W., Beausoleil-Morrison I., Reardon J. (2009). Evaluation of the Alberta air infiltration model using measurements and inter-model comparisons. Building and Environment, 44, 309-318.
- Won D., Corsi R.L., Rynes M. (2000). New indoor carpet as an adsorptive reservoir for volatile organic compounds. Environmental Science and Technology, 34, 4193–4198.
- Won D., Corsi R.L., Rynes M. (2001a). Sorptive interactions between VOCs and indoor materials. Indoor Air, 11, 246–256.
- Won, D., Sander, D. M., Shaw, C. Y., & Corsi, R. L. (2001b). Validation of the one-sink model for sorptive interactions between VOCs and indoor materials. Atmospheric Environment, 35, 4479–4488.
- Yang X., Chen Q., Zhang J.S., An Y., Zeng J., Shaw C.Y. (2001). A mass transfer model for simulating VOC sorption on building materials. Atmospheric Environment, 35, 1291–1299.
- You Y., Bai Z., Jia C., Wan Z., Ran W., Zhang J. (2007). Measuring Air Exchanges Rates Using Continuous CO2 Sensors. *Proceedings of Clima 2007 Well Being Indoors*.
- Yuan L.L. (2000). Sheltering effects of buildings from biological weapons. Science and Global Security, 8, 329–355.
- Zhang J., Zhang J.S., Chen Q. (2002b). Effects of environmental conditions on the VOC sorption by building materials. Part I: experimental results. ASHRAE Transactions, 108, 273–282.

Zhang J., Zhang J.S., Chen Q., Yang X. (2002a). A critical review on studies of volatile organic compound (VOC) sorption on building materials. *ASHRAE Transactions*, 108, 162–174.

Zhang J., Zhang J.S., Chen Q. (2003). Effects of environmental conditions on the VOC sorption by building materials. Part II: model evaluations. *ASHRAE Transactions*, 109, 167–178.

Zhao D., Little J.C., Hodgson A.T. (2002). Modeling the reversible, diffusive sink effect in response to transient contaminant sources. *Indoor Air*, 12, 184–190.

Zill D.G. (1988). *Ecuaciones diferenciales con aplicaciones* (2nd Spanish ed.). Mexico city.

European Directives

Directiva 96/82/CE del Consell, de 9 de desembre de 1996, relativa al control de riscos inherents als accidents greus en els que intervenen substàncies perilloses.

Directiva 2003/105/CE del Parlament Europeu i del Consell, de 16 de desembre de 2003, pel qual es modifica la Directiva 96/82/CE, relativa al control de riscos inherents als accidents greus en els que intervenen substàncies perilloses.

Spanish Directives

Ley Orgánica 5/1985, de 19 de junio de 1985. Ley Electoral. Last visit: 15/01/210 .Available at: <<http://www.senado.es/leyelect/indices/index.html>>

Real Decret 1324/1972 de 20 de abril, pel que s'aprova la norma d'edificació MV-201/72 "Muros resistentes de fábrica de ladrillo".

Real Decret 1254/1999, de 16 de juliol, pel que s'aproven mesures de control dels riscos inherents als accidents greus en els que intervenen substàncies perilloses.

Real Decret 1196/2003, de 19 de setembre, pel que s'aprova la "Directriz Básica de protección civil para el control y planificación delante del riesgo de accidentes graves en los que intervienen sustancias peligrosas".

Real Decret 119/2005, de 4 de febrer, pel qual es modifica el Real Decret 1254/1999, pel que s'aproven mesures de control dels riscos inherents als accidents greus en els que intervenen substàncies perilloses.

Real Decret 948/2005, de 29 de juliol, pel qual es modifica el Real Decret 1254/1999, pel que s'aproven mesures de control dels riscos inherents als accidents greus en els que intervenen substàncies perilloses.

Catalan Directives

Decret 174/2001, de 26 de juny, pel qual es regula l'aplicació a Catalunya del Real Decret 1254/1999, de 16 de juliol, pel que s'aproven mesures de control dels riscos inherents als accidents greus en els que intervenen substàncies perilloses.

Webs

Belt Iberica S.A. Analistas de Prevención. (18-07-2003) Una nube tóxica en el Vallés Oriental (Cataluña) activa el Plan de Emergencia Exterior. Available at: <<http://www.belt.es/noticias/2003/julio/18/nube.htm>>

Instituto Tecnológico del Fuego. (31-01-2002) Una nube tóxica paraliza el complejo industrial del Valle de Escombreras en Cartagena, España. Last visit: 15/01/2010. Available at: <http://www.itfuego.com/nube_toxica_cartagena.htm>

La Region Internacional. Edición Digital. (06/03/2009). Un incendio en Química del Nalón genera una nube tóxica. Last visit: 11/01/2010. Available at: <<http://www.laregioninternacional.com/noticia/47300/incendio/Qu%C3%ADmica/>>

IDESCAT. 2001. Statistical Institute of Catalunya. Dwelling Census of 2001. Last visit: 15/02/2010. Available at: <<http://www.idescat.cat>>

INEbase. 2001. Instituto Nacional de Estadística Statistical National Institute). Censo de población y viviendas 2001 (Population and housing census). Last visit: 22/10/2009. Available at: <http://www.ine.es/inebmenu/mnu_construc.htm>

Servei Meteorològic de Catalunya. Available at: <http://www.meteo.cat/mediambxemec/servmet/marcs/marc_dades.html>

Annex A. Distribution of dwellings characteristics by census tracts

This Annex presents the format on which the data concerning dwellings characteristics was provided by the IDESCAT. Data was obtained in excel files, organized by census codes (lines) and frequencies (columns) by categories. The second table shown presents an example of the computed discrete probability distribution of the variable by census tract.

A.1 Floor area

Table A.1 Dwellings' frequencies by floor area (m²) and census tract

Census code	<30	30-39	40-49	50-59	60-69	70-79	80-89	90-99	100-109	110-119	120-129	130-139	140-149	150-179	180-209	>209	total
0800101001	0	0	1	1	1	3	7	34	29	23	8	6	9	14	8	6	150
0800101002	0	0	0	0	1	5	8	78	29	27	73	13	24	43	27	6	334
0800101003	0	0	0	0	6	8	7	44	16	7	12	4	3	10	3	5	125
0800101004	0	0	2	2	3	6	27	43	27	19	22	2	1	23	9	6	192
0800101005	0	0	0	0	0	1	0	0	0	8	3	0	0	0	0	0	12
0800101007	1	0	2	11	33	48	68	63	36	23	26	9	9	21	10	10	370
0800201001	0	0	1	1	1	6	7	8	13	4	9	3	0	9	7	5	74
0800301001	0	1	5	15	21	23	14	59	34	10	24	12	12	48	20	40	338
0800301002	0	1	2	7	12	17	16	35	46	18	37	17	24	73	88	114	507

Table A.2 Discrete probability distributions of dwellings by floor area (m²) and census tract

Census code	<30	30-39	40-49	50-59	60-69	70-79	80-89	90-99	100-109	110-119	120-129	130-139	140-149	150-179	180-209	>209
0800101001	0.000	0.000	0.007	0.007	0.007	0.020	0.047	0.227	0.193	0.153	0.053	0.040	0.060	0.093	0.053	0.040
0800101002	0.000	0.000	0.000	0.000	0.003	0.015	0.024	0.234	0.087	0.081	0.219	0.039	0.072	0.129	0.081	0.018
0800101003	0.000	0.000	0.000	0.000	0.048	0.064	0.056	0.352	0.128	0.056	0.096	0.032	0.024	0.080	0.024	0.040
0800101004	0.000	0.000	0.010	0.010	0.016	0.031	0.141	0.224	0.141	0.099	0.115	0.010	0.005	0.120	0.047	0.031
0800101005	0.000	0.000	0.000	0.000	0.000	0.083	0.000	0.000	0.000	0.667	0.250	0.000	0.000	0.000	0.000	0.000
0800101007	0.003	0.000	0.005	0.030	0.089	0.130	0.184	0.170	0.097	0.062	0.070	0.024	0.024	0.057	0.027	0.027
0800201001	0.000	0.000	0.014	0.014	0.014	0.081	0.095	0.108	0.176	0.054	0.122	0.041	0.000	0.122	0.095	0.068
0800301001	0.000	0.003	0.015	0.044	0.062	0.068	0.041	0.175	0.101	0.030	0.071	0.036	0.036	0.142	0.059	0.118
0800301002	0.000	0.002	0.004	0.014	0.024	0.034	0.032	0.069	0.091	0.036	0.073	0.034	0.047	0.144	0.174	0.225

A.2 Year of constuction

Table A.3 Dwellings' frequencies by year of construction and census tract

Census code	<1900	1900-1920	1921-1940	1941-1950	1951-1960	1961-1970	1971-1980	1981-1990	1991-2001	without data	total
0800101001	0	4	0	0	1	2	37	103	3	0	150
0800101002	1	0	0	0	0	0	0	18	315	0	334
0800101003	2	0	0	3	1	14	17	72	16	0	125
0800101004	15	5	2	2	1	16	46	78	27	0	192
0800101005	0	0	0	0	0	0	9	0	3	0	12
0800101007	5	2	0	1	5	7	59	132	159	0	370
0800201001	48	2	1	1	2	5	1	2	12	0	74
0800301001	39	6	12	97	7	17	42	75	43	0	338
0800301002	6	0	1	6	19	44	115	222	94	0	507

Table A.4 Discrete probability distributions of dwellings by year of construction and census tract

Census code	<1900	1900-1920	1921-1940	1941-1950	1951-1960	1961-1970	1971-1980	1981-1990	1991-2001	without data
0800101001	0.000	0.027	0.000	0.000	0.007	0.013	0.247	0.687	0.020	0.000
0800101002	0.003	0.000	0.000	0.000	0.000	0.000	0.000	0.054	0.943	0.000
0800101003	0.016	0.000	0.000	0.024	0.008	0.112	0.136	0.576	0.128	0.000
0800101004	0.078	0.026	0.010	0.010	0.005	0.083	0.240	0.406	0.141	0.000
0800101005	0.000	0.000	0.000	0.000	0.000	0.000	0.750	0.000	0.250	0.000
0800101007	0.014	0.005	0.000	0.003	0.014	0.019	0.159	0.357	0.430	0.000
0800201001	0.649	0.027	0.014	0.014	0.027	0.068	0.014	0.027	0.162	0.000
0800301001	0.115	0.018	0.036	0.287	0.021	0.050	0.124	0.222	0.127	0.000
0800301002	0.012	0.000	0.002	0.012	0.037	0.087	0.227	0.438	0.185	0.000

A.3 Number of stories

Table A.5 Dwellings' frequencies by number of stories and census tract

Census code	1	2	3	4	5	6	7	8 ≥	total
0800101001	14	124	12	0	0	0	0	0	150
0800101002	1	144	189	0	0	0	0	0	334
0800101003	123	2	0	0	0	0	0	0	125
0800101004	191	0	0	1	0	0	0	0	192
0800101005	1	11	0	0	0	0	0	0	12
0800101007	190	150	30	0	0	0	0	0	370
0800201001	41	29	4	0	0	0	0	0	74
0800301001	79	217	42	0	0	0	0	0	338

Table A.6 Discrete probability distributions of dwellings by number of stories and census tract

Census code	1	2	3	4	5	6	7	8 ≥
0800101001	0.093	0.827	0.080	0.000	0.000	0.000	0.000	0.000
0800101002	0.003	0.431	0.566	0.000	0.000	0.000	0.000	0.000
0800101003	0.984	0.016	0.000	0.000	0.000	0.000	0.000	0.000
0800101004	0.995	0.000	0.000	0.005	0.000	0.000	0.000	0.000
0800101005	0.083	0.917	0.000	0.000	0.000	0.000	0.000	0.000
0800101007	0.514	0.405	0.081	0.000	0.000	0.000	0.000	0.000
0800201001	0.554	0.392	0.054	0.000	0.000	0.000	0.000	0.000
0800301001	0.234	0.642	0.124	0.000	0.000	0.000	0.000	0.000

Annex B. Programs used in the estimation of the *ACH* distribution applying the stochastic simulation

B.1 Programs to estimate the *ACH* distribution in Catalunya using the stochastic simulation.

Matlab codes *.m	Text files necessities to run the codes *.txt
distrdiscreta	año
estocastica	area
infiltración	plantas
nxestacion	secciones
	temperatura
	velocidad
	Text files generated *.txt
	no
	codigo

A description of the codes used to estimate the *ACH* of Catalan dwellings using the stochastic simulation, the LBNL airtightness model, the UPC-CETE model and the AIM-2 ventilation model are shown next:

Input	Output
estocastica.m	
distrdiscreta.m	codigo.txt
año.txt	
area.txt	
estructura.txt	
plantas.txt	
puntosT.txt	
secciones.txt	
infiltracion.m	
secciones.txt	Cp.txt
nxestacion.m	
Cp.txt	no.txt
temperatura.txt	
velocidad.txt	

Description of the codes

distrdiscreta.m

This code generates random numbers in accordance to a discrete probability distribution. Random numbers are generated using the *rand* function of matlab.

estocastica.m

This code writes random values of area, age, number of stories and structure type for each dwelling inside the affected census tracts with more than 10 dwellings (código.txt). This procedure is done taking into account the real distribution of discrete probabilities in the census tract.

infiltracion.m

This code estimates the airtightness of every dwelling using the building characteristics obtained through the stochastic simulation, stored in files codigo.txt, and the LBNL airtightness model or the UPC-CETE model, for chapters 4 and 5 respectively.

nxestación.m

This code calculates the air infiltration flow through the AIM-2 ventilation model for each dwelling by season.

distrdiscreta.m

```

function [sample] = distrdiscreta(npoints,pdf,error)
% SIMDISCR random numbers from a discrete random
% variable X which attains values x1,...,xn with probabilities
p1,...,pn
%
% Inputs: npoints - sample size
%         pdf - vector of probabilities (p1, ..., pn). They should
%         sum up to 1.
%
if (sum(pdf)<0.90)
    suma=sum(pdf)
    error('Probabilities does not sum up to 1');
elseif (sum(pdf)>1.1)
    suma=sum(pdf)
    error('Probabilities does not sum up to 1')
end
pdf1=(round(pdf*npoints))/sum(round(pdf*npoints));
pdf=pdf1;
n = length(pdf);
val=[1:n];
a=zeros(1, n);
cumprob = [0 cumsum(pdf)]; % cumulative distribution
runi = rand(1, npoints); % random uniform sample
sample = zeros(1, npoints);
for j=1:n
    % if the value of U(0,1) falls into the interval (p_j,)
    %p_j+1) assign the value xj to X
    ind = find((runi>cumprob(j)) & (runi<=cumprob(j+1)));
    sample(ind) = val(j);
end
pdis=tabulate(sample);% es una tabla de frecuencias, en la 1era
%columna van los numeros, en la 2da las repeticiones y en el 3ra
%el porcentaje.
a(pdis(:,1))=pdis(:,3)./100;
k=0;
while any(abs(pdf-a)>1e-2)
    if k>30,
        clear aux aux1 aux6 aux7 aux2 aux8 aux3 pdis k
        a=zeros(1, n);
        break,
    end
    aux=find((pdf-a)<-1*error);
    if any(aux)==0
        clear aux aux1 aux6 aux7 aux2 aux8 aux3 pdis k
        a=zeros(1, n);
        break,
    end
    aux1=val(aux); %valores que son cambiados a 0 porque tienen
                    % mayor del que deberian
    aux6=find((pdf-a)>-1*error & (pdf-a)<error);
    aux7=val(aux6);%valores que no se deben adicionar porque ya
                    %tienen la probabilidad que es
    if any(aux1)==0 | (n-length(aux6))==1
        break
    end
    for i=1:length(aux1)

```

```

        aux2=find(sample==aux1(i));
        sample(aux2(1))=0;
    end
    aux3=find(sample==0);
    for i=1:length(aux3)
        u = rand;
        I = find(u<cumsum(pdf));
        aux5=find(aux1==min(I));
        aux8=find(aux7==min(I));
        while any(aux5)==1 | any(aux8)==1
            u = rand;
            I = find(u<cumsum(pdf));
            aux5=find(aux1==min(I));
            aux8=find(aux7==min(I));
        end
        sample(aux3(i)) = min(I);
    end
    pdis=tabulate(sample);
    a(pdis(:,1))=pdis(:,3)./100;
    pr=pdf-a;
    pr1=sum(abs(pdf-a));
    k=k+1;
end

```

estocastica.m

```

%% THIS PROGRAM GENERATES RANDOM DATA FOR AREA, YEAR OF CONSTRUCTION,
# OF STORIES AND ESTRUCTURE TYPE, FOR THE NUMBER OF EXISTING DWELLINGS
IN EACH CENSUS TRACK

```

```

clear all
fid=fopen('secciones.txt','r'); %This file contains 2
columns:LETRA,número de casas
P=fscanf(fid, '%g %g', [2,inf]);
fclose(fid);
P=P';
seccion=P(:,1);
npoints=P(:,2);
clear P;
i=1;
error=1e-5;
while i<=length(seccion)

    while npoints(i)<=10 %Sections with less than 10 dwellings are not
    taken into account
        i=i+1;
    end

    % Random numbers generation for the area
    fid=fopen('area.txt', 'r');
    P=fscanf(fid, '%g %g', [18 5223]);
    fclose(fid);
    P=P';
    valver=P(1,3:18); %values of area, the 1st and 2nd column
    represent the census code and the number of single family dwellings
    a=find(P==seccion(i));
    pdf=P(a,3:18);

```

```

clear P a
sample(:,1) = distrdiscretav2(npoints(i), pdf,error);
%Asignation of real values, it is, values between 30 y 255 m2
val=(1:length(pdf));
for j=1:length(val)
    aux4=find(sample==val(j));
    if j==1
        sample(aux4) = valver(j);
    else
        sample(aux4) = valver(j-1)+(valver(j)-(valver(j-
1)+1))*rand(length(aux4),1);
    end
end
clear pdi valver pdf aux4 val

% Random numbers generation for the year of construction
fid=fopen('año.txt', 'r');
P=fscanf(fid, '%g %g', [11 5223]);
fclose(fid);
P=P';
valver=P(1,3:11); %values of year, the 1st and 2nd column
represent the census code and the number of single family dwellings
a=find(P==seccion(i));
pdf=P(a,3:11);
clear P a
sample(:,2) = distrdiscretav2(npoints(i), pdf,error);
%Asignation of real values, it is, values between 1900 & 2001 m2
val=(1:length(pdf));
for j=1:length(val)
    aux4=find(sample==val(j));
    if j==1
        sample(aux4) = valver(j);
    else
        sample(aux4) = valver(j-1)+(valver(j)-(valver(j-
1)+1))*rand(length(aux4),1);
    end
end
clear pdi valver pdf aux4 val

% Random numbers generation for the number of stories
fid=fopen('plantas.txt', 'r');
P=fscanf(fid, '%g %g', [5 5223]);
fclose(fid);
P=P';
valver=P(1,3:5); %values of number of stories, the 1st and 2nd
column represent the census code and the number of single-family
dwellings
a=find(P==seccion(i));
pdf=P(a,3:5);
clear P a
sample(:,3) = distrdiscretav2(npoints(i), pdf,error);
clear pdi valver pdf aux4 val
sample(:,4)=0; %we assumed all dwellings have a heavy structure
% Writing data to a text file
a=sprintf('%f.txt', seccion(i));
dlmwrite(a,sample,'delimiter',' ', 'precision', 4);
i=i+1;
clear sample
end

```

infiltracion.m (UPC-CETE model)

```

%% ESTE PROGRAMA ESTIMA c' DE CADA CASA, CON LOS DATOS GENERADOS
ALEATORIAMENTE EN estocastica.m USANDO EL MODELO UPC-CETE
clear all

fid=fopen('secciones.txt','r'); %Este archivo contiene los codigos de
las
    %secciones afectadas y el número de viviendas unifamiliares
P1=fscanf(fid, '%g %g', [2,inf]);
fclose(fid);
P1=P1';
P7=find(P1(:,2)>10);
P1=P1(P7,:); %matrix with census tracks with more than 10 dwellings. 1
col: census code, 2 col:# of dwellings
b=max(P1(:,2));
seccion=P1(:,1);
i=1;
Bage=0.2278;
while i<=length(seccion)
    P3=sprintf('%f.txt', seccion(i));
    fid=fopen(P3,'r');
    P=fscanf(fid, '%g %g', [4,inf]);%1 col:area, 2 col:year, 3 col:#
stories, 4 col:structure
    fclose(fid);
    P=P';
    casas=P;
    clear P P2 P3 P7 fid P1

    casas(:,2)=2009-casas(:,2); %2009: year for the age estimation
    Cp=zeros(b,1); [m3*h-1*Pa^(-2/3)]
    P4=find(casas(:,2)<=9 & 1<casas(:,2) & casas(:,3)==1); %Age<9,
    #p=1
    if any(P4)==1
        Cp(P4,1)=exp(2.50721+0.00697995.*casas(P4,1)+0.50749.*casas(P4,4)+...
            0.0783752.*casas(P4,2)+0.345047.*1); % [m3*h-1*Pa^(-2/3)]
    end
    clear P4
    P4=find(casas(:,2)<=9 & 1<casas(:,2) & casas(:,3)>=2); %Age<9,
    #p>=2
    if any(P4)==1
        Cp(P4,1)=exp(2.50721+0.00697995.*casas(P4,1)+0.50749.*casas(P4,4)+...
            0.0783752.*casas(P4,2)+0.345047.*2); % [m3*h-1*Pa^(-2/3)]
    end
    clear P4

    P4=find(9<casas(:,2) & casas(:,2)<=64 & casas(:,3)==1); %Age entre
9 & 64, #p=1
    if any(P4)==1
        Cp(P4,1)=exp(2.50721+0.00697995.*casas(P4,1)+0.50749.*casas(P4,4)+...
            0.0783752.*9+0.345047.*1)+((2.5/(50^(2/3))).*casas(P4,1).*Bage.*(casas
(P4,2)-9));
    end
    clear P4

    P4=find(9<casas(:,2) & casas(:,2)<=64 & casas(:,3)>=2); %Age entre
9 & 64, #p>=2
    if any(P4)==1

```

```

Cp(P4,1)=exp(2.50721+0.00697995.*casas(P4,1)+0.50749.*casas(P4,4)+...
0.0783752.*9+0.345047.*2)+((2.5/(50^(2/3))).*casas(P4,1).*Bage.*(casas
(P4,2)-9));
end
clear P4

P4=find(casas(:,2)>64 & casas(:,3)==1); %Age>64 & #p=1
if any(P4)==1
Cp(P4,1)=exp(2.50721+0.00697995.*casas(P4,1)+0.50749.*casas(P4,4)+...
0.0783752.*9+0.345047.*1)+((2.5/(50^(2/3))).*casas(P4,1).*Bage.*(64-
9));
end
clear P4

P4=find(casas(:,2)>64 & casas(:,3)>=2); %Age>64 & #p>=2
if any(P4)==1
Cp(P4,1)=exp(2.50721+0.00697995.*casas(P4,1)+0.50749.*casas(P4,4)+...
0.0783752.*9+0.345047.*2)+((2.5/(50^(2/3))).*casas(P4,1).*Bage.*(64-
9));
end
clear P4

Cp=Cp./3600; %[m3*s-1*Pa^(-2/3)]
dlmwrite('Cp.txt',Cp,'-append','delimiter',' ','precision',
10)%Cp is a matrix where lines represent sections and columns
dwellings
i=i+1;
clear casas Cp
end

```

infiltracion.m (LBNL airtightness model)

```

%% ESTE PROGRAMA ESTIMA el c DE CADA CASA, CON LOS DATOS GENERADOS
ALEATORIAMENTE EN estocastica.m USANDO EL MODELO LBNL
.
clear all

fid=fopen('seccioneslbnl.txt','r'); %Este archivo contiene los codigos
de las secciones afectadas (1col), el número de viviendas
unifamiliares (2col) y el clima de la seccion (3col)húmeda:1, seca:2
P1=fscanf(fid, '%g %g', [3,inf]);
fclose(fid);
P1=P1';
P7=find(P1(:,2)>10);
P1=P1(P7,:); %matrix with census tracks with more than 10 dwellings. 1
col: census code, 2 col:# of dwellings, 3 col:climatic zone
b=max(P1(:,2));
seccion=P1(:,1);
zona=P1(:,3);
i=1;

while i<=length(seccion)
    P3=sprintf('%f.txt', seccion(i));
    fid=fopen(P3,'r');
    P=fscanf(fid, '%g %g', [4,inf]);%1 col:area, 2 col:year, 3 col:#
stories, 4 col:structure
    fclose(fid);

```

```

P=P';
casas=P;
clear P P3 P7 fid P1

casas(:,2)=2009-casas(:,2); %2009: year for the age estimation

if zona(i,1)==1 %zona húmeda
    nlcz=0.35;
else
    nlcz=0.61;
end
al=zeros(b,1);
nl=zeros(b,1);
Cplbnl=zeros(b,1);
% no se consideró la posibilidad de infiltracion por el suelo, es
decir posibilidad de sótano
nl(1:length(casas(:,1)),1)=nlcz.*(0.841.^(casas(:,1)./100-
1)).*(1.156.^(casas(:,3)-1)).*(1.0118.^(casas(:,2)));

Cplbnl(1:length(casas(:,1)),1)=nl(1:length(casas(:,1))).*casas(:,1).*(
(2/1.2)^0.5)./(1000*(4^(0.67-0.5)).*casas(:,3).^(0.3)); %m3/(s*Pa^n)

dlmwrite('Cplbnl.txt',Cplbnl,'-append','delimiter',' ','precision',
10)

i=i+1;
clear casas nl al Cplbnl
end
clear P1 seccion

```

nxestación.m

```

%% ESTIMATION OF THE AIR INFILTRATION RATE APPLYING THE AIM-2 MODEL
%without taking into account houses with crawl spaces.

clear all

%c SE REFIERE A LA ESTACION 2.INV,3.PRIM,4.VER,5.OTO,6.MAX INV,7.MAX
%PRIM,8.MAX VER,9.MAX OTO
c=9;

fid=fopen('secciones.txt','r'); %Este archivo contiene los codigos de
las secciones afectadas y el número de viviendas unifamiliares
P1=fscanf(fid, '%g %g', [2,inf]);
fclose(fid);
P1=P1';
P7=find(P1(:,2)>10);
P1=P1(P7,:); %matrix with census tracks with more than 10 dwellings. 1
col: census code, 2 col:# of dwellings
seccion=P1(:,1);

fid=fopen('Cp.txt','r');
%fid=fopen('Cplbnl.txt','r'); %para usar la hermeticidad del modelo
LBNL
Cp=fscanf(fid, '%g %g', [1648,length(seccion)]); %columns represent
%census traks, in the same order as seccion, and lines dwellings

```

```

fclose(fid);

fid=fopen('velocidad.txt','r');
v=fscanf(fid, '%g %g', [9,inf]);
fclose(fid);
v=v([1 c],:); % velocidades ya corregidas a 3m por tanto G=1, m/s.
    %1.CosSeccion,2.Inv,3.Prim,4.Ver,5.Oto,6.Max inv,7.Max prim,8.Max
ver,9.Max oto

fid=fopen('temperatura.txt','r');
To=fscanf(fid, '%g %g', [9,inf]);
fclose(fid);
To=To([1 c],:); %Temperaturas °C,
    %1.CosSeccion,2.Inv,3.Prim,4.Ver,5.Oto,6.Max inv,7.Max prim,8.Max
ver,9.Max oto

if c==4 || c==8 %For summer
    Ti=25;
else
    Ti=20;%for winter, autumn, and spring.
end

b=max(P1(:,2));
clear P1 fid P7
i=1;
% AIM2 model parameters
R=0;%Ceiling-floor sum fraction (Cc+Cf)/C, C=Cc+Cf+Cw+Cflue;
X=0;%Ceiling-floor difference fraction (Cc-Cf)/C;
Y=0.2;%Flue fraction Cflue/C
n=2/3;
swo=0.5; %shelter coefficient, for shelter class 4: heavily shielded,
many large obstructions within one building height
swflue=1;% flue shelter coefficient, shelter class 1: unsheltered
hf=1.5;%height of the flue above the ceiling level
G=1;%wind speed multiplier
%Outdoor air density calculation, assuming P=latm y hr (relative
humidity)
Pre=101325;%Pa
hr=0.5;

while i<=length(seccion)
    P3=find(To(:,1)==seccion(i));
    while any(P3)==0
        i=i+1;
        P3=find(To(:,1)==seccion(i));
    end
    a=sprintf('%f.txt', seccion(i));
    fid=fopen(a,'r');
    P=fscanf(fid, '%g %g', [4,inf]);
    fclose(fid);
    P=P';
    ns=P(:,3);
    vol=P(:,1)*2.5; %m3
    clear P fid

    [ro]=densidad(To(P3(1),2),Pre,hr);
    Zf=(hf+2.5*ns)./(2.5*ns);
    Xc=R+(2*(1-R-Y)/(n+1))-2*Y.*(Zf-1).^n;

```


Generated files

codigo.txt

The name código refers to the numeric code of each census tracts, for example 800101001.txt. Each one of these files contains 4 columns and lines as the number of dwellings of the respective census tract. The columns represent the floor area, the year of construction, the number of stories and the structure type.

105	1905	2	0
99.09	1911	2	0
181.6	1988	2	0
⋮	⋮	⋮	⋮

Cp.txt

This file contains the airtightness (c') of each one of the dwellings in $\text{m}^3 \cdot \text{s}^{-1} \cdot \text{Pa}^{-0.67}$. Lines represent census tracts and columns dwellings.

	Casa	Casa	
Sección 1	0.05767	0.05574	...
Sección 2	0.03274	0.06298	...
	⋮	⋮	

no.txt

This file contains the calculated ACH of each dwelling in s^{-1} . Lines represent census tracts and columns dwellings

	Casa	Casa	
Sección 1	0.0001232	0.00044641	...
Sección 2	8.65 E-04	0.00021026	...
	⋮	⋮	

Annex C. Analysis of the distributions obtained using the stochastic simulation

First test (see section 4.3.2)

Table C.1 Statistics for the different distributions of c ($\text{m}^3/(\text{h}\cdot\text{Pa}^n)$) obtained with the stochastic simulation and the LBNL model ($\text{m}^3\cdot\text{h}^{-1}\cdot\text{Pa}^{0.67}$)

Number of dwellings	Simulation	By simulation						Accumulated					
		Average c'	σ	P10 th	P50 th	P90 th	Average c'	σ	P10 th	P50 th	P90 th	Average c'	σ
10	1	195.10	65.56	186.14	121.43	186.14	305.16	195.10	65.56	186.14	121.43	186.14	305.16
10	2	196.06	82.73	184.12	104.60	184.12	337.75	195.58	72.65	184.33	108.69	184.33	317.44
10	3	190.53	67.57	176.51	107.04	176.51	280.58	193.90	69.86	184.33	107.04	184.33	305.16
10	4	190.04	63.34	183.05	115.12	183.05	291.75	192.93	67.51	184.33	113.08	184.33	302.78
10	5	189.76	50.28	181.65	139.79	181.65	273.37	192.30	63.98	184.33	115.72	184.33	297.66
10	6	193.35	77.53	167.80	111.01	167.80	319.71	192.47	65.70	181.35	115.72	181.35	300.67
20	1	239.23	117.82	205.63	109.30	205.63	409.85	239.23	117.82	205.63	109.30	205.63	409.85
20	2	233.86	107.48	196.36	130.92	196.36	404.20	236.55	111.35	202.92	122.56	202.92	404.20
20	3	243.74	141.15	187.11	130.63	187.11	404.57	238.94	120.93	200.29	126.67	200.29	404.57
20	4	245.63	148.82	215.25	108.57	215.25	409.40	240.62	127.50	202.92	122.05	202.92	404.57

Table C.1 Statistics for the different distributions of c (m3/(h·Pan)) obtained with the stochastic simulation and the LBNL model (m3·h-1·Pa0.67)

Number of dwellings	Simulation	By simulation					Accumulated						
		Average c'	σ	P10 th	P50 th	P90 th	Average c'	σ	P10 th	P50 th	P90 th	Average c'	σ
20	5	254.97	172.78	195.62	105.99	195.62	498.01	243.49	136.88	202.92	119.60	202.92	420.31
20	6	236.34	112.09	200.15	123.28	200.15	433.95	242.30	132.66	201.71	119.60	201.71	422.53
20	7	237.37	126.15	182.09	105.40	182.09	452.99	241.59	131.32	200.29	115.42	200.29	435.65
20	8	232.65	111.17	184.80	138.49	184.80	405.24	240.47	128.69	196.79	119.60	196.79	432.97
20	9	224.16	84.91	187.23	146.86	187.23	363.83	238.66	124.51	193.94	123.80	193.94	411.51
20	10	233.65	118.38	205.23	114.74	205.23	434.38	238.16	123.63	193.94	123.80	193.94	412.07
20	11	230.07	107.43	215.24	111.26	215.24	397.97	237.42	122.05	194.92	121.55	194.92	412.07
20	12	238.51	138.40	196.18	138.71	196.18	389.50	237.51	123.18	194.92	123.80	194.92	412.07
30	1	194.55	89.87	169.50	116.46	169.50	309.50	194.55	89.87	169.50	116.46	169.50	309.50
30	2	190.68	75.39	174.16	111.83	174.16	284.67	192.61	82.26	170.13	113.82	170.13	294.79
30	3	196.67	87.85	169.40	106.50	169.40	350.46	193.97	83.69	170.13	111.83	170.13	309.50
30	4	197.03	84.33	168.00	117.65	168.00	327.99	194.73	83.51	169.35	112.94	169.35	309.50
30	5	195.25	79.41	179.24	113.19	179.24	288.27	194.84	82.44	170.30	112.94	170.30	306.24
40	1	191.32	87.87	161.98	111.88	161.98	319.34	191.32	87.87	161.98	111.88	161.98	319.34
40	2	185.77	54.45	170.36	128.08	170.36	270.04	188.55	72.69	167.71	125.25	167.71	274.64
40	3	183.01	52.78	173.13	126.87	173.13	254.75	186.70	66.54	171.54	126.20	171.54	270.04
40	4	186.64	59.91	181.41	116.61	181.41	266.79	186.68	64.76	172.99	120.85	172.99	269.39
50	1	204.68	86.24	196.77	91.99	196.77	289.21	204.68	86.24	196.77	91.99	196.77	289.21
50	2	207.62	90.87	200.41	93.39	200.41	317.71	206.15	88.15	198.45	93.39	198.45	300.83
50	3	202.59	78.27	196.99	98.62	196.99	289.68	204.96	84.74	197.87	97.61	197.87	296.62
50	4	203.51	85.55	186.40	101.55	186.40	328.25	204.60	84.73	196.77	97.61	196.77	309.33
50	5	206.77	101.61	195.87	100.78	195.87	292.02	205.03	88.15	196.77	97.61	196.77	304.93
50	6	200.28	79.08	186.47	110.16	186.47	285.10	204.24	86.59	195.79	99.07	195.79	296.62
50	7	204.57	93.05	185.36	104.61	185.36	349.37	204.29	87.41	193.84	100.35	193.84	304.93
60	1	445.64	161.17	433.88	250.48	433.88	677.31	445.64	161.17	433.88	250.48	433.88	677.31
60	2	449.47	182.97	432.12	225.19	432.12	706.08	447.56	171.70	433.88	237.32	433.88	678.39
60	3	451.92	172.03	438.88	243.36	438.88	685.03	449.01	171.34	435.23	239.31	435.23	679.42
60	4	450.62	177.09	421.12	263.41	421.12	712.01	449.41	172.42	430.98	246.87	430.98	689.76
70	1	184.82	86.47	163.24	91.32	163.24	302.94	184.82	86.47	163.24	91.32	163.24	302.94
70	2	182.58	81.40	164.88	105.14	164.88	296.44	183.70	83.68	163.24	100.07	163.24	299.02
70	3	181.90	77.48	168.38	90.14	168.38	300.73	183.10	81.48	166.77	94.50	166.77	300.06
70	4	181.51	75.22	157.21	101.58	157.21	298.20	182.70	79.83	164.87	99.22	164.87	300.06
70	5	185.04	81.66	172.98	100.25	172.98	304.61	183.17	80.09	166.65	99.22	166.65	300.06
70	6	179.36	71.20	170.14	102.12	170.14	300.34	182.53	78.61	167.46	99.84	167.46	300.06
70	7	187.61	90.63	173.19	92.50	173.19	313.29	183.26	80.35	168.02	99.60	168.02	301.67
70	8	180.80	73.99	163.86	98.19	163.86	289.12	182.95	79.53	166.68	98.87	166.68	299.75
70	9	184.82	82.83	157.54	104.94	157.54	295.64	183.16	79.84	165.94	99.78	165.94	298.71
70	10	184.04	86.39	157.68	111.98	157.68	298.83	183.25	80.45	165.24	101.27	165.24	298.71

Table C.1 Statistics for the different distributions of c (m3/(h·Pan)) obtained with the stochastic simulation and the LBNL model (m3·h-1·Pa0.67)

Number of dwellings	Simulation	By simulation						Accumulated					
		Average c'	σ	P10 th	P50 th	P90 th	Average c'	σ	P10 th	P50 th	P90 th	Average c'	σ
80	1	238.11	111.48	201.67	120.31	201.67	408.34	238.11	111.48	201.67	120.31	201.67	408.34
80	2	240.13	124.56	223.76	118.46	223.76	395.66	239.12	117.83	212.34	119.18	212.34	402.21
80	3	236.75	111.82	205.47	115.78	205.47	371.32	238.33	115.63	209.25	118.63	209.25	396.84
80	4	238.23	106.39	225.44	123.33	225.44	390.18	238.30	113.23	211.58	119.79	211.58	396.84
90	1	281.54	160.66	234.21	137.60	234.21	425.95	281.54	160.66	234.21	137.60	234.21	425.95
90	2	271.37	130.76	239.80	130.97	239.80	450.73	276.46	146.15	237.92	132.74	237.92	441.15
90	3	283.18	158.78	231.97	137.49	231.97	437.85	278.70	150.22	235.51	134.92	235.51	441.15
90	4	273.86	137.46	242.17	125.40	242.17	439.17	277.49	146.96	237.14	130.99	237.14	441.15
90	5	273.84	141.30	232.96	135.15	232.96	451.58	276.76	145.70	237.14	131.47	237.14	446.98
90	6	271.34	134.67	236.41	142.03	236.41	428.73	275.86	143.81	236.45	134.03	236.45	444.65
90	7	269.91	130.32	242.96	132.75	242.96	454.49	275.01	141.88	238.06	133.75	238.06	445.62
90	8	280.74	154.79	238.74	134.16	238.74	455.01	275.72	143.46	238.25	133.75	238.25	446.98
90	9	280.64	163.54	238.61	125.44	238.61	461.87	276.27	145.72	238.25	133.20	238.25	446.98
90	10	270.86	142.48	234.84	144.59	234.84	435.01	275.73	145.33	238.25	133.75	238.25	444.65
90	11	280.87	161.22	225.47	133.26	225.47	493.61	276.20	146.77	237.92	133.47	237.92	447.81
90	12	269.04	120.32	240.00	139.89	240.00	425.34	275.60	144.71	237.92	134.03	237.92	445.62
90	13	272.29	139.19	249.76	143.38	249.76	433.77	275.35	144.24	238.11	134.47	238.11	445.62
100	1	204.07	83.99	183.88	118.91	183.88	312.69	204.07	83.99	183.88	118.91	183.88	312.69
100	2	204.52	70.51	200.19	119.11	200.19	301.93	204.29	77.35	193.99	118.91	193.99	306.64
100	3	205.87	79.15	189.43	111.22	189.43	316.69	204.82	77.82	193.21	116.02	193.21	312.45
100	4	204.48	79.14	182.44	123.89	182.44	306.39	204.74	78.05	187.44	119.13	187.44	309.78
120	1	211.09	104.31	174.84	116.15	174.84	338.79	211.09	104.31	174.84	116.15	174.84	338.79
120	2	218.98	116.73	178.51	118.18	178.51	352.13	215.04	110.53	177.45	117.08	177.45	346.02
120	3	211.75	108.43	176.12	121.16	176.12	342.46	213.94	109.70	177.33	118.71	177.33	346.02
120	4	212.10	100.12	181.71	112.66	181.71	363.64	213.48	107.28	177.60	117.55	177.60	351.54
120	5	221.77	117.07	178.22	106.53	178.22	392.77	215.14	109.26	177.73	114.91	177.73	363.10
120	6	214.96	113.14	182.74	123.58	182.74	359.83	215.11	109.84	178.62	115.60	178.62	363.10
140	1	254.97	131.32	219.50	135.32	219.50	400.87	254.97	131.32	219.50	135.32	219.50	400.87
140	2	256.42	113.41	231.72	133.58	231.72	419.04	255.69	122.47	226.12	134.27	226.12	412.64
140	3	252.02	125.63	223.38	134.36	223.38	386.24	254.47	123.40	225.32	134.36	225.32	404.25
140	4	253.82	127.75	221.74	126.38	221.74	433.74	254.31	124.38	223.38	133.09	223.38	411.18
160	1	385.89	136.11	365.16	219.25	365.16	567.10	385.89	136.11	365.16	219.25	365.16	567.10
160	2	385.24	140.30	379.42	202.24	379.42	570.45	385.57	138.01	373.83	207.95	373.83	569.55
180	1	343.27	170.86	318.38	156.31	318.38	569.70	343.27	170.86	318.38	156.31	318.38	569.70
180	2	344.93	174.14	313.42	148.06	313.42	607.77	344.10	172.27	314.88	149.67	314.88	590.16
180	3	342.12	179.78	320.46	150.12	320.46	606.05	343.44	174.65	315.54	149.83	315.54	598.61

Table C.1 Statistics for the different distributions of c (m3/(h·Pan)) obtained with the stochastic simulation and the LBNL model (m3·h-1·Pa0.67)

Number of dwellings	Simulation	By simulation					Accumulated						
		Average c'	σ	P10 th	P50 th	P90 th	Average c'	σ	P10 th	P50 th	P90 th	Average c'	σ
180	4	346.50	175.18	322.59	140.42	322.59	608.43	344.21	174.66	318.29	147.41	318.29	602.19
180	5	347.27	175.86	325.26	149.18	325.26	622.20	344.82	174.81	320.61	148.40	320.61	606.05
180	6	348.43	175.59	333.70	144.37	333.70	609.92	345.42	174.86	321.61	147.60	321.61	606.05
180	7	348.95	179.24	310.40	141.80	310.40	640.15	345.93	175.43	321.52	146.72	321.52	612.63
180	8	343.86	172.30	318.74	142.13	318.74	609.40	345.67	174.98	321.38	145.47	321.38	610.83
200		185.70	53.85	183.53	118.44	183.53	248.33	185.70	53.85	183.53	118.44	183.53	248.33
200	1	186.18	58.75	188.68	115.96	188.68	242.11	185.94	56.29	185.84	117.14	185.84	246.79
200	2	187.56	60.99	189.12	112.28	189.12	254.11	186.48	57.85	186.79	114.27	186.79	248.33
200	3	188.51	61.34	187.12	114.53	187.12	262.51	186.99	58.71	186.79	114.27	186.79	250.57
200	4	185.23	53.52	189.25	115.20	189.25	248.35	186.64	57.69	187.40	114.50	187.40	249.78
200	5	188.47	59.04	188.07	114.93	188.07	254.32	186.94	57.89	187.40	114.50	187.40	251.42
200	6	189.25	58.18	187.54	119.98	187.54	257.07	187.27	57.92	187.52	115.86	187.52	251.93
200	7	185.80	58.09	183.06	112.99	183.06	254.68	187.09	57.92	187.03	115.86	187.03	252.06
250	1	280.02	147.70	233.10	128.05	233.10	492.51	280.02	147.70	233.10	128.05	233.10	492.51
250	2	275.35	138.03	243.77	125.23	243.77	475.72	277.69	142.82	239.31	126.44	239.31	482.26
250	3	278.38	139.18	245.86	123.82	245.86	490.34	277.92	141.53	242.09	125.23	242.09	483.47
300	1	187.25	57.31	179.19	119.38	179.19	272.88	187.25	57.31	179.19	119.38	179.19	272.88
300	2	190.00	61.84	178.15	121.60	178.15	270.86	188.62	59.59	179.12	121.52	179.12	271.66
300	3	189.15	62.56	177.38	116.96	177.38	272.13	188.80	60.56	178.69	119.68	178.69	271.66
400	1	205.33	92.76	179.28	125.31	179.28	302.69	205.33	92.76	179.28	125.31	179.28	302.69
400	2	209.67	97.76	185.99	119.52	185.99	319.07	207.50	95.26	182.28	122.28	182.28	309.89
400	3	206.90	95.23	182.26	115.47	182.26	308.66	207.30	95.21	182.28	120.23	182.28	309.59
499	1	255.38	144.37	202.63	122.71	202.63	451.16	255.38	144.37	202.63	122.71	202.63	451.16
499	2	263.29	157.65	196.85	123.32	196.85	501.10	259.33	151.13	200.13	122.82	200.13	479.69
499	3	254.30	143.08	202.51	119.96	202.51	446.75	257.65	148.47	200.38	121.88	200.38	465.19
499	4	255.41	148.04	196.46	121.12	196.46	456.09	257.09	148.33	199.12	121.47	199.12	461.20
499	5	256.65	145.88	196.13	125.11	196.13	462.82	257.01	147.81	198.62	122.69	198.62	461.29
599	1	208.62	83.90	186.41	124.77	186.41	306.86	208.62	83.90	186.41	124.77	186.41	306.86
599	2	205.72	87.61	180.60	126.37	180.60	306.10	207.17	85.76	183.09	125.76	183.09	306.39
599	3	205.91	79.99	187.77	124.64	187.77	304.27	206.75	83.86	184.44	125.35	184.44	306.14
599	4	208.55	87.98	183.18	126.28	183.18	317.51	207.20	84.89	184.00	125.48	184.00	307.38
599	5	205.27	78.21	185.26	125.59	185.26	306.15	206.81	83.59	184.35	125.48	184.35	307.06
599	6	206.47	80.89	185.39	124.92	185.39	309.84	206.76	83.13	184.36	125.42	184.36	307.69
699	1	252.79	147.31	199.96	123.03	199.96	465.49	252.79	147.31	199.96	123.03	199.96	465.49
699	2	252.75	148.57	197.55	122.88	197.55	467.01	252.77	147.89	199.46	122.87	199.46	465.51
792	1	211.84	73.33	203.99	122.72	203.99	306.78	211.84	73.33	203.99	122.72	203.99	306.78
792	2	210.07	70.88	204.83	122.00	204.83	304.53	210.95	72.10	204.52	122.28	204.52	305.97
792	3	211.06	73.98	203.40	122.70	203.40	307.69	210.99	72.72	204.28	122.56	204.28	306.37

Table C.1 Statistics for the different distributions of c ($\text{m}^3/(\text{h}\cdot\text{Pan})$) obtained with the stochastic simulation and the LBNL model ($\text{m}^3\cdot\text{h}^{-1}\cdot\text{Pa}^{0.67}$)

Number of dwellings	Simulation	By simulation					Accumulated						
		Average c'	σ	P10 th	P50 th	P90 th	Average c'	σ	P10 th	P50 th	P90 th	Average c'	σ
902	1	207.68	96.33	184.06	117.46	184.06	312.98	207.68	96.33	184.06	117.46	184.06	312.98
902	2	204.47	94.85	180.63	119.84	180.63	303.48	206.08	95.58	182.15	118.91	182.15	310.35
902	3	206.02	91.56	187.87	120.17	187.87	305.20	206.06	94.24	184.06	119.35	184.06	307.70
967	1	181.76	81.37	160.47	108.05	160.47	276.39	181.76	81.37	160.47	108.05	160.47	276.39
967	2	177.64	73.04	160.70	106.44	160.70	270.94	179.70	77.32	160.53	107.34	160.53	274.84
967	3	179.92	77.30	161.59	108.49	161.59	272.04	179.77	77.30	160.86	107.61	160.86	273.75
1648	1	199.92	92.99	175.17	121.36	175.17	303.53	199.92	92.99	175.17	121.36	175.17	303.53
1648	2	198.63	88.94	175.59	120.59	175.59	291.97	199.28	90.98	175.35	120.65	175.35	297.36
1648	3	201.57	95.02	177.15	122.65	177.15	293.63	200.04	92.34	175.88	121.17	175.88	296.44
1648	4	197.22	84.22	175.98	122.64	175.98	284.51	199.33	90.38	175.88	121.71	175.88	293.56
1648	5	198.52	89.56	175.84	121.45	175.84	293.65	199.17	90.21	175.88	121.58	175.88	293.57

Second test

Results of the ANOVA test for c ($\text{m}^3\cdot\text{h}^{-1}\cdot\text{Pa}^{0.67}$). Medians of 20 simulations by census tract.

Number of dwellings	Section code
10	801509044

ANOVA Table

Source	SS	df	MS	F	Prob>F
Columns	0.0421	19	0.00221	0.02	1
Error	24.2208	180	0.13456		
Total	24.2629	199			

Kruskal-Wallis ANOVA Table

Source	SS	df	MS	Chi-sq	Prob>Chi-sq
Columns	2996	19	157.68	0.89	1
Error	663654	180	3686.97		
Total	666650	199			

Number of dwellings	Section code
20	801503002

ANOVA Table					
Source	SS	df	MS	F	Prob>F
Columns	0.0421	19	0.00221	0.01	1
Error	90.984	380	0.23943		
Total	91.0261	399			

Kruskal-Wallis ANOVA Table					
Source	SS	df	MS	Chi-sq	Prob>Chi-sq
Columns	10707.7	19	563.6	0.8	1
Error	5322592.3	380	14006.8		
Total	5333300	399			

Number of dwellings	Section code
30	801507015

ANOVA Table					
Source	SS	df	MS	F	Prob>F
Columns	0.0657	19	0.00346	0.02	1
Error	94.3248	580	0.16263		
Total	94.3904	599			

Kruskal-Wallis ANOVA Table					
Source	SS	df	MS	Chi-sq	Prob>Chi-sq
Columns	26595.7	19	1399.8	0.89	1
Error	17973354.3	580	30988.5		
Total	17999950	599			

Number of dwellings	Section code
40	801507005

ANOVA Table					
Source	SS	df	MS	F	Prob>F
Columns	0.0315	19	0.00166	0.01	1
Error	92.332	780	0.11837		
Total	92.3635	799			

Kruskal-Wallis ANOVA Table					
Source	SS	df	MS	Chi-sq	Prob>Chi-sq
Columns	64742.7	19	3407.5	1.21	1
Error	42601857.3	780	54617.8		
Total	42666600	799			

Number of dwellings	Section code
50	801507010

ANOVA Table					
Source	SS	df	MS	F	Prob>F
Columns	0.067	19	0.00352	0.02	1
Error	182.156	980	0.18587		
Total	182.223	999			

Kruskal-Wallis ANOVA Table					
Source	SS	df	MS	Chi-sq	Prob>Chi-sq
Columns	61752.6	19	3250.1	0.74	1
Error	83271497.4	980	84970.9		
Total	83333250	999			

Number of dwellings	Section code
60	800801001

ANOVA Table					
Source	SS	df	MS	F	Prob>F
Columns	0.025	19	0.00132	0.01	1
Error	229.478	1180	0.19447		
Total	229.503	1199			

Kruskal-Wallis ANOVA Table					
Source	SS	df	MS	Chi-sq	Prob>Chi-sq
Columns	165327	19	8701.4	1.38	1
Error	143834573	1180	121893.7		
Total	143999900	1199			

Number of dwellings	Section code
70	801907188

ANOVA Table					
Source	SS	df	MS	F	Prob>F
Columns	0.043	19	0.00225	0.01	1
Error	257.42	1380	0.18654		
Total	257.463	1399			

Kruskal-Wallis ANOVA Table

Source	SS	df	MS	Chi-sq	Prob>Chi-sq
Columns	46329.2	19	2438.4	0.28	1
Error	228620220.8	1380	165666.8		
Total	228666550	1399			

Number of dwellings	Section code
80	801907067

ANOVA Table

Source	SS	df	MS	F	Prob>F
Columns	0.042	19	0.00224	0.01	1
Error	315.262	1580	0.19953		
Total	315.305	1599			

Kruskal-Wallis ANOVA Table

Source	SS	df	MS	Chi-sq	Prob>Chi-sq
Columns	216108.7	19	11374.1	1.01	1
Error	341117091.3	1580	215896.9		
Total	341333200	1599			

Number of dwellings	Section code
90	810201001

ANOVA Table

Source	SS	df	MS	F	Prob>F
Columns	0.071	19	0.00373	0.02	1
Error	426.286	1780	0.23949		
Total	426.357	1799			

Kruskal-Wallis ANOVA Table

Source	SS	df	MS	Chi-sq	Prob>Chi-sq
Columns	130197	19	6852.5	0.48	1
Error	485869653	1780	272960.5		
Total	485999850	1799			

Number of dwellings	Section code
100	810201001

ANOVA Table

Source	SS	df	MS	F	Prob>F
Columns	0.077	19	0.00407	0.03	1
Error	284.795	1980	0.14384		
Total	284.872	1999			

Kruskal-Wallis ANOVA Table

Source	SS	df	MS	Chi-sq	Prob>Chi-sq
Columns	363208.6	19	19116.2	1.09	1
Error	666303291.4	1980	336516.8		
Total	666666500	1999			

Number of dwellings	Section code
120	801502001

ANOVA Table

Source	SS	df	MS	F	Prob>F
Columns	0.175	19	0.0092	0.05	1
Error	461.272	2380	0.19381		
Total	461.447	2399			

Kruskal-Wallis ANOVA Table

Source	SS	df	MS	Chi-sq	Prob>Chi-sq
Columns	583479.6	19	30709.5	1.22	1
Error	1151416320.4	2380	483788.4		
Total	1151999800	2399			

Number of dwellings	Section code
140	800902002

ANOVA Table

Source	SS	df	MS	F	Prob>F
Columns	0.169	19	0.00888	0.04	1
Error	550.371	2780	0.19798		
Total	550.54	2799			

Kruskal-Wallis ANOVA Table

Source	SS	df	MS	Chi-sq	Prob>Chi-sq
Columns	1.04938e+006	19	55230.6	1.61	1
Error	1.82828e+009	2780	657656		
Total	1.82933e+009	2799			

Number of dwellings	Section code
160	256101001

ANOVA Table

Source	SS	df	MS	F	Prob>F
Columns	0.086	19	0.00451	0.03	1
Error	509.961	3180	0.16037		
Total	510.047	3199			

Kruskal-Wallis ANOVA Table

Source	SS	df	MS	Chi-sq	Prob>Chi-sq
Columns	660161.5	19	34745.3	0.77	1
Error	2730006238.5	3180	858492.5		
Total	2730666400	3199			

Number of dwellings	Section code
180	807601002

ANOVA Table

Source	SS	df	MS	F	Prob>F
Columns	0.118	19	0.00621	0.02	1
Error	975.078	3580	0.27237		
Total	975.196	3599			

Kruskal-Wallis ANOVA Table

Source	SS	df	MS	Chi-sq	Prob>Chi-sq
Columns	689707.9	19	36300.4	0.64	1
Error	3887309992.1	3580	1085840.8		
Total	3887999700	3599			

Number of dwellings	Section code
200	818707001

ANOVA Table

Source	SS	df	MS	F	Prob>F
Columns	0.158	19	0.0083	0.08	1
Error	398.799	3980	0.1002		
Total	398.957	3999			

Kruskal-Wallis ANOVA Table

Source	SS	df	MS	Chi-sq	Prob>Chi-sq
Columns	2.69689e+006	19	141941.5	2.02	1
Error	5.33064e+009	3980	1339355.8		
Total	5.33333e+009	3999			

Number of dwellings	Section code
250	812601001

ANOVA Table

Source	SS	df	MS	F	Prob>F
Columns	0.2	19	0.0105	0.04	1
Error	1226.28	4980	0.24624		
Total	1226.48	4999			

Kruskal-Wallis ANOVA Table

Source	SS	df	MS	Chi-sq	Prob>Chi-sq
Columns	3.03894e+006	19	159944.3	1.46	1
Error	1.04136e+010	4980	2091089.8		
Total	1.04167e+010	4999			

Number of dwellings	Section code
300	813601005

ANOVA Table

Source	SS	df	MS	F	Prob>F
Columns	0.151	19	0.00796	0.08	1
Error	606.549	5980	0.10143		
Total	606.7	5999			

Kruskal-Wallis ANOVA Table

Source	SS	df	MS	Chi-sq	Prob>Chi-sq
Columns	3.51049e+006	19	184762.7	1.17	1
Error	1.79965e+010	5980	3009446.3		
Total	1.8e+010	5999			

Number of dwellings	Section code
400	820002013

ANOVA Table

Source	SS	df	MS	F	Prob>F
Columns	0.3	19	0.01587	0.11	1
Error	1164.09	7980	0.14588		
Total	1164.4	7999			

Kruskal-Wallis ANOVA Table

Source	SS	df	MS	Chi-sq	Prob>Chi-sq
Columns	1.83373e+007	19	965119.1	3.44	1
Error	4.26483e+010	7980	5344402.1		
Total	4.26667e+010	7999			

Number of dwellings	Section code
499	4313701001

ANOVA Table

Source	SS	df	MS	F	Prob>F
Columns	0.44	19	0.02326	0.08	1
Error	2796.81	9960	0.2808		
Total	2797.25	9979			

Kruskal-Wallis ANOVA Table

Source	SS	df	MS	Chi-sq	Prob>Chi-sq
Columns	1.95126e+007	19	1.02698e+006	2.35	1
Error	8.28148e+010	9960	8.31474e+006		
Total	8.28343e+010	9979			

Number of dwellings	Section code
599	804201001

ANOVA Table

Source	SS	df	MS	F	Prob>F
Columns	0.47	19	0.02484	0.19	1
Error	1584.28	11960	0.13246		
Total	1584.75	11979			

Kruskal-Wallis ANOVA Table

Source	SS	df	MS	Chi-sq	Prob>Chi-sq
Columns	5.44911e+007	19	2.86795e+006	4.56	0.9997
Error	1.43227e+011	11960	1.19755e+007		
Total	1.43281e+011	11979			

Number of dwellings	Section code
699	4302801001

ANOVA Table

Source	SS	df	MS	F	Prob>F
Columns	0.84	19	0.04445	0.17	1
Error	3576.7	13960	0.25621		
Total	3577.54	13979			

Kruskal-Wallis ANOVA Table

Source	SS	df	MS	Chi-sq	Prob>Chi-sq
Columns	4.32592e+007	19	2.2768e+006	2.66	1
Error	2.27645e+011	13960	1.63069e+007		
Total	2.27688e+011	13979			

Number of dwellings	Section code
792	820505001

ANOVA Table					
Source	SS	df	MS	F	Prob>F
Columns	0.21	19	0.01126	0.09	1
Error	2024.62	15820	0.12798		
Total	2024.83	15839			

Kruskal-Wallis ANOVA Table					
Source	SS	df	MS	Chi-sq	Prob>Chi-sq
Columns	2.91848e+007	19	1.53604e+006	1.4	1
Error	3.31166e+011	15820	2.09334e+007		
Total	3.31195e+011	15839			

Number of dwellings	Section code
902	823401001

ANOVA Table					
Source	SS	df	MS	F	Prob>F
Columns	0.75	19	0.03942	0.26	0.9995
Error	2775.85	18020	0.15404		
Total	2776.6	18039			

Kruskal-Wallis ANOVA Table					
Source	SS	df	MS	Chi-sq	Prob>Chi-sq
Columns	1.31201e+008	19	6.90532e+006	4.84	0.9996
Error	4.89116e+011	18020	2.7143e+007		
Total	4.89247e+011	18039			

Number of dwellings	Section code
967	829101001

ANOVA Table					
Source	SS	df	MS	F	Prob>F
Columns	0.95	19	0.04986	0.35	0.9955
Error	2716.72	19320	0.14062		
Total	2717.67	19339			

Kruskal-Wallis ANOVA Table					
Source	SS	df	MS	Chi-sq	Prob>Chi-sq
Columns	2.15916e+008	19	1.1364e+007	6.93	0.9946
Error	6.02605e+011	19320	3.11907e+007		
Total	6.02821e+011	19339			

Number of dwellings	Section code
1648	802301001

ANOVA Table

Source	SS	df	MS	F	Prob>F
Columns	1.99	19	0.10458	0.73	0.7877
Error	4698.69	32940	0.14264		
Total	4700.68	32959			

Kruskal-Wallis ANOVA Table

Source	SS	df	MS	Chi-sq	Prob>Chi-sq
Columns	1.1725e+009	19	6.17103e+007	12.95	0.8411
Error	2.9827e+012	32940	9.05495e+007		
Total	2.98387e+012	32959			

Results obtained with the UPC-CETE model (see section 5.3)

First test

Table C.2 Statistics for the different distributions of c ($\text{m}^3/(\text{h}\cdot\text{Pa}^n)$) obtained with the stochastic simulation and the UPC-CETE model ($\text{m}^3\cdot\text{h}^{-1}\cdot\text{Pa}^{0.67}$)

Number of dwellings	Simulation	By simulation					Acumulated				
		Average c'	σ	P10 th	P50 th	P90 th	Average c'	σ	P10 th	P50 th	P90 th
10	1	184.814	108.395	79.862	146.726	350.783	184.814	108.395	79.862	146.726	350.783
	2	185.866	91.560	76.750	160.210	298.416	185.340	97.657	79.862	155.713	327.753
	3	186.612	102.618	77.744	171.138	353.695	185.764	97.554	79.041	160.210	328.618
	4	183.698	74.184	103.056	162.606	292.256	185.248	91.364	87.167	160.210	312.541
	5	174.057	46.368	121.921	165.924	238.678	183.009	84.019	92.525	163.137	311.677
	6	174.236	63.653	93.534	154.339	255.711	181.547	80.570	92.525	163.050	306.552
	7	180.285	82.507	88.600	166.634	309.722	181.367	80.243	92.525	163.050	306.552
20	1	216.346	121.330	106.516	165.116	395.249	216.346	121.330	106.516	165.116	395.249
	2	223.887	145.301	83.816	185.719	508.669	220.116	132.181	94.280	178.985	460.591
	3	207.714	104.690	124.485	179.650	356.221	215.982	122.937	98.238	178.985	418.235
	4	209.971	109.678	94.793	171.953	401.478	214.480	119.110	98.238	175.334	408.956
	5	222.120	127.993	74.789	190.740	460.663	216.008	120.311	94.280	181.142	428.462
	6	206.629	94.895	118.184	178.927	318.280	214.444	116.155	97.319	180.193	408.956
	7	206.519	101.763	98.761	174.918	377.476	213.312	113.904	98.329	178.632	400.156
	8	206.173	93.064	113.491	187.443	343.662	212.420	111.277	98.329	180.895	386.446
	9	220.173	123.878	83.749	188.106	413.248	213.281	112.401	95.508	181.515	388.652
	10	217.853	128.784	108.344	164.708	470.268	213.738	113.796	96.264	180.895	400.156
	11	199.283	91.533	136.738	165.277	326.737	212.424	111.854	98.329	180.193	388.652
	12	216.828	115.277	104.780	178.969	406.115	212.791	111.903	98.329	179.552	388.652
	13	209.522	107.975	96.311	169.077	309.105	212.540	111.406	98.329	178.969	381.481
	14	209.772	103.453	104.292	191.061	319.202	212.342	110.684	98.329	180.193	378.967
30	1	190.399	104.453	101.379	157.269	312.336	190.399	104.453	101.379	157.269	312.336
	2	184.169	81.425	109.794	167.226	266.576	187.284	92.906	101.379	159.678	293.649
	3	193.458	123.991	102.949	167.750	332.692	189.342	103.634	101.379	165.160	293.649
	4	188.833	97.681	123.417	158.102	289.474	189.215	101.773	105.578	164.055	293.649

Table C.2 Statistics for the different distributions of c (m³/(h·Pan)) obtained with the stochastic simulation and the UPC-CETE model (m³·h⁻¹·Pa0.67) Continuation

Number of dwellings	Simulation	By simulation					Accumulated				
		Average c'	σ	P10 th	P50 th	P90 th	Average c	σ	P10 th	P50 th	P90 th
40	1	163.369	55.040	97.779	155.416	230.695	163.369	55.040	97.779	155.416	230.695
	2	172.907	84.473	87.217	157.481	263.715	168.138	71.002	91.803	155.891	252.097
	3	166.427	61.917	93.681	158.474	231.578	167.568	67.851	92.395	156.750	243.334
	4	168.790	70.592	88.492	163.063	273.469	167.873	68.324	89.836	159.232	249.779
	5	169.794	66.290	90.025	158.860	256.796	168.257	67.762	89.858	159.197	251.368
	6	168.119	85.395	89.258	157.802	255.783	168.234	70.804	89.728	159.197	251.368
50	1	346.685	126.999	192.594	352.260	527.060	346.685	126.999	192.594	352.260	527.060
	2	350.068	131.001	212.265	338.387	526.198	348.376	128.483	199.206	346.229	526.198
	3	354.426	154.944	199.190	318.817	535.815	350.393	137.462	199.190	336.900	526.604
	4	348.105	141.849	186.256	338.892	536.520	349.821	138.276	196.334	336.900	529.087
	5	348.045	125.087	192.809	345.572	525.945	349.466	135.541	196.334	339.678	529.087
	6	355.699	151.716	182.594	333.282	560.475	350.505	138.164	192.215	336.926	531.873
	7	350.203	133.748	194.285	322.018	533.695	350.461	137.385	193.141	334.647	531.873
60	1	346.685	126.999	192.594	352.260	527.060	346.685	126.999	192.594	352.260	527.060
	2	350.068	131.001	212.265	338.387	526.198	348.376	128.483	199.206	346.229	526.198
	3	354.426	154.944	199.190	318.817	535.815	350.393	137.462	199.190	336.900	526.604
	4	348.105	141.849	186.256	338.892	536.520	349.821	138.276	196.334	336.900	529.087
	5	348.045	125.087	192.809	345.572	525.945	349.466	135.541	196.334	339.678	529.087
	6	355.699	151.716	182.594	333.282	560.475	350.505	138.164	192.215	336.926	531.873
	7	350.203	133.748	194.285	322.018	533.695	350.461	137.385	193.141	334.647	531.873
70	1	178.547	107.748	80.785	162.737	317.115	178.547	107.748	80.785	162.737	317.115
	2	178.605	106.666	75.683	149.939	294.665	178.576	106.822	78.423	155.313	311.697
80	1	201.137	88.192	114.837	173.447	322.921	201.137	88.192	114.837	173.447	322.921
	2	211.678	121.074	99.481	185.859	388.210	206.408	105.716	108.475	178.347	335.151
	3	207.346	110.409	103.273	180.298	400.821	206.721	107.073	104.849	178.831	352.978
	4	210.987	123.636	104.861	178.907	396.749	207.787	111.258	104.849	178.831	375.885
	5	213.865	129.853	98.333	182.759	381.836	209.003	115.069	104.243	179.050	377.964
	6	210.081	116.613	110.689	174.662	379.063	209.182	115.206	104.849	177.898	377.964
90	1	238.501	122.104	116.639	208.744	430.229	238.501	122.104	116.639	208.744	430.229
	2	232.094	103.520	132.739	222.758	363.960	235.298	112.923	120.927	215.485	387.043
	3	232.550	102.915	120.225	219.450	362.952	234.382	109.504	120.927	218.164	386.149
	4	239.305	137.073	121.889	216.993	394.023	235.613	116.823	120.927	218.043	387.043
	5	241.441	136.898	113.358	203.543	409.246	236.779	120.964	118.779	212.989	388.770
	6	237.830	126.504	119.392	202.633	416.200	236.954	121.785	118.779	210.581	390.090

Table C.2 Statistics for the different distributions of c (m³/(h·Pan)) obtained with the stochastic simulation and the UPC-CETE model (m³·h⁻¹·Pa0.67) Continuation

Number of dwellings	Simulation	By simulation					Acumulated				
		Average c'	σ	P10 th	P50 th	P90 th	Average c	σ	P10 th	P50 th	P90 th
100	1	205.603	87.806	116.188	191.583	298.516	205.603	87.806	116.188	191.583	298.516
	2	216.214	113.441	109.984	188.833	360.117	210.909	101.321	111.271	191.112	333.944
	2	212.616	101.213	107.575	185.555	356.911	211.478	101.119	109.984	187.303	347.075
	4	211.355	93.099	107.858	187.610	350.006	211.447	99.060	108.876	187.303	347.075
120	1	177.815	100.801	83.444	149.324	330.279	177.815	100.801	83.444	149.324	330.279
	2	181.942	116.210	82.360	153.421	312.175	179.879	108.570	83.444	150.366	315.819
	3	173.952	82.112	90.068	156.628	260.816	177.903	100.450	86.124	152.486	294.013
	4	173.349	87.831	85.632	164.333	273.053	176.765	97.379	86.039	154.311	288.251
	5	178.288	93.370	85.761	151.096	278.044	177.069	96.516	86.039	153.853	284.444
	6	169.751	85.571	83.377	147.672	273.611	175.850	94.763	85.419	152.486	284.123
	7	177.322	105.985	87.288	146.423	290.098	176.060	96.380	85.924	151.069	284.123
	8	173.414	82.546	86.850	156.553	275.367	175.729	94.726	86.251	151.946	283.931
	9	177.552	96.460	91.135	153.498	276.676	175.932	94.877	86.410	152.129	283.442
	10	177.958	103.603	84.628	152.470	312.078	176.134	95.741	86.355	152.129	283.931
	11	180.128	103.367	81.167	146.725	329.742	176.497	96.424	86.251	151.577	287.602
	12	180.399	104.901	90.240	157.925	288.700	176.823	97.126	86.355	151.836	287.602
	13	174.286	77.197	86.498	160.532	272.762	176.627	95.722	86.355	152.388	284.719
	14	176.676	107.497	89.326	141.910	304.402	176.631	96.576	86.366	151.965	287.436
140	1	239.030	125.243	107.562	218.967	395.825	239.030	125.243	107.562	218.967	395.825
	2	239.504	126.214	113.774	206.832	434.706	239.267	125.504	110.293	207.901	415.131
160	1	318.765	128.755	180.191	283.941	504.079	318.765	128.755	180.191	283.941	504.079
	2	315.232	123.938	196.166	282.469	486.869	316.999	126.183	189.160	283.941	490.691
	3	316.969	128.623	198.046	287.169	487.424	316.989	126.867	193.255	284.909	488.744
180	1	286.723	163.122	116.367	253.440	526.854	286.723	163.122	116.367	253.440	526.854
	2	278.439	143.962	118.373	256.111	466.009	282.581	153.682	117.437	254.822	473.963
	3	280.891	151.520	107.960	251.779	479.857	282.017	152.826	115.968	253.546	476.978
	4	271.567	130.033	125.358	253.196	437.717	279.405	147.441	116.996	253.546	467.431
	5	274.607	124.675	117.701	261.024	432.672	278.445	143.125	116.996	254.049	461.603
	6	279.752	138.680	112.660	249.237	469.832	278.663	142.332	116.492	253.837	465.766
200	1	161.491	56.874	96.967	155.310	234.408	161.491	56.874	96.967	155.310	234.408
	2	164.603	63.111	101.263	158.057	244.707	163.047	60.018	100.069	156.759	239.171
	3	164.837	62.922	101.232	158.894	225.497	163.644	60.955	100.939	157.441	235.544
	4	162.774	59.784	92.674	157.964	246.200	163.426	60.628	98.540	157.518	237.002
	5	163.801	62.370	97.384	157.436	245.295	163.501	60.949	98.540	157.518	238.378

Table C.2 Statistics for the different distributions of c (m³/(h·Pan)) obtained with the stochastic simulation and the UPC-CETE model (m³·h⁻¹·Pa0.67) Continuation

Number of dwellings	Simulation	By simulation					Accumulated				
		Average c'	σ	P10 th	P50 th	P90 th	Average c	σ	P10 th	P50 th	P90 th
250	1	241.910	126.443	95.842	212.215	436.011	241.910	126.443	95.842	212.215	436.011
	2	248.230	142.190	101.192	201.645	450.912	245.070	134.450	98.714	205.655	439.903
	3	248.498	144.038	95.481	201.897	477.234	246.213	137.633	96.977	203.453	459.074
	4	253.132	155.788	95.317	210.106	451.669	247.942	142.340	96.977	208.101	456.121
	5	238.152	126.945	103.988	199.054	416.928	245.984	139.403	97.482	204.095	447.509
	6	253.199	143.187	96.193	228.237	468.139	247.187	140.018	97.218	208.271	449.273
	7	247.232	142.828	97.550	198.628	456.886	247.193	140.382	97.218	206.605	449.437
300	1	178.126	76.126	96.063	160.920	282.810	178.126	76.126	96.063	160.920	282.810
	2	185.439	95.475	98.327	162.376	311.915	181.782	86.350	96.651	161.856	300.241
	3	180.644	93.587	97.257	156.925	304.254	181.403	88.777	96.929	160.330	301.381
	4	182.261	89.422	95.853	160.736	291.217	181.617	88.902	96.651	160.330	298.248
	5	179.086	79.885	93.369	163.266	293.401	181.111	87.154	95.802	161.148	297.282
	6	180.801	82.465	97.279	162.660	285.783	181.060	86.368	95.967	161.303	293.856
400	1	190.883	96.776	97.192	159.232	331.456	190.883	96.776	97.192	159.232	331.456
	2	195.907	109.344	98.287	163.136	347.951	193.395	103.218	97.287	162.114	338.029
	3	193.403	98.724	102.715	163.868	318.144	193.398	101.701	99.433	162.739	331.456
499	1	195.182	105.173	93.122	169.391	330.078	195.182	105.173	93.122	169.391	330.078
	2	196.042	105.598	93.182	170.360	327.929	195.612	105.334	93.177	170.195	329.879
	3	193.547	101.989	92.015	168.279	326.232	194.923	104.201	92.929	169.391	329.270
	4	197.252	105.744	89.689	176.598	323.722	195.505	104.567	91.876	170.910	327.550
	5	198.042	105.595	92.028	172.264	333.756	196.013	104.757	91.977	171.381	329.338
	6	193.685	105.482	88.685	174.112	317.632	195.625	104.864	91.607	171.483	326.386
	7	199.007	106.234	89.078	173.080	331.805	196.108	105.052	91.331	171.552	327.638
	8	191.618	99.790	90.428	168.781	318.497	195.547	104.408	91.216	171.436	326.681
	9	193.543	103.609	91.301	166.954	316.373	195.324	104.310	91.213	171.042	325.642
	10	195.772	102.287	94.230	173.407	321.729	195.369	104.099	91.570	171.314	324.481
599	1	194.408	106.498	95.649	162.579	336.964	194.408	106.498	95.649	162.579	336.964
	2	195.889	105.004	94.361	165.286	335.991	195.149	105.712	95.031	164.071	336.036
	3	196.892	102.622	100.767	162.643	333.545	195.730	104.667	97.245	163.294	335.566
	4	194.201	97.698	99.677	165.475	333.586	195.348	102.951	97.619	163.944	334.813
	5	193.184	101.563	101.236	159.199	336.130	194.915	102.661	98.313	162.643	335.362
	6	199.495	105.857	98.429	169.840	335.778	195.678	103.200	98.370	164.228	335.399
	7	195.160	108.216	97.211	164.906	321.769	195.604	103.918	98.274	164.298	333.763

Table C.2 Statistics for the different distributions of c (m³/(h·Pan)) obtained with the stochastic simulation and the UPC-CETE model (m³·h⁻¹·Pa0.67) Continuation

Number of dwellings	Simulation	By simulation					Accumulated				
		Average c'	σ	P10 th	P50 th	P90 th	Average c	σ	P10 th	P50 th	P90 th
699	1	200.457	106.333	95.615	174.142	346.496	200.457	106.333	95.615	174.142	346.496
	2	203.798	111.737	94.595	176.207	354.956	202.128	109.043	95.086	175.132	348.717
	3	200.194	106.747	95.673	170.601	330.171	201.483	108.261	95.402	174.358	340.982
	4	204.620	112.101	95.914	177.307	348.217	202.267	109.222	95.616	175.113	343.478
	5	201.523	109.026	96.859	175.993	335.608	202.118	109.168	95.935	175.444	342.033
792	1	204.129	101.562	97.055	181.078	346.832	204.129	101.562	97.055	181.078	346.832
	2	205.136	102.296	98.651	181.785	349.815	204.632	101.899	97.992	181.190	348.439
	3	206.855	107.592	93.766	179.413	349.815	205.373	103.814	96.800	180.543	348.817
	4	205.368	104.724	100.168	179.139	340.949	205.372	104.026	98.187	180.091	348.503
902	1	167.361	96.742	77.210	141.120	299.556	167.361	96.742	77.210	141.120	299.556
	2	167.650	95.615	78.416	143.610	288.016	167.505	96.154	77.819	142.387	292.905
967	3	131.264	74.617	65.322	108.193	230.762	131.264	74.617	65.322	108.193	230.762
	4	134.413	78.929	66.037	109.802	240.720	132.839	76.799	65.654	108.608	236.502
	5	134.436	76.830	67.880	111.065	229.038	133.371	76.800	66.426	109.628	234.491
	6	133.461	75.181	66.436	111.010	228.837	133.394	76.389	66.427	109.730	232.578
1648	1	177.868	99.225	87.836	151.189	300.922	177.868	99.225	87.836	151.189	300.922
	2	180.107	101.284	88.297	149.481	303.908	178.987	100.251	87.987	150.269	302.191
	3	179.189	97.916	88.911	150.986	305.424	179.054	99.469	88.391	150.442	303.536

Table C.3 Number of simulations that fit a log-normal distribution with the UPC-CETE model based on Lilliefors' test

Number of dwellings	Yes	No	Number of dwellings	Yes	No
10	20	0	180	10	10
20	18	2	200	16	4
30	15	5	250	13	7
40	17	3	300	17	3
50	18	2	400	1	19
60	20	0	499	4	16
70	15	5	599	1	19
80	14	6	699	3	17
90	15	5	792	6	14
100	19	1	902	0	20
120	16	4	967	0	20
140	19	1	1648	0	20
160	8	12			

Second test

Results of the ANOVA test for c' ($\text{m}^3 \cdot \text{h}^{-1} \cdot \text{Pa}^{0.67}$). Medians of 20 simulations by census tract.

Number of dwellings	Section code
10	801509044

Anova

Source	SS	df	MS	F	Prob>F
Columns	0.096	20	0.0048	0.02	1
Error	37.2657	189	0.19717		
Total	37.3617	209			

Kruscal-Wallis

Source	SS	df	MS	Chi-sq	Prob>Chi-sq
Columns	7580	20	379	2.05	1
Error	764152.5	189	4043.13		
Total	771732.5	209			

Number of dwellings	Section code
20	801503002

Anova

Source	SS	df	MS	F	Prob>F
Columns	0.07	19	0.00369	0.01	1
Error	99.8438	380	0.26275		
Total	99.9138	399			

Kruscal-Wallis

Source	SS	df	MS	Chi-sq	Prob>Chi-sq
Columns	63235.1	31	2039.8	1.85	1
Error	21781984.9	608	35825.6		
Total	21845220	639			

Number of dwellings	Section code
30	801507015

Anova

Source	SS	df	MS	F	Prob>F
Columns	0.044	19	0.00229	0.01	1
Error	138.049	580	0.23802		
Total	138.093	599			

Kruscal-Wallis

Source	SS	df	MS	Chi-sq	Prob>Chi-sq
Columns	29188.3	19	1536.2	0.97	1
Error	17970761.7	580	30984.1		
Total	17999950	599			

Number of dwellings	Section code
40	801507005

Anova

Source	SS	df	MS	F	Prob>F
--------	----	----	----	---	--------

Columns	0.088	19	0.00462	0.03	1
---------	-------	----	---------	------	---

Error	127.245	780	0.16313		
-------	---------	-----	---------	--	--

Total	127.333	799			
-------	---------	-----	--	--	--

Kruscal-Wallis

Source	SS	df	MS	Chi-sq	Prob>Chi-sq
--------	----	----	----	--------	-------------

Columns	86315.6	19	4542.9	1.62	1
---------	---------	----	--------	------	---

Error	42580284.4	780	54590.1		
-------	------------	-----	---------	--	--

Total	42666600	799			
-------	----------	-----	--	--	--

Number of dwellings	Section code
50	801507010

Anova

Source	SS	df	MS	F	Prob>F
--------	----	----	----	---	--------

Columns	0.066	19	0.00345	0.02	1
---------	-------	----	---------	------	---

Error	198.992	980	0.20305		
-------	---------	-----	---------	--	--

Total	199.057	999			
-------	---------	-----	--	--	--

Kruscal-Wallis

Source	SS	df	MS	Chi-sq	Prob>Chi-sq
--------	----	----	----	--------	-------------

Columns	56713.6	19	2984.9	0.68	1
---------	---------	----	--------	------	---

Error	83276531.4	980	84976.1		
-------	------------	-----	---------	--	--

Total	83333245	999			
-------	----------	-----	--	--	--

Number of dwellings	Section code
60	800801001

Anova

Source	SS	df	MS	F	Prob>F
--------	----	----	----	---	--------

Columns	0.042	19	0.00219	0.01	1
---------	-------	----	---------	------	---

Error	201.482	1180	0.17075		
-------	---------	------	---------	--	--

Total	201.523	1199			
-------	---------	------	--	--	--

Kruscal-Wallis

Source	SS	df	MS	Chi-sq	Prob>Chi-sq
--------	----	----	----	--------	-------------

Columns	92492.5	19	4868	0.77	1
---------	---------	----	------	------	---

Error	143907407.5	1180	121955.4		
-------	-------------	------	----------	--	--

Total	143999900	1199			
-------	-----------	------	--	--	--

Number of dwellings	Section code
70	801907188

Anova

Source	SS	df	MS	F	Prob>F
--------	----	----	----	---	--------

Columns	0.205	19	0.0108	0.04	1
Error	375.747	1380	0.27228		
Total	375.952	1399			

Kruscal-Wallis

Source	SS	df	MS	Chi-sq	Prob>Chi-sq
--------	----	----	----	--------	-------------

Columns	236641.8	19	12454.8	1.45	1
Error	228429908.2	1380	165528.9		
Total	228666550	1399			

Number of dwellings	Section code
80	801907067

Anova

Source	SS	df	MS	F	Prob>F
--------	----	----	----	---	--------

Columns	0.057	19	0.00301	0.01	1
Error	381.951	1580	0.24174		
Total	382.008	1599			

Kruscal-Wallis

Source	SS	df	MS	Chi-sq	Prob>Chi-sq
--------	----	----	----	--------	-------------

Columns	258988.4	19	13631	1.21	1
Error	341074211.6	1580	215869.8		
Total	341333200	1599			

Number of dwellings	Section code
90	810201001

Anova

Source	SS	df	MS	F	Prob>F
--------	----	----	----	---	--------

Columns	0.09	20	0.00449	0.02	1
Error	393.236	1869	0.2104		
Total	393.326	1889			

Kruscal-Wallis

Source	SS	df	MS	Chi-sq	Prob>Chi-sq
--------	----	----	----	--------	-------------

Columns	359343.2	20	17967.2	1.21	1
Error	562246249.3	1869	300827.3		
Total	562605592.5	1889			

Number of dwellings	Section code
100	810201001

Anova

Source	SS	df	MS	F	Prob>F
--------	----	----	----	---	--------

Columns	0.076	18	0.00421	0.02	1
Error	349.166	1881	0.18563		
Total	349.242	1899			

Kruscal-Wallis

Source	SS	df	MS	Chi-sq	Prob>Chi-sq
--------	----	----	----	--------	-------------

Columns	218353.5	18	12130.7	0.73	1
Error	571364821.5	1881	303755.9		
Total	571583175	1899			

Number of dwellings	Section code
120	801502001

Anova

Source	SS	df	MS	F	Prob>F
--------	----	----	----	---	--------

Columns	0.308	19	0.0162	0.07	1
Error	527.852	2380	0.22179		
Total	528.16	2399			

Kruscal-Wallis

Source	SS	df	MS	Chi-sq	Prob>Chi-sq
--------	----	----	----	--------	-------------

Columns	1.19068e+006	19	62667.2	2.48	1
Error	1.15081e+009	2380	483533.2		
Total	1.152e+009	2399			

Number of dwellings	Section code
140	800902002

Anova

Source	SS	df	MS	F	Prob>F
--------	----	----	----	---	--------

Columns	0.14	19	0.00739	0.03	1
Error	766.76	2780	0.27581		
Total	766.9	2799			

Kruscal-Wallis

Source	SS	df	MS	Chi-sq	Prob>Chi-sq
--------	----	----	----	--------	-------------

Columns	857734.2	19	45143.9	1.31	1
Error	1828475365.8	2780	657725		
Total	1829333100	2799			

Number of dwellings	Section code
160	256101001

Anova

Source	SS	df	MS	F	Prob>F
--------	----	----	----	---	--------

Columns	0.076	19	0.00401	0.03	1
Error	465.293	3180	0.14632		
Total	465.369	3199			

Kruscal-Wallis

Source	SS	df	MS	Chi-sq	Prob>Chi-sq
--------	----	----	----	--------	-------------

Columns	1.12163e+006	19	59033	1.31	1
Error	2.72954e+009	3180	858347.4		
Total	2.73067e+009	3199			

Number of dwellings	Section code
180	807601002

Anova

Source	SS	df	MS	F	Prob>F
--------	----	----	----	---	--------

Columns	0.086	19	0.00451	0.02	1
Error	922.385	3580	0.25765		
Total	922.47	3599			

Kruscal-Wallis

Source	SS	df	MS	Chi-sq	Prob>Chi-sq
--------	----	----	----	--------	-------------

Columns	891949	19	46944.7	0.83	1
Error	3887107751	3580	1085784.3		
Total	3887999700	3599			

Number of dwellings	Section code
200	818707001

Anova

Source	SS	df	MS	F	Prob>F
--------	----	----	----	---	--------

Columns	0.201	19	0.01056	0.08	1
Error	510.45	3980	0.12825		
Total	510.651	3999			

Kruscal-Wallis

Source	SS	df	MS	Chi-sq	Prob>Chi-sq
--------	----	----	----	--------	-------------

Columns	1.55942e+006	19	82074.7	1.17	1
Error	5.33177e+009	3980	1339641.6		
Total	5.33333e+009	3999			

Number of dwellings	Section code
250	812601001

Anova

Source	SS	df	MS	F	Prob>F
--------	----	----	----	---	--------

Columns	0.45	19	0.02378	0.07	1
Error	1642.73	4980	0.32987		
Total	1643.19	4999			

Kruscal-Wallis

Source	SS	df	MS	Chi-sq	Prob>Chi-sq
--------	----	----	----	--------	-------------

Columns	3.26262e+006	19	171717	1.57	1
Error	1.04134e+010	4980	2091044.9		
Total	1.04167e+010	4999			

Number of dwellings	Section code
300	813601005

Anova

Source	SS	df	MS	F	Prob>F
--------	----	----	----	---	--------

Columns	0.41	19	0.02153	0.12	1
Error	1119.37	5980	0.18719		
Total	1119.78	5999			

Kruscal-Wallis

Source	SS	df	MS	Chi-sq	Prob>Chi-sq
--------	----	----	----	--------	-------------

Columns	7.35491e+006	19	387100.6	2.45	1
Error	1.79926e+010	5980	3008803.4		
Total	1.8e+010	5999			

Number of dwellings	Section code
400	820002013

Anova

Source	SS	df	MS	F	Prob>F
--------	----	----	----	---	--------

Columns	0.32	18	0.01802	0.08	1
Error	1709.3	7581	0.22547		
Total	1709.63	7599			

Kruscal-Wallis

Source	SS	df	MS	Chi-sq	Prob>Chi-sq
--------	----	----	----	--------	-------------

Columns	5.35045e+006	18	297247.1	1.11	1
Error	3.6576e+010	7581	4824691		
Total	3.65813e+010	7599			

Number of dwellings	Section code
499	4313701001

Anova

Source	SS	df	MS	F	Prob>F
--------	----	----	----	---	--------

Columns	0.83	19	0.04377	0.18	1
Error	2446.95	9960	0.24568		
Total	2447.78	9979			

Kruscal-Wallis

Source	SS	df	MS	Chi-sq	Prob>Chi-sq
--------	----	----	----	--------	-------------

Columns	2.76868e+007	19	1.4572e+006	3.34	1
Error	8.28066e+010	9960	8.31392e+006		
Total	8.28343e+010	9979			

Number of dwellings	Section code
599	804201001

Anova

Source	SS	df	MS	F	Prob>F
--------	----	----	----	---	--------

Columns	0.68	19	0.03577	0.16	1
Error	2623.74	11960	0.21938		
Total	2624.42	11979			

Kruscal-Wallis

Source	SS	df	MS	Chi-sq	Prob>Chi-sq
--------	----	----	----	--------	-------------

Columns	4.15255e+007	19	2.18555e+006	3.47	1
Error	1.4324e+011	11960	1.19766e+007		
Total	1.43281e+011	11979			

Number of dwellings	Section code
699	4302801001

Anova

Source	SS	df	MS	F	Prob>F
--------	----	----	----	---	--------

Columns	0.8	19	0.04186	0.17	1
Error	3445.19	13960	0.24679		
Total	3445.98	13979			

Kruscal-Wallis

Source	SS	df	MS	Chi-sq	Prob>Chi-sq
--------	----	----	----	--------	-------------

Columns	4.9531e+007	19	2.60689e+006	3.04	1
Error	2.27639e+011	13960	1.63065e+007		
Total	2.27688e+011	13979			

Number of dwellings	Section code
792	820505001

Anova

Source	SS	df	MS	F	Prob>F
--------	----	----	----	---	--------

Columns	0.74	19	0.03875	0.17	1
Error	3662.23	15820	0.23149		
Total	3662.97	15839			

Kruscal-Wallis

Source	SS	df	MS	Chi-sq	Prob>Chi-sq
--------	----	----	----	--------	-------------

Columns	7.31533e+007	19	3.85017e+006	3.5	1
Error	3.31122e+011	15820	2.09306e+007		
Total	3.31195e+011	15839			

Number of dwellings	Section code
902	823401001

Anova

Source	SS	df	MS	F	Prob>F
--------	----	----	----	---	--------

Columns	1.1	19	0.05766	0.22	0.9999
Error	4770.53	18020	0.26474		
Total	4771.62	18039			

Kruscal-Wallis

Source	SS	df	MS	Chi-sq	Prob>Chi-sq
--------	----	----	----	--------	-------------

Columns	1.18537e+008	19	6.2388e+006	4.37	0.9998
Error	4.89129e+011	18020	2.71437e+007		
Total	4.89247e+011	18039			

Number of dwellings	Section code
967	829101001

Anova

Source	SS	df	MS	F	Prob>F
--------	----	----	----	---	--------

Columns	1.55	19	0.08165	0.35	0.9957
Error	4480.63	19320	0.23192		
Total	4482.19	19339			

Kruscal-Wallis

Source	SS	df	MS	Chi-sq	Prob>Chi-sq
--------	----	----	----	--------	-------------

Columns	3.14605e+008	19	1.65582e+007	10.09	0.9506
Error	6.02506e+011	19320	3.11856e+007		
Total	6.02821e+011	19339			

Number of dwellings	Section code
1648	802301001

Anova

Source	SS	df	MS	F	Prob>F

Columns	1.12	19	0.05875	0.26	0.9995
Error	7546.53	32940	0.2291		
Total	7547.65	32959			

Kruscal-Wallis

Source	SS	df	MS	Chi-sq	Prob>Chi-sq

Columns	2.7054e+008	19	1.4239e+007	2.99	1
Error	2.9836e+012	32940	9.05769e+007		
Total	2.98387e+012	32959			

Annex D. Statistical analysis of the CETE de Lyon air leakage database

D.1 ANOVA test made in Minitab

Structure type, ST

One-way ANOVA: ln(c') versus ST

Source	DF	SS	MS	F	P
ST	1	9.379	9.379	27.45	0.000
Error	233	79.614	0.342		
Total	234	88.993			

S = 0.5845 R-Sq = 10.54% R-Sq(adj) = 10.16%

Level	N	Mean	StDev
Heavy	181	-4.4007	0.5749
Ligth	54	-3.9258	0.6161

Insulation type, IT

One-way ANOVA: ln(c') versus Insulation

Source	DF	SS	MS	F	P
Isolation	2	2.771	1.386	3.47	0.034
Error	138	55.148	0.400		
Total	140	57.919			

S = 0.6322 R-Sq = 4.78% R-Sq(adj) = 3.40%

Level	N	Mean	StDev
Inner	86	-4.3639	0.5454
Integrated	44	-4.1596	0.7892
Outer	11	-3.9030	0.5555

Heating system, HS

One-way ANOVA: ln(c') versus HS

Source	DF	SS	MS	F	P
HS	1	1.359	1.359	3.67	0.058
Error	127	47.004	0.370		
Total	128	48.363			

S = 0.6084 R-Sq = 2.81% R-Sq(adj) = 2.04%

Level	N	Mean	StDev
Electric	64	-4.3678	0.5574
Non Electric	65	-4.1625	0.6547

Age

One-way ANOVA: ln(c') versus Age when tested

Source	DF	SS	MS	F	P
Age testé	6	7.948	1.325	3.65	0.002
Error	215	77.963	0.363		
Total	221	85.911			

S = 0.6022 R-Sq = 9.25% R-Sq(adj) = 6.72%

Level	N	Mean	StDev
0	182	-4.3844	0.6194
1	20	-3.9975	0.4957
2	5	-3.8425	0.4994
3	2	-5.1275	0.0381
4	4	-4.1199	0.8807
5	1	-3.8658	*
9	8	-3.7830	0.2721

Floor area, Area

Regression Analysis: ln(c') versus Floor area

The regression equation is
 ln_Cps = - 5.09 + 0.00825 Floor area

Predictor	Coef	SE Coef	T	P
Constant	-5.0894	0.1187	-42.89	0.000
Floor area	0.008247	0.001174	7.02	0.000

S = 0.563264 R-Sq = 16.5% R-Sq(adj) = 16.2%

Analysis of Variance

Source	DF	SS	MS	F	P
Regression	1	15.653	15.653	49.34	0.000
Residual Error	249	78.999	0.317		
Total	250	94.652			

Climatic zone, CZ

One-way ANOVA: ln(c') versus CZ

Source	DF	SS	MS	F	P
CZ	2	8.100	4.050	11.60	0.000
Error	248	86.552	0.349		
Total	250	94.652			

S = 0.5908 R-Sq = 8.56% R-Sq(adj) = 7.82%

Level	N	Mean	StDev
H1	126	-4.1409	0.5757
H2	113	-4.4914	0.5901
H3	12	-4.0450	0.7460

One-way ANOVA for heavy structures only: ln(c') versus CZ

Source	DF	SS	MS	F	P
CZ	2	5.456	2.728	8.99	0.000
Error	178	54.039	0.304		
Total	180	59.495			

S = 0.5510 R-Sq = 9.17% R-Sq(adj) = 8.15%

Level	N	Mean	StDev
H1	78	-4.2665	0.5012
H2	92	-4.5612	0.5620
H3	11	-4.0096	0.7717

D.2 Regressions made in Minitab

Regression 1 (Eq. 5.3)

The regression equation is

$$\ln(c') = -5.54 + 0.00641 \text{ area} + 0.311 \text{ ST} + 0.0881 \text{ Age} + 0.124 \text{ NS} \\ + 0.108 \text{ H1} + 0.049 \text{ H2} + 0.583 \text{ IT} + 0.411 \text{ HS}$$

84 cases used, 167 cases contain missing values

Predictor	Coef	SE Coef	T	P
-----------	------	---------	---	---

Constant	-5.5438	0.4060	-13.65	0.000
Floor area	0.006415	0.001968	3.26	0.002
ST	0.3107	0.1359	2.29	0.025
Age	0.08807	0.02377	3.71	0.000
NS	0.1240	0.1305	0.95	0.345
H1	0.1076	0.3220	0.33	0.739
H2	0.0488	0.3293	0.15	0.883
IT	0.5832	0.2174	2.68	0.009
HS	0.4105	0.1279	3.21	0.002

S = 0.507123 R-Sq = 41.1% R-Sq(adj) = 34.9%

Analysis of Variance

Source	DF	SS	MS	F	P
Regression	8	13.4829	1.6854	6.55	0.000
Residual Error	75	19.2881	0.2572		
Total	83	32.7709			

Source	DF	Seq SS
Floor area	1	4.7672
ST	1	1.8736
Age	1	2.3088
NS	1	0.4689
H1	1	0.0771
H2	1	0.2982
IT	1	1.0413
HS	1	2.6478

Regression 2 (Eq. 5.4)

The regression equation is

$$\ln(c') = -5.51 + 0.0102 \text{ area} + 0.324 \text{ ST} + 0.0704 \text{ Age} + 0.176 \text{ NS} \\ + 0.429 \text{ IT} - 0.141 \text{ H1} - 0.254 \text{ H2}$$

117 cases used, 134 cases contain missing values

Predictor	Coef	SE Coef	T	P
Constant	-5.5078	0.3118	-17.66	0.000
Floor area	0.010204	0.001718	5.94	0.000
ST	0.3239	0.1231	2.63	0.010
Age	0.07039	0.02213	3.18	0.002
NS	0.1764	0.1107	1.59	0.114
IT	0.4288	0.2115	2.03	0.045
H1	-0.1411	0.2073	-0.68	0.497
H2	-0.2538	0.2133	-1.19	0.237

S = 0.519238 R-Sq = 43.6% R-Sq(adj) = 40.0%

Analysis of Variance

Source	DF	SS	MS	F	P
Regression	7	22.7295	3.2471	12.04	0.000
Residual Error	109	29.3873	0.2696		
Total	116	52.1168			

Source	DF	Seq SS
Floor area	1	12.5167
ST	1	3.6150
Age	1	3.6512
NS	1	1.5979
IT	1	0.8843
H1	1	0.0828
H2	1	0.3816

Regression 3 (Eq. 5.5)

The regression equation is

$$\ln(c') = -5.40 + 0.00709 \text{ area} + 0.480 \text{ ST} + 0.0699 \text{ Age} + 0.293 \text{ NS} \\ - 0.139 \text{ H1} - 0.286 \text{ H2}$$

201 cases used, 50 cases contain missing values

Predictor	Coef	SE Coef	T	P
Constant	-5.4049	0.2304	-23.45	0.000
Floor area	0.007090	0.001191	5.95	0.000
ST	0.47977	0.08929	5.37	0.000
Age	0.06987	0.02002	3.49	0.001
NS	0.29315	0.07771	3.77	0.000
H1	-0.1388	0.1725	-0.80	0.422
H2	-0.2861	0.1698	-1.68	0.094

S = 0.498395 R-Sq = 40.2% R-Sq(adj) = 38.4%

Analysis of Variance

Source	DF	SS	MS	F	P
Regression	6	32.4127	5.4021	21.75	0.000
Residual Error	194	48.1891	0.2484		
Total	200	80.6018			

Source	DF	Seq SS
Floor area	1	9.9775
ST	1	10.5634
Age	1	5.1485
NS	1	5.5194
H1	1	0.4986
H2	1	0.7052

Regression 4 (Eq. 5.6)

The regression equation is

$$\ln(c') = -5.68 + 0.00698 \text{ area} + 0.507 \text{ ST} + 0.0784 \text{ Age} + 0.345 \text{ NS}$$

201 cases used, 50 cases contain missing values

Predictor	Coef	SE Coef	T	P
Constant	-5.6815	0.1463	-38.84	0.000
Floor area	0.006980	0.001175	5.94	0.000
ST	0.50749	0.08581	5.91	0.000
Age	0.07838	0.01922	4.08	0.000

NS 0.34505 0.07373 4.68 0.000
 S = 0.502001 R-Sq = 38.7% R-Sq(adj) = 37.5%

Analysis of Variance

Source	DF	SS	MS	F	P
Regression	4	31.2089	7.8022	30.96	0.000
Residual Error	196	49.3929	0.2520		
Total	200	80.6018			

Source	DF	Seq SS
Floor area	1	9.9775
ST	1	10.5634
Age	1	5.1485
NS	1	5.5194

Regression for the adjustment of the Age variable (Eq. 5.8)

The regression equation is
 ACH50 = - 0.00239 + 0.00131 CT + 0.000063 Age

Predictor	Coef	SE Coef	T	P
Constant	-0.0023894	0.0003587	-6.66	0.000
CT	0.0013056	0.0001310	9.96	0.000
Age	0.00006328	0.00000577	10.97	0.000

S = 0.000414392 R-Sq = 94.8% R-Sq(adj) = 94.0%

Analysis of Variance

Source	DF	SS	MS	F	P
Regression	2	0.000037716	0.000018858	109.82	0.000
Residual Error	12	0.000002061	0.000000172		
Total	14	0.000039776			

Source	DF	Seq SS
CT	1	0.000017045
Age	1	0.000020671

D.3 Non parametric analysis of variance made in Matlab

Original versus predicted values of c'

Kruskal-Wallis ANOVA Table					
Source	SS	df	MS	Chi-sq	Prob>Chi-sq
Columns	3744.3	1	3744.3	0.18	0.6731
Error	10538361.7	500	21076.7		
Total	10542106	501			

Annex E. Protocols followed in the experimental trials

E.1 Informative brochures about the trials

Catalan version:

IMPORTÀNCIA DE LA TAXA DE RENOVACIÓ

Econòmica: Influeix en el consum energètic durant l'hivern i l'estiu. Si el cabal d'aire infiltrat és alt, es perd fred i/o calor amb l'aire que surt i es consumeix més energia per condicionar l'aire que entra.

Salut: Si les finestres i portes resten tancades, la infiltració és l'única via de transport de contaminants des de l'exterior a l'interior i des de l'interior a l'exterior. Per això és un dels paràmetres que determinen la qualitat de l'aire que respirem.

PRESENTACIÓ

El Centre d'Estudis del Risc Tecnològic (CERTEC), creat l'any 1992 per la Universitat Politècnica de Catalunya i l'Institut d'Estudis Catalans, és una entitat que té per objectiu la recerca i la formació en els diferents camps del risc tecnològic i de l'impacte ambiental.

L'objectiu d'aquest treball és caracteritzar la taxa de renovació dels habitatges unifamiliars catalans. Els resultats que s'obtinguin han de permetre la determinació de la qualitat de la protecció que poden oferir els habitatges a les persones en el cas de fugites de gasos tòxics així com facilitar el càlcul del radi d'evacuació.

ESTUDI PER DETERMINAR LA TAXA DE RENOVACIÓ D'AIRE EN HABITATGES



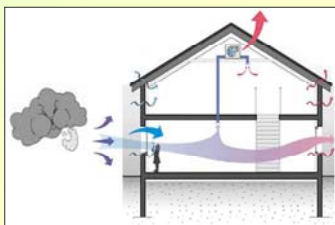
Centre d'Estudis del Risc Tecnològic



Universitat Politècnica de Catalunya

TAXA DE RENOVACIÓ D'AIRE

La taxa de renovació d'aire es refereix al nombre de vegades per hora que es renova tot l'aire dins l'habitatge. Quan totes les obertures voluntàries, com ara les finestres i les portes, es tanquen l'aire només pot entrar per infiltració. La infiltració depèn de 2 factors: l'hermeticitat de l'habitatge (especialment la unió entre els marcs i les parets) i les condicions meteorològiques (temperatura exterior i velocitat del vent).



PASSOS PER DETERMINAR LA TAXA DE RENOVACIÓ D'AIRE UTILITZANT CO₂



Tancar les finestres, portes i altres obertures voluntàries. Aturar tots els sistemes mecànics de ventilació.



Mesurar la concentració interior de CO₂ i la temperatura abans d'iniciar la prova.



Descarregar una quantitat determinada de CO₂ a la casa per assolir ràpidament una concentració de 1500 ppm. Aquesta concentració no representa cap perill, fins i tot es pot assolir durant la nit en habitacions tancades.



Posar en marxa el sistema de mesura i enregistrament de la concentració de CO₂, sortir de la casa i esperar que passin 2h. Durant aquest temps la concentració anirà disminuint a causa de la infiltració d'aire exterior. Amb l'anàlisi de les dades es pot estimar la taxa de renovació.



Finalitzada la prova, obrir les portes i finestres perquè es dispersi el CO₂ restant.



Mesurar les condicions meteorològiques durant la prova: temperatura i velocitat del vent.

Spanish version:

IMPORTANCIA DE LA TASA DE RENOVACIÓN

Económica: Influye en el consumo energético durante invierno y verano. Si el caudal de aire infiltrado es alto, se pierde frío y/o calor con el aire que sale y se consume mayor energía para acondicionar el aire que entra.

Salud: Si las ventanas y puertas se encuentran cerradas, la infiltración es la única vía de transporte de contaminantes desde el exterior al interior y desde el interior al exterior. Por ello es uno de los parámetros que determinan la calidad del aire que respiramos.

PRESENTACIÓN

El Centro de Estudios del Riesgo Tecnológico (CERTEC), creado en el año 1992 por la Universitat Politècnica de Catalunya y el Institut d'Estudis Catalans, es una entidad que tiene por objetivo la investigación y la formación en los distintos campos del riesgo tecnológico y el impacto ambiental.

El objetivo de este trabajo es caracterizar la tasa de renovación de las viviendas unifamiliares catalanas. Los resultados que se obtengan permitirán la determinación de la calidad de la protección que pueden brindar las viviendas a las personas en el caso de escapes de gases tóxicos y facilitarán el cálculo del radio de evacuación.

ESTUDIO PARA DETERMINAR LA TASA DE RENOVACIÓN DE AIRE EN VIVIENDAS



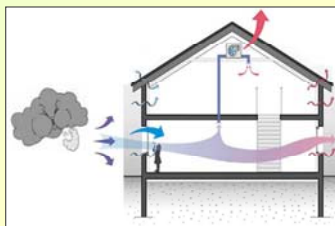
Centre d'Estudis
del Risc
Tecnològic



Universitat
Politècnica de
Catalunya

TASA DE RENOVACIÓN DE AIRE

La tasa de renovación de aire se refiere al número de veces por hora que se renueva todo el aire dentro de la vivienda. Cuando todas las aberturas voluntarias, como las ventanas y puertas se cierran, el aire solo puede entrar por infiltración. La infiltración depende de 2 factores: la hermeticidad de la casa (especialmente la unión entre los marcos y las paredes) y las condiciones meteorológicas (temperatura exterior y velocidad del viento).



PASOS PARA DETERMINAR LA TASA DE RENOVACIÓN DE AIRE UTILIZANDO CO₂



Cerrar las ventanas, puertas y demás aberturas voluntarias, y apagar todos los sistemas mecánicos de ventilación.



Medir la concentración interior de CO₂ y la temperatura antes de iniciar la prueba.



Descargar una cantidad determinada de CO₂ en la casa para alcanzar rápidamente una concentración de 1500 ppm. Esta concentración no representa ningún peligro, incluso puede alcanzarse durante la noche en habitaciones cerradas.



Iniciar el sistema de medición y almacenamiento de concentraciones de CO₂, salir de la casa y esperar a que pasen 2h. Durante este tiempo la concentración irá disminuyendo debido a la infiltración de aire exterior. Mediante el análisis de los datos se puede estimar la tasa de renovación.




Terminada la prueba, abrir las puertas y ventanas para que se disperse el CO₂ remanente.



Medir las condiciones meteorológicas durante la prueba: temperatura y velocidad del viento.

E.2 Safety data sheet of CO₂

	FICHA DE DATOS DE SEGURIDAD	Página : 1
		Edición revisada no : 2
		Fecha : 2 / 2 / 2009
		Reemplaza : 1 / 6 / 2004
ANH. CARBÓNICO/ DIÓXIDO DE CARBONO/LASAL 2		018A-1



Etiqueta 2.2 : Gas no inflamable, no tóxico.

1 IDENTIFICACIÓN DE LA SUSTANCIA O PREPARADO Y DE LA SOCIEDAD O EMPRESA

Nombre comercial	: ANH. CARBÓNICO/ DIÓXIDO DE CARBONO/LASAL 2
Número de la Ficha de Datos de Seguridad del producto	: 018A-1
Uso	: Varios.
Fórmula química	: CO ₂
Identificación de la Compañía	: AL AIR LIQUIDE ESPAÑA S.A. Pº DE LA CASTELLANA ,35 28046 MADRID (ESPAÑA)
	E-mail: e-business.ALE@airliquide.com
Número de teléfono de emergencia	: 915029300

2 IDENTIFICACIÓN DE LOS PELIGROS

Identificación de riesgos	: Gas licuado. Puede causar asfixia en altas concentraciones.
Primeras vías de exposición	: Inhalación. Ojos. Piel.

3 COMPOSICIÓN / INFORMACIÓN SOBRE LOS COMPONENTES

Sustancia / Mezcla	: Sustancia.				
Nombre del componente	Contenido	Nº CAS	Nº EC	Nº Indiso	Clasificación
Dióxido de carbono	: 100 %	124-38-9	204-696-9	—	
No contiene otros componentes o impurezas que puedan influir en la clasificación del producto.					


4 PRIMEROS AUXILIOS

Primeros auxilios	
- Inhalación	: A elevadas concentraciones puede causar asfixia. Los síntomas pueden incluir la pérdida de la consciencia o de la movilidad. La víctima puede no haberse dado cuenta de la asfixia. Concentraciones pequeñas (3 a 5%) provocan aumento de la frecuencia respiratoria y dolor de cabeza. Retirar a la víctima a un área no contaminada llevando colocado el equipo de respiración autónoma de presión positiva. Mantener a la víctima caliente y en reposo. Llamar al doctor. Aplicar la respiración artificial si se para la respiración.
- Contacto con la piel y con los ojos	: Lavar inmediatamente los ojos con agua durante, al menos, 15 minutos. En caso de congelación rociar con agua durante 15 minutos. Aplicar un vendaje estéril. Obtener asistencia médica.
- Ingestión	: La ingestión no está considerada como una vía potencial de exposición.

5 MEDIDAS DE LUCHA CONTRA INCENDIOS

Tipo de inflamabilidad	: No inflamable.
Riesgos específicos	: La exposición al fuego puede causar la rotura o explosión de los recipientes.
Productos peligrosos de la	: Ninguno.

AL AIR LIQUIDE ESPAÑA S.A.
Pº DE LA CASTELLANA ,35 28046 MADRID (ESPAÑA)
E-mail: e-business.ALE@airliquide.com

	FICHA DE DATOS DE SEGURIDAD	Página : 2
		Edición revisada no : 2
		Fecha : 2 / 2 / 2009
		Reemplaza : 1 / 6 / 2004
ANH. CARBÓNICO/ DIÓXIDO DE CARBONO/LASAL 2		018A-1

5 MEDIDAS DE LUCHA CONTRA INCENDIOS /...

combustión

Medios para extinguir incendios

- Medios de extinción adecuados : Se pueden utilizar todos los extintores conocidos.

Métodos específicos : Si es posible detener la fuga de producto.
Colocarse lejos del recipiente y enfriarlo con agua desde un recinto protegido.

Equipo de protección especial para la actuación en incendios : En espacios confinados se recomienda utilizar equipos de respiración autónoma de presión positiva.

6 MEDIDAS EN CASO DE VERTIDO ACCIDENTAL

Precauciones personales : Evacuar el área.
Utilizar equipos de respiración autónoma de presión positiva cuando entren en el área a menos que esté probado que la atmósfera es segura.
Asegurar la adecuada ventilación de aire.

Precauciones para la protección del medio ambiente : Intentar parar el escape/derrame.
Prevenir la entrada en alcantarillas, sótanos, fosos de trabajo o en cualquier otro lugar donde la acumulación pueda ser peligrosa.

Métodos de limpieza : Ventilar la zona.

7 MANIPULACIÓN Y ALMACENAMIENTO

Almacenamiento : Mantener el contenedor por debajo de 50°C, en un lugar bien ventilado.

Manipulación : Debe prevenirse la filtración de agua al interior del recipiente.
No permitir el retroceso hacia el interior del recipiente.
Utilizar solo equipo específicamente apropiado para este producto y para su presión y temperatura de suministro, en caso de duda contacte con su suministrador.
Solicitar del suministrador las instrucciones de manipulación de las botellas.

8 CONTROLES DE LA EXPOSICIÓN / PROTECCIÓN PERSONAL

Protección personal : Asegurar una ventilación adecuada.

- Protección de las vías respiratorias : En caso de ventilación insuficiente, úsese equipo respiratorio de presión positiva adecuado.

- Protección de las manos : Usen guantes.

- Protección para la piel : Úsese indumentaria protectora adecuada. Guantes y zapatos de seguridad para el manejo de botellas.


- Protección para los ojos : Gafas de seguridad.

Límite de exposición laboral : Dióxido de carbono : TLV® -TWA [ppm] : 5000
Dióxido de carbono : TLV® -STEL [ppm] : 30000
Dióxido de carbono : OEL (UK)-LTEL [ppm] : 5000
Dióxido de carbono : OEL (UK)-STEL [ppm] : 15000
Dióxido de carbono : ILV (EU) - 8 H - [mg/m³] : 9000
Dióxido de carbono : ILV (EU) - 8 H - [ppm] : 5000
Dióxido de carbono : HTP-värden - 8 H - [ppm] : 5000
Dióxido de carbono : HTP-värden - 8 H - [mg/m³] : 9100
Dióxido de carbono : NGV - [ppm] : 5000
Dióxido de carbono : NGV - [mg/m³] : 9000
Dióxido de carbono : KTV - [ppm] : 10
Dióxido de carbono : KTV - [mg/m³] :
Dióxido de carbono : MAK (AU) Tagesmittelwert (ml/m³) : 5000
Dióxido de carbono : MAK (AU) Kurzzeitwerte (mg/m³) : 18000
Dióxido de carbono : MAK (AU) Tagesmittelwert (mg/m³) : 9000
Dióxido de carbono : MAK (AU) Kurzzeitwerte (ml/m³) : 10000
Dióxido de carbono : Arbeitsplatzgrenzwert AGW - Germany [mg/m³] TRGS 900 :

AL AIR LIQUIDE ESPAÑA S.A.

Pº DE LA CASTELLANA,35 28046 MADRID (ESPAÑA)

E-mail: e-business.ALE@airliquide.com

	FICHA DE DATOS DE SEGURIDAD	Página : 3
		Edición revisada no : 2
		Fecha : 2 / 2 / 2009
		Reemplaza : 1 / 6 / 2004
ANH. CARBÓNICO/ DIÓXIDO DE CARBONO/LASAL 2		018A-1

8 CONTROLES DE LA EXPOSICIÓN / PROTECCIÓN PERSONAL /...

5000
 Dióxido de carbono : Arbeitsplatzgrenzwert AGW - Germany [ppm] TRGS 900 : 9100
 Dióxido de carbono : Spitzenbegrenzung / Überschreitungsfaktor AGW - Germany TRGS 900 : 2
 Dióxido de carbono : VLA EC [ppm] : 15000
 Dióxido de carbono : VLA ED [ppm] : 5000

9 PROPIEDADES FÍSICAS Y QUÍMICAS

Estado físico a 20°C : Gas licuado.
 Color : Incoloro.
 Olor : Sin olor que advierta de sus propiedades.
 Masa molecular : 44
 Punto de fusión [°C] : -56,6
 Punto de ebullición [°C] : -78,5 (s)
 Temperatura crítica [°C] : 30
 Presión de vapor, 20°C : 57,3 bar
 Densidad relativa del gas (aire=1) : 1,52
 Densidad relativa del líquido (agua=1) (Condiciones normales T*:15°C ;1 atm) : 0,82
 Solubilidad en agua [mg/l] : 2000
 Rango de inflamabilidad [% de volumen en aire] : No inflamable.
 Otros datos : El vapor es mas pesado que el aire. Puede acumularse en espacios confinados, particularmente al nivel del suelo o en sótanos.

10 ESTABILIDAD Y REACTIVIDAD

Estabilidad y reactividad : Estable en condiciones normales.
 Productos de descomposición peligrosos : Cuando se expone a temperaturas elevadas, puede descomponerse, desprendiendo : Monóxido de carbono a temperaturas superiores a 2000 °C
 Materiales a evitar : Goma de butilo (Poliisobutileno) (IIR). Caucho Nitrilo (NBR; n-Buna). Cloropreno (CR; Clorobutadieno). Vitón (FKM). Agua. Bases fuertes Metales.
 Condiciones a evitar : Humedad.


11 INFORMACIÓN TOXICOLÓGICA

Información sobre Toxicidad : A elevadas concentraciones producen una rápida insuficiencia circulatoria. Los síntomas son dolor de cabeza, náuseas y vómitos, los cuales pueden conducir a la inconsciencia.
 - Dermal : Este gas líquido puede causar quemaduras similares a las causadas por congelación. Enrojecimiento. Congelación.
 - Ocular : Este gas líquido puede causar quemaduras similares a las causadas por congelación. Enrojecimiento. Riesgo de lesiones oculares. Congelación.
 - Ingestión : La ingestión no está considerada como una vía potencial de exposición.

12 INFORMACIÓN ECOLÓGICA

Información sobre efectos ecológicos : Cuando se descarga en grandes cantidades puede contribuir al efecto invernadero.
 Potencial del Calentamiento Global (: 1

AL AIR LIQUIDE ESPAÑA S.A.
 Pº DE LA CASTELLANA ,35 28046 MADRID (ESPAÑA)
 E-mail: e-business.ALE@airliquide.com

	FICHA DE DATOS DE SEGURIDAD	Página : 4
		Edición revisada no : 2
		Fecha : 2 / 2 / 2009
		Reemplaza : 1 / 6 / 2004
ANH. CARBÓNICO/ DIÓXIDO DE CARBONO/LASAL 2		018A-1

12 INFORMACIÓN ECOLÓGICA /...

PCG)

13 CONSIDERACIONES RELATIVAS A LA ELIMINACIÓN

General : No descargar dentro de ningún lugar donde su acumulación pudiera ser peligrosa.
A la atmósfera en un lugar bien ventilado.
Se debe evitar descargar a la atmósfera en grandes cantidades.
Contactar con el suministrador si se necesita orientación.

14 INFORMACIÓN RELATIVA AL TRANSPORTE

No UN : 1013
H.I. n° : 20
ADR/RID
- Nombre propio para el transporte : UN1013 DIOXIDO DE CARBONO (Dióxido de carbono), 2.2, 2A
- ADR Clase : 2
- Código de clasificación ADR/RID : 2 A
- Grupo de embalaje ADR : A
- Etiquetado según ADR : Etiqueta 2.2 : Gas no inflamable, no tóxico.
Otras informaciones para el transporte :
- Asegúrese de que los recipientes están bien sujetos.
Evitar el transporte en los vehículos donde el espacio de la carga no esté separado del compartimiento del conductor.
Asegurar que el conductor está enterado de los riesgos potenciales de la carga y que conoce que hacer en caso de un accidente o de una emergencia.
Antes de transportar las botellas :
- Asegurarse que las válvulas de las botellas están cerradas y no fugan.
- Asegurar una ventilación adecuada.
- Asegurarse que el tapón del acoplamiento de la válvula (cuando exista) está adecuadamente apretado.
- Asegurarse que la caperuza de la válvula o la tulipa, (cuando exista), está adecuadamente apretada.
- Asegurarse de cumplir con la legislación aplicable.

15 INFORMACIÓN REGLAMENTARIA

Clasificación CE : No clasificada como mezcla peligrosa.
No incluido en el anexo I.
Etiquetado CE : No requiere etiquetado CE.
- Símbolo(s) : Ninguno.
- Frase(s) R : Ninguno.
- Frase(s) S : Ninguno.

16 OTRA INFORMACIÓN

Asfixiante a altas concentraciones.
Consérvese el recipiente en lugar bien ventilado.
No respirar los gases.
El contacto con el líquido puede causar quemaduras por frío o congelación.
Asegúrese que se cumplen las normativas nacionales y locales.
El riesgo de asfixia es a menudo despreciado y debe ser recalado durante la formación de los operarios.
La presente Ficha de Datos de Seguridad está establecida de acuerdo con las Directivas Europeas en vigor y se aplica a todos los países que han transpuesto las Directivas en su derecho nacional.
Antes de utilizar el producto en un nuevo proceso o experimento, debe llevarse a cabo un estudio completo de seguridad y de compatibilidad de los materiales.

AL AIR LIQUIDE ESPAÑA S.A.
Pº DE LA CASTELLANA, 35 28046 MADRID (ESPAÑA)
E-mail: e-business.ALE@airliquide.com

E.3 Protocols followed

1. Equipos

- Alargadores
- Balanza
- Baterías: 3A (4u), 9v (1u)
- Botella de CO₂
- Brújula
- Cámara fotográfica
- Carro del CERTEC
- Cinta adhesiva
- Conversor RS-232/USB
- Cronómetro
- Cutter
- Decámetro (2).
- Destornilladores pequeños
- Guantes para abrir la bombona
- Metro
- Pulpos
- Ordenador
- Tijeras
- Sensor de CO₂
- Software para la transferencia y almacenamiento de los datos
- Termopar y datalogger (3)
- Ventiladores (1 por planta)

2. Ficha técnica de la vivienda

Fecha de la prueba		Esquema de la vivienda (numerar las fachadas)			
Dirección					
Orientación de la vivienda (de acuerdo con la numeración del esquema)					
Coordenadas UTM	x:				
	y:				
Presión atmosférica (P_a)					
Fachadas expuestas al exterior	1.	2.	3.	4.	
Año de construcción					
Año de rehabilitación	Tipo de rehabilitación	Puertas Ventanas Otro			
Material de construcción	Hormigón				
	Ladrillo				
	Madera				
	Prefabricado				
	Tapia				
	Otro				
Modo constructivo	Vigas				
	Pared estructural				
	Otro				
Aislamiento	Interno				
	Externo				
	Integrado				
	Ninguno				
	No se sabe				
Altura (incluyendo el techo)					
Altura de cada planta					
Número de plantas					
Sistema de calefacción	Gas				
	Eléctrico				
	Gasoil				
	Madera				
	Bomba de calor				
	Otro				
	Ninguno				

 Área construida

 Área de planta

 Volumen¹

Existencia de conductos:	Dimensiones		Ubicación (interior, exterior)	
chimenea				
cocina				
calefacción				
baño				
otro				
Existencia de cámara sanitaria	si	no		
Aislada de la vivienda	si	no		
Dimensiones				
Existencia de sótano ¹ :	si	no		
Espacio acondicionado	si	no		
Calefacción	si	no		
Existencia de desván ¹ :	si	no		
Espacio acondicionado	si	no		
Calefacción	si	no		
Puertas exteriores	Nº pared ubicación ²	de	Material (M:madera, PVC, A:aluminio, O:otro)	Dimensiones
Ventanas exteriores	Nº pared ubicación ²	de	Material (M:madera, PVC, A:aluminio, O:otro)	Dimensiones

 Notas

¹ Tanto el sótano como el desván y el garaje se deben considerar como parte de la vivienda en la realización de las pruebas siempre que sean un espacio habitable, es decir, adecuado para esto y por tanto haya plena accesibilidad a ellos, estén aislados térmicamente y tengan calefacción. En caso de que no se usen, o se usen solo para guardar cosas, su acceso se deberá sellar con cinta y no se tendrán en cuenta en la prueba ni dentro del cálculo del volumen.

² De acuerdo con la numeración de las paredes en los planos o diagrama de la casa que se realiza en el punto 3 del protocolo de preparación

3. Protocolo de preparación de la vivienda

Al exterior

1. Tomar fotos del lugar.
2. Medir la concentración de CO₂ al exterior en diferentes puntos alrededor de la vivienda. La ubicación debe ir de acuerdo con la numeración de la fachada.

Hora:

Ubicación	C _o	Ubicación	C _o	Ubicación	C _o
⋮	⋮	⋮	⋮	⋮	⋮

Al interior

1. Conseguir un plano de la vivienda o hacer un diagrama de la misma.
 - 1.1. Numerar las paredes exteriores.
 - 1.2. Escoger el lugar a utilizar como shelter, numérelo (). Una habitación interior ó con el mínimo de aberturas al exterior, que no tenga más de una puerta de acceso y con una superficie mínima de 1-1.5 m² por persona.
2. Determinar el volumen de la vivienda y del shelter, a partir de medidas y de los planos de la casa. No incluir dentro del volumen aquellos espacios que no estén acondicionados para ser habitables, como pueden ser el desván, el sótano o el garaje.

V =

V_s =

3. Cerrar el acceso a los espacios que no se tendrán en cuenta dentro del volumen para la prueba (deshván, sótano, garaje).
4. Apagar todos los sistemas mecánicos de ventilación.
5. Escoja un lugar representativo para medir la temperatura en cada planta.

Planta	Planta	Planta	Planta	Planta

6. Determine los lugares para realizar la prueba de uniformidad de concentraciones. Cómo mínimo se debe muestrear en 3 ubicaciones por cada planta a una altura media. Numérelas:

Planta	Planta	Planta	Planta	Planta

7. Determine el lugar para tomar la concentración en el shelter.
8. Determine el lugar para tomar la concentración durante la prueba. La concentración se debe tomar a media altura. Numérela:
9. Determine el lugar (o los lugares) para llevar a cabo la descarga del CO₂. Un lugar donde el CO₂ se pueda dispersar fácilmente por toda la vivienda.

Planta	Planta	Planta	Planta	Planta

10. Ubicar los ventiladores en las posiciones adecuadas para inducir un buen mezclado del aire teniendo en cuenta el punto de descarga del CO₂.
11. Encender los ventiladores y asegurarse de su correcto funcionamiento.
12. Cerrar todas las puertas y ventanas que tienen contacto con el exterior y demás aberturas intencionales por donde pueda pasar aire exterior como la chimenea.
13. Abrir todas las puertas y ventanas interiores de la casa para permitir un ambiente homogéneo.
14. Realizar un muestreo de concentraciones y temperaturas al interior de la vivienda y en el shelter para obtener los valores de concentración de CO₂ y temperatura anteriores a la prueba. Hacer como mínimo 3 muestreos por cada planta, utilizando la misma numeración de los lugares seleccionados para la prueba de homogeneidad.

Hora:

Ubicación	C _i	T _i	Ubicación	C _i	T _i
⋮	⋮	⋮	⋮	⋮	⋮
Promedio					

Presión absoluta de la vivienda (Pa):

4. Prueba en el shelter

1. Iniciar la adquisición de temperaturas exterior e interior.
2. Tome la temperatura y la concentración de CO₂ en el punto medio del shelter (promedio de 30s).

T _s	
----------------	--

C _s	
----------------	--

3. Determine el volumen y la masa de CO₂ a inyectar. Para este cálculo se usará una concentración inicial de referencia (C_{ref}) de 1500 ppm.

$$V_{CO_2} = (C_{ref} - C_s) \cdot 10^{-6} \cdot V_s$$

$$V_{CO_2} =$$

$$m_{CO_2} = \frac{P_a \cdot V_{CO_2} \cdot 44}{T_s' \cdot 8.314}, (g)$$

$$m_{CO_2} =$$

donde: P_a esta en Pa, V_s y V_{CO₂} en m³, T_i' en K, C_{ref} y C_s (ppm)

4. Ubique la balanza y la botella de CO₂ dentro del shelter, al igual que un ventilador y entre.
5. Cierre la puerta y selle con cinta adhesiva las ventanas y/o aberturas existentes.
6. Inyección del gas. Dependiendo del volumen de CO₂ que debe inyectarse a T_i' y P_a, que equivale a una masa de CO₂ (m_{CO₂}), se controla la descarga del CO₂ por peso, utilizando una balanza.

- 6.1. Colocar la botella de CO₂ sobre la balanza y anotar la masa inicial m₁

$$m_1 =$$

- 6.2. Calcular la masa final teórica de la botella.

$$m_2 = m_1 - m_{CO_2} =$$

- 6.3. Manteniendo la botella sobre la balanza, abrir la válvula de la botella y dejar salir el gas hasta alcanzar m₂.

- 6.4. Anotar la masa final de la botella.

$$m_2 =$$

7. Realizar la prueba de uniformidad de concentraciones

7.1. Medir las concentraciones en la parte superior, intermedia e inferior del shelter.

7.2. Calcular la concentración promedio del shelter (C_s'). Si las concentraciones medidas difieren en menos de 10% de C_s' , se satisface el criterio de uniformidad de concentraciones y la prueba puede empezar. En caso contrario, colocar el ventilador en funcionamiento, esperar 5 min y volver a realizar las mediciones de concentración. Si aún no se consigue la uniformidad, iniciar la prueba y reportar esto en los resultados. Calcular solamente el porcentaje de error.

Primera prueba.

Hora: $C_s' =$ $S_c =$ $V_{meas} =$

Ubicación	C	% error	v_c	Ubicación	C	% error	v_c
Superior				Intermedio			
Inferior							

Segunda prueba.

Hora: $C_s' =$ $S_c =$ $V_{meas} =$

Ubicación	C	% error	v_c	Ubicación	C	% error	v_c
Superior				Intermedio			
Inferior							

S_c desviación estándar de las concentraciones

$v_c = S_c / C$ coeficiente de variación

V_{meas} error de precisión de las mediciones, el mayor de los v_c

8. Ubicar el sensor de CO_2 en el lugar determinado para medir la concentración. Tome el tiempo actual como el tiempo de inicio de la prueba e inicie la prueba.

Hora:

9. Inicie el sistema de adquisición de datos de concentración y temperatura en el shelter cada 5 segundos.

10. Salga y cierre la puerta de acceso al shelter, séllela con cinta por la parte exterior.

11. Espere a que la concentración no cambie mas con el tiempo, ó como mínimo haya pasado hora y media de prueba.

12. Reporte cualquier alteración durante la prueba. Es decir, cambio de estado de las aberturas, como puertas, ventanas; entrada y salida de personas, etc.

Hora	Evento
⋮	⋮

13. Para terminar: tome la hora, abra la puerta, entre y ciérrela nuevamente.

Hora:

14. Realice la prueba de uniformidad de concentraciones.

14.1. Medir las concentraciones en cada punto de muestreo seleccionado.

14.2. Calcular la concentración promedio del shelter (C_s'). Si las concentraciones medidas difieren en menos de 10% de C_s' , se satisface el criterio de uniformidad de concentraciones y los resultados pueden reportarse con una incertidumbre inferior al 10%.

Hora:

$C_s' =$

$S_c =$

$V_{\text{meas}} =$

Ubicación	C	% error	v_c	Ubicación	C	% error	v_c
Superior				Intermedio			
Inferior							

15. Realizar un muestreo de concentraciones y temperaturas al interior de la vivienda para obtener los valores de concentración de CO_2 y temperatura posteriores a la prueba. Utilizar la misma ubicación que durante la preparación de la vivienda.

Hora:

Ubicación	C_i	T_i	Ubicación	C_i	T_i
⋮	⋮	⋮	⋮	⋮	⋮
Promedio					

16. Abra la puerta

17. Inicie la prueba en la vivienda.

5. Prueba en la vivienda

1. Iniciar la adquisición de temperaturas exterior e interior.
2. Realizar un muestreo de concentraciones al exterior si no se ha hecho antes.

Hora:

Ubicación	C _o	Ubicación	C _o	Ubicación	C _o
⋮	⋮	⋮	⋮	⋮	⋮

3. Realizar un muestreo de concentraciones y temperaturas al interior para obtener los valores anteriores a la prueba. Asegurar como mínimo tres muestreos por cada planta, utilizando la misma numeración de los lugares seleccionados para la prueba de homogeneidad.

Hora:

Ubicación	C _i	T _i	Ubicación	C _i	T _i
⋮	⋮	⋮	⋮	⋮	⋮
Promedio					

4. Determine el volumen de CO₂ a inyectar. Para este cálculo se usará una concentración inicial de referencia (C_{ref}) de 1500 ppm.

$$V_{CO_2} = (C_{ref} - C_i) \cdot 10^{-6} \cdot V$$

$$m_{CO_2} = \frac{P_a \cdot V_{CO_2} \cdot 44}{T_i' \cdot 8.314}, (g)$$

donde: P_a esta en Pa, V y V_{CO2} en m³, T_i' en K, C_{ref} y C_i en ppm.

5. Descarga por habitación

Ubicación	Masa a descargar	Masa descargada
⋮	⋮	⋮

6. Inyección del gas. Dependiendo del volumen de CO_2 que debe inyectarse a T_i' y P_a , que equivale a una masa de CO_2 (m_{CO_2}), se controla la descarga del CO_2 por peso, utilizando una balanza.

6.1. Colocar la botella de CO_2 sobre la balanza, anotar la masa inicial m_1 y tarar

m_1 :

6.2. Montar la botella sobre el carro, abrir la válvula y dejar salir el gas en cada ubicación. Empezar por la última planta e ir descendiendo.

6.3. Anotar la masa descargada en cada ubicación en la tabla anterior

6.4. Anotar la masa final de la botella.

$m_2 =$

7. Esperar 15 min con los ventiladores en marcha para homogenizar el CO_2 descargado.

8. Realizar la prueba de uniformidad de concentraciones

8.1. Medir las concentraciones en cada punto de muestreo seleccionado.

8.2. Calcular la concentración promedio de la vivienda (C_i'). Si las concentraciones medidas difieren en menos de 10% de C_i' , se satisface el criterio de uniformidad de concentraciones y la prueba puede empezar. En caso contrario, colocar los ventiladores nuevamente en funcionamiento, esperar 15 min y volver a realizar las mediciones de concentración. Si aún no se consigue la uniformidad, iniciar la prueba y reportar esto en los resultados. Calcular solamente el porcentaje de error.

Hora: $C_i' =$ $S_c =$ $V_{\text{meas}} =$

Ubicación	Prueba 1		Prueba 2		Prueba 3		V_c
	C	% error	C	% error	C	% error	
⋮	⋮	⋮	⋮	⋮	⋮	⋮	⋮

S_c desviación estándar de las concentraciones

$V_c = S_c / C$ coeficiente de variación

V_{meas} error de precisión de las mediciones, el mayor de los V_c

9. Ubicar los termopares en los lugares seleccionados para medir la temperatura por planta e iniciar el registro de los datos cada 5 segundos.

10. Ubicar el sensor de CO_2 en el lugar determinado para medir la concentración en la vivienda. Tome el tiempo actual como el tiempo de inicio de la prueba e inicie la prueba.

Hora:

11. Inicie el sistema de adquisición de datos de concentración cada 5 segundos.
12. Espere a que la concentración no cambie más con el tiempo, ó como mínimo hayan pasado dos horas de prueba.
13. Reporte cualquier alteración durante la prueba. Es decir, cambio de estado de las aberturas, como puertas, ventanas; entrada y salida de personas, etc.

Hora	Evento
⋮	⋮

14. Terminada la prueba, realizar nuevamente el test de uniformidad de concentraciones en la vivienda, para asegurar la homogeneidad durante la prueba.

14.1. Medir las concentraciones en cada punto de muestreo seleccionado.

- 14.2. Calcular la concentración promedio de la vivienda (C_i'). Si las concentraciones medidas difieren en menos de 10% de C_i' , se satisface el criterio de uniformidad de concentraciones y los resultados pueden reportarse con una incertidumbre del 10%.

Hora: $C_i' =$ $S_c =$ $V_{meas} =$

Ubicación	C	% error	v_c	Ubicación	C	% error	v_c
⋮	⋮	⋮	⋮	⋮	⋮	⋮	⋮

15. Abrir las ventanas y puertas que conectan al exterior y ventilar la casa.

16. Realizar un muestreo de concentraciones al exterior.

Hora:

Ubicación	C_o	Ubicación	C_o	Ubicación	C_o
⋮	⋮	⋮	⋮	⋮	⋮

6. Puesta en marcha de la sonda de CO₂, adquisición y transferencia de datos

1. Asegurarse de que el instrumento multifunción tenga suficiente batería..
2. Conectar la sonda IAQ al instrumento multifunción.
3. Poner en marcha el instrumento.
4. Configuración
 - 4.1. Mantener presionada la tecla del menú (central) hasta que se visualice config.
 - 4.2. Seleccionar el perfil a configurar utilizando las flechas y luego aceptar (tecla que se corresponde con el texto de la parte inferior del visualizador). Entre los perfiles se encuentran las unidades, la fecha y hora, la desconexión automática después de 10 min (solo en caso de que no se estén guardando datos), el reset (se resetean todas las configuraciones a excepción de la fecha y la hora) y el idioma; para su configuración utilizar las flechas.

Registro de lecturas por puntos y promedio

Útil para la prueba de homogeneidad de concentraciones

1. Ir al menú
2. Con las flechas buscar seleccionar la opción de promedio
3. Seleccionar multipunto y aceptar
4. Para cada nuevo punto presionar la tecla seleccionar
5. Cuando se hayan tomado todos los puntos (esperar mínimo 30s en cada punto) presionar la tecla finalizar y leer el promedio.

Programación para el registro automático de lecturas.

1. Ir al menú
2. Con las flechas seleccionar la opción situación, la situación es la carpeta donde se guardarán los datos. Así, para el shelter se escogerá la situación shelter y para la vivienda la situación casa.
3. Seleccionada la situación, buscar dentro del menú la opción de Prog. Med.
4. Seleccionar auto
5. Seleccionar el intervalo de medición

6. Seleccionar el número de mediciones. Poner 9999 (presionar la tecla $\frac{\square}{\square}$ para cambiar de unidades a miles). De esta forma, la medición se realiza hasta llenar la memoria o detenerla manualmente.
7. Para iniciar la medición, presionar la tecla inicio.
8. Para finalizar, presionar la tecla final.

Transferencia de datos al ordenador

1. Conectar el instrumento al ordenador (puerto USB)
2. Ejecutar el programa Comfort Software. Inicio/Todos los programas/ Cientific/ Testo/
3. Hacer click sobre el instrumento. Se muestran todas las situaciones.
4. Seleccionar la situación a copiar. Con el click derecho seleccionar la opción de copiar.
5. Pegar los datos en una hoja de Excel.
6. Para borrar la memoria, hacer click derecho sobre el instrumento e ir a la opción control de equipo.
7. Ir a programas de medición
8. Seleccionar borrar memoria. Se borran los registros pero no los nombres de las situaciones.
9. Desconectar el equipo, para ello hacer click derecho y seleccionar cerrar. Luego, retirar el software con seguridad.

7. Adquisición de temperaturas

1. Conectar el termopar al datalogger.
2. Encender el datalogger, el número que aparece en la pantalla indica el número de registros que se pueden guardar. Asegurarse que hayan 100 como mínimo.
3. Ajuste de la hora
 - 3.1. Apague el datalogger y vuelva a encenderlo manteniendo presionada la tecla "T1-T2"
 - 3.2. Presione la tecla "Hold"
 - 3.3. Presione la tecla "REC" o "°C/°F" para corregir hacia arriba o hacia abajo el número mostrado. El orden de ajuste es: año/mes/día/hora/minuto/segundo
 - 3.4. Presione la tecla "Hold" para grabar el ajuste de la hora.
4. Ajuste del intervalo de grabación
 - 4.1. Apague el datalogger y vuelva a encenderlo manteniendo presionada la tecla "T1-T2"
 - 4.2. Presione la tecla "MAXMIN"
 - 4.3. Presione la tecla "REC" o "°C/°F" para corregir hacia arriba o hacia abajo el número mostrado.
 - 4.4. Presione la tecla "MAXMIN" para seleccionar el valor correspondiente (5 min) y vuelva a presionar la tecla "MAXMIN" para grabar el valor en el aparato. Si desea interrumpir el proceso, apague el datalogger.
5. Cuando se vaya a iniciar la prueba, presionar la tecla "REC" para iniciar el almacenamiento de los datos.
6. Para terminar el almacenamiento de los datos presionar la tecla "REC" nuevamente.

Descarga de los datos

1. Conectar el datalogger a un PC a través del cable de comunicaciones RS-232 del equipo y un conversor RS-232/USB.
2. Encender el datalogger.
3. Abrir el programa de descarga de datos: inicio/todos los programas/SE 309/ SE 309. Está instalado en las laptops.

4. Descargar los datos: Data logger/ Load. Aparece una ventana que dice: Data retriving process.
5. En el costado izquierdo del programa se verá el data set .Se crea un data set con los valores que se guarden desde el momento de iniciar la grabación hasta que se termina. Seleccionar el data set e iniciar el proceso de grabación: File/Save
6. El data set se almacena como un archivo de texto con el nombre y ubicación designados.
7. Aparece una nueva ventana que permite seleccionar cuantos datos se desean, por defecto se guardan todas.
8. Para borrar los datos luego de la transferencia, presionar la tecla "REC" y el botón verde simultáneamente durante el tiempo que dure el proceso. Finalmente aparecen las letras CLR en la pantalla.

Annex F. Experimental data analysis

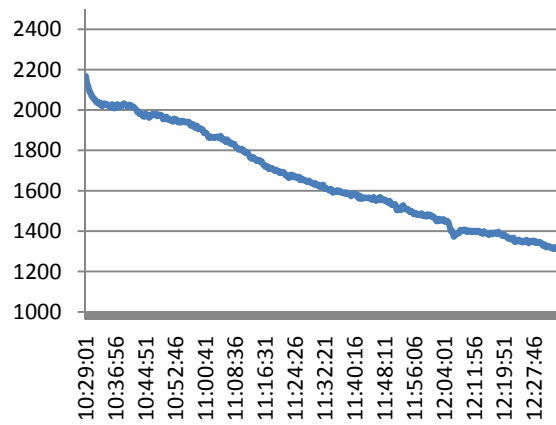
This Annex shows the experimental data for each dwelling, which comprises data related to dwelling features like location, year of construction, nearest meteorological station, etc; and data concerning the decay of CO₂ concentration in both the shelter and the dwelling.

Dwelling 1

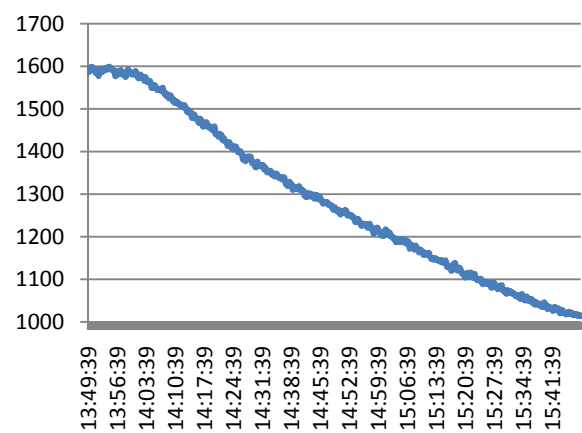
Material de construcción	Termoarcilla
Año de construcción	1994
Material puertas y ventanas	Aluminio, excepto la puerta de entrada (M)
Área total	72.27
No. plantas	2
Caras expuestas al viento	2
Estación Meteorológica próxima	Vinyols i els arcs (2m de altura)
Volumen shelter	9 m ³
Chimenea	Si

Summer

Shelter



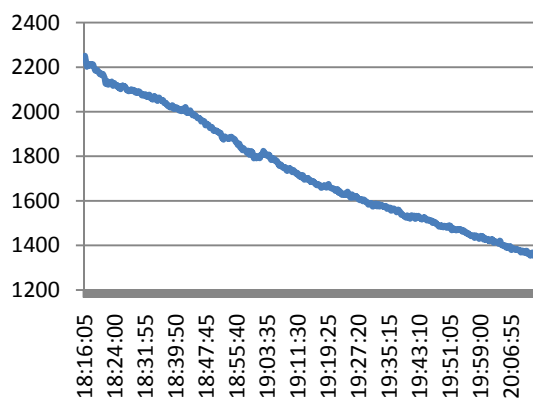
Dwelling

**Dwelling 2**

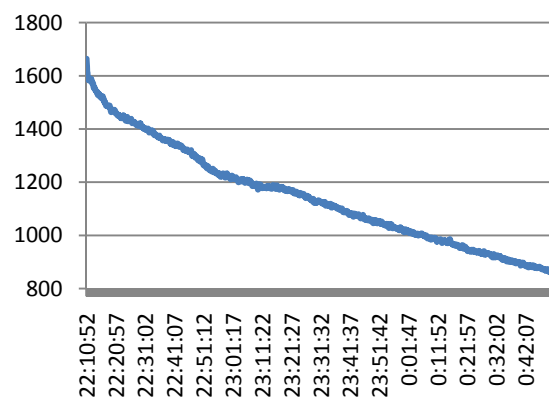
Material de construcción	Ladrillo
Año de construcción	reformada 2009
Material puertas y ventanas	PVC imitación madera, doble vidrio.
Área total	87
No. plantas	4
Caras expuestas al viento	1
Estación Meteorológica próxima	34-L'Ametlla de mar (2m de altura)
Volumen shelter	10.7 m ³
Chimenea	No

Summer

Shelter

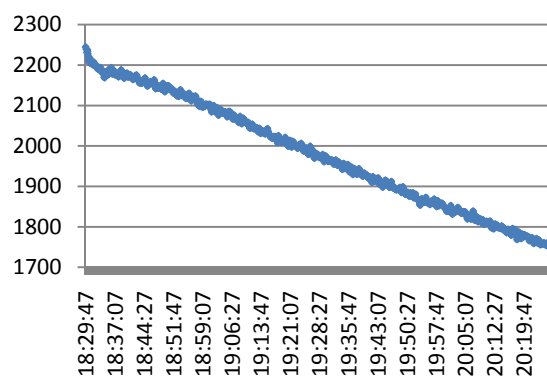


Dwelling

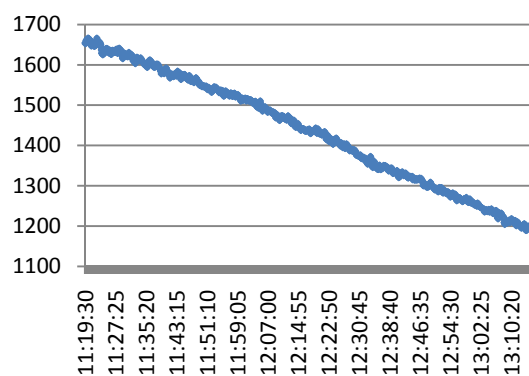


Winter

Shelter



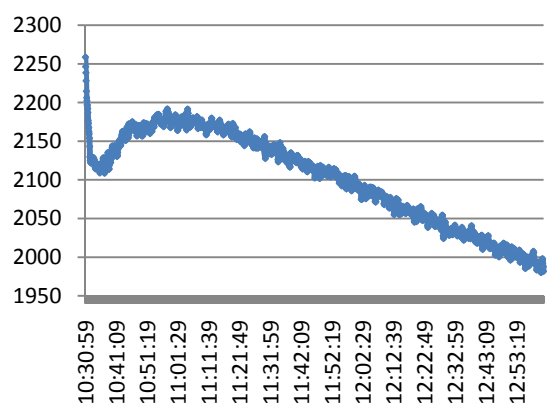
Dwelling

**Dwelling 3**

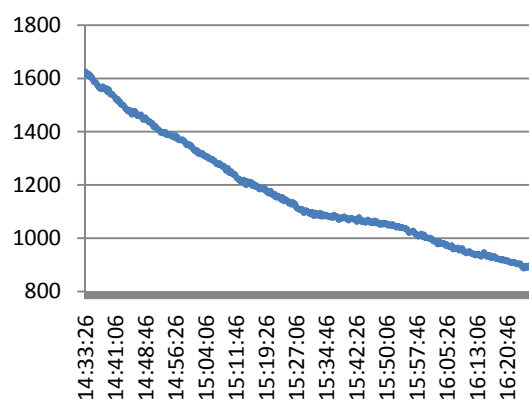
Material de construcción	Piedra
Año de construcción	1945
Material puertas y ventanas	Madera
Área estudiada (P0 y P1)	83
No. plantas	4+sótano. Sólo se analizaron la P0 y la P1. Las demás plantas no estaban completamente terminadas ni acondicionadas y solo se comunicaban por la puerta de las escaleras, por lo que se aislaron de la prueba cerrando y sellando la puerta.
Caras expuestas al viento	2
Estación Meteorológica próxima	34-L'Ametlla de mar (2m de altura)
Volumen shelter	7.8 m ³
Chimenea	Si

Summer

Shelter



Dwelling

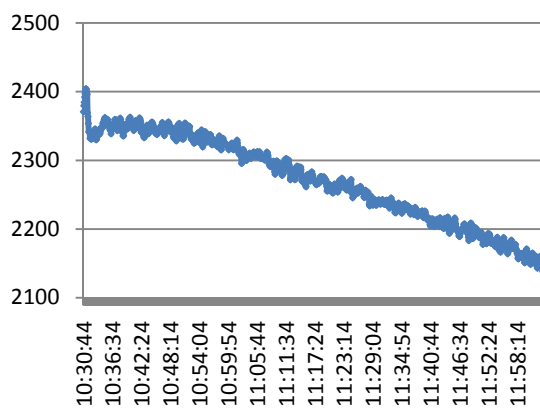


Dwelling 4

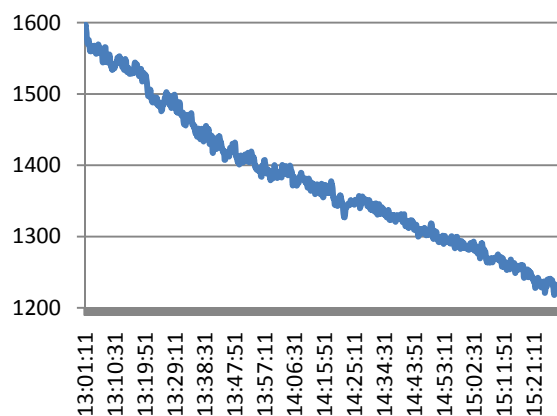
Material de construcción	Ladrillo, exterior en piedra
Año de construcción	2003
Material puertas y ventanas	Madera, doble vidrio.
Área total	112.6 m ² sin garaje (no se incluyó)
No. plantas	1 sobre rasante +desván. Garaje en la planta -1 (aislado completamente de la casa).
Caras expuestas al viento	4
Estación Meteorológica próxima	111-Nuria (10 m altura)
Volumen shelter	8 m ³
Chimenea	Si

Summer

Shelter

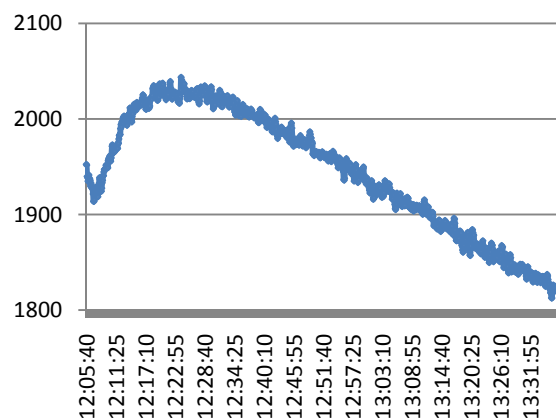


Dwelling

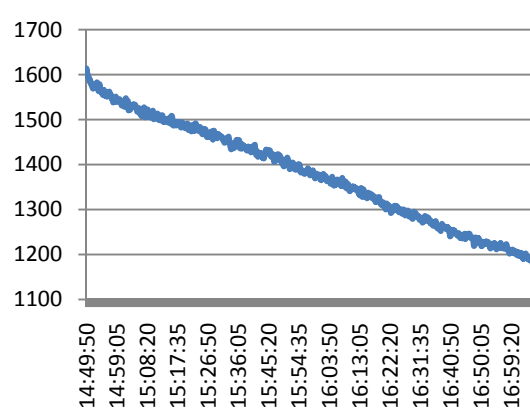


Winter

Shelter



Dwelling

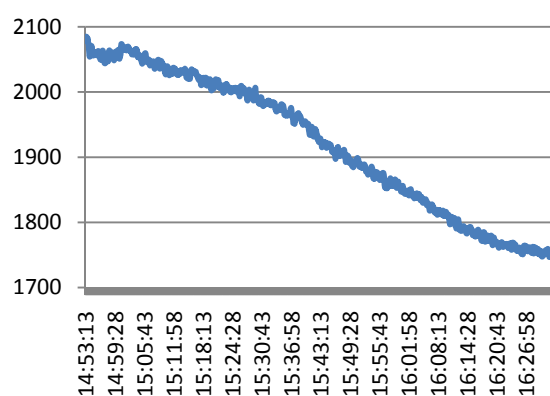


Dwelling 5

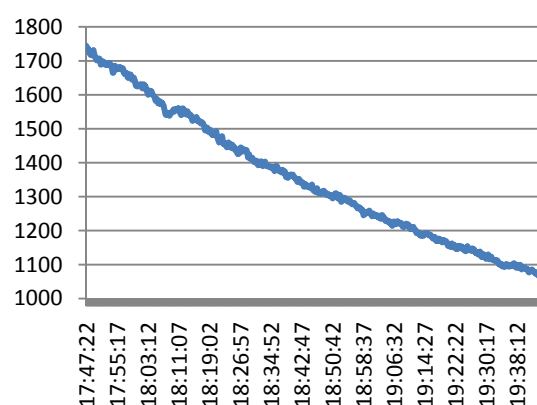
Material de construcción	Ladrillo
Año de construcción	1958
Material puertas y ventanas	Madera.
Área total	77 m ² sin garaje ni desván (no se incluyeron)
No. plantas	2 sobre rasante +desván. Garaje en la planta 0 sin acondicionar, se comunica con la casa por una puerta en la P0 que da a las escaleras. El desván se encuentra en la terraza y está completamente aislado de la casa por lo que no se tuvo en cuenta.
Caras expuestas al viento	3
Estación Meteorológica próxima	120-Lleida-Bordeta 2m
Volumen shelter	8.9 m ³
Chimenea	No

Summer

Shelter

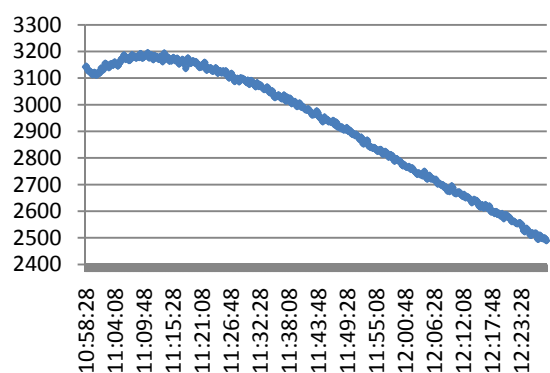


Dwelling

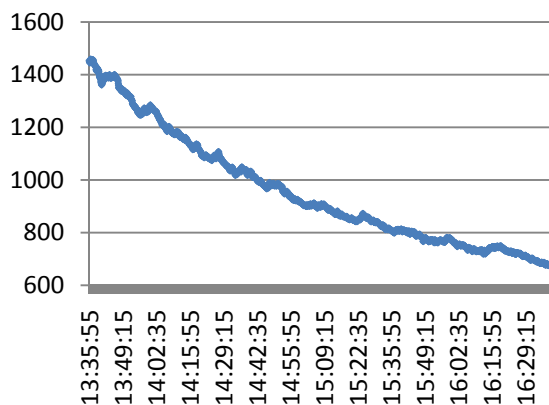


Winter

Shelter



Dwelling

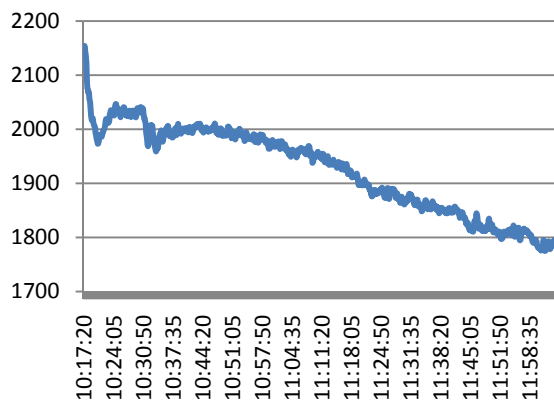


Dwelling 6

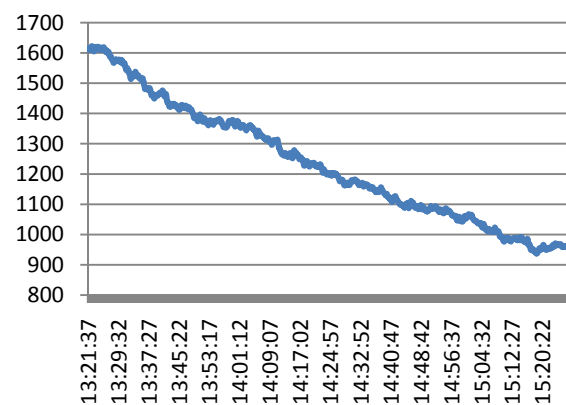
Material de construcción	Ladrillo
Año de construcción	1977
Material puertas y ventanas	Aluminio
Área total	147.7 m ² sin garaje (es independiente de la casa)
No. plantas	2 sobre rasante. Garaje en la planta -1 independiente de la casa.
Caras expuestas al viento	4
Estación Meteorológica próxima	Tagamanent Parc Natural del Montseny
Volumen shelter	9 m ³
Chimenea	Si

Summer

Shelter

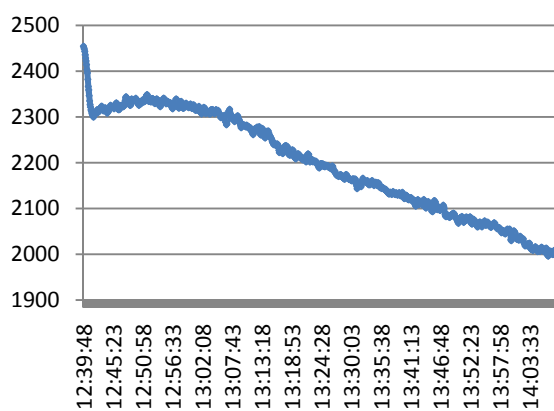


Dwelling

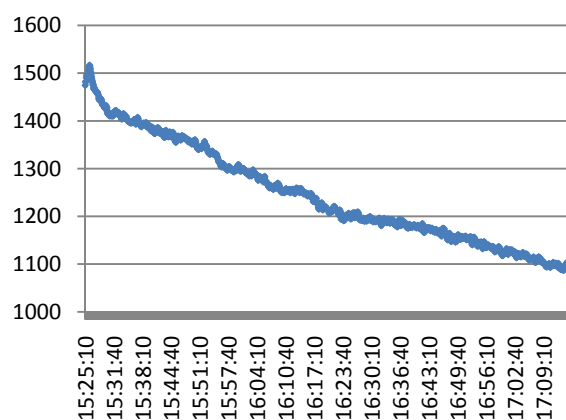


Winter

Shelter



Dwelling

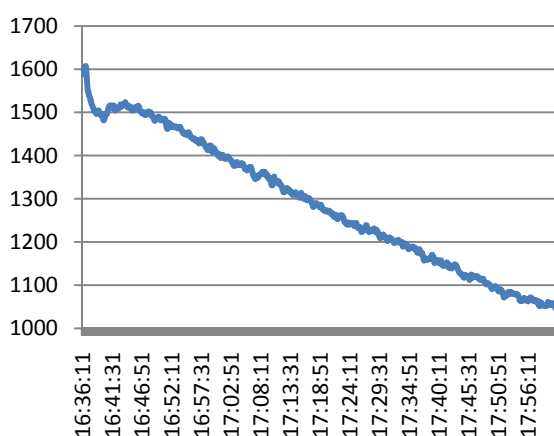


Dwelling 7

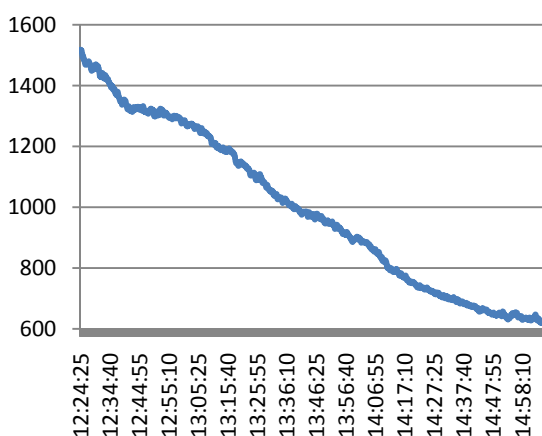
Material de construcción	Ladrillo
Año de construcción	2003
Material puertas y ventanas	Aluminio
Área total	184.7 m ² sin garaje (es independiente de la casa)
No. plantas	4 sobre rasante. Garaje y almacén en la P 0 comunicados con la casa por puertas y pasillo que comunica el exterior con las escaleras. Para la prueba se cerraron las puertas que comunicaban el almacén con las escaleras y el pasillo de entrada con la casa.
Caras expuestas al viento	3
Estación Meteorológica próxima	Tagamanent Parc Natural del Montseny (2m)
Volumen shelter	9.6 m ³
Chimenea	Si

Summer

Shelter

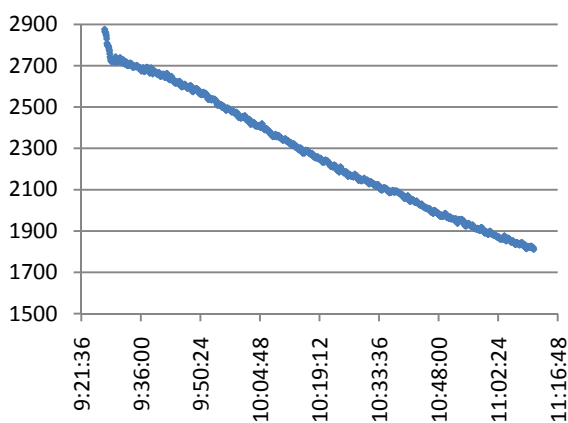


Dwelling

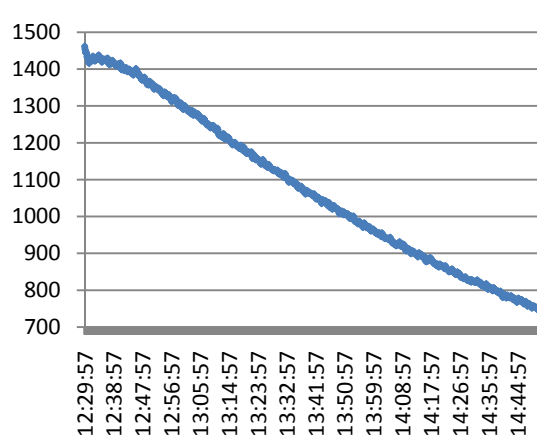


Winter

Shelter



Dwelling

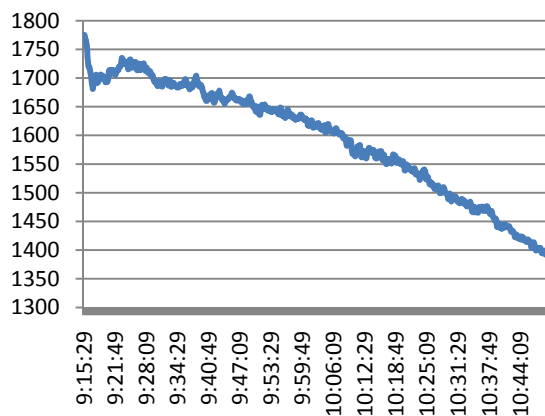


Dwelling 8

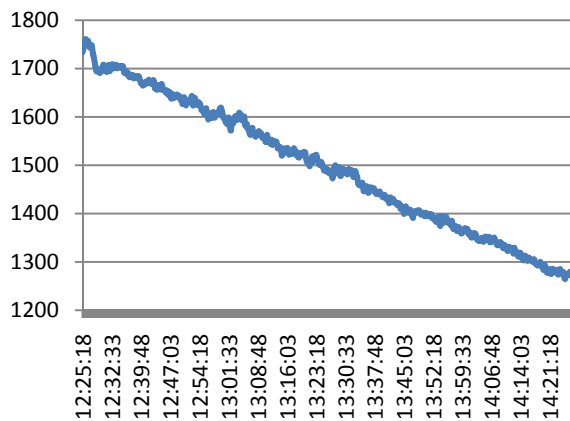
Material de construcción	Ladrillo
Año de construcción	1950
Material puertas y ventanas	Madera y PVC
Área total	172 m ²
No. plantas	2
Caras expuestas al viento	4
Estación Meteorológica próxima	Barcelona - Observatori Fabra (10m)
Volumen shelter	12.8
Chimenea	No

Summer

Shelter



Dwelling

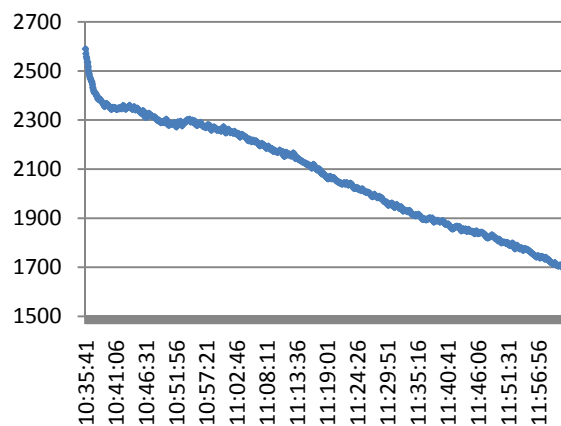


Dwelling 9

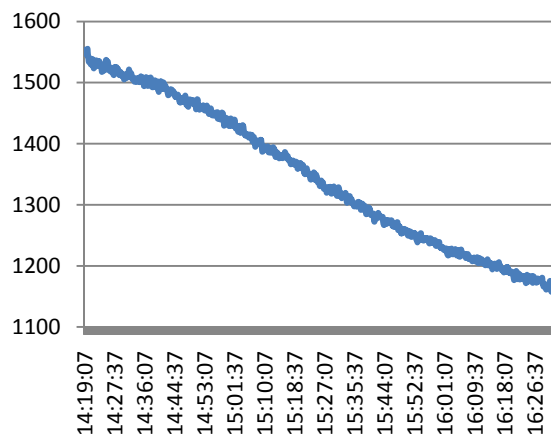
Material de construcción	Hormigón
Año de construcción	2004 (reformada totalmente)
Material puertas y ventanas	PVC principalmente. Algunas puertas de Al
Área total	172.3
No. plantas	4
Caras expuestas al viento	2
Uniformidad de concentraciones <10%	No
Estación Meteorológica próxima	Barcelona Raval (10m)
Volumen shelter	4.7 m ³
Chimenea	No

Summer

Shelter

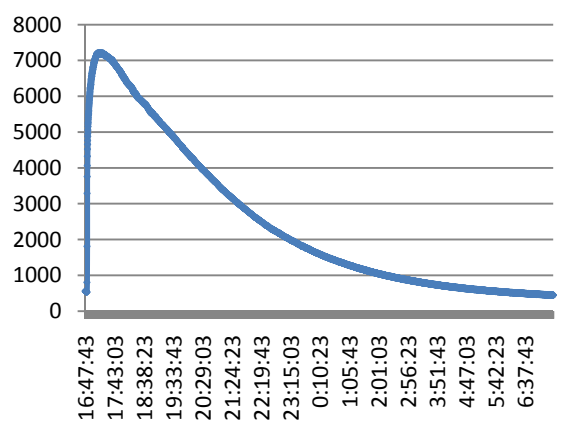


Dwelling

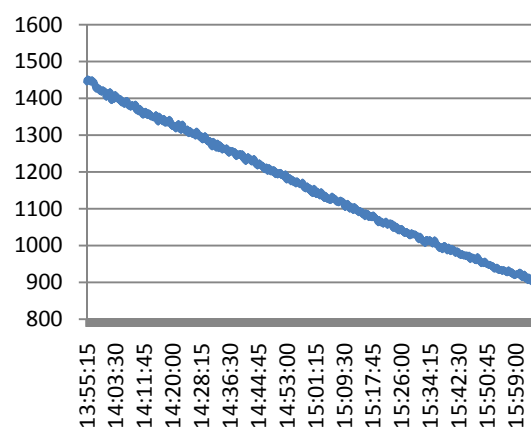


Winter

Shelter



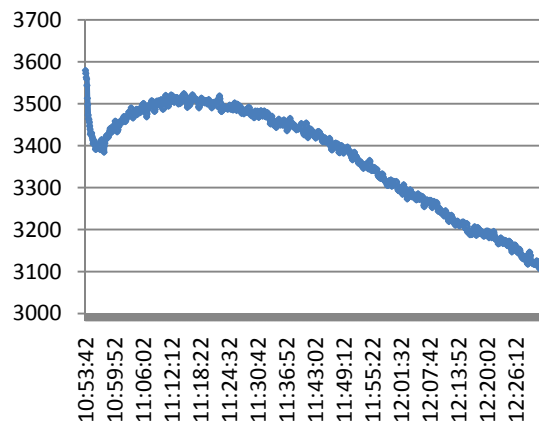
Dwelling

**Dwelling 10**

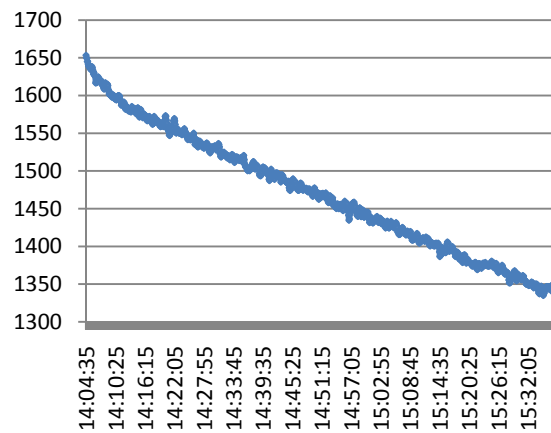
Material de construcción	Hormigón
Año de construcción	1989
Material puertas y ventanas	PVC principalmente. Algunas puertas de Al
Área total	175.96
No. plantas	3
Caras expuestas al viento	4
Estación Meteorológica próxima	Montserrat (11 km), 6m de altura
Volumen shelter	5.8
Chimenea	Si

Summer

Shelter

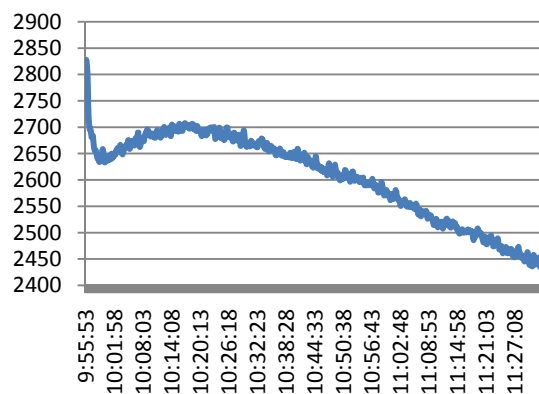


Dwelling

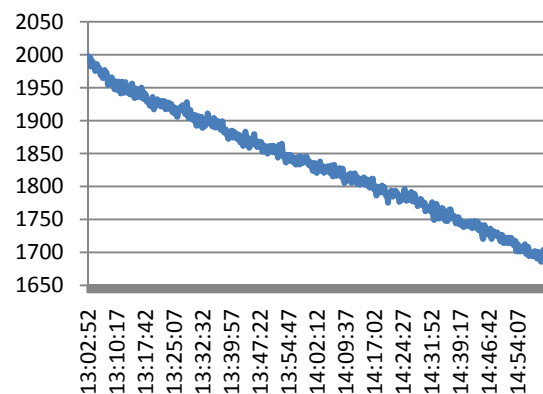


Winter

Shelter



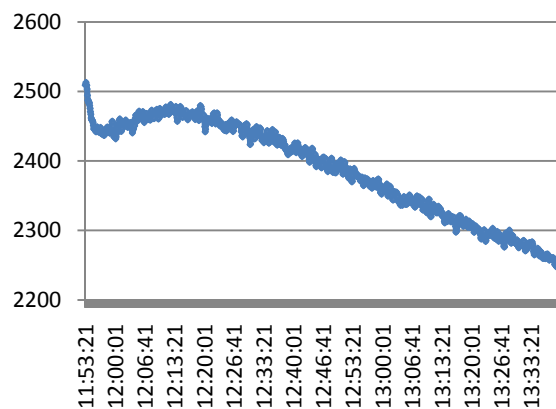
Dwelling

**Dwelling 11**

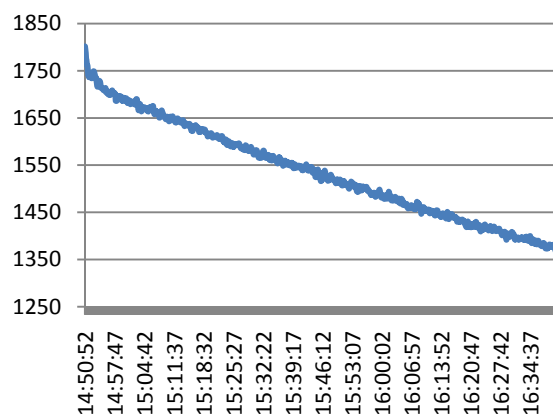
Material de construcción	Hormigón
Año de construcción	1995
Material puertas y ventanas	Madera
Área total	84.5
No. plantas	2 sobre rasante
Caras expuestas al viento	3
Estación Meteorológica próxima	Torredembarra (2.5 km), a 10 m
Volumen shelter	12.3 m ³
Chimenea	Si

Summer

Shelter

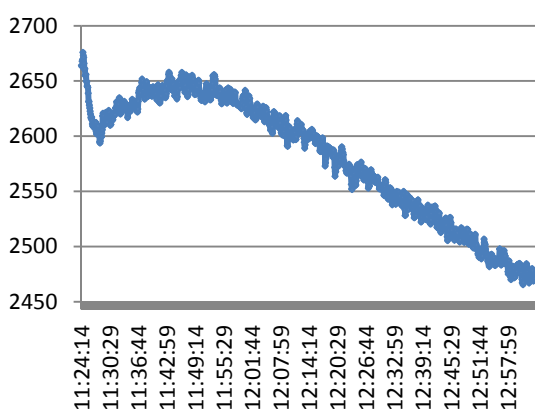


Dwelling

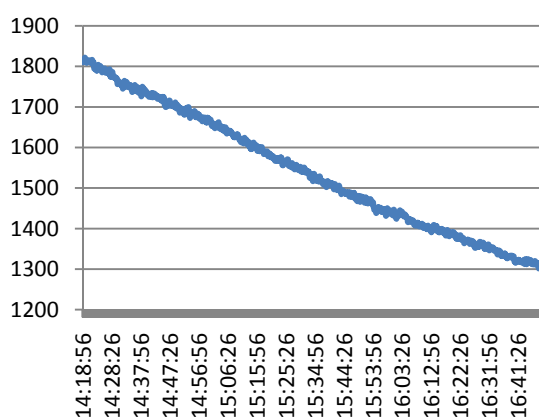


Winter

Shelter



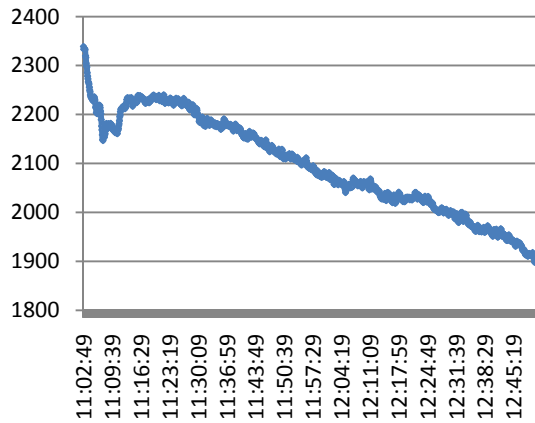
Dwelling

**Dwelling 12**

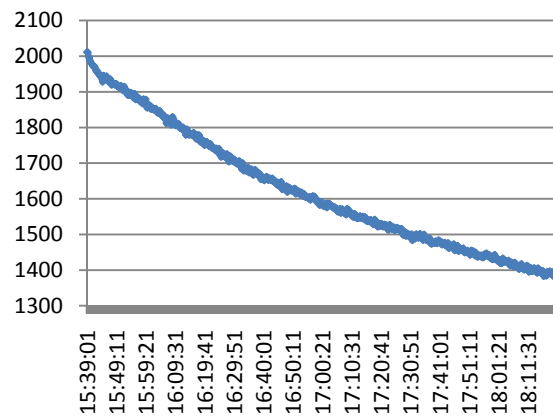
Material de construcción	Hormigón, ladrillo
Año de construcción	1960, reformada 1989
Material puertas y ventanas	Aluminio y vidrio. La mayoría de las ventanas son de doble vidrio. La puerta de la calle es de madera
Área total	172.61 m ² (con garaje) 137 m ² (sin garaje)
No. plantas	2 sobre rasante
Caras expuestas al viento	2
Estación Meteorológica próxima	Barcelona-Raval (10 m)
Volumen shelter	10.6 m ³
Chimenea	No

Summer

Shelter

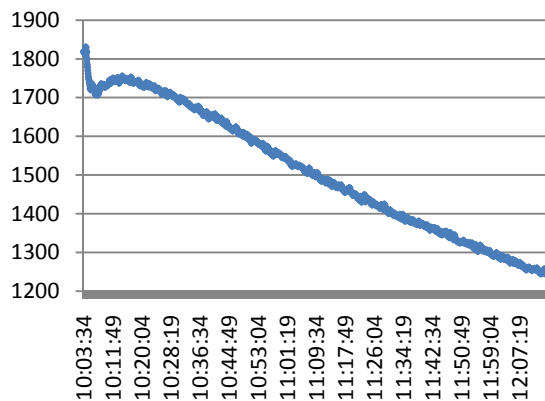


Dwelling

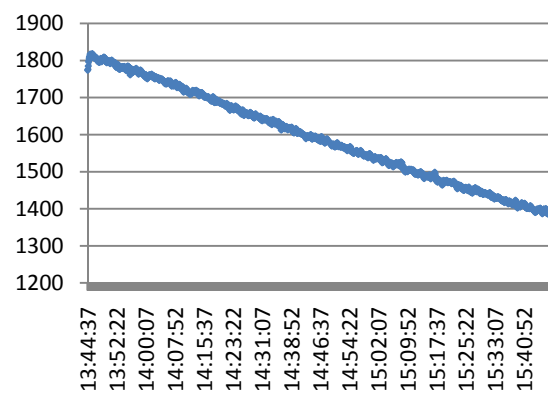


Winter

Shelter



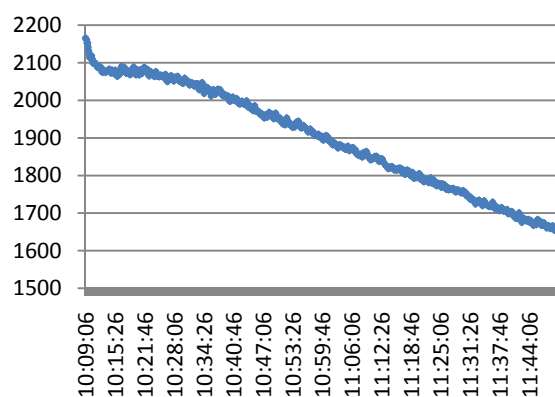
Dwelling

***Dwelling 13***

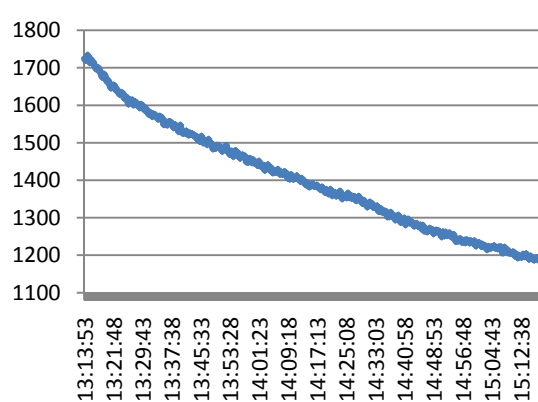
Material de construcción	Hormigón, ladrillo
Año de construcción	1929- Por el 65 se reformo y se unieron las 2 casas
Material puertas y ventanas	Aluminio y vidrio. La mayoría de las ventanas son de doble vidrio. La puerta de la calle es de madera
Área total	74 m ²
No. plantas	2 sobre rasante
Caras expuestas al viento	2
Estación Meteorológica próxima	Barcelona-Raval (10 m)
Volumen shelter	18.8 m ³
Chimenea	No

Summer

Shelter

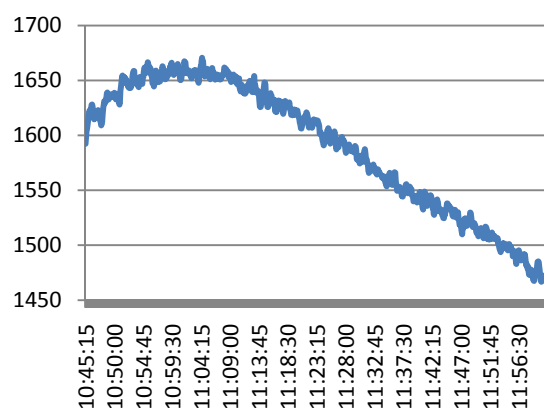


Dwelling

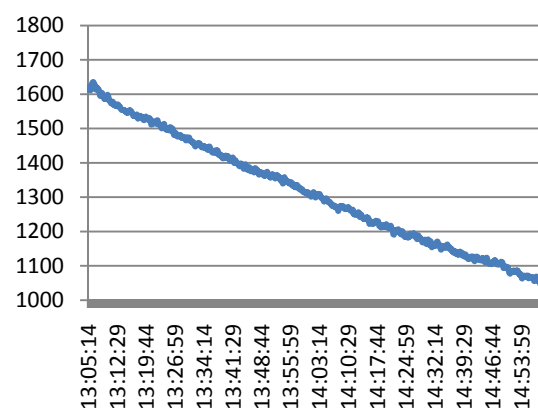


Winter

Shelter



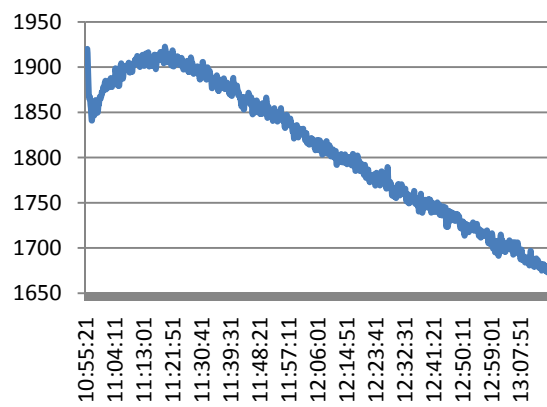
Dwelling

**Dwelling 14**

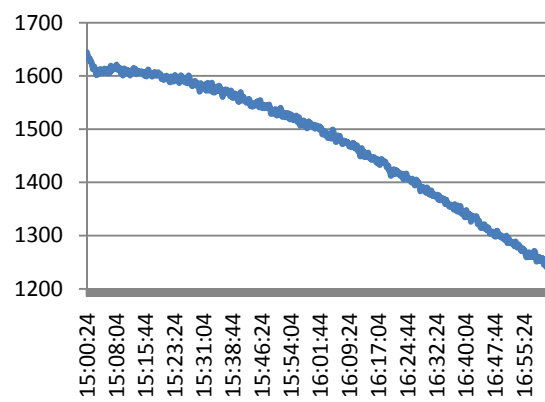
Material de construcción	Hormigón, ladrillo
Año de construcción	1920, remodelación 1990
Material puertas y ventanas	Aluminio y vidrio. La mayoría de las ventanas son de doble vidrio. La puerta de la calle, la del garaje y la de comunicación de la casa con el garaje son de metal.
Área total	142.3m ² (usados para la prueba), en total 210.81 m ²
No. plantas	4 sobre rasante. No se tuvo en cuenta el garaje ni la planta 0, ya que se encuentran completamente aislados del resto de la casa.
Caras expuestas al viento	2
Estación Meteorológica próxima	Barcelona-Raval (10 m)
Volumen shelter	7.9 m ³
Chimenea	Si

Summer

Shelter

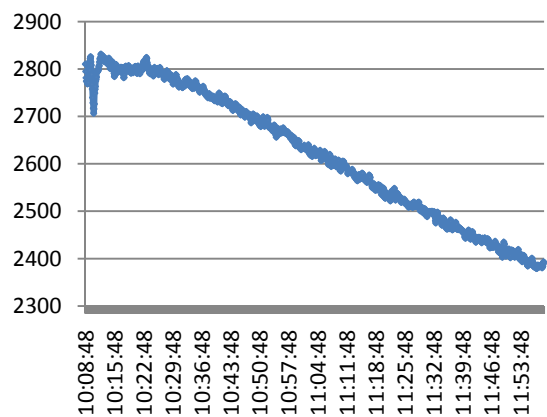


Dwelling

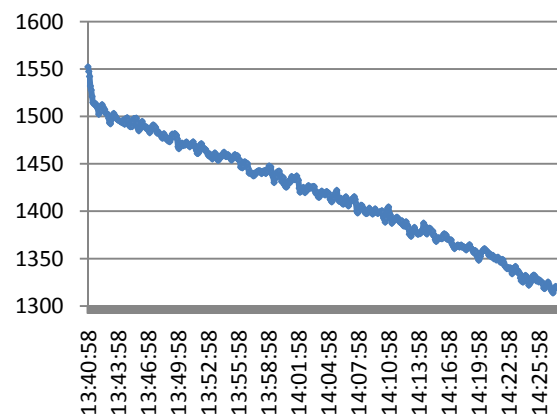


Winter

Shelter



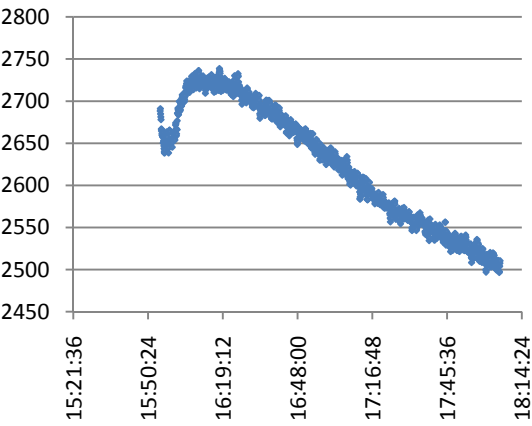
Dwelling

***Dwelling 15***

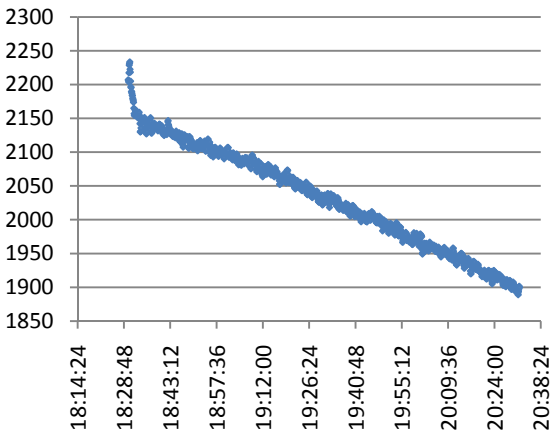
Material de construcción	Ladrillo
Año de construcción	1997
Material puertas y ventanas	PVC, doble vidrio
Área estudiada (P0 y P1)	127.3
No. plantas	2 plantas
Caras expuestas al viento	4
Estación Meteorológica próxima	Barcelona - Observatori Fabra 10 m
Volumen Shelter	29m ³
Chimenea	No

Winter

Shelter



Dwelling

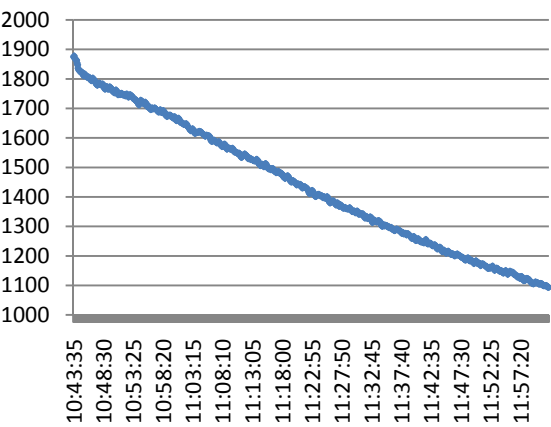


Dwelling 16

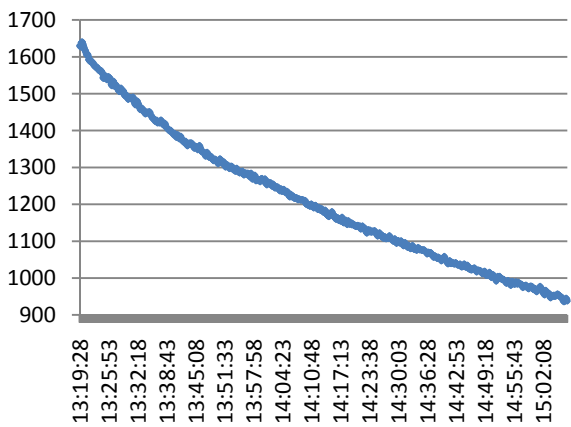
Material de construcción	Ladrillo
Año de construcción	2004
Material puertas y ventanas	Aluminio, doble vidrio
Área estudiada (P0 y P1)	177
No. plantas	2 plantas + garaje (no se tuvo en cuenta)
Caras expuestas al viento	4
Volumen shelter	7.5 m ³
Estación Meteorológica próxima	Hospitalet de l’Infant (10 m)

Winter

Shelter



Dwelling



Annex G. Publications derived from this thesis

From the results obtained and the work done through this thesis, the following publications in scientific journals and congresses were derived.

María I. Montoya, Elsa Pastor, F. Rémi Carrié, Gaelle Guyot, Eulàlia Planas. (2010). "Air leakage in Catalan dwellings: Developing an airtightness model and leakage airflow predictions". *Building and Environment* 45, 1458–1469.

María I. Montoya, Eulàlia Planas, Joaquim Casal. (2009). "A comparative analysis of mathematical models for relating indoor and outdoor toxic gas concentrations in accidental releases". *Journal of Loss Prevention in the Process Industries* 22, 381–391.

María I. Montoya, Eulàlia Planas. (2010). "Effect of additional measures when evaluating shelter-in-place effectiveness in the case of a toxic gas release". European Meeting on Chemical Industry and Environment. pp 1097-1106. Mechelen.

María I. Montoya, F. Rémi Carrié, Gaelle Guyot, Eulàlia Planas. (2009) "Analysis of Air Leakage of French Residential Dwellings". 30th AIVC Conference and 4th International BUILDAIR-Symposium. pp. 1-7. Berlín.

María I. Montoya, Eulàlia Planas. (2008). "Comparison of different methodologies to estimate the evacuation radius in the case of a toxic release". Annual Risk, Safety and Reliability Conference. ESREL 2008 AND 17th SRA-EUROPE CONFERENCE. Vol. 2, pp. 1089-1096. Valencia.

María I. Montoya, Eulàlia Planas. (2008) "A way of assessment shelter-in-place effectiveness in Catalunya". 11th MEDITERRANEAN CONGRESS OF CHEMICAL ENGINEERING. Proceedings en CD. Barcelona.



Contents lists available at ScienceDirect

Building and Environment

journal homepage: www.elsevier.com/locate/buildenv

Air leakage in Catalan dwellings: Developing an airtightness model and leakage airflow predictions

María I. Montoya^a, Elsa Pastor^a, F. Rémi Carrié^b, Gaelle Guyot^b, Eulàlia Planas^{a,*}^a Centre d'Estudis de Risc Tecnològic (CERTEC), Departament d'Enginyeria Química, Universitat Politècnica de Catalunya, ETSEB, Diagonal 647, Pav. G, planta 1, 08028 Barcelona, Spain^b Centre d'Etudes Techniques de l'Équipement de Lyon (CETE), 46 rue Saint Théobald, F-38081 L'Isle d'Abeau Cedex, France

ARTICLE INFO

Article history:

Received 19 October 2009

Received in revised form

9 December 2009

Accepted 11 December 2009

Keywords:

Airtightness

Infiltration

Air exchange rate

Residential dwellings

ABSTRACT

In this study we estimate the air leakage distribution of single-family dwellings in Catalonia and use a statistical analysis of an airtightness database for single-family dwellings in France to identify the building characteristics that have the greatest influence on airtightness. The most significant variables are found to be the structure type, the floor area, the age of the building, the number of stories and the insulation type. A multiple linear regression technique is then applied to establish a predictive model for deriving an estimated value of airtightness from these characteristics. To estimate the infiltration airflow, a stochastic simulation of the building characteristics was performed per census tract using real data on the distributions of building variables taken from the census information. The model is then applied to determine the power law coefficient and the airtightness distribution. The predicted flow coefficients are combined with the AIM-2 model and given meteorological conditions to determine the infiltration airflow. Two sets of meteorological conditions are considered: average conditions and extreme conditions for each season.

© 2009 Elsevier Ltd. All rights reserved.

1. Introduction

This paper forms part of a general study focused on the assessment of shelter-in-place effectiveness of Catalan dwellings in the event of a toxic gas release. Catalonia is a highly industrialized region in the north-east of Spain in which 180 companies are regulated by the Seveso II Directive [1]. In a shelter-in-place situation, air infiltration is one of the variables with the greatest influence on shelter-in-place effectiveness, as discussed by Chan et al. [2] and Montoya et al. [3], because it conditions the speed of toxic gas inflow and therefore the indoor gas concentration.

Air infiltration flow refers to the flow of outdoor air through envelope leaks (i.e. through non-intentional openings) generated by meteorological conditions. Therefore, this flow depends on the airtightness of the building and the pressure difference between outdoors and indoors. The pressure difference is a function of the stack effect and the wind, whereas the airtightness depends on the envelope leakage characteristics and is therefore independent of weather conditions [4]. However, no experimental data on air

infiltration exchange rate (ACH) or airtightness is available for Catalan dwellings.

Air infiltration in single-family dwellings has become a popular research area over the last three decades, because it greatly influences the energy performance of buildings and indoor air quality. Recently, European legislation concerning the energy performance of buildings has become more demanding. Possible solutions to meet the new requirements, as described by Erhorn et al. [5], are based not only on additional insulation or more effective building systems, but also on reducing infiltration losses by improving building airtightness. Air infiltration also affects indoor air quality and, since single-family dwellings in southern Europe are not usually fitted with mechanical ventilation systems, infiltration is the only means of pollutant transport between outdoors and indoors when all intentional openings are closed. Consequently, air infiltration conditions the inflow of outdoor common pollutants and toxic substances in the event of an accidental release and influences the outflow and retention of contaminants of indoor origin such as tobacco smoke.

Consequently, as expressed by Sherman [6], there is a need to determine the real distribution of building stock airtightness and the resulting magnitude of the air infiltration flow. This information is essential for characterizing the status of the current building stock and for establishing a foundation for future research into aspects

* Corresponding author. Present address: ETSEB, Diagonal 647, Pav. G, planta 1, 08028 Barcelona, Spain. Tel.: +34 93 4011736; fax: +34 93 4017150.
E-mail address: eulalia.planas@upc.edu (E. Planas).



Contents lists available at ScienceDirect

Journal of Loss Prevention in the Process Industries

journal homepage: www.elsevier.com/locate/jlpi

A comparative analysis of mathematical models for relating indoor and outdoor toxic gas concentrations in accidental releases

María I. Montoya, Eulàlia Planas*, Joaquim Casal

Centre d'Estudis de Risc Tecnològic (CERTEC), Departament d'Enginyeria Química, Universitat Politècnica de Catalunya, Barcelona, Spain

ARTICLE INFO

Article history:
Received 11 July 2008
Received in revised form
30 January 2009
Accepted 30 January 2009

Keywords:
Sheltering
Toxic release
Atmospheric dispersion
Indoor concentration

ABSTRACT

This paper surveys various models for estimating indoor concentration as a function of outdoor concentration in the event of an accidental release or chemical attack involving toxic substances. It is essential to know indoor concentration in order to estimate the effectiveness of shelter in place as a protective measure. Several models—deposition, one-sink, sink-diffusion and two-sink—were considered. These models can be derived from a general model by making different assumptions. The models showed significant variations in terms of the adsorption/desorption considerations. Since indoor materials act as reservoirs, adsorption may lead to a significant decrease in indoor concentration, but subsequent desorption may also take place. The models require the knowledge of a set of parameters that are specific to each compound and material, which are currently scarce in the literature. As a result, the more complex and complete the model, the more limited its applicability. Outdoor concentrations obtained from a Gaussian model and originating from three source types (continuous, temporary and instantaneous) were used as inputs in the reviewed models. Indoor concentrations of chlorine and sarin from a temporary source were estimated in order to compare the predictions of the models.

© 2009 Elsevier Ltd. All rights reserved.

1. Introduction

Toxic gas clouds can be caused by a variety of events, including accidental releases on industrial premises, accidents during the transportation of hazardous materials, and attacks involving chemical warfare agents. When a toxic plume appears, one usual protection measure is to shelter in a building and wait until the plume has passed. Evacuation would involve exposure to the toxic release. Since most people spend most of their time inside buildings, they are advised to stay indoors, where the concentration of the toxic substance is supposed to be lower than it is outside. Thus, people are exposed to lower doses of the substance (Chan, Price, Gadgil, & Nazaroff, 2004; Glickman & Ujihara, 1990; Jetter & Whitfield, 2005; Karlsson, 1994; TNO, 1989, chap. 6; Yuan, 2000). Doses are estimated on the basis of the relationship between inside and outside concentrations as a function of time. This paper surveys this relationship for the models analyzed.

Studies in the field of technological risk have focused more on developing models for estimating the outdoor dispersion of neutral and heavy gases in the event of a toxic release than on developing

models for relating indoor concentration to outdoor concentration. Indoor concentration is often determined by a mass balance without taking into account indoor processes (i.e. reactions, sorptive interactions with indoor materials, etc.) that can increase or decrease the concentration. Processes of this type have received more attention in the field of indoor air quality where outside concentration is seldom assumed to follow a predefined behavior. In this paper, indoor concentration is related to outdoor concentration using a single model that includes several sorption processes. The paper also evaluates the solutions of various models by using the Gaussian dispersion model to estimate outdoor concentration for cases of continuous and instantaneous releases.

Indoor concentration models were originally developed as a means of estimating the indoor concentration of common pollutants that affect indoor air quality (i.e. CO₂, ozone, VOCs, etc.). One of the first models was proposed by Shair and Heitner (1974). This model uses the approximation of a well-mixed chemical reactor and develops a case study of ozone by using a sinusoidal input and a ramp input to simulate outdoor concentration. Recent research in this area has essentially focused on the effects that sorptive interactions between gases and indoor materials have on concentration. Won, Corsi, and Rynes (2001), for example, studied the interactions between eight VOCs and various indoor materials (e.g. carpet, gypsum board, upholstery, vinyl and wood flooring, acoustic tiles, and fruit). They obtained the adsorption/desorption

* Corresponding author. ETSEIB (UPC), Campus Sud, Edif. PG, Av. Diagonal, 647, 08028 Barcelona, Spain. Tel.: +34 934011736; fax: +34 934017150.

E-mail addresses: maria.isabel.montoya@upc.edu (M.I. Montoya), eulalia.planas@upc.edu (E. Planas), joaquim.casal@upc.edu (J. Casal).

EFFECT OF ADDITIONAL MEASURES WHEN EVALUATING SHELTER IN PLACE EFFECTIVENESS IN THE CASE OF A TOXIC GAS RELEASE

Maria Isabel Montoya^a, Eulàlia Planas^a

^aCentre d'Estudis de Risc Tecnològic (CERTEC), Universitat Politècnica de Catalunya, Av. Diagonal 647, CP-08028 Barcelona, Spain.

Abstract

When a shelter-in-place event take place, additional measures like go into an interior room close the door, seal vents and window and door frames with tape, are often advised to people with the aim of reduce the amount of air infiltration and prevent people from being exposed to a high concentration. In this study, we determine experimentally the air exchange rate of several dwellings under normal sheltering, as well as the air exchange of an interior room where expedient measures were applied. In most of the cases, we found a reduction on the ACH of shelters in relation to those of dwellings, which born out that even in the worst case (only outdoor air infiltrates to the shelter), expedient measures increase shelter in place effectiveness in relation to normal sheltering.

Keywords:

Shelter-in-place, building airtightness, air infiltration, toxic release, human vulnerability, expedient measures, interior rooms.

Analysis of Air Leakage of French Residential Dwellings

Maria Isabel Montoya^{1,a}, François Rémi Carrié^{2,b},
Gaëlle Guyot^{2,c}, Eulàlia Planas^{1,d}

¹Centre d'Estudis de Risc Tecnològic (CERTEC), Universitat Politècnica de Catalunya, Av. Diagonal 647, CP-08028 Barcelona, Spain. Tel. +34 934016675 - Fax. +34 934017150

²Centre d'Etudes Techniques de l'Équipement de Lyon (CETE), 46 rue Saint Théobald, F-38081 L'Isle d'Abeau Cedex, France. Tel. +33 474275161 - Fax. +33 474275118

^amaria.isabel.montoya@upc.edu ^bRemi.Carrie@developpement-durable.gouv.fr

^cGaëlle.Guyot@developpement-durable.gouv.fr ^deulalia.planas@upc.edu,

ABSTRACT

In this work the air leakage database of French single family dwellings, available at the CETE de Lyon (Centre d'Études Techniques de L'Équipement), has been analysed. This database accounts for 251 blower-door measurements of single family dwellings, made after 1983 as a result of several campaigns carried out across France to quantify the performance of French dwellings in terms of envelope airtightness and the existing directives. A statistical analysis was performed in order to find out the available buildings characteristics that most influence dwellings airtightness, represented by the flow coefficient C of the leakage function. The floor area, the number of stories, the structure type and the age were found to be the most significant characteristics. Finally, a linear model to estimate C was developed using these variables as predictors.

KEYWORDS

Air leakage database, air exchange rate, residential dwellings, shelter-in-place

INTRODUCTION

In the last decades, building airtightness has become a growing concern in the research field due to several problems that arise from the uncontrolled or inadequate leakage of buildings (e.g. thermal comfort, high energy consumption, poor indoor air quality). Main efforts on airtightness characterization have been done in the field of buildings energy performance and indoor air quality (Litvak et al. 2000a; Litvak et al. 2000b; Erhorn, Erhorn-Kluttig & Carrié 2008). However, after some catastrophic chemicals accidents (i.e the Bophal accident) where a toxic cloud disperses over the population, the concern regarding shelter in place as a protective measure has been growing and therefore the interest on building airtightness stock in the risk assessment field has also grown (Chan et al. 2007a, Carrié et al. 2006). When all intentional openings are closed and mechanical ventilations systems are shut down, air infiltration becomes the only media of pollutant transport between outdoors and indoors, and it conditions the entrance of outdoor common pollutants and toxic substances (in the case of an accidental release), as well as the exit and retention of contaminants of indoor origin (TNO 1989; Chan et al. 2005, 2007a; Montoya et al. 2009). The magnitude of the infiltration flow depends mainly on the building envelope leakage sites, the indoor configuration of the building, the site topography and the pressure difference across each leakage site generated by meteorological conditions



Comparison of different methodologies to estimate the evacuation radius in the case of a toxic release

M.I. Montoya & E. Planas

Center for Technological Risk Studies, Universitat Politècnica de Catalunya, Barcelona, Spain

ABSTRACT: A comparison of different methodologies used to estimate the evacuation radius, is presented. The evaluation is accomplished doing some modifications in the way of computing indoor concentration (taking into account the profile of outdoor concentration and the possible sorption into indoor surfaces) and toxic load. The casualties' probability estimation is made using the probit analysis, but a parallel analysis to assess the effectiveness of shelter in place, based on the AEGL-3, is also made with the aim of comparison and to confirm the results obtained with the probit analysis. Five substances of different toxicity (chlorine, methyl isocyanate, acrolein, hydrogen fluoride and mustard gas) are used to study the performance of one or another methodology, finding that for cumulative substances there is an overestimation with the method used by Catalanian government. Concerning meteorological conditions, larger distances were obtained when increasing the atmospheric stability.

1 INTRODUCTION

Dispersion of toxic gas clouds can be originated by diverse events, including accidental releases in the industry or during transportation of hazardous materials, and biological or chemical warfare agent's attacks. One protection way against this phenomenon is to shelter in a building and wait until the toxic plume has passed. Since most people spend the majority of their daily time inside buildings they could stay indoors, where the concentration of the toxic substance is supposed to be lower than outside and thus, the toxic load (TL) to which people are exposed is lower. Even though, there is not a unified or totally reliable method to determine the effectiveness of this protection method, and thus, there are several methodologies used by authorities and local emergency commissions which underestimate or overestimate the evacuation radius, leading to unexpected deaths, health affections or unnecessary efforts, respectively.

As community protection measures, Catalanian government has established three actuation zones: alert, intervention and LC01, based on outside concentrations (PlaseQcat 2005). The first zone refers to the region in which accident's consequences, although perceptible by the community, does not justify intervention. The second is a zone in which those consequences generate such a level of damages that immediately protection measures might be taken. The last zone involves the area in which 1% casualties are expected at the exterior. The first two zones are defined using the threshold values given by the Spanish

government (Directriz básica 2003), which are the Acute Exposure Guidelines Levels (AEGL-1 and AEGL-2, respectively), the Emergency Response Planning Guidelines (ERPG-1, ERPG-2) or the Temporary Emergency Exposure Limits (TEEL-1, TEEL-2) if the first ones (AEGL) are not available for the substance studied. The LC01 involves the estimation of a percentage of casualties which is usually accomplished through a vulnerability study using the probit analysis (Purple book 1999). In addition to this zones, and taking into account that protection measures in the case of a toxic gas dispersion recommend shelter, emergency managers should have established the radius within shelter in place is effective and thus an evacuation radius must be defined. The criteria used by Catalanian government to calculate this radius is that casualties inside the building, within this distance, are 0.1% (PlaseQcat 2005).

For the vulnerability study one of the most common techniques is the probit analysis which relates the magnitude of the incident with the damage caused (Casal et al. 1999a, El Harbawi et al. 2008, Geeta et al. 1993). In the case of toxic dispersion, the magnitude of the incident is the TL received by people exposed. This magnitude is used to calculate the probit variable and then, the casualties' probability. The TL depends on the time and the concentration to which people are exposed, that is why the estimation of the indoor concentration (C_i) is so important.

Indoor concentration depends mainly on the air exchange rate of the building -since it conditions the entrance of outdoor air- and on the sorption

A WAY OF ASSESSMENT SHELTER-IN-PLACE EFFECTIVENESS IN CATALONIA

María Isabel Montoya^a, Eulàlia Planas^b

Center for Technological Risk Studies. Chemical Engineering Department. Universitat Politècnica de Catalunya. Diagonal, 647. 08028-Barcelona

^aTel. 34 93 4016675. Fax. 34 93 4017150. e-mail: maria.isabel.montoya@upc.edu

^bTel. 34 93 4011736. Fax. 34 93 4017150. e-mail: eulalia.planas@upc.edu

Sustainable Development, Risk Analysis and Environmental Impact

Shelter-in-place as an emergency protection action is used with the aim of reducing human exposure to toxic gas clouds in the event of an accidental or intentional airborne release. As the concentration of the toxic substance inside buildings is supposed to be lower than outside, the toxic load (TL) to which people are exposed is lower, and since most people spend the majority of their daily time inside buildings, shelter-in-place could be an easy and very effective protection measure that saves money and evacuation efforts to emergency managers. Even though, an assessment of its effectiveness should be made to assure its applicability since, although indoor concentration and indoor toxic load are lower than outdoors, they could, in some cases, be greater than the toxic load limit (TLL) and that would represent a real hazard. In assessing shelter-in-place effectiveness in a population, one of the most important parameters is the air exchange rate distribution among buildings, since it conditions the air infiltration into the buildings and thus the indoor concentration perceived.

To assess shelter-in-place effectiveness there are two type of indicators: ones that are used to evaluate if the TLL is exceeded; and others that are used to evaluate the TL reduction gained as being indoors. In the first case, there are some indicators known as safety factors (indoor and outdoor safety factors) that represent the constant by which the exposure concentrations can be multiplied without exceeding the TLL (Chan et al. 2007) and gave a general idea of the situation in each one of the affected zones. In the other type of indicators there are two approaches: the toxic load reduction factor (TLRF) which relates the TL that is avoided by being indoors (TLi) with the TL that is perceived outside (TLo) and the safety factor multiplier (SFM), which represents the relation between the indoor and outdoor safety factors. In the case of the TLRF a value near 1 means a good TL reduction is achieved and a value near 0 means an ineffective shelter, while a high value of the SFM indicates an effective shelter and a value approaching 1 means an ineffective shelter.

In this work, a methodology to evaluate the effectiveness of shelter-in-place is presented and developed within an example of an accidental toxic release in Catalonia. Especial emphasis was made on the estimation of the air exchange rate distribution, which was assessed by census track taking into account buildings airtightness (represented by the normalized leakage area) and meteorological conditions. As a result a map with the normalized leakage area distribution for single-family dwellings within census track for Catalonia was obtained. Then, according to the release location (coordinates), the wind direction and the relation between outdoor and indoor concentrations, the area affected by the toxic cloud, established as the area where the $TLo > TLL$, could be determined in a geographical information system (GIS). The indoor and outdoor safety factors and the SFM were evaluated for this area as the indicators of the shelter-in-place effectiveness.

References

Chan W.R., Nazaroff W.W., Price P.N., Gadgil A.J. 2007. Effectiveness of urban shelter-in-place—I: Idealized conditions. *Atmospheric Environment*. 41, 4962–4976.